

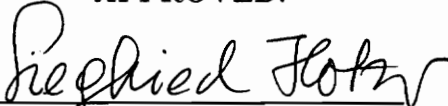
3-D FINITE ELEMENT BEAM/CONNECTOR MODEL
FOR A GLULAM DOME CAP

by


Moses T. Tsang

Thesis submitted to the Faculty of the
Virginia Polytechnic Institute and State University
in partial fulfillment of the requirements for the degree of
Master of Science
in
Civil Engineering

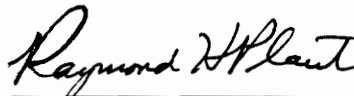
APPROVED:



S. M. Holzer, Chairman



J. D. Dolan



R. H. Plaut

December, 1992
Blacksburg, Virginia

C.2

LD
5655
V855
1992
T827
C.2

3-D Finite Element Beam/Connector Model for a Glulam Dome Cap

by

Moses T. Tsang

Committee Chairman: Dr. S. M. Holzer

Civil Engineering

(ABSTRACT)

The purpose of this study is to model the beam/decking connectors (nails) of a glulam dome cap by beam/connector elements, and to analyze various dome cap models in order to investigate the potential of the beam/connector model to simulate the decking. Two- and three-dimensional beam/connector elements are formulated, tested, and evaluated.

The dome cap is modeled with I-DEAS, and the modeling procedures are briefly discussed. Four series of beam/connector dome cap models are created and analyzed: (1) models with the nailed joints at bracing points (rigid link $h=0$), (2) models with the nailed joints at bracing points ($h>0$), (3) models with 16 nailed joints per beam element ($h=0$), and (4) models with 16 nailed joints per beam element ($h>0$). Their results are compared with the dome cap models with the truss bracings. Finally, conclusions and recommendations for future research are presented.

Acknowledgements

I am very grateful to Dr. S. M. Holzer for his excellent teaching, and his continued support and encouragement throughout this study. I also wish to express my gratitude to Dr. R. H. Plaut and Dr. J. D. Dolan for their help and suggestions during the course of my study, and for serving on my committee.

I am very thankful to my fellow students, Sandeep Kavi, Niket Telang, Chris Earls, Budi Widjaja, and Yu-Wen Yang for their lively discussions, and innovative ideas. I am especially grateful to Dr. Abatan for his help and valuable suggestions for this study.

I would like to thank my family for providing constant moral support during my education. My heart goes to my parents and Eunice Chiu to whom I dedicate this thesis and thank for their support, love, and patience.

TABLE OF CONTENTS

1.	INTRODUCTION	1
2.	REVIEW OF THE LITERATURE	
2.1	Introduction	6
2.2	Nailed Connections	7
2.2.1	Types of Nails	8
2.2.2	Lateral Load Connections	9
2.2.3	Factors Affecting Strength of Nailed Connections	9
2.3	Load Slip Relationship of Nailed Connections	11
2.3.1	Elastic Theory	13
2.3.2	Generalized Model for Lateral Load Slip of Nailed Connections	17
2.4	Present Design Criteria	24
2.4.1	Lateral Resistance of Nailed Connections	24
2.4.2	Validity of Lateral Load Design Values	26
2.5	Behavior of Timber Joints with Multiple Nails	28
3.	FORMULATION OF BEAM/CONNECTOR ELEMENTS	
3.1	Introduction	31

3.2	Formulation of 2-D Connector Stiffness Matrix	33
3.3	Formulation of 3-D Connector Stiffness Matrix	41
3.4	Testing of 3-D Connector Stiffness Matrix for a Special Case	53
4.	TESTING OF BEAM/CONNECTOR ELEMENTS	
4.1	Introduction	57
4.2	Testing of 2-D Beam/Connector Element	58
4.2.1	Test Models and Procedures	58
4.2.2	Creation of Input File for 2-D Beam/Connector Element in ABAQUS	62
4.2.3	Comparison and Discussion of Test Results	67
4.3	Testing of 3-D Beam/Connector Element	75
4.3.1	Testing of a Special Case	75
4.3.2	Test Models and Procedures	82
4.3.3	Input File for 3-D Beam/Connector Element in ABAQUS	86
4.3.4	Comparison and Discussion of Test Results	91
5.	DOME CAP MODEL	
5.1	Introduction	97
5.2	Finite Element Modeling of Dome Cap	99
5.2.1	Modeling of Beams, Purlins and Tension Ring	100
5.2.2	Modeling of Decking	104
5.3	Boundary Conditions	112
5.4	Material Properties	113

5.5	Design Loads	116
5.6	Creation of ABAQUS Input File	117
5.6.1	Nodal Loads	117
5.6.2	Beam Orientations	118
5.6.3	Beam/Connector Element Properties	118
6.	DOME CAP ANALYSIS	
6.1	Introduction	128
6.2	Nonlinear Analysis Procedures	129
6.3	Dome Cap Analysis with Nailed Joints at Bracing Points	131
6.3.1	Rigid Link Length $h=0$	132
6.3.2	Rigid Link Length $h>0$	142
6.4	Dome Cap Analysis with 16 Nailed Joints per Beam Element	147
6.4.1	Rigid Link Length $h=0$	147
6.4.2	Rigid Link Length $h>0$	152
7.	CONCLUSIONS AND RECOMMENDATIONS	
7.1	Conclusions	157
7.2	Recommendations	159
	REFERENCES	160
	APPENDIX A	166
	APPENDIX B	171
	APPENDIX C	177
Table of Contents		vi

APPENDIX D	179
APPENDIX E	195
APPENDIX F	219
APPENDIX G	224
VITA	229

LIST OF FIGURES

Figure 2.1:	Lateral load connections	10
Figure 2.2:	(a) Load-slip curve; (b) Joint slip of nailed joint	12
Figure 2.3:	Method of testing for nailed joints	15
Figure 2.4:	Test specimen. (a) Plan view; (b) Elevation view	21
Figure 3.1:	Beam/connector assembly	32
Figure 3.2:	Beam with discrete connector	34
Figure 3.3:	Degrees of freedom (a) Plane beam; (b) Plane frame	39
Figure 3.4:	(a) Beam cross section; (b) Space beam element	43
Figure 3.5:	(a) Beam/connector model; (b) Beam cross section	44
Figure 3.6:	Deformations of beam/connector element	47
Figure 4.1:	Beam/connector assembly (n=1)	59
Figure 4.2:	Results of test problem 1 in Table 4.1	68
Figure 4.3:	Results of test problem 2 in Table 4.1	69
Figure 4.4:	Results of test problem 3 in Table 4.1	70
Figure 4.5:	Results of test problem 4 in Table 4.1	71

Figure 4.6:	Results of test problem 5 in Table 4.1	72
Figure 4.7:	Results of test problem 6 in Table 4.1	73
Figure 4.8:	3-D beam/connector assembly for Section 4.3.1	77
Figure 4.9:	Results of a beam/connector assembly (by statics)	78
Figure 4.10:	Results of beam/connector assembly (a) By approach 2 (b) By approach 3	80
Figure 4.11:	3-D beam/connector assembly (n=1)	83
Figure 4.12:	Results of test problem 1 in Table 4.2	92
Figure 4.13:	Results of test problem 2 in Table 4.2	93
Figure 4.14:	Results of test problem 3 in Table 4.2	94
Figure 4.15:	Results of test problem 4 in Table 4.2	95
Figure 5.1:	Plan of dome	98
Figure 5.2:	Members of dome model	101
Figure 5.3:	Dome cap model	103
Figure 5.4:	Plan of dome decking	105
Figure 5.5:	Load-slip curve of nailed joint	110
Figure 5.6:	Location of nailed joints on beam element (unrefined mesh)	111
Figure 5.7:	Stress-strain curve for wood (nonlinear material law)	115
Figure 5.8:	Local axes of beam/connector models	120
Figure 5.9:	Local main beam element of dome cap model	124
Figure 5.10:	Reactions of cap rib models	126
Figure 6.1:	Dome cap model with truss bracings	133
Figure 6.2:	Location of nailed joints (at bracing points) in dome cap model	136
Figure 6.3:	Load-slip curve with constant nail stiffnesses	138

Figure 6.4:	Load deflection paths of dome cap models with nailed joints at bracing points ($h=0$); Linear material law	140
Figure 6.5:	Load deflection paths of dome cap models with nailed joints at bracing points ($h=0$); Nonlinear material law	141
Figure 6.6:	Load deflection paths of dome cap models with nailed joints at bracing points ($h>0$); Linear material law	144
Figure 6.7:	Load deflection paths of dome cap models with nailed joints at bracing points ($h>0$); Nonlinear material law	145
Figure 6.8:	Load deflection paths of dome cap models with 16 nailed joints per beam element ($h=0$); Linear material law	150
Figure 6.9:	Load deflection paths of dome cap models with 16 nailed joints per beam element ($h=0$); Nonlinear material law	151
Figure 6.10:	Load deflection paths of dome cap models with 16 nailed joints per beam element ($h>0$); Linear material law	154
Figure 6.11:	Load deflection paths of dome cap models with 16 nailed joints per beam element ($h>0$); Nonlinear material law	155

LIST OF TABLES

Table 4.1	Test program and results for 2-D beam/connector elements	60
Table 4.2	Test program and results for 3-D beam/connector elements	84
Table 6.1	Models with truss bracing and nailed joints at bracing points ($h=0$)	134
Table 6.2	Models with truss bracing and nailed joints at bracing points ($h>0$)	143
Table 6.3	Models with truss bracing and 16 nailed joints per beam element ($h=0$)	149
Table 6.4	Models with truss bracing and 16 nailed joints per beam element ($h>0$)	153

Chapter 1

INTRODUCTION

The purpose of this study is to model the beam/decking connectors (nails) of a glulam dome cap by beam/connector elements, and to analyze various dome cap models in order to investigate the potential of the beam/connector model to simulate the decking. The dome cap models are analyzed with the finite element program ABAQUS.

The roof decking effects on the beams of the dome were modeled by truss bracing by Wu (1991) and Telang (1992). However, the truss bracing does not simulate the closely spaced nail connections; therefore, the beam/connector model is created. The 3-D beam/connector element is formulated to model the beam/decking connector in this study (Chapter 3). This element consists of a beam element, a linear spring element with one end fixed, and a rigid link. The linear spring element is attached laterally to the top of the beam by the rigid link

in order to model the lateral resistance of the nail by which the beam and the decking are connected. The decking is modeled by the fixed end based on an assumption that the decking is very stiff in membrane action. The advantage of the beam/connector element is that the connector elements (spring elements), which model the nails, are transformed into an element which shares the same nodes with the beam instead of placing nodes on the beam. As a result, the beam/connector element has the same number of degrees-of-freedom as the beam itself no matter how many connectors are attached. Thus, it saves a significant amount of computer memory and computer time when analyzing a large structure like a glulam dome.

The 2-D and 3-D beam/connector elements are formulated. The stiffness matrix of the beam/connector element is simply a superposition of the beam stiffness matrix and the connector stiffness matrix. The beam stiffness matrix can be generated from the element library in ABAQUS but the connector stiffness matrix is not provided by ABAQUS. However, ABAQUS provides a powerful option called USER ELEMENT, which introduces a user-defined element type. Since the behavior of the connector is assumed to be purely linear, the connector stiffness matrix is simply input by using the suboption MATRIX (ABAQUS 4.8, User's Manual, p.6.5.20-1).

In order to study the effects of the number of connectors and the connector stiffness on the response of the 2-D beam/connector element, five test problems are analyzed with ABAQUS. In each test problem, the simply supported beam/connector assembly (different in each test problem) is modeled by: (1) the

beam/connector elements, and (2) the beam and the linear spring elements. The results of these two models are compared. Similarly, four test problems are analyzed with ABAQUS for testing the 3-D beam/connector element, and for studying the effects of the number of connectors and the connector stiffness on the response of the element.

The dome cap model is created, based on the triax dome at Raleigh, North Carolina. The dome cap model is the top ring of the complete dome. This model is created because it is more economical to analyze the model in terms of computer time. Besides, since the model is a part of the complete dome, its behavior is similar to that of the entire dome. Thus, potential modeling and analysis problems can be identified before analysis of the complete dome.

The dome cap models are created graphically using I-DEAS, which is a finite element program with excellent graphical capabilities. I-DEAS has the option for writing an input file for ABAQUS. The input file, which is obtained from I-DEAS, is modified to include the beam orientations, the material law of wood (linear or nonlinear), and the user elements for the beam/connector elements.

In the dome cap models, the 2-noded straight beam elements (B33) are used. In order to simulate the complete dome behavior, the geometric properties and the orientations of the edge beams (beams at the base of the dome cap) for these models are the same as those of the edge beams for the complete dome. The tension ring and the purlins are modeled with the truss elements (C1D2). When the beam/decking connectors (nails) are modeled by the beam/connector

elements, the connector stiffness matrices (in ABAQUS input format) for the main beams and the edge beams are generated by the FORTRAN programs MKS1 and MKS3, respectively. Both linear and nonlinear material laws are used for the models, and only full snow load is considered.

Four dome cap models with the nailed joints at the bracing points (rigid link length $h=0$) were analyzed with ABAQUS. A linear material law ($E=1.8 \times 10^6$ psi; $G=1.6 \times 10^5$ psi) is applied to the first two models while a nonlinear material law (Telang, 1992, p.15) is applied to the other two models. For a nonlinear material law, the initial longitudinal modulus of wood in tension $E_{(tension)} = 1.81 \times 10^6$ psi and in compression $E_{(compression)} = 2.19 \times 10^6$ psi. The shear modulus is taken as $G = 1.6 \times 10^5$ psi (Telang, 1992, p.65). The rigid link length h is taken as zero so that the spring element of the beam/connector model is attached to the centroid of the beam cross section. The nailed joints are modeled by the spring elements of the beam/connector model. Each nailed joint is assumed to be composed of two identical nails. The choice of the values of the connector stiffness (spring stiffness) is based on the load-slip curve of the 16-d common nail, which is the type of nail used in the construction of the dome. The load-slip curve is predicted by Wilkinson's formula (Wilkinson, 1971, 1972a, 1972b, 1974a, 1974b) and McLain's formula (McLain, 1975). The results from these beam/connector models are compared with the truss bracing model (Table 6.1). Another three series of beam/connector models (see Tables 6.2 - 6.4) are analyzed with ABAQUS: (1) models with the nailed joints at the bracing points ($h>0$), (2) models with 16 nailed joints per beam element ($h=0$), and (3) models with 16 nailed joints per beam element ($h>0$). The results are compared with those of the

truss bracing models and discussed. In the case of $h > 0$, the rigid link length h is taken as 5.5 in. for the main beams and 6.125 in. for the edge beams, respectively. Thus, the spring element of the beam/connector model is attached to the top of the beam cross section.

Equilibrium paths, critical loads, maximum stresses, apex deflections (node 1 deflection), and maximum nail deflections are presented for all the models. Based on the present research, conclusions are presented, and recommendations are made as to further study of glulam domes.

Chapter 2

REVIEW OF THE LITERATURE

2.1 Introduction

Many modern roof structures are composed of several widely spaced deep beams and a tongue-and-groove timber decking, which is attached to the top of the beams by nails. The decking is necessary because it greatly increases the resistance of the beams against lateral buckling. The roof deck stabilizes the compression flanges of the beams by diaphragm action, which is defined as a process by which the deck resists in-plane shear distortion. For plank decking, the shear stiffness depends primarily on the nails joining the adjacent planks. In addition, the stabilizing effect of the plank decking is taken into account by considering the lateral resistance of the nail fasteners (Jenkinson and Zahn, 1972, p.599). Since the decking effect on the beams is considered in this study, the review of the nail behavior under lateral load, which is transmitted from the decking to the beams and the nail joints, becomes crucial.

The objective of this chapter is to give a summary of the load deformation relationship of nailed joints. An introduction to the nailed connections is given in Section 2.2. This section is divided into three subheadings of types of nails, lateral load connections, and factors affecting the strength of nailed connections. The elastic theory developed by Wilkinson (1971) on the load-slip relationship of nailed connections is presented in Section 2.3.1. The generalized model for lateral load slip of nailed connections is discussed in Section 2.3.2. The lateral resistance of nailed joints in design and its validity are given in Sections 2.4.1 and 2.4.2, respectively. In Section 2.5, the behavior of timber joints with multiple nails is presented.

2.2 Nailed Connections

Nails are commonly used as fasteners in timber structures. They are used when the loads on the structures are relatively small, and other types of fasteners (e.g., bolts) are used for larger loads (Breyer, 1980, p.359). If the nails fail, the whole structure collapses. Therefore, it is necessary to study the behavior of nailed connections under different types of loads. This section serves as an introduction to the nailed connections (Section 2.2.1 and 2.2.2), and some factors that influence the stiffness of nailed connections are presented (Section 2.2.3).

2.2.1 Types of Nails

Four basic types of nails mentioned in Table 8.8A of the National Design Specification for Wood Construction (NDS, 1986) are

1. Common nails
2. Box nails
3. Common spikes
4. Threaded hardened steel nails

The nail size is specified by the pennyweight of the nail, abbreviated by d. The pennyweight specifies the length of the nail.

For a given pennyweight, all four types of nails have the same length but a different diameter. The first three types of nails are made of low-carbon-steel wire and have a flat head, plain shank, and diamond point. The last type of nail is made of high-carbon-steel and has a flat head, annularly or helically threaded shank, and a diamond point (Breyer, 1980, pp. 360-361).

2.2.2 Lateral Load Connections

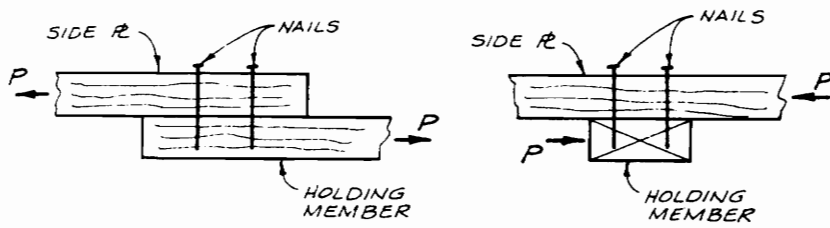
Three types of nailed connections are: lateral load connection, withdrawal-type connection, and toenailed connection (Breyer, 1980, pp.367-384). Since lateral forces are transmitted to the beams as well as to the nailed joints from the decking (Mohammad, 1990, p.6), only the lateral load connection will be discussed in the following paragraph.

In a lateral load connection, the load is applied perpendicular to the length of the nail. There are two types of lateral load connections. One of them has the nail driven into the side grain (i.e., perpendicular to the grain) of the holding member (Fig. 2.1a). This is the strongest type of nailed connection and it is recommended over the other types. The second type has the nail driven into the end grain (i.e., parallel to the grain) of the holding member (Fig. 2.1b). This is a weaker connection and the allowable lateral load is two-thirds of that obtained for the first type (Breyer, 1980, pp. 366-368).

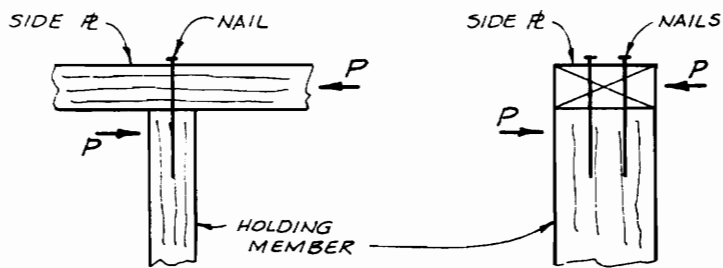
2.2.3 Factors Affecting Strength of Nailed Connections

There are a number of factors that affect the strength of nailed connections. These include (Breyer, 1980, pp. 365-366):

1. Number, size, and type of nail



(a)



(b)

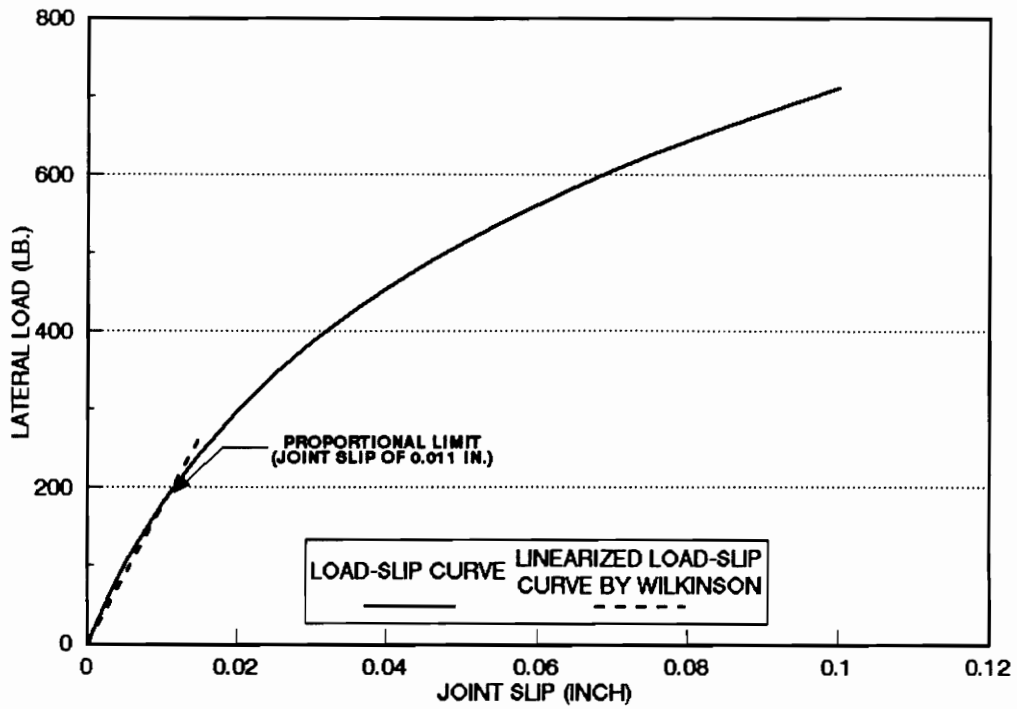
Figure 2.1 Lateral load connections. (a) Side grain nailing; (b) end grain nailing.

2. Species of lumber
3. Type of connection (lateral or withdrawal)
4. Direction of nailing (side grain, end grain or toenail)
5. Moisture content
6. Duration of load
7. Type of side plate
8. Spacing of nails

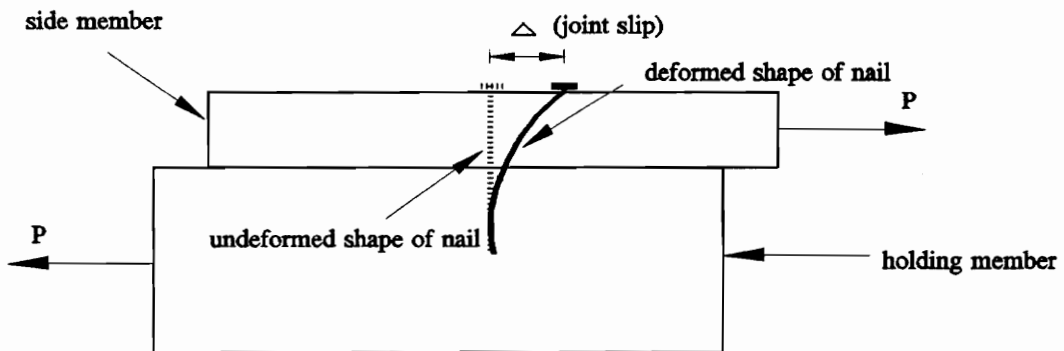
In design, the allowable load values of nailed connections are tabulated in the NDS (1986) for different types of nails (Section 2.2.1) and various lumber species. The values are applicable to the nailed connections under certain conditions. For example, the moisture content of the lumber species should be equal to 19% or less. Otherwise, adjustment to the allowable values is needed. Thus, the capacities of nailed connections are sensitive to the factors mentioned above.

2.3 Load-Slip Relationship of Nailed Connections

When a nailed joint is subjected to a lateral load, the resulting load versus interlayer slip relationship is curvilinear (Fig. 2.2a). While certain researchers have tried to model the load-slip curve (Foschi, 1969; Goodman 1967; Jansson 1955; Mack 1977; McLain 1975; Morris 1967), other investigators have used some linear approximations to the actual curve in order to simplify the relationship. Both theoretical and empirical formulas to describe the load-slip relationship are



(a)



(b)

Fig. 2.2 Load and slip in joint. (a) Load-slip curve; (b) joint slip of nailed joint.

summarized by Mohammad (1990, pp. 12-21) and discussed in detail by Ehlbeck (1979, pp. 52-74) and Smith (1980).

2.3.1 Elastic Theory

One of the theoretical formulas that describes the linear load-slip relationship of nailed connections is an equation derived by Wilkinson (1971). This equation is based on elastic theory, and is used to provide the value for the initial slope of the load-slip curve. The value of a point on the initial slope is used to calculate one of the parameters in an empirical formula in the next section. This formula was derived by McLain (1975) to predict the entire load-slip curve. Therefore, it is important to know how Wilkinson's equation applies to different joint configurations to compute the initial slope of the curve.

Kuenzi (1955) developed a theoretical formula of nailed joints subjected to lateral loads. The nail is assumed to be a beam supported on an elastic foundation in which the pressure under the beam is assumed to be proportional to the beam deflection (Wilkinson, 1971, pp. 1381-1382). Another assumption is that the friction between the members is negligible and thus frictional shear forces are not developed between the members and the nail. The details concerning the formula may be found in Kuenzi (1955).

Wilkinson (1971) simplified the expressions presented by Kuenzi (1955) and

derived the following formula for similar wood members (two wood members are made of the same density materials):

$$P = 0.1667 E^{1/4} k_o^{3/4} d^{7/4} \Delta \quad (2.1)$$

where

P = lateral load (lb)

E = modulus of elasticity of the nail (psi)

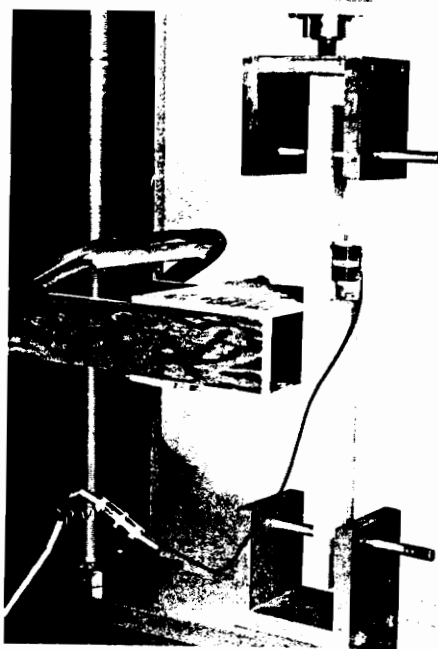
k_o = elastic bearing constant (lb/in.³)

d = nail diameter (in.)

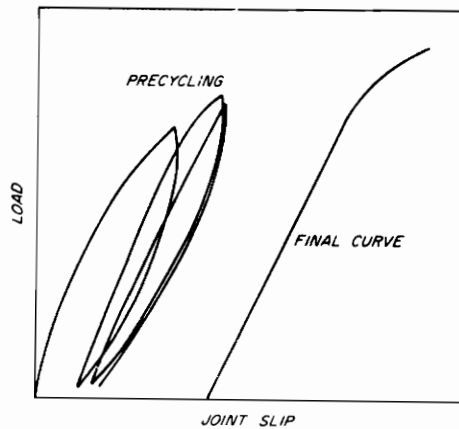
Δ = joint slip (in.)

Joint slip is defined as the deformation in a nailed joint subjected to the lateral load (Fig. 2.2b). Eq. (2.1) is limited to a two-member joint connected with a single round nail with load applied parallel to the grain. This equation is only valid up to the proportional limit slip of 0.011 inch (see Fig. 2.2a) and gives good agreement with experimental results for the initial slope of the load-slip curve (Wilkinson, 1971). The proportional limit slip is defined as an upper limit beyond which the load slip curve is no longer linear. The elastic bearing constant is a species property which describes the behavior of wood acting as an elastic foundation and is found to vary linearly with the specific gravity of wood members having 12 % moisture content.

Numerous experiments were conducted to verify Eq. (2.1). The experimental arrangement for loading the nailed joints is shown in Fig. 2.3a. Joint slip was



(a)



(b)

Fig. 2.3 Method of Testing for nailed joints. (a) Experimental arrangement; (b) cyclic loading.

measured with a microformer, which allowed for continuous recording of the load slip curve. The joints were loaded at a constant rate of 0.1 inch per minute.

Each joint was first subjected to precycling by loading to a low level of slip. The level of slip was then gradually increased until a fairly linear load slip curve was obtained. This is demonstrated by the curves presented in Fig. 2.3b (Wilkinson, 1971, p.1388).

A study was undertaken to determine the effect of different types of nail shanks, prebored lead holes, and grain orientation on the elastic bearing constant. The elastic bearing constant, k_o , was found to be related to average species specific gravity, G (lb/in.³), by the following relations (Wilkinson, 1972a):

a. $k_o = 3,200,000 G$ for smooth shank nails driven in prebored holes (about 90% of the nail diameter) and loaded parallel to the grain. For no prebored holes, $k_o = 2,144,000 G$.

b. $k_o = 2,880,000 G$ for annularly threaded nails driven in prebored holes and loaded parallel to the grain. For no prebored holes, $k_o = 2,240,000 G$.

c. $k_o = 2,496,000 G$ for helically threaded nails driven in prebored holes and loaded parallel to the grain. For no prebored holes, $k_o = 1,920,000 G$.

d. $k_o = 1,280,000 G$ for smooth shank nails driven in prebored holes and loaded perpendicular to the grain. For no prebored holes, $k_o = 1,280,000 G$.

The proportional limit slip was between 0.011 and 0.012 inch for smooth, annularly threaded, and helically threaded shank nails with the load parallel to the grain. This indicates that the form of the nail shank has no effect upon the proportional limit slip. When the loading was perpendicular to the grain, the proportional limit slip for smooth round nail was about 0.018 inch (Wilkinson, 1972a).

Another study was carried out to determine the effects of moisture content on the elastic bearing constant of wood members. There was no effect of moisture content on the elastic bearing constant if drying did not occur after the joints were assembled. However, when the joints were assembled and allowed to dry, the elastic bearing constant was reduced by as much as 45 percent. In addition, the proportional limit slip was unaffected by different moisture content conditions.

Since this section only gives an overview of Wilkinson's expressions, details concerning the other joint configurations not covered in this section may be found in Wilkinson (1971, 1972a, 1972b, 1974a, 1974b).

2.3.2 Generalized Model for Lateral Load-Slip of Nailed Connections

The model that is widely used in the United States to predict the load slip curve of nailed connections is the empirical equation developed by McLain (1975). This

model is of the form:

$$P = A \log_{10} (1 + B\Delta) \quad (2.2)$$

where

P = lateral load (lb)

A, B = empirically-derived constants

Δ = joint slip (in.)

The details concerning the development of this model are presented by McLain (1975).

Although the model has gained popularity in the United States, its value is limited because the model was developed for a specific joint configuration. The joint consisted of a solid-wood holding member and a 3/4 in-thick side member connected with an 8d common wire nail. Friction between the side and the holding members was eliminated by placing a 0.015 in-thick metal shim between the two members when the joint was being constructed. The shim was removed before the joint was tested. The interlayer gap was less than the shim thickness due to the relaxation of the wood members. The objective of this section is to give a summary of how the above model can be extended to a wider range of joint configurations (Pellicane, Stone and Vanderbilt, 1991, p. 61).

Before using Eq. (2.2) to predict the load slip relationship, the parameters A and B should be determined. There are three equations to compute the parameter A , depending on the type of side member used in the joint. The equation suggested

for joints with all types of side members (including solid wood, plywood, particleboard, insulation board, hardboard, and metal) is

$$A = 248.6 - \frac{42.1}{SGS} + 41.36 \text{ SGM} \times \text{SGS}^2 \quad (2.3)$$

where

SGS,SGM = specific gravity (based on volume at 12% moisture
(lb/in.³) content) of the side and holding members,
respectively

For joints with wood and wood-based members only, the following equation is recommended:

$$A = 227.3 - \frac{9.813}{\text{SGS}^2} - \frac{2.221}{\text{SGM}^2} \quad (2.4)$$

For joints with solid wood members only (Pellicane, Stone and Vanderbilt, 1991, pp. 61-62),

$$A = 205.3 + \frac{232.2}{\text{SGS}} - \frac{32.4}{\text{SGS} \times \text{SGM}} \quad (2.5)$$

In order to determine parameter B, Eq. (2.2) is rearranged and parameter B has the form:

$$B = \frac{10^{P/A} - 1}{\Delta} \quad (2.6)$$

Once parameter A is predicted from the most appropriate equation (Eqs. (2.3) -

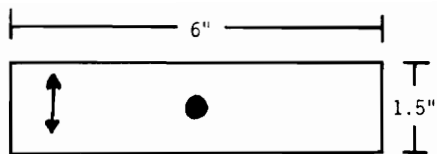
(2.5)), a point on the load-slip curve can be determined by using the procedure developed by Wilkinson (1971, 1972a, 1972b, 1974a, 1974b). The Wilkinson technique enables the prediction of the load associated with a joint slip of 0.015 in. By substituting the value of P corresponding to $\Delta = 0.015$ in., and the value of A, into Eq. 2.6, one obtains a value for B.

The goal of the study conducted experimentally by Pellicane, Stone, and Vanderbilt (1991, pp. 60-77) was to predict parameters A and B in Eq. (2.2) including the effects of nail size, side member thickness, interlayer gap, and specific gravities of the side and the holding members. As a result, Eq. (2.2) can apply to a wide range of joint configurations.

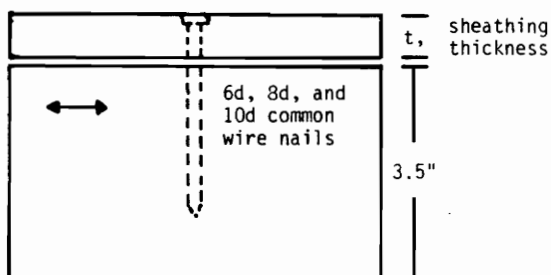
A two member, single-nail test specimen (Fig. 2.4) was used for the testing program. The testing program consisted of four test series. The first three series were used to investigate the interlayer gap, member thickness, and nail diameter effects on nail joints. They were designed to determine the correction factors for A and B. Series 4 was designed to evaluate the applicability of the prediction technique developed in the first three series to the nailed joints constructed with the materials not tested in series 1-3. Several wood and wood-based materials were tested in series 4. The details concerning the testing procedure and the testing program may be found in Pellicane, Stone and Vanderbilt (1991).

The predicted values of the parameters A and B for the first three series are:

$$A_p = A' C_{Ag} C_{At} C_{Ad} \quad (2.7)$$



(a)



(b)

Fig. 2.4 Test Specimen. (a) Plan view; (b) elevation view.

$$B_p = B' C_{Bg} C_{Bt} C_{Bd} \quad (2.8)$$

where

A_p, B_p = predicted values

A', B' = parameters predicted using Eq. (2.3)-(2.5) and the
Wilkinson technique

C_{Ai}, C_{Bi} = correction factors

For the interlayer gap effect on nailed connections, the correction factors are:

$$C_{Ag} = 1.223 \quad (2.9)$$

$$C_{Bg} = 10^{(0.284 - 8.05g)} \quad (2.10)$$

and

g = interlayer gap (in.)

The correction factors for the member thickness effect are expressed as follows:

$$C_{At} = 0.17 + 2.04 t - 1.24 t^2 \quad (2.11)$$

(for side member thickness $t \leq 0.822$ in.)

or

$$C_{At} = 1.02 \quad (\text{for } t > 0.822 \text{ in.}) \quad (2.12)$$

and

$$C_{Bt} = 1.0 \quad (\text{for all thicknesses}) \quad (2.13)$$

For nail diameter effects, the correction factors are given as follows:

$$C_{Ad} = -2.21 + 39.3 d - 113.0 d^2 \quad (2.14)$$

(for nail diameter $d \leq 0.174$ in.)

or

$$C_{Ad} = 1.21 \quad (\text{for } d > 0.174 \text{ in.}) \quad (2.15)$$

and

$$C_{Bd} = 2.83 - 14.6 d \quad (2.16)$$

To determine whether the prediction technique is conservative or not, the average ratios of predicted to experimental loads were computed at several slip values. Each ratio is based on the following expressions:

$$P_p = A_p \log_{10} (1 + B_p \Delta) \quad (2.17)$$

$$P_e = A \log_{10} (1 + B\Delta) \quad (2.18)$$

where

P_p, P_e = predicted and experimental load at joint slip (in.),
respectively

A_p, B_p = predicted value of model parameters

A, B = experimental value of model parameters

Δ = joint slip of interest (in.)

The prediction technique gives somewhat conservative values because inconsistent test results forced a lower bound approach for one of the correction factors for B. It yields reasonable values for low density materials and sheathing materials. However, it has not been verified for 16d and larger nails or for a side-member thickness outside of the 1/2 in. - 3/4 in. range. Further research is recommended to concentrate on this area. Although the prediction technique cannot cover all combinations of nailed joints, it predicts the load slip relationship of nailed

connections over a wide range of joint configurations.

2.4 Present Design Criteria

Wood structures commonly use nails as the primary type of mechanical fastener. In the design of these structures, the lateral load resistance of nails is of primary concern in providing strength and stiffness. The following two subsections present an outline of the allowable lateral load values of nailed joints (Section 2.4.1) and their validity (Section 2.4.2).

2.4.1 Lateral Resistance of Nail Connections

An empirical formula that expresses the test load at a joint slip of 0.015 in. with bright, common wire nails in lateral resistance driven into the side grain (perpendicular to the wood fibers) of seasoned wood is (Wood Handbook, 1987, p. 7-6):

$$P = K/D^{3/2} \tag{2.19}$$

where

- P = lateral load in lb/nail at a joint slip of 0.015 in.
(approximate proportional limit load)
- K = coefficient

D = diameter of nail in inches

The ultimate lateral nail loads for softwoods may approach 3.5 times the loads expressed by Eq. (2.19). The joint slip at maximum load is about 0.3 in. It has been the practice to reduce the value of the lateral load in Eq. (2.19) to account for variability of the wood and duration of load effects. A reduction factor of 1.6 is used to obtain a value for longtime loading, which is the design load applied for a duration of more than ten years (Wood Handbook, 1987, p. 7-7). For normal loading (design load applied for a duration of approximately ten years), the resulting value may be increased by 10 percent. In practice, an additional increase of 10 percent is used as an engineering judgement factor. Therefore, the reduction factor for normal loading is $1.6 / (1.1 \times 1.1) = 1.32$.

The value of the lateral load for normal loading is taken as the lateral load design value of nailed joints in the NDS, and the design values are tabulated in Table 8.8c of the NDS. These values apply only where the depth of penetration of the nails into the holding member is not less than the following requirements (NDS, 1986, p.53):

<u>Species Group</u> (Table 8.1A of NDS)	<u>Depth of Penetration</u>
Group I (specific gravity (lb./in. ³) of wood member greater than 0.61)	10 D
Group II (specific gravity between 0.51 and 0.55)	11 D
Group III (specific gravity between 0.42 and 0.49)	13 D
Group IV (specific gravity between 0.31 and 0.41)	14 D

where

$$D = \text{nail diameter (in.)}$$

When the penetration of the nail is less than that specified above, the design value can be obtained from the straight line interpolation except when the penetration is less than one-third of that specified.

2.4.2 Validity of Lateral Load Design Values

The purpose of this section is to list the conditions under which the design values apply. There are several factors affecting the strength of nailed joints (Section 2.2.3). A designer should be aware of what conditions the nailed joints are under before he/she uses the design values. The design values apply to the following conditions (Wood Handbook, 1987, pp. 7-6 - 7-8; NDS, 1986, pp. 53-55):

- 1). The side member and the holding member have approximately the same density. Otherwise, the member with lighter density controls.
- 2). The thickness of the side member should be about one-half the depth of penetration of the nail in the holding member.
- 3). End distance (distance from the center of a nail to the end of a member), edge distance (distance from the center of a nail to the side of a member) and spacing

of nails should be such as to prevent unusual splitting. According to the Uniform Building Code (1976), the spacing requirement is recommended as follows:

End distance = one half required penetration of nail

Edge distance = one half required penetration of nail

Spacing in row = required penetration of nail

- 4). The load is in a direction parallel to the grain of the members or at right angles to it.
- 5). The wood members have a moisture content of 19 percent or less.
- 6). The depth of penetration of the nail into the holding member is not less than that specified in Table 8.8c of NDS.
- 7). The nails are driven into the side grain of the holding member.
- 8). In order to avoid splitting of the wood, a prebored lead hole of a diameter not exceeding nine-tenths of the nail diameter for Group I species or three-fourths for Group II, III and IV species should be used (Timber Construction Manual, 1985, p. 6-491).
- 9). Normal duration of load

10). A nail in single shear

11). Wood side member is used, and the member is nominal by one inch thick or larger. The distance of the nail along the grain to the end of the side member is 2 inches, and the distance across the grain to the edge is 1 inch (Holye, 1973, p.140).

When more than one nail is used, the total design value is the sum of the design values for individual nails (Timber Construction Manual, 1985).

If the conditions for the design values are not satisfied in a joint under consideration, then adjustments should be made in reference to the NDS (1986) and Wood Handbook (1987).

2.5 Behavior of Timber Joints with Multiple Nails

At present, the allowable load in design on a group of nails is equal to the product of the allowable single nail load and the number of nails in the group. It is based on the assumption that all nails share the applied load on the joint equally and each nail carries a load equivalent to the lateral load capacity of a single nail joint. However, Lantos (1969) found out that the fasteners in a row of a joint (bolted joint) do not transmit the load applied to the joint uniformly. Therefore, the assumption may be somewhat of an overestimation of the overall capacity of the nailed joint (Thomas and Malhotra, 1985, p.973). Nevertheless, it should be

noted that nails are very ductile and distribute the load equally after yielding of the nails.

Although in recent years mathematical models have been developed to describe the load-slip behavior of timber joints with a single nail, there is a lack of information about the behavior of multi-nailed timber joints.

A theoretical model was developed by Thomas and Malhotra (1985) to predict the behavior of laterally-loaded timber joints with multiple nails. The results of the research were used to check the validity of the current design practice for multi-nailed joints. The scope of the research was limited to the joints with two to eight nails. The joints under consideration were laterally loaded single shear joints with common wire nails located along a single row parallel to the grain direction. Modification factors were developed to account for the effect of the number of nails in a row on the stiffness of a joint with multiple nails. The load-slip curves of tested joints and the curves obtained from the theoretical model were compared with each other to verify the model. The theoretical model yielded an upper bound solution for seven different types of joints tested in the research. Details concerning the development of the model and the testing procedures may be found in Thomas and Malhotra (1985, pp. 973-991).

The results of the research indicate that the lateral load carried by each of the multiple nails in a row of a joint is not the same as that carried by a corresponding joint with a single nail. Thus, modification factors, C_N , are developed to account for the effect of the number of nails in a row of a joint on

the overall joint stiffness. For design purposes, it is suggested that the modification factor, C_N , should be taken as 1.0 for joints with up to three nails in a row, and 0.9 for those with more than three nails in a row. The actual capacity of proportional limit slip of a joint with two to eight nails in a row is about 0-10 % less than the present design capacity. At the ultimate slip, the reduction in capacity is within 0-7 %.

Chapter 3

FORMULATION OF BEAM/CONNECTOR ELEMENTS

3.1 Introduction

In the glulam dome in Raleigh, North Carolina (Mohammad, 1990, p.36; Telang, 1992, p.54), beams and decking are connected by nails. Nails are modeled by linear springs in this study. In general, a nail is called a connector.

The simplest way to model a connector in a beam/connector assembly is to place a node at every point along a beam where a spring is attached (Fig.3.1). However, this method results in an assembly with many degrees of freedom in addition to those required at the nodes of the beam assembly. For a large structure, such as the glulam dome, this approach is not feasible because a computer may not have enough memory to analyze the structure.

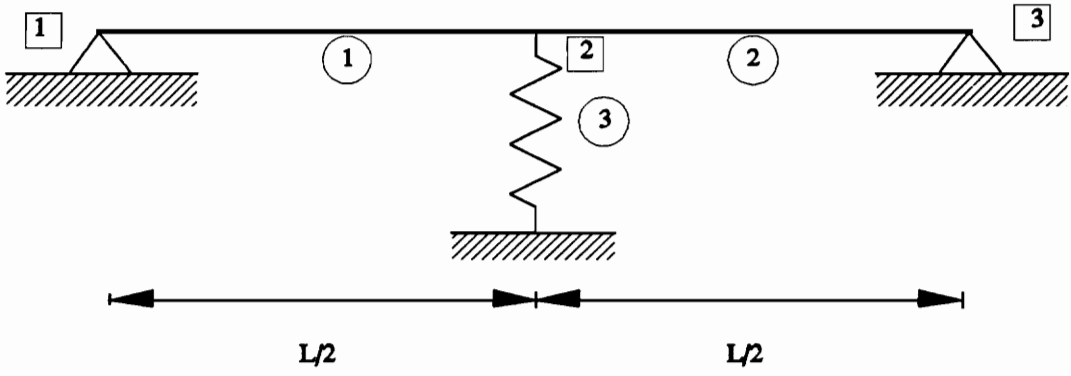


Figure 3.1 Beam/connector assembly.

Nevertheless, the beam/connector element can be used to solve this problem. The connector is transformed into an element that shares the same nodes with the beam instead of placing a node on the beam. This method was used by Dolan (1989, pp. 52-71). As a result, the beam/connector element has the same number of degrees of freedom as the beam itself, no matter how many connectors are attached. Thus, this approach is feasible for analyzing a large structure because it saves a significant amount of computer memory and computer time.

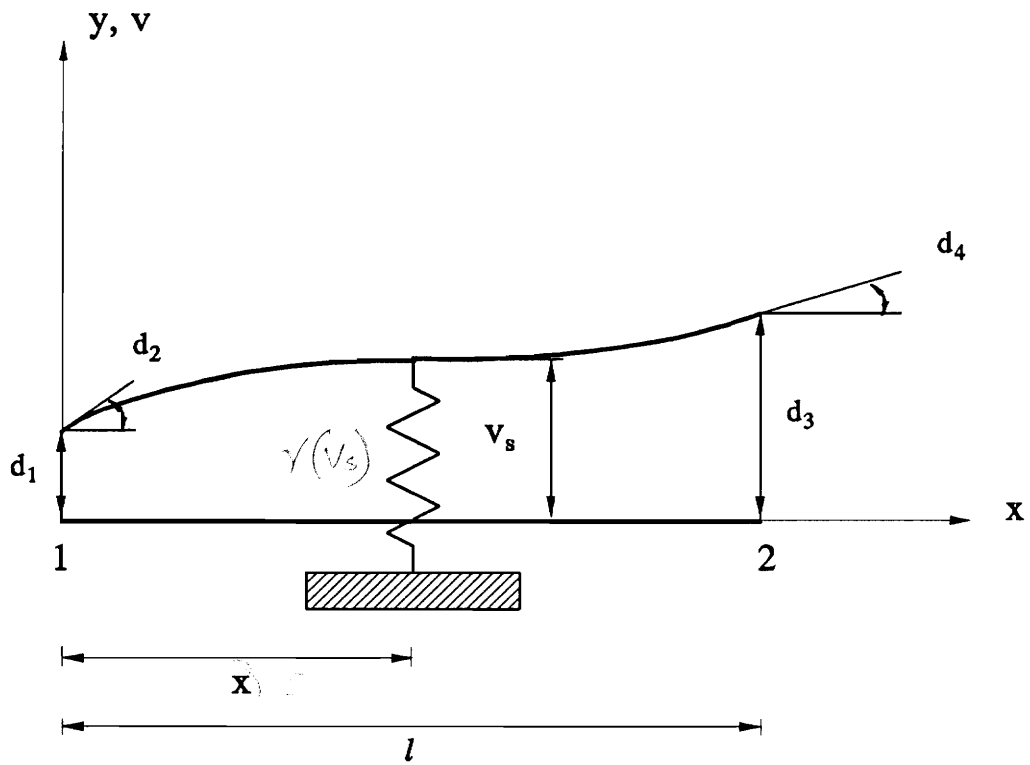
The 2-D and 3-D connector stiffness matrices are formulated in Section 3.2 and Section 3.3 (Holzer, 1991; Dolan, 1989), respectively.

3.2 Formulation of 2-D Connector Stiffness Matrix

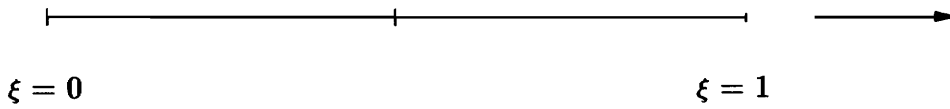
A plane beam with a connector attached is shown in Fig. 3.2a. The beam element has four degrees of freedom, $d_1 - d_4$, and its parent element is shown in Fig. 3.2b. The connector element is modeled as a linear spring with the constant stiffness γ and the displacement v_s (Fig. 3.2a). The spring energy U_s is given as follows:

$$U_s = \frac{1}{2} \gamma v_s^2 = \frac{1}{2} v_s^T \gamma v_s \quad (3.1)$$

The spring deflection can be obtained from the beam interpolation functions as follows (Holzer, 1985, p.8):



(a)



(b)

Figure 3.2 Beam with discrete connector. (a) Beam/connector assembly;
 (b) parent element.

$$v_s(\xi) = N_1(\xi) d_1 + N_2(\xi) d_2 + N_3(\xi) d_3 + N_4(\xi) d_4 \quad (3.2)$$

where

$$\begin{aligned} N_1 &= 1 - 3\xi^2 + 2\xi^3 \\ N_2 &= (\xi - 2\xi^2 + \xi^3) l \\ N_3 &= 3\xi^2 - 2\xi^3 \\ N_4 &= (-\xi^2 + \xi^3) l \end{aligned} \quad (3.3)$$

and

$$\xi = \frac{x}{l}$$

In matrix form

$$v_s(\xi) = N_s d \quad (3.4)$$

where

$$N_s = [N_1 \quad N_2 \quad N_3 \quad N_4]$$

$$d = \begin{bmatrix} d_1 \\ d_2 \\ d_3 \\ d_4 \end{bmatrix}$$

By substituting Eq. (3.4) into Eq. (3.1), U_s becomes

$$U_s = \frac{1}{2} d^T N_s^T \gamma N_s d = \frac{1}{2} d^T k_s d \quad (3.5)$$

where the connector stiffness matrix

$$k_s = N_s^T \gamma N_s$$

or

$$k_s = \begin{bmatrix} g_1 & g_2 & g_4 & g_7 \\ & g_3 & g_5 & g_8 \\ & & g_6 & g_9 \\ \text{sym.} & & & g_{10} \end{bmatrix} \quad (3.6)$$

where

$$\begin{aligned} g_1 &= \gamma N_1 N_1 \\ g_2 &= \gamma N_1 N_2 \\ g_3 &= \gamma N_2 N_2 \\ g_4 &= \gamma N_1 N_3 \\ g_5 &= \gamma N_2 N_3 \\ g_6 &= \gamma N_3 N_3 \\ g_7 &= \gamma N_1 N_4 \\ g_8 &= \gamma N_2 N_4 \\ g_9 &= \gamma N_3 N_4 \\ g_{10} &= \gamma N_4 N_4 \end{aligned} \quad (3.7)$$

and N_i 's are defined in Eq. (3.3).

The interpolation functions in Eq. (3.3) are used instead of the standard ones ($-1 < \xi < 1$) because it is more convenient to compute the connector stiffness matrix according to the location of the spring on the beam relative to one end ($\xi = \frac{x}{l}$),

especially in the case of a large number of springs.

To test the connector stiffness matrix in Eq. (3.6), suppose a connector is attached to the mid-span of a beam. In this case, $\xi = 0.5$ and the connector stiffness matrix becomes

$$k_s = \gamma \begin{bmatrix} 1/4 & l/16 & 1/4 & -l/16 \\ & l^2/64 & l/16 & -l^2/64 \\ & & 1/4 & -l/16 \\ \text{sym.} & & & l^2/64 \end{bmatrix} \quad (3.8)$$

The connector stiffness matrix above is the same as that in the notes of CE 5414 (Holzer, 1991), and the concept used to derive this matrix may be found in Dolan (1989, pp. 52-71).

For the whole system, which is composed of the beam and the spring, the total energy U is presented as:

$$U = U_b + U_s = \frac{1}{2} d^T k_b d + \frac{1}{2} d^T k_s d \quad (3.9)$$

where

U_b = internal energy of the beam

k_b = plane beam stiffness matrix

U can also be written as:

$$U = \frac{1}{2} d^T [k_b + k_s] d = \frac{1}{2} d^T k d \quad (3.10)$$

where

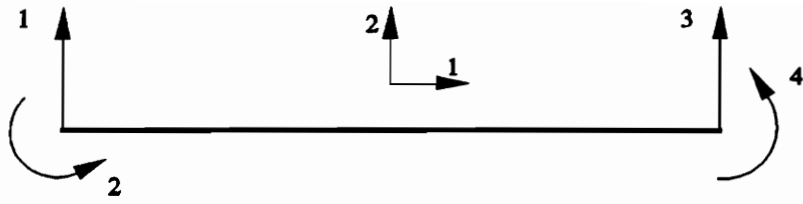
$$k = k_b + k_s$$

and k is called the beam/connector stiffness matrix.

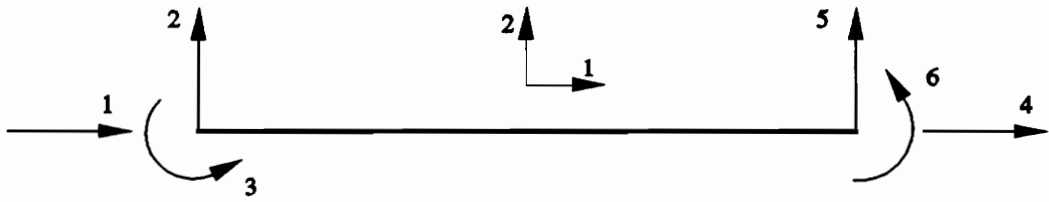
Therefore, after the beam/connector stiffness matrix is obtained, the system stiffness matrix can be constructed using the member code matrix (Holzer, 1985). Since the connector and the beam stiffness matrices share the same degrees of freedom, the size of the system stiffness matrix does not depend on the number of connectors attached to the beam.

The connector stiffness matrix for a plane frame element can be generated by following the idea discussed at the beginning of this section. However, since the connector has no resistance to the axial deformation of the beam, the connector stiffness matrix for a beam element can be extended to that of a frame element by using the member code method (Holzer, 1985). According to Fig. 3.3, the member code matrix is obtained as follows:

$$M = \begin{bmatrix} 2 \\ 3 \\ 5 \\ 6 \end{bmatrix} \quad (3.11)$$



(a)



(b)

Figure 3.3 Degrees of freedom. (a) Plane beam; (b) plane frame.

The member code is then assigned to k_s in Eq. (3.6):

$$\begin{array}{cccc}
 & 2 & 3 & 5 & 6 \\
 k_s = & \left[\begin{array}{cccc}
 g_1 & g_2 & g_4 & g_7 \\
 & g_3 & g_5 & g_8 \\
 & & g_6 & g_9 \\
 \text{sym.} & & & g_{10}
 \end{array} \right] & \begin{array}{l} 2 \\ 3 \\ 5 \\ 6 \end{array}
 \end{array} \quad (3.12)$$

The k_s for plane frame is obtained as below:

$$\begin{array}{cccc}
 k_s = & \left[\begin{array}{cccccc}
 0 & 0 & 0 & 0 & 0 & 0 \\
 & g_1 & g_2 & 0 & g_4 & g_7 \\
 & & g_3 & 0 & g_5 & g_8 \\
 & & & 0 & 0 & 0 \\
 & & & & g_6 & g_9 \\
 \text{sym.} & & & & & g_{10}
 \end{array} \right] & (3.13)
 \end{array}$$

where the g_i 's are defined in Eq. (3.7).

The stiffness matrix for a plane frame element is (Holzer, 1985, p.125)

$$k_b = \alpha \begin{bmatrix} \beta & 0 & 0 & -\beta & 0 & 0 \\ & 12 & 6l & 0 & -12 & 6l \\ & & 4l^2 & 0 & -6l & 2l^2 \\ & & & \beta & 0 & 0 \\ & & & & 12 & -6l \\ \text{sym.} & & & & & 4l^2 \end{bmatrix} \quad (3.14)$$

where

$$\alpha = EI / l^3, \quad \beta = Al^2 / I, \quad \gamma = \alpha\beta = EA / l$$

E = modulus of elasticity of plane frame element

I = moment of inertia

l = length of plane frame element

A = cross sectional area of plane frame element

3.3 Formulation of 3-D Connector Stiffness Matrix

The two dimensional connector stiffness matrix for a plane beam is formulated in Eq. (3.6). As the beam/connector element is used three dimensionally in dome analysis, the formulation of a three dimensional connector stiffness matrix is necessary.

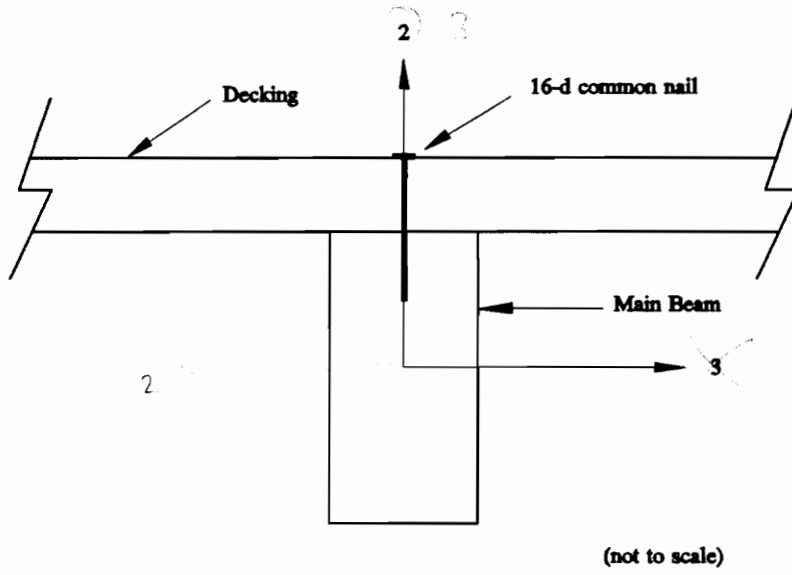
In the dome, the beams and purlins are connected to a 2" tongue-and-groove

decking, which has a stabilizing effect on the lateral buckling of the beams. According to Mohammad (1990, pp. 73-74), the decking reduces the nodal deflections and the maximum member stresses of the beams. A typical beam and decking assembly, and a local space frame element, are shown in Fig. 3.4a and 3.4b, respectively (Holzer, 1985, p.263).

A beam/connector model is shown in Fig. 3.5. The model consists of a beam, a rigid link and a linear spring. The spring is placed horizontally to model the nail because the nail resists and deforms laterally when the beam is subjected to torsion about the 1-axis and bending about the 2-axis. In this study, since the nail is assumed to have lateral resistance only to the beam, one spring is enough to model the nailed joint. Another assumption in this study is that the decking is stiffer than the nail and it does not move so that it is modeled by a fixed end support. The rigid link with length h is used as a connection for the spring to attach to the top of the beam because it is unrealistic to attach the spring to the centroid of the beam (Zahn, 1972; Mohammad, 1990, p.48).

We model the lateral restraint offered by the decking via the nails because it is vital to the integral action of the dome. However, we neglect the effect of the decking on the bending of the beams (i.e. T-beam action). Therefore, the axial degrees of freedom of the beam are neglected in the beam/connector model (Fig. 3.5).

Although glulam beams and nails are orthotropic in nature, the assumption of transverse isotropy (isotropic in the plane of beam cross section) greatly simplifies



(a)

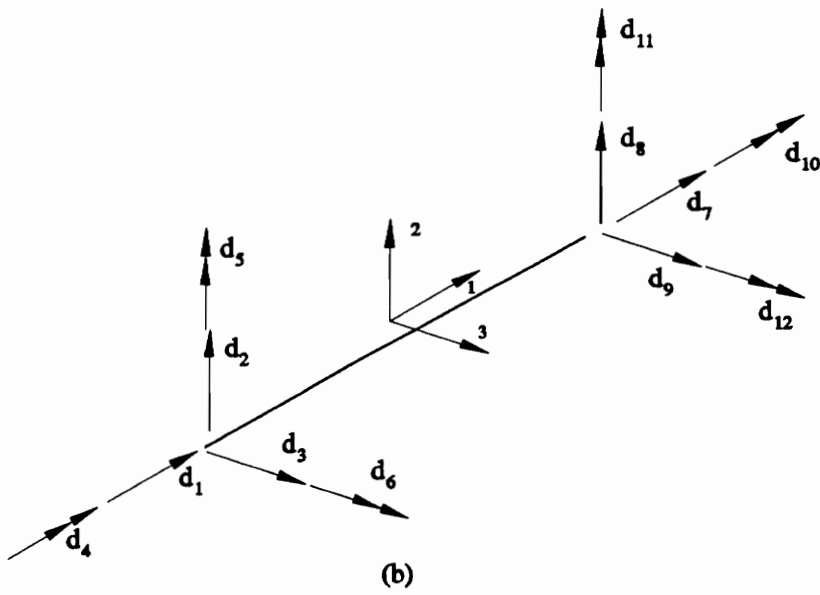


Fig. 3.4 Beam and decking assembly. (a) Beam cross section;
(b) space beam element.

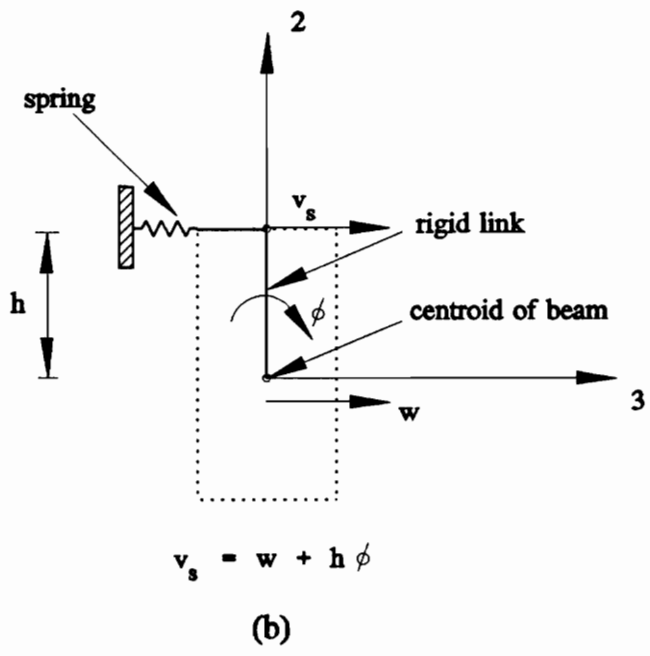
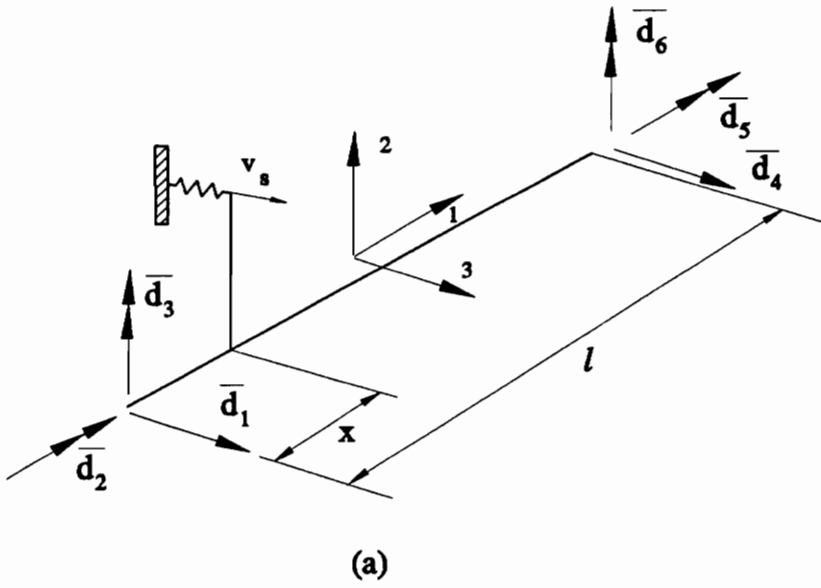


Fig. 3.5 Beam and decking model. (a) Beam/connector model; (b) beam cross section.

the modeling of glulam beams. It is because to model a glulam beam as orthotropic will require tensor transformation of axes for each layer of the beam cross section. Though it is theoretically possible to model the growth rings of the cross section of individual beams, it is not practical in the analysis of structural systems consisting of a large number of members. To efficiently analyze skeletal glulam systems, the beams can be modeled as isotropic in the plane of the cross section based on the experimental tests conducted by Davalos (1989, pp. 29-49) on wood and glulam samples. According to Davalos (1989, p.56), the material of glulam beams are assumed to be continuous, homogeneous, and transversely isotropic. The longitudinal elastic modulus E is taken as 1.8×10^6 psi, and the shear modulus, G , obtained from torsion tests of small glulam samples, is taken as 1.6×10^5 psi (Davalos, 1989, p. 154). In this study, the material properties of the glulam beams for linear material law (nonlinear material law has different E value) are the same as those used by Davalos (1989).

By using the idea discussed in Section 3.2, the spring deflection has the form (Fig. 3.5):

$$v_s(\xi) = w(\xi) + h\phi(\xi) \quad (3.15)$$

where

$w(\xi)$ = deflection of beam subjected to bending about 2-axis

$\phi(\xi)$ = rotation of beam subjected to torsion about 1-axis

h = length of rigid link

and

$$\xi = \frac{x}{l}$$

Since the deflection and rotation of the beam are independent of each other, they are expressed in terms of different interpolation functions shown as follows (Holzer, 1985, pp. 6-8):

$$\phi(\xi) = [N_1^1 \quad N_2^1] \begin{bmatrix} \bar{d}_2 \\ \bar{d}_5 \end{bmatrix} \quad (3.16)$$

where

$$\begin{aligned} N_1^1 &= 1 - \xi \\ N_2^1 &= \xi \end{aligned} \quad (3.17)$$

and

$$w(\xi) = [N_1^2 \quad N_2^2 \quad N_3^2 \quad N_4^2] \begin{bmatrix} \bar{d}_1 \\ \bar{d}_3 \\ \bar{d}_4 \\ \bar{d}_6 \end{bmatrix} \quad (3.18)$$

where

$$\begin{aligned} N_1^2 &= N_1 = 1 - 3\xi^2 + 2\xi^3 \\ N_2^2 &= -N_2 = -(\xi - 2\xi^2 + \xi^3) l \\ N_3^2 &= N_3 = 3\xi^2 - 2\xi^3 \\ N_4^2 &= -N_4 = (\xi^2 - \xi^3) l \end{aligned} \quad (3.19)$$

The interpolation functions, N_i , are defined in Eq. (3.3).

To verify the functions defined in Eq. (3.19), two models are used in Fig. 3.6. The

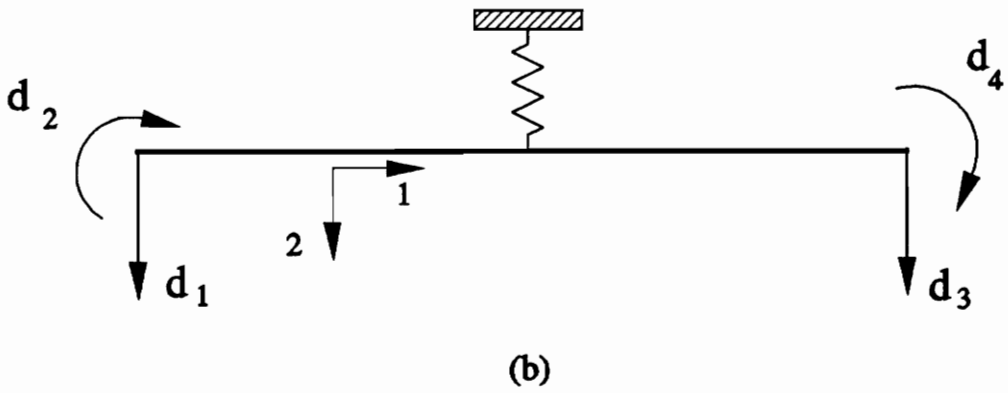
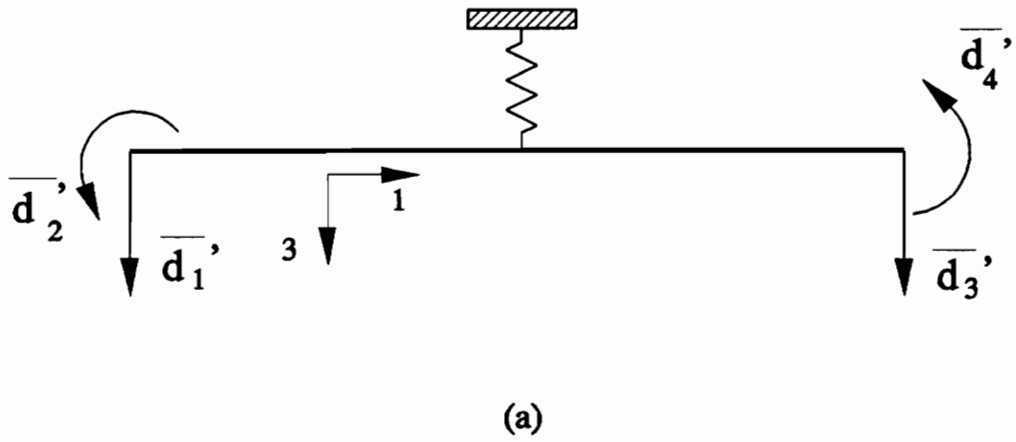


Fig. 3.6 Deformations of beam/connector element.
 (a) Bending about 2 axis; (b) bending about 3 axis.

first model is obtained by letting $h=0$ in Fig. 3.5 and has the interpolation functions N_i^2 (Eq. (3.19)). The second model is the model used in Section 3.2 and has the interpolation functions N_i in Eq. (3.3). The relationship between the displacements of the models is (see Fig. 3.6)

$$d_1 = \bar{d}_1', \quad d_2 = -\bar{d}_2', \quad d_3 = \bar{d}_3', \quad d_4 = -\bar{d}_4' \quad (3.20)$$

The displacement function of the second model has the form (Section 3.2)

$$w(\xi) = N_1(\xi) d_1 + N_2(\xi) d_2 + N_3(\xi) d_3 + N_4(\xi) d_4 \quad (3.21)$$

The substitution of Eq. (3.20) into Eq. (3.21) yields

$$w(\xi) = N_1(\xi) \bar{d}_1' + (-N_2(\xi)) \bar{d}_2' + N_3(\xi) \bar{d}_3' + (-N_4(\xi)) \bar{d}_4' \quad (3.22)$$

or

$$w(\xi) = N_1^2(\xi) \bar{d}_1' + N_2^2(\xi) \bar{d}_2' + N_3^2(\xi) \bar{d}_3' + N_4^2(\xi) \bar{d}_4' \quad (3.23)$$

where

$$N_1^2 = N_1, \quad N_2^2 = -N_2, \quad N_3^2 = N_3, \quad N_4^2 = -N_4 \quad (3.24)$$

Since Eq. (3.19) is identical to Eq. (3.24), the relationship between the functions N_i^2 and N_i is verified.

By substituting Eqs. (3.16) and (3.18) into Eq. (3.15), one obtains the spring deflection

$$v_s(\xi) = \begin{bmatrix} N_1^2 & hN_1^1 & N_2^2 & N_3^2 & hN_2^1 & N_4^2 \end{bmatrix} \begin{bmatrix} \bar{d}_1 \\ \bar{d}_2 \\ \bar{d}_3 \\ \bar{d}_4 \\ \bar{d}_5 \\ \bar{d}_6 \end{bmatrix} \quad (3.25)$$

or

$$v_s(\xi) = N \bar{d} \quad (3.26)$$

where

$$N = \begin{bmatrix} N_1^2 & hN_1^1 & N_2^2 & N_3^2 & hN_2^1 & N_4^2 \end{bmatrix}$$

$$\bar{d} = \begin{bmatrix} \bar{d}_1 \\ \bar{d}_2 \\ \bar{d}_3 \\ \bar{d}_4 \\ \bar{d}_5 \\ \bar{d}_6 \end{bmatrix}$$

The substitution of Eq. (3.26) into Eq(3.1) yields the spring energy

$$U_s = \frac{1}{2} \bar{d}^T N^T \gamma_s N \bar{d} \quad (3.27)$$

or

$$U_s = \frac{1}{2} \bar{d}^T k_s \bar{d} \quad (3.28)$$

where

$$\mathbf{k}_s = \mathbf{N}^T \gamma_s \mathbf{N} \quad (3.29)$$

After being expanded, the connector stiffness matrix \mathbf{k}_s can be expressed as

$$\mathbf{k}_s = \begin{bmatrix} g_1 & g_2 & g_4 & g_7 & g_{11} & g_{16} \\ & g_3 & g_5 & g_8 & g_{12} & g_{17} \\ & & g_6 & g_9 & g_{13} & g_{18} \\ & & & g_{10} & g_{14} & g_{19} \\ & & & & g_{15} & g_{20} \\ \text{sym.} & & & & & g_{21} \end{bmatrix} \quad (3.30)$$

where the twenty-one distinct coefficients are defined as

$$\begin{aligned} g_1 &= \gamma N_1^2 N_1^2 = \gamma (1 - 3\xi^2 + 2\xi^3)^2 \\ g_2 &= \gamma h N_1^2 N_1^1 = \gamma h (1 - 3\xi^2 + 2\xi^3)(1 - \xi) \\ g_3 &= \gamma h^2 N_1^1 N_1^1 = \gamma h^2 (1 - \xi)^2 \\ g_4 &= \gamma N_1^2 N_2^2 = -\gamma l (1 - 3\xi^2 + 2\xi^3)(\xi - 2\xi^2 + \xi^3) \\ g_5 &= \gamma h N_1^1 N_2^2 = -\gamma h l (1 - \xi)(\xi - 2\xi^2 + \xi^3) \\ g_6 &= \gamma N_2^2 N_2^2 = \gamma l^2 (\xi - 2\xi^2 + \xi^3)^2 \\ g_7 &= \gamma N_1^2 N_3^2 = \gamma (1 - 3\xi^2 + 2\xi^3)(3\xi^2 - 2\xi^3) \\ g_8 &= \gamma h N_1^1 N_3^2 = \gamma h (1 - \xi)(3\xi^2 - 2\xi^3) \\ g_9 &= \gamma N_2^2 N_3^2 = -\gamma l (\xi - 2\xi^2 + \xi^3)(3\xi^2 - 2\xi^3) \\ g_{10} &= \gamma N_3^2 N_3^2 = \gamma (3\xi^2 - 2\xi^3)^2 \\ g_{11} &= \gamma h N_1^2 N_2^1 = \gamma h (1 - 3\xi^2 + 2\xi^3)\xi \\ g_{12} &= \gamma h^2 N_1^1 N_2^1 = \gamma h^2 (1 - \xi)\xi \end{aligned} \quad (3.31)$$

$$\begin{aligned}
g_{13} &= \gamma h N_2^2 N_2^1 = -\gamma h l (\xi - 2\xi^2 + \xi^3)\xi \\
g_{14} &= \gamma h N_3^2 N_2^1 = \gamma h (3\xi^2 - 2\xi^3)\xi \\
g_{15} &= \gamma h^2 N_2^1 N_2^1 = \gamma h^2 \xi^2 \\
g_{16} &= \gamma N_1^2 N_4^2 = \gamma l (1 - 3\xi^2 + 2\xi^3)(\xi^2 - \xi^3) \\
g_{17} &= \gamma h N_1^1 N_4^2 = \gamma h l (1 - \xi)(\xi^2 - \xi^3) \\
g_{18} &= \gamma N_2^2 N_4^2 = -\gamma l^2 (\xi - 2\xi^2 + \xi^3)(\xi^2 - \xi^3) \\
g_{19} &= \gamma N_3^2 N_4^2 = \gamma l (3\xi^2 - 2\xi^3)(\xi^2 - \xi^3) \\
g_{20} &= \gamma h N_2^1 N_4^2 = \gamma h l (\xi^2 - \xi^3)\xi \\
g_{21} &= \gamma N_4^2 N_4^2 = \gamma l^2 (\xi^2 - \xi^3)^2
\end{aligned}$$

The interpolation functions N_i^1 and N_i^2 are defined in Eq. (3.17) and (3.19), respectively.

In order to extend the connector stiffness matrix (6 x 6) to a 12 x 12 matrix which is compatible with the space frame element matrix, the member code matrix is used and obtained by comparing Fig. 3.5a with Fig. 3.4b (Holzer, 1985, p. 265):

$$M = \begin{bmatrix} 3 \\ 4 \\ 5 \\ 9 \\ 10 \\ 11 \end{bmatrix} \quad (3.32)$$

The member code matrix is then assigned to the matrix in Eq. (3.30) and the 3-D connector stiffness matrix is obtained as

$$\mathbf{k}_s = \begin{bmatrix}
0 & 0 & 0 & 0 & 0 & 0 & 0 & 0 & 0 & 0 & 0 & 0 & 0 \\
& 0 & 0 & 0 & 0 & 0 & 0 & 0 & 0 & 0 & 0 & 0 & 0 \\
& & g_1 & g_2 & g_4 & 0 & 0 & 0 & g_7 & g_{11} & g_{16} & 0 & 0 \\
& & & g_3 & g_5 & 0 & 0 & 0 & g_8 & g_{12} & g_{17} & 0 & 0 \\
& & & & g_6 & 0 & 0 & 0 & g_9 & g_{13} & g_{18} & 0 & 0 \\
& & & & & 0 & 0 & 0 & 0 & 0 & 0 & 0 & 0 \\
& & & & & & 0 & 0 & 0 & 0 & 0 & 0 & 0 \\
& & & & & & & 0 & 0 & 0 & 0 & 0 & 0 \\
& & & & & & & & g_{10} & g_{14} & g_{19} & 0 & 0 \\
& & & & & & & & & g_{15} & g_{20} & 0 & 0 \\
& & & & & & & & & & g_{21} & 0 & 0 \\
\text{sym.} & & & & & & & & & & & & 0
\end{bmatrix} \quad (3.33)$$

where the g_i 's are defined in Eq. (3.31).

By using the same concept as in Section 3.2, the 3-D beam/connector stiffness matrix can be expressed as

$$\mathbf{k} = \mathbf{k}_b + \mathbf{k}_s \quad (3.34)$$

where

\mathbf{k}_b = space frame stiffness matrix

\mathbf{k}_s = 3-D connector stiffness matrix

In the case of multiple springs on the beam, the total energy of the whole system is (see Eq. (3.9))

$$U = U_b + \sum_{i=1}^n U_{s_i}$$

$$U = \frac{1}{2} \bar{d}^T (k_b + \sum_{i=1}^n k_{s,i}) \bar{d} \quad (3.35)$$

where

$$\begin{aligned} U_b &= \text{internal energy of beam} \\ U_{s,i} &= \text{spring energy of } i^{th} \text{ spring} \\ k_{s,i} &= \text{connector stiffness matrix of } i^{th} \text{ spring} \\ n &= \text{total number of springs} \end{aligned}$$

Thus the beam/connector stiffness matrix for multiple springs is

$$k = k_b + \sum_{i=1}^n k_{s,i} \quad (3.36)$$

3.4 Testing of 3-D Connector Stiffness Matrix for a Special Case

The 3-D connector stiffness matrix needs to be tested to make sure it is correct for the dome analysis. A simple way to check the matrix in Eq.(3.30) is to set $h=0$ and finally compare the matrix with Eq. (3.8) (Holzer, 1991; Dolan, 1989). The details will be discussed in the following paragraphs.

On the basis of Fig. 3.5, if $h=0$ and $x=\frac{l}{2}$ ($\xi=0.5$), the spring is attached to the

centroid of the beam and the spring deflection is expressed as (see Fig. 3.6a)

$$v_s(\xi) = [N_1^2 \quad N_2^2 \quad N_3^2 \quad N_4^2] \begin{bmatrix} \bar{d}_1' \\ \bar{d}_2' \\ \bar{d}_3' \\ \bar{d}_4' \end{bmatrix} \quad (3.37)$$

or

$$v_s(\xi) = N \bar{d}' \quad (3.38)$$

where

$$N = [N_1^2 \quad N_2^2 \quad N_3^2 \quad N_4^2] \quad (3.39)$$

$$\bar{d}' = \begin{bmatrix} \bar{d}_1' \\ \bar{d}_2' \\ \bar{d}_3' \\ \bar{d}_4' \end{bmatrix}$$

The substitution of Eq. (3.39) into Eq. (3.29) yields

$$k_s = \gamma \begin{bmatrix} 1/4 & -l/16 & 1/4 & l/16 \\ & l^2/64 & -l/16 & -l^2/64 \\ & & 1/4 & l/16 \\ \text{sym.} & & & l^2/64 \end{bmatrix} \quad (3.40)$$

The connector stiffness matrix in Eq. (3.40) applies to the model shown in Fig. 3.6a. The other model shown in Fig. 3.6b is obtained by rotating the model in Fig. 3.6a about the 1-axis through 180° . On the basis of Fig. 3.6, the displacements of the two models have the following relation (in matrix form):

$$\begin{bmatrix} \bar{d}_1' \\ \bar{d}_2' \\ \bar{d}_3' \\ \bar{d}_4' \end{bmatrix} = \begin{bmatrix} 1 & 0 & 0 & 0 \\ & -1 & 0 & 0 \\ & & 1 & 0 \\ \text{sym.} & & & -1 \end{bmatrix} \begin{bmatrix} d_1 \\ d_2 \\ d_3 \\ d_4 \end{bmatrix} \quad (3.41)$$

or

$$\bar{\mathbf{d}}' = \mathbf{T} \mathbf{d} \quad (3.42)$$

where

$$\mathbf{T} = \begin{bmatrix} 1 & 0 & 0 & 0 \\ & -1 & 0 & 0 \\ & & 1 & 0 \\ \text{sym.} & & & -1 \end{bmatrix} \quad (3.43)$$

The spring energy of the model in Fig. 3.6a is

$$U_s = \frac{1}{2} \bar{\mathbf{d}}'^T \mathbf{k}_s \bar{\mathbf{d}}' \quad (3.44)$$

By substituting Eq. (3.42) into Eq. (3.44), the spring energy becomes

$$U_s = \frac{1}{2} \mathbf{d}^T \mathbf{T}^T \mathbf{k}_s \mathbf{T} \mathbf{d} \quad (3.45)$$

or

$$U_s = \frac{1}{2} d^T \bar{k}_s d \quad (3.46)$$

where

$$\bar{k}_s = T^T k_s T \quad (3.47)$$

It is noted that Eq. (3.46) also represents the spring energy for the model in Fig. 3.6b with the connector stiffness matrix \bar{k}_s . After being expanded, the matrix \bar{k}_s can be expressed as

$$\bar{k}_s = \gamma \begin{bmatrix} 1/4 & l/16 & 1/4 & -l/16 \\ & l^2/64 & l/16 & -l^2/64 \\ & & 1/4 & -l/16 \\ \text{sym.} & & & l^2/64 \end{bmatrix} \quad (3.48)$$

The matrix \bar{k}_s is the same as the connector stiffness matrix in Eq. (3.8) (Holzer, 1991), and the concept used to derive the matrix may be found in Dolan (1989, pp. 52-71).

Chapter 4

TESTING OF BEAM/CONNECTOR ELEMENTS

4.1 Introduction

The 2-D and 3-D connector stiffness matrices are formulated in Chapter 3. The stiffness matrix of a beam/connector element is simply a superposition of the beam and connector stiffness matrices. Some simple testing programs are carried out to study the response of the element before the element is used in the dome cap analysis (Chapter 6). The purpose of this chapter is to present the results of the testing programs for the 2-D (Section 4.2) and 3-D beam/connector elements (Section 4.3).

4.2 Testing of 2-D Beam/Connector Element

The objectives of this section are to present the results from some simple test runs for the 2-D beam/connector element, and to study the element response. This section is divided into three subheadings of test models and procedures (Section 4.2.1), creation of input file for the 2-D beam/connector element (Section 4.2.2), and comparison and discussion of test results (Section 4.2.3).

4.2.1 Test Models and Procedures

A beam/connector assembly is used for testing and is shown in Fig. 4.1. The geometric and material properties of the beam selected are the same as those of the main beams in the dome cap. In order to study the effects of number of connectors and connector stiffness on the element, the configuration of the assembly (Fig. 4.1) is subjected to change. There are two variables on the assembly:

1. Number of connectors n
2. Connector stiffness γ

The test program outlined in Table 4.1 consists of six test problems. The first problem is designed to study the effect of the number of beam elements. Test

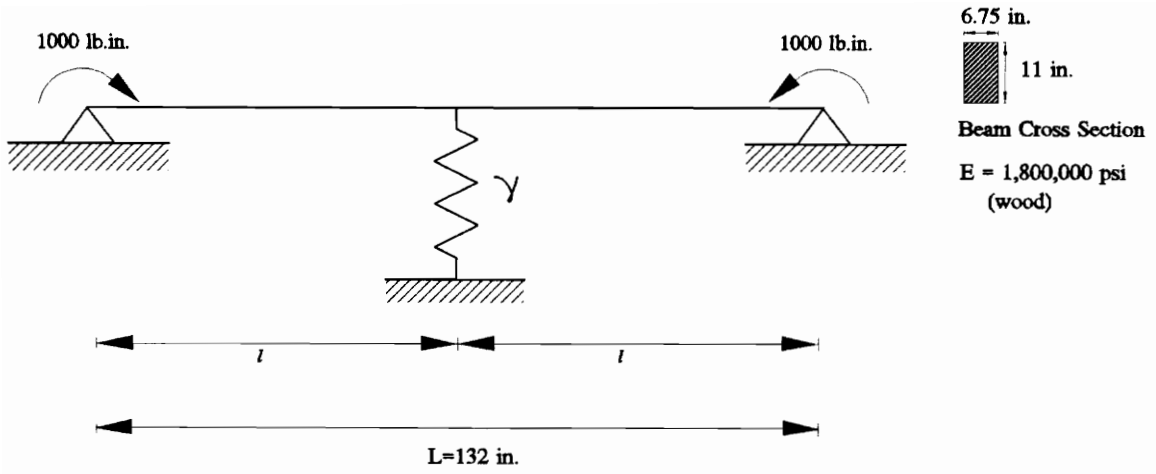


Fig. 4.1 Beam/connector assembly ($n=1$).

Table 4.1 Test program and results for 2-D beam/connector elements (linear analysis).

Test Problem	Beam/ Connector		Assembly	Model 1		Model 2		Max. % difference in reactions of models 1 & 2	% difference in end rotations of models 1 & 2
	No. of Connectors n	Spacing of Connectors $l = L/(n+1)$		Connector Stiffness γ	No. of B23	No. of User Elements	No. of B23		
1	0	-	-	1	0	2	0	0	0
2	1	66	14400	1	1	2	1	9.27	3.15
3	3	33	14400	1	3	4	3	14.16	7.24
4	15	8.25	14400	1	15	16	15	33.9	32.39
5	15	8.25	7200	1	15	16	15	21.96	16.83
6	15	8.25	1000	1	15	16	15	5.24	0.91

* Reaction values for each test problem are shown in Fig. 4.2 through Fig. 4.7.

problem 2, 3, and 4 are designed to study the effect of the number of connectors on the response of the beam/connector element. In order to model a real case, 15 connectors are attached to the beam in test problem 4 because the spacing of nailed joints (connectors) on the beam elements (132 inches long) in the dome cap is assumed to be 8 - 9 inches. Another assumption made is that each connector models a nailed joint which is composed of two nails. In other words, the connector stiffness should be equal to two times the value of lateral stiffness of a single nail. According to NDS (1986), the lateral stiffness of a 16-d nail (type of nail used in dome) is $108/0.015 = 7200$ lb/in. Therefore, the value of the connector stiffness is taken as $2 \times 7200 = 14400$ lb/in. for test problems 2, 3, and 4. Test problems 4, 5, and 6 are used to study the connector stiffness effects.

In test problem 1, the connector stiffness of the spring is taken as zero and the beam (Fig. 4.1) is modeled by a plane frame element, B23, in ABAQUS in model 1, while in model 2, the beam is modeled by two B23 elements. Each of the other test problems consists of two models. Model 1 simulates the beam/connector assembly in Fig. 4.1 by using a beam/connector element. The element is composed of a beam element and connector elements. The plane frame element in ABAQUS, B23, is used to model the beam, and each connector element is modeled by a user element which has the connector stiffness matrix shown in Eq. (3.13). The details concerning the creation of the input file for model 1 will be discussed in Section 4.2.2. For model 2, the B23 elements are used to model the beam, and the Spring2 elements, which are linear spring elements in ABAQUS, are used to model the connectors. It is important to note that in model 2, a node is placed at every point along the beam where a connector is attached. Therefore,

the beam is modeled by $n+1$ B23 elements where n represents the number of connectors in the assembly. This model serves as a check for model 1.

A linear analysis in ABAQUS is conducted for each model in the testing program. The test results of model 1 are compared with that of model 2 in each test problem and a discussion of the results is given (Section 4.2.3).

4.2.2 Creation of Input File for 2-D Beam/Connector Element in ABAQUS

The beam stiffness matrix k_b can be generated from the element library in ABAQUS. The connector element, however, is not provided by the element library. Nevertheless, ABAQUS provides a powerful option called USER ELEMENT, which introduces a user-defined element type. Since the behavior of the connector is assumed to be purely linear in this study, k_s is simply input by using the suboption MATRIX (ABAQUS 4.8, User's Manual p. 6.5.20-1).

Model 1 in the test problem 1 (Table 4.1) is used as an example to illustrate how the input file is created. The list of commands to describe the geometric and material properties of the beam is as follows:

```
*NODE
```

```
1,0.,0.
```

2,132.,0.

*ELEMENT,TYPE=B23,ELSET=BEAM

1,1,2

*BEAM SECTION,SECTION=RECT,ELSET=BEAM,MATERIAL=WOOD

6.75,11.

*MATERIAL,NAME=WOOD

*ELASTIC

1.8E6

So far only the beam is defined in the input file. If the connector has stiffness of 14400 lb/in. attached to the mid-span of the beam, k_s is obtained from Eq. (3.13) as follows:

$$k_s = \begin{bmatrix} 0 & 0 & 0 & 0 & 0 & 0 \\ & 3600 & 118800 & 0 & 3600 & -118800 \\ & & 3920000 & 0 & 118800 & -3920000 \\ & & & 0 & 0 & 0 \\ & & & & 3600 & -118800 \\ \text{sym.} & & & & & 3920000 \end{bmatrix} \quad (4.1)$$

The connector element is defined as a user element in the input file. It is activated as follows:

```
*USER ELEMENT,NODES=2,TYPE=U1,LINEAR
1,2,6
```

The number of nodes is the same as that of the beam element so 2 is assigned to the parameter NODES. Since the format of the parameter TYPE must be Un where n is a positive integer, U1 is chosen to identify the connector element (ABAQUS 4.8, User's Manual p.6.5.20-1). Parameter LINEAR indicates that the behavior of the element is linear and its stiffness or mass matrix is defined under the suboption *MATRIX. The numbers 1, 2, 6 specify the active degrees of freedom at nodes of the connector element.

The following statements define the connector stiffness matrix of Eq. (4.1):

```
*MATRIX,TYPE=STIFFNESS
0.
0.,3600.
0.,118800.,3920000.
0.,0.,0.,0.
0.,3600.,118800.,0.
3600.
0.,-118800.,-3920000,0.
-118800.,3920000.
```

The first line, the keyword line, indicates that a stiffness matrix is being defined.

The following lines represent the entries in the connector stiffness matrix. Since the matrix is symmetric, the entries from the top of each column to the main diagonal are entered. The entries should be input in the following fashion (ABAQUS 4.8 User's Manual p. 6.5.20-4):

```
A11  
A12,A22  
A13,A23,A33  
A14,A24,A34,A44  
A15,A25,A35,A45  
A55  
A16,A26,A36,A46  
A56,A66
```

where

A_{ij} = the entry in the matrix for row i column j

The commands for element definition and user element property are given below:

```
*ELEMENT,TYPE=U1,ELSET=CONNECTR  
2,1,2  
*UEL PROPERTY,ELSET CONNECTR
```

The first two lines above define that user element U1 is used as element 2 and is also directed from node 1 to node 2. Element 2 is in the element set called

CONNECTR. The last line represents that the connector stiffness matrix, which is the property of the user element, is also the stiffness matrix of element 2.

As a result, the beam and the connector are defined; k_b and k_s are generated automatically in ABAQUS. Since the beam element is also directed from node 1 to node 2, k_b is combined with k_s to form the beam/connector stiffness matrix k in ABAQUS.

In the case of multiple connectors, there are two methods to input the connector stiffness matrices. In the first method, one user element is used for each individual connector. Thus, the number of user elements is equal to the number of connectors because each connector has a different connector stiffness matrix. Alternatively, all the connector stiffness matrices can be combined into one matrix and then this matrix is written to the input file to be the property of one user element.

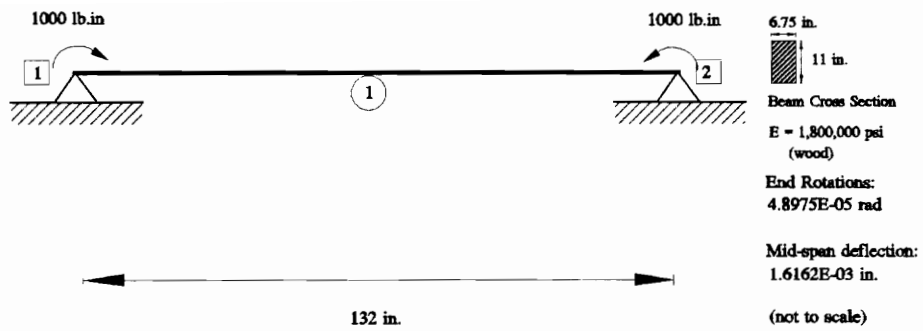
The rest of the input file including the boundary conditions, type of analysis, loading condition, and output request is shown as follows (ABAQUS 4.8 User's Manual):

```
*BOUNDARY
1,1,2
2,1,2
*STEP,LINEAR
*CLOAD
```

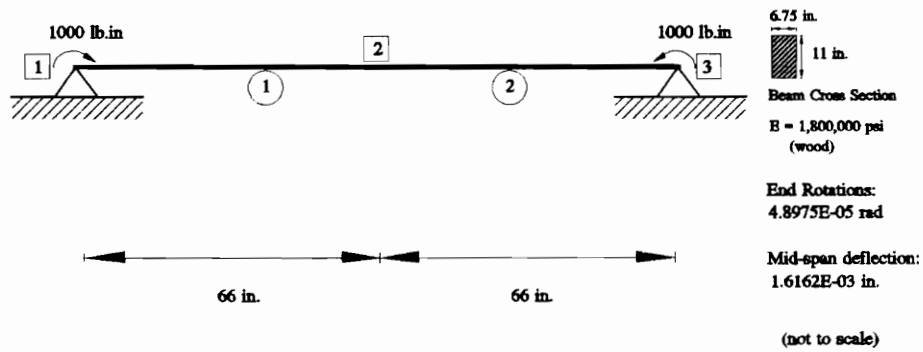
```
1,6,-1000.  
2,6,1000.  
*EL PRINT,SUMMARY=NO  
S  
*NODE PRINT,SUMMARY=NO  
U  
*NODE PRINT,SUMMARY=NO  
RF  
*END STEP
```

4.2.3 Comparison and Discussion of Test Results

The reactions for each model are shown in Fig. 4.2 through Fig. 4.7. In model 1, the deflections at the connectors are obtained by interpolation from the end displacements of the beam (see Eq. (3.4)) while in model 2, the connector displacements are obtained directly from the displacements of the nodes to which each connector is joined. Since the cubic interpolation functions are used in beam elements, and the springs are attached at the nodes of the beam elements, the connector displacements are the same as those obtained from the beam deflection function (from beam differential equation), which is a cubic function. Thus, exact results are obtained in model 2. The reaction at the connector support in model 1 is calculated as the connector displacement times the connector stiffness. For each test problem, the percentage difference between the reaction at each support



(a)



(b)

Figure 4.2 Results of Test Problem 1 in Table 4.1. (a) Model 1; (b) Model 2.

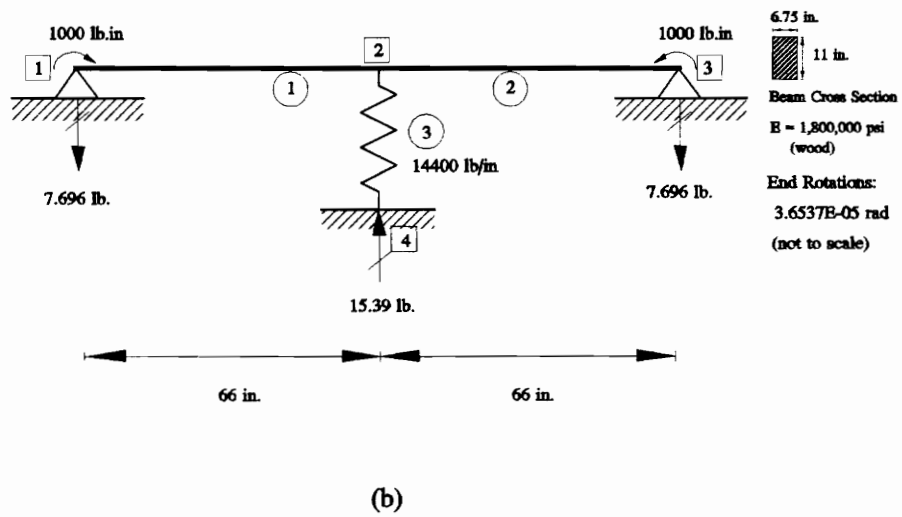
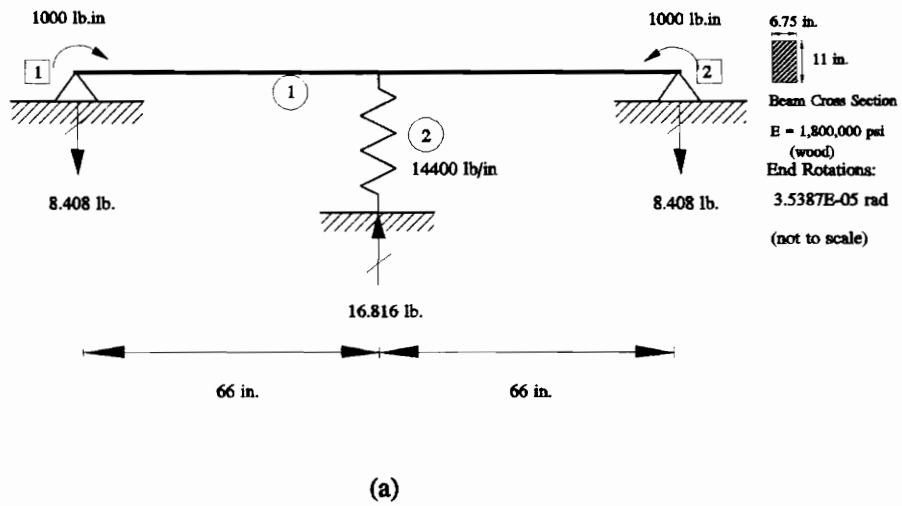
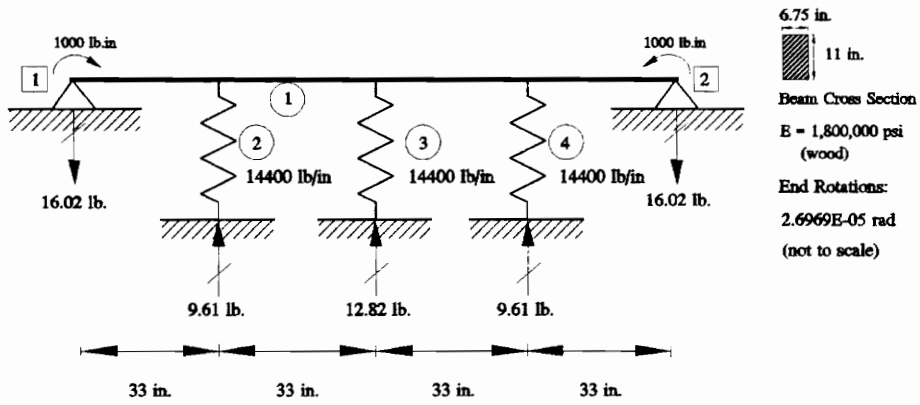
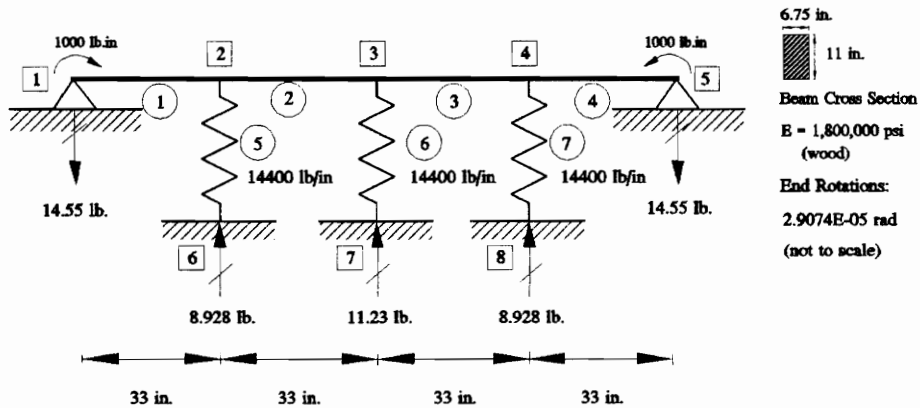


Figure 4.3 Results of Test Problem 2 in Table 4.1. (a) Model 1; (b) Model 2.

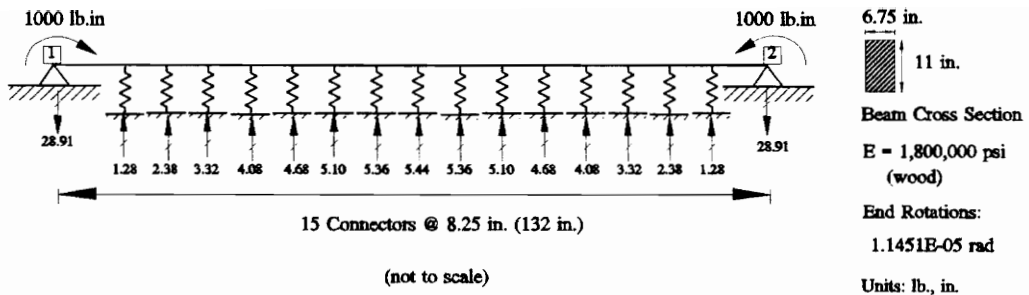


(a)

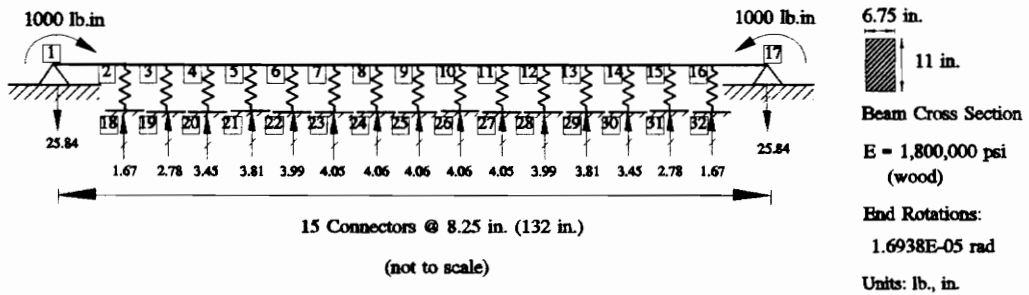


(b)

Figure 4.4 Results of Test Problem 3 in Table 4.1. (a) Model 1; (b) Model 2.



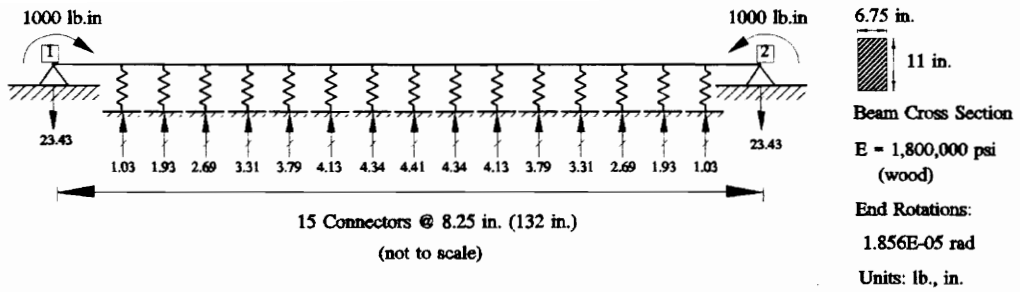
(a)



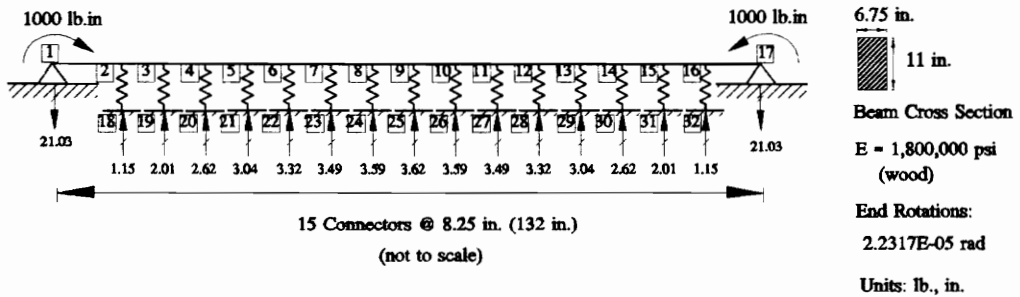
(b)

Figure 4.5 Results of test problem 4 in Table 4.1 (connector stiffness = 14400 lb/in.).

(a) Model 1; (b) Model 2.



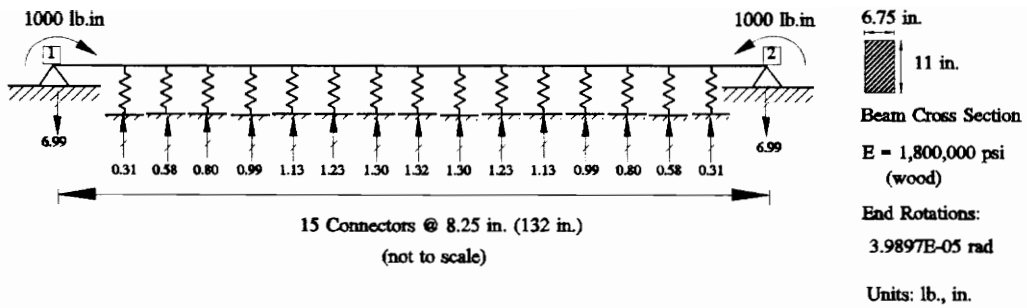
(a)



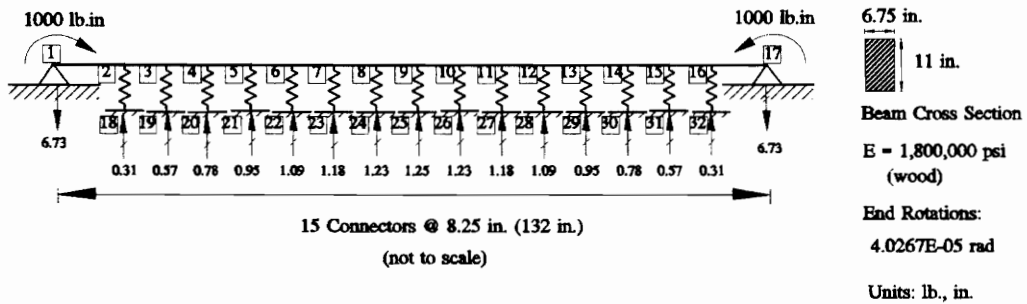
(b)

Figure 4.6 Results of test problem 5 in Table 4.1 (connector stiffness = 7200 lb/in.)

(a) Model 1; (b) Model 2.



(a)



(b)

Figure 4.7 Results of test problem 6 in Table 4.1 (connector stiffness = 1000 lb/in.)
(a) Model 1; (b) Model 2.

(including connector supports) in model 1 and the reaction at the corresponding support in model 2 is computed. Only the maximum percentage difference for each test problem is shown in the second to last column of Table 4.1. The percentage difference between the end rotations at the beam supports in model 1 and those in model 2 for each test problem is computed and is shown in the last column of Table 4.1.

Test problem 1 indicates that an increase in the number of beam elements does not cause any difference in response between model 1 and model 2. Test problems 2, 3, and 4 indicate that an increase in the number of connectors increases the percentage difference between model 1 and model 2. The reason is model 1, which has only two nodes, is stiffer than model 2, which has more than two nodes. In model 1, the deflections at the connectors are obtained by interpolation from the end displacements of the beam. Since the interpolation functions are approximate functions, the connector displacements in models 1 and 2 are different. In addition, when there are more connectors attached to the beam, more approximations are involved to obtain the connector displacements from the interpolation in model 1. As the reactions at the connector supports (fixed ends) depend on the connector displacements, an increase in the number of connectors increases the difference in reactions between the two models.

On the basis of test problems 4, 5, and 6, one can see that a decrease in connector stiffness results in a decrease in percentage difference between two models. This is because when the connector stiffness is high comparable to the beam stiffness, it is like a cable (beam) that lies on the rigid poles (connectors). Therefore, when the

connector stiffness decreases, and the beam is stiffer than the connectors, the two models simulate the real beam/connector assembly so that their differences are small.

4.3 Testing of 3-D Beam/Connector Element

The objective of this section is to present the results of some simple test runs for the 3-D beam/connector element and to study the element response. This section is divided into four subheadings: testing of a special case (Section 4.3.1), test models and procedures (Section 4.3.2), input file for a 3-D beam/connector element (Section 4.3.3), a comparison and discussion of test results (Section 4.3.4).

4.3.1 Testing of a Special Case

According to Section 4.2.3, the difference of the results between model 1 and model 2 in each test problem is due to the difference in the assumed deflection functions of the beam. If a connector is attached at one end of the beam, the assumed deflection functions would be the same. The response of the model with

the beam/connector element should be the same as that of the model with the connector modeled by a linear spring because there is no approximation introduced by interpolation when the spring is attached at the end of the beam. The purpose of this section is to present the results of a test of the 3-D beam/connector element for this special case.

The beam/connector assembly used for testing is shown in Fig. 4.8. The connector stiffness is taken as 14400 lb./in., and the shear modulus is 1.6×10^5 psi. The assembly is analyzed by three approaches shown below:

- 1) by hand (statics)
- 2) by two beam/connector elements (the beam is modeled by two B33 elements)
- 3) by two B33 elements and one Spring2 element

For approach 1, the free body diagrams and the joint forces of the assembly are shown in Fig. 4.9. On the basis of Fig. 4.9a, the connector displacement is $160/14400 = 0.0111$ in. The net torsional rotation (angle of twist) of the beam cross section is obtained by the following torsion formula (Holzer, 1985, p.27):

$$T = \frac{GJ}{L} \Delta\omega \quad (4.2)$$

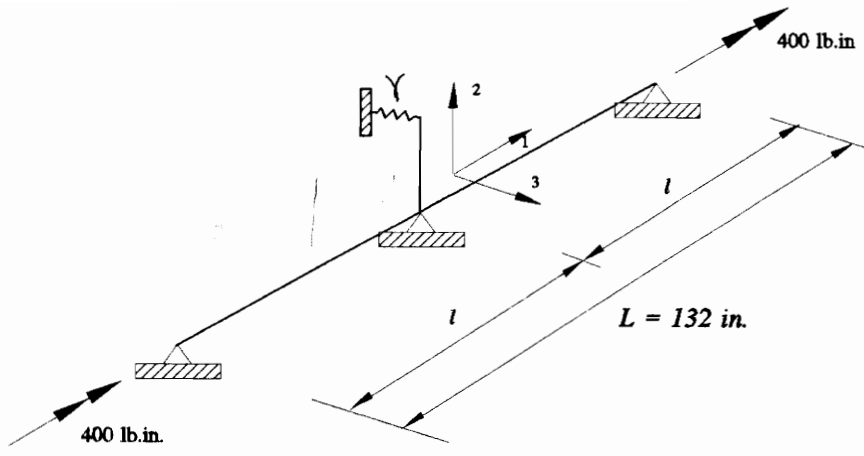
or

$$\Delta\omega = \frac{TL}{GJ} \quad (4.3)$$

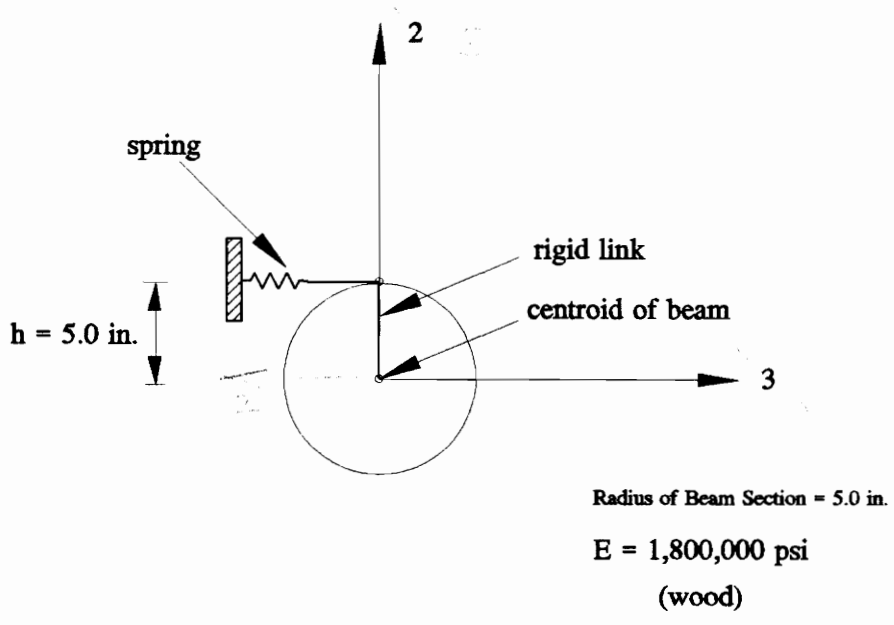
where

$\Delta\omega$ = net torsional rotation of the beam cross section (rad)

T = torque applied to the beam (lb.in.)



(a)



(b)

Fig. 4.8 3-D Beam/connector assembly for Section 4.3.1.

(a) Assembly in space; (b) beam cross section.

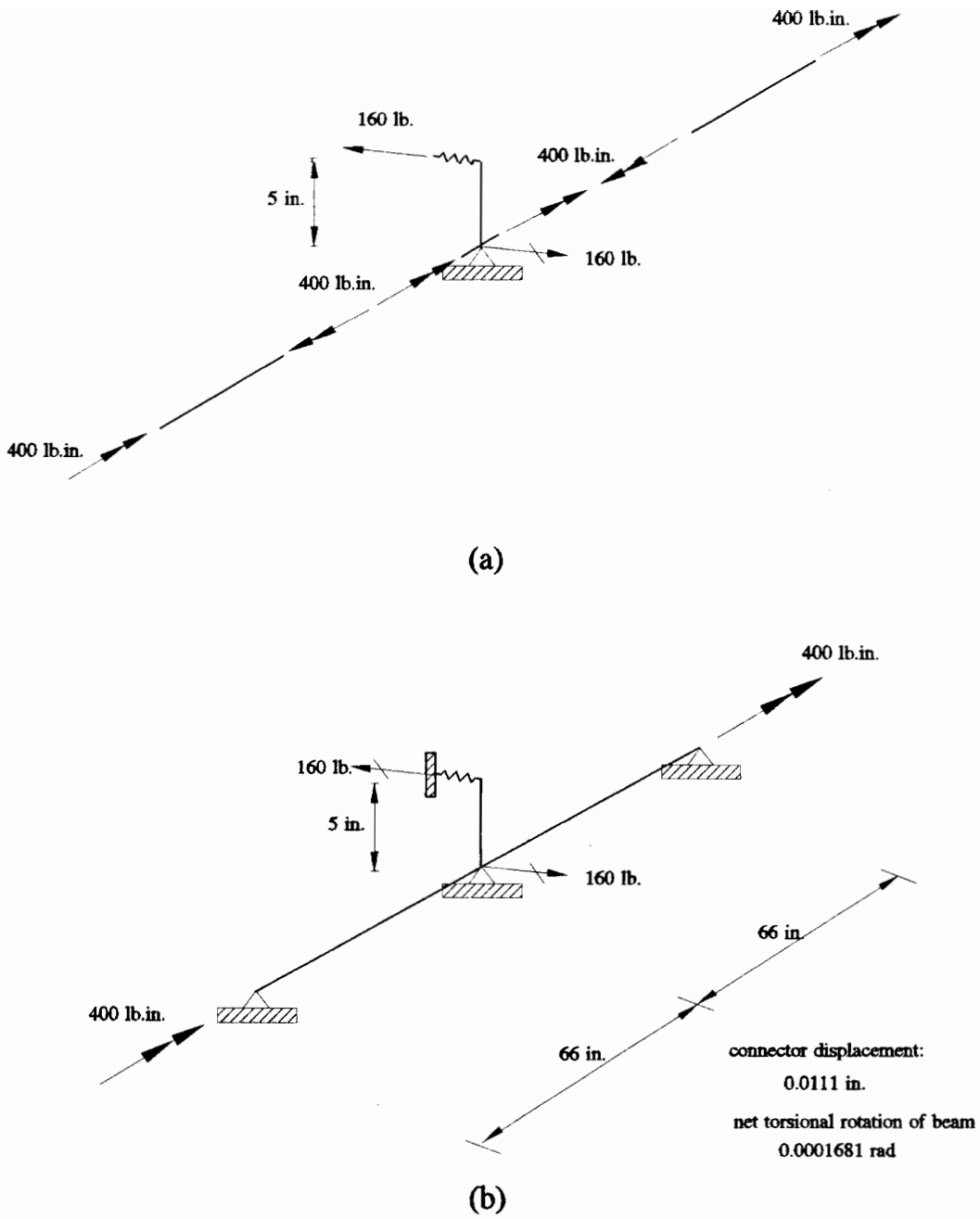


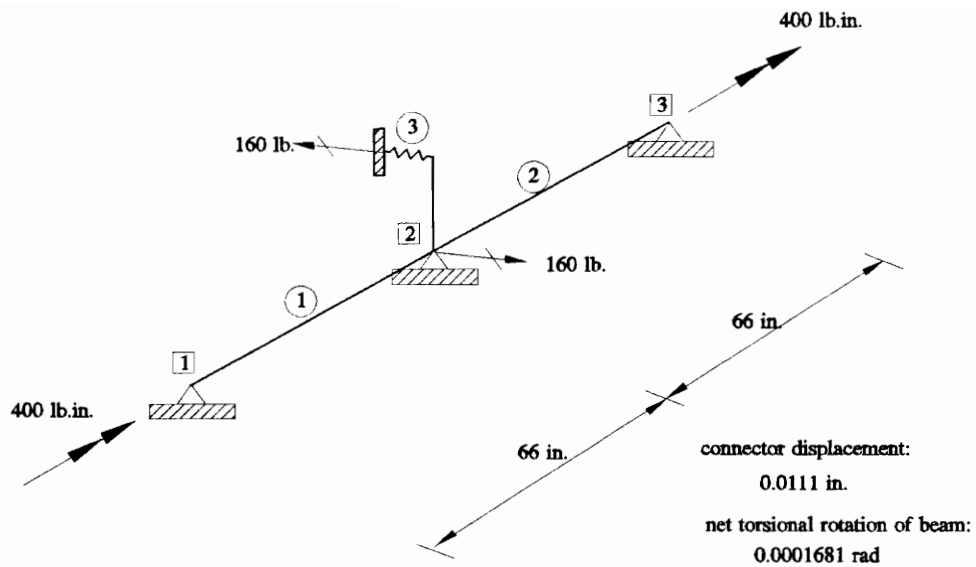
Fig. 4.9 Results of a beam/connector assembly (by statics).
 (a) Free body diagrams; (b) joint forces.

- L = beam length (in.)
- G = shear modulus of elasticity (psi)
- J = polar moment of inertia of the cross section (in.⁴)
 (J = $\frac{\pi}{2} r^4$ for circular cross section where r = radius)

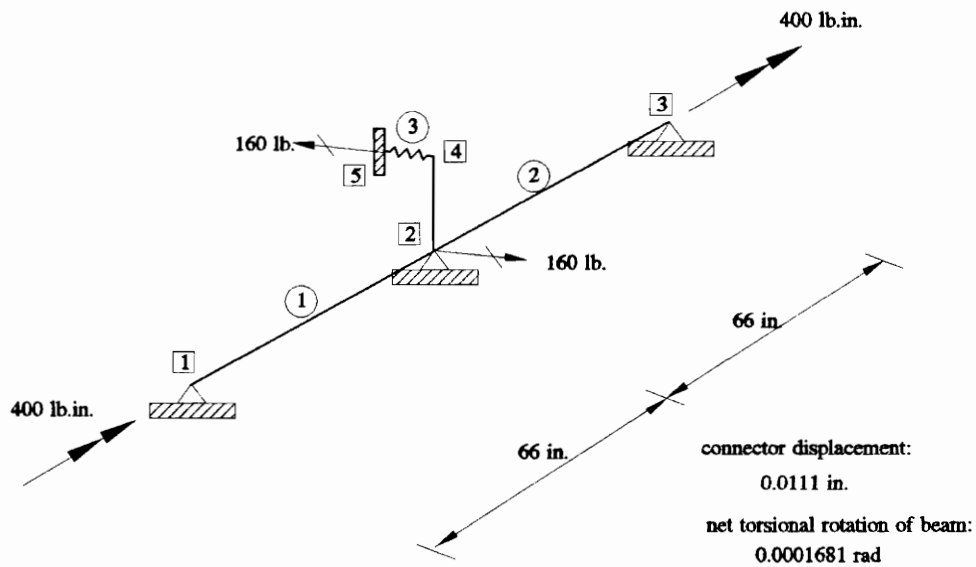
By substituting T = 400 lb.in., L = 66 in., G = 1.6 x 10⁵ psi, and J = $\frac{\pi}{2} 5^4 = 981.75$ in⁴ into Eq. 4.3, the net torsional rotation of the beam is

$$\begin{aligned} \Delta\omega &= \frac{400 \times 66}{1.6 \times 10^5 \times 981.75} \\ &= 1.681 \times 10^{-4} \text{ rad} \end{aligned} \quad (4.4)$$

The assembly is analyzed by approach 2 with ABAQUS. The joint forces, which are obtained from the ABAQUS output file, are shown in Fig. 4.10a. For approach 2, the connector is attached to the end of the beam element 1, and the connector displacement is calculated by the interpolation from end displacements of the beam (Eq. (3.25)). From the ABAQUS output file, the torsional rotation for both node 1 and node 3 is 2.3903 x 10⁻³ rad while the torsional rotation at node 2 is 2.2222 x 10⁻³ rad. On the basis of Fig. 3.5, \bar{d}^2 and \bar{d}^5 are taken as 2.3903 x 10⁻³ rad and 2.2222 x 10⁻³ rad, respectively. All the other displacements according to Eq. (3.25) are zero. By the substitutions of $\xi = 1$ (connector attached to the end of the beam 1), h = 5 in., and the above values for \bar{d}^2 and \bar{d}^5 into Eq. (3.25), the connector displacement is



(a)



(b)

Fig. 4.10 Results of a beam/connector assembly.

(a) By approach 2; (b) by approach 3.

$$\begin{aligned}
 v_s(1) &= \begin{bmatrix} 0 & 0 & 0 & 1 & 5 & 0 \end{bmatrix} \begin{bmatrix} 0 \\ 2.3903 \times 10^{-3} \\ 0 \\ 0 \\ 2.2222 \times 10^{-3} \\ 0 \end{bmatrix} \\
 &= 0.0111 \text{ in.}
 \end{aligned} \tag{4.5}$$

The reaction force P at the connector support is

$$\begin{aligned}
 P &= v_s \gamma \\
 &= 0.0111 \times 14400 \\
 &= 160 \text{ lb.}
 \end{aligned} \tag{4.6}$$

The net torsional rotation of the beam element 1 is obtained by subtracting the torsional rotation at node 2 from that at node 1. Therefore the net torsional rotation is

$$\begin{aligned}
 \Delta\omega &= 2.3903 \times 10^{-3} - 2.2222 \times 10^{-3} \\
 &= 1.681 \times 10^{-4} \text{ rad}
 \end{aligned} \tag{4.7}$$

The net torsional rotation of the beam element 2 is the same as that in Eq. (4.7).

The assembly is then analyzed by approach 3 with ABAQUS. The joint forces and

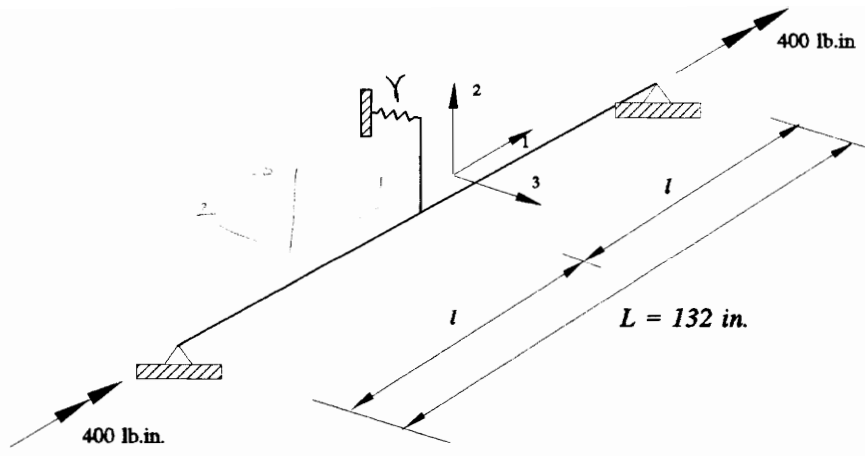
the connector displacement, which are obtained from the ABAQUS output file, are shown in Fig. 4.10b. The torsional rotation for both node 1 and node 3 is 2.3903×10^{-3} rad, and the torsional rotation for both node 2 and node 4 is 2.2222×10^{-3} rad. Therefore, the net torsional rotation for the beam elements 1 and 2 is $2.3903 \times 10^{-3} - 2.2222 \times 10^{-3} = 1.681 \times 10^{-4}$ rad.

According to Fig. 4.9 and Fig. 4.10, the results of the three approaches are the same. This indicates that the beam/connector element has no error in analyzing the assembly compared with approach 3 because there is no approximation involved from interpolation to obtain the connector displacement when the connector is attached at one end of the beam element 1.

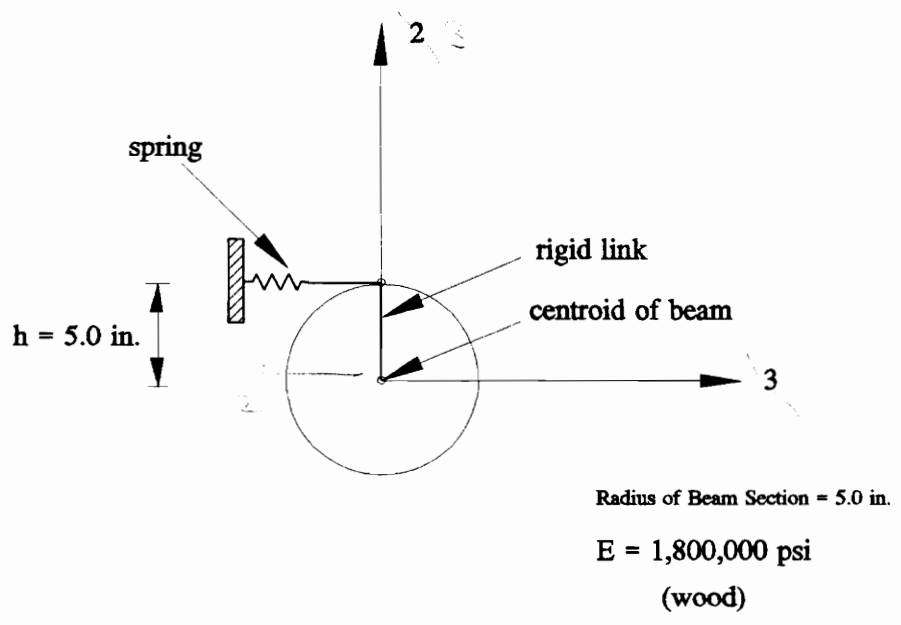
4.3.2 Test Models and Procedures

A 3-D beam/connector assembly, shown in Fig. 4.11, is used for testing. The cross section of the beam is circular because we do not want to consider warping effects. In order to study the effects of a number of connectors and connector stiffness on the beam/connector element, the configuration of the assembly in Fig. 4.11 is subjected to change according to the two variables below:

1. Number of connectors n
2. Connector stiffness γ



(a)



(b)

Fig. 4.11 3-D Beam/connector assembly (n=1).

(a) Assembly in space; (b) beam cross section.

Table 4.2 Test program and results for 3-D beam/connector elements (linear analysis).

Test Problem	Beam/ Connector Element			Model 1			Model 2		Max. % difference in reactions of models 1 & 2	% difference in end rotations of models 1 & 2
	No. of Connectors n	Spacing of Connectors $l = L/(n+1)$	Connector Stiffness γ	No. of B33	No. of User Elements	No. of B33	No. of Spring2			
1	1	66	14400	1	1	2	1	0	21.4	
2	3	33	14400	1	3	4	3	15	28.24	
3	15	8.25	14400	1	15	16	15	131.81	50.1	
4	15	8.25	1000	1	15	16	15	6.84	8.21	

* Reaction values for each test problem are shown in Fig. 4.12 through Fig. 4.15.

The test program outlined in Table 4.2 is similar to that in Table 4.1. The first three test problems are designed to study the effects of the number of connectors attached to the beam. The value of connector stiffness is taken as 14400 lb/in. for the first three test problems (see Section 4.2.1). In order to study the effect of the connector stiffness, the connector stiffness is changed to 1000 lb/in. in test problem 4. The beams are constrained in all directions except the axial torsional direction. Two torques are applied 400 lb/in. at the supports. The link length, h , which is measured from the centroid to the top of the beam, is taken as 5.0 inches.

Each test problem consists of two models. Model 1 simulates the beam/connector assembly (Fig. 4.11) by a beam/connector element. The element is composed of a beam element and connector elements. The space frame element in ABAQUS, B33, is used to model the beam, and each connector element is modeled by a user element which has the connector stiffness matrix shown in Eq. (3.33). For model 2, the B33 elements and the Spring2 elements are used. The beam is modeled by $n+1$ B33 elements where n represents the number of springs in the assembly.

A linear analysis in ABAQUS is conducted for each model in each test problem. The test results of model 1 are compared with those of model 2 and a discussion of the results is presented (Section 4.3.4).

4.3.3 Input File for 3-D Beam/Connector Element in ABAQUS

The input format for the 3-D beam/connector element in ABAQUS is similar to that for the 2-D beam/connector element (Section 4.2.2). In order to specify the shear modulus of 1.6×10^5 psi along with the Young's modulus of 1.8×10^6 psi, a user subroutine developed by Niket (1992, p.51) is used in the input file. This subroutine specifies the linear material law for testing.

The input file for model 1 in test problem 1 (Table 4.2) is shown as follows:

```
*NODE
1,0.,0.,0.
2,132.,0.,0.
*NSET,NSET=NBC
1,2
*ELEMENT,TYPE=B33,ELSET=BEAM
1,1,2
*BEAM SECTION,SECTION=CIRC,ELSET=BEAM,MATERIAL=UWOOD
5.
*TRANSVERSE SHEAR STIFFNESS
9972128.26,9972128.26
*MATERIAL,NAME=UWOOD
*USER MATERIAL,CONSTANT=3
12.00,0.52,4.625
```

```

*USER ELEMENT,NODES=2,TYPE=U 1,LINEAR
1,2,3,4,5,6
*ELEMENT,TYPE=U 1,ELSET=C 1
2, 1, 2
*MATRIX,TYPE=STIFFNESS
0.0000E+00
0.0000E+00, 0.0000E+00
0.0000E+00, 0.0000E+00, 3600.
0.0000E+00, 0.0000E+00, 0.1800E+05, 0.9000E+05
0.0000E+00, 0.0000E+00, -0.1188E+06, -0.5940E+06
0.3920E+07
0.0000E+00, 0.0000E+00, 0.0000E+00, 0.0000E+00
0.0000E+00, 0.0000E+00
0.0000E+00, 0.0000E+00, 0.0000E+00, 0.0000E+00
0.0000E+00, 0.0000E+00, 0.0000E+00
0.0000E+00, 0.0000E+00, 0.0000E+00, 0.0000E+00
0.0000E+00, 0.0000E+00, 0.0000E+00, 0.0000E+00
0.0000E+00, 0.0000E+00, 3600. , 0.1800E+05
-0.1188E+06, 0.0000E+00, 0.0000E+00, 0.0000E+00
3600.
0.0000E+00, 0.0000E+00, 0.1800E+05, 0.9000E+05
-0.5940E+06, 0.0000E+00, 0.0000E+00, 0.0000E+00
0.1800E+05, 0.9000E+05
0.0000E+00, 0.0000E+00, 0.1188E+06, 0.5940E+06
-0.3920E+07, 0.0000E+00, 0.0000E+00, 0.0000E+00

```

```
0.1188E+06, 0.5940E+06, 0.3920E+07
0.0000E+00, 0.0000E+00, 0.0000E+00, 0.0000E+00
0.0000E+00, 0.0000E+00, 0.0000E+00, 0.0000E+00
0.0000E+00, 0.0000E+00, 0.0000E+00, 0.0000E+00
*UEL PROPERTY,ELSET=C 1
*BOUNDARY
NBC,1,3
NBC,5,6
**THIS COMPLETES THE DEFINITION OF STRUCTURE
*STEP
*STATIC,PTOL=0.1,MTOL=0.1
*CLOAD
1,4,400.
2,4,400.
*EL PRINT,SUMMARY=NO
S
*NODE PRINT,SUMMARY=NO
U
*NODE PRINT,SUMMARY=NO
CF
*NODE PRINT,SUMMARY=NO
RF
*END STEP
*USER SUBROUTINE
```

```

*****
*****      SUBROUTINE TO TEST USER SUBROUTINE UMAT      *****
*****
*****                      *****
*****      NIKET M. TELANG .....10 APRIL'91      *****
*****
*****
C
      SUBROUTINE UMAT(STRESS,STATEV,DDSDDE,SSE,SPD,SCD,
1 RPL,DDSDDT,DRPLDE,DRPLDT,
2 STRAN,DSTRAN,TIME,DTIME,TEMP,DTEMP,PREDEF,DPRED,CMNAME,
3 NDI,NSHR,NTENS,NSTATV,PROPS,NPROPS,COORDS,DROT)
C
      IMPLICIT REAL*8(A-H,O-Z)
C
C      CHARACTER*8 CMNAME
C
C
C
      DIMENSION STRESS(NTENS),STATEV(NSTATV),
1 DDSDDE(NTENS,NTENS),
2 DDSDDT(NTENS),DRPLDE(NTENS),
3 STRAN(NTENS),DSTRAN(NTENS),PREDEF(1),DPRED(1),
4 PROPS(NPROPS),COORDS(3),DROT(3,3)
C
      DIMENSION DSTRES(2)
C
C
C
      DO 20 I=1,NTENS

```

```

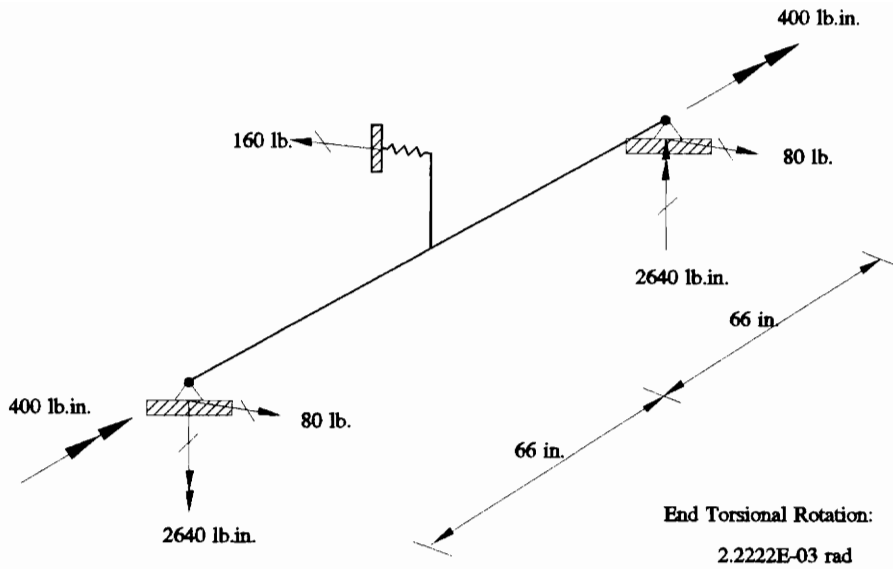
        DO 10 J=1,NTENS
            DDSDE(I,J)=0.0
10      CONTINUE
20      CONTINUE
C
C      *LONGITUDINAL STRESS*
C
        TS=0.0
        TS=STRAN(1) + DSTRAN(1)
C
C      *TENSION ZONE*
C
        DDSDE(1,1)=1.8E+06
        STRESS(1)=DDSDE(1,1)*TS
C
C      *TORSIONAL SHEAR STRESS*
C
        TT=0.0
        TT=STRAN(2) + DSTRAN(2)
C
        DDSDE(2,2)=1.80E+06/(2.*(1+PROPS(3)))
        STRESS(2)=DDSDE(2,2)*TT
C
        RETURN
        END

```

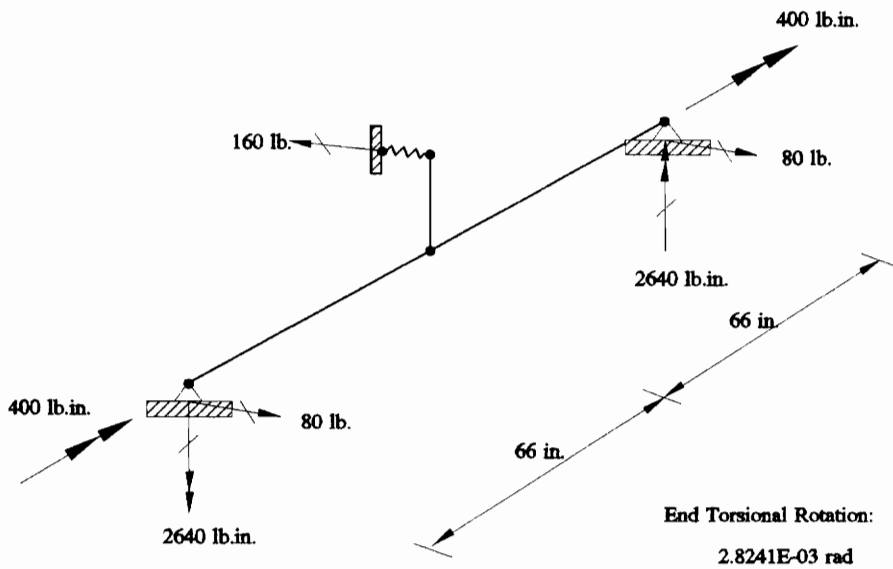
4.3.4 Comparison and Discussion of Test Results

The reactions and end rotations for each model are shown in Fig. 4.12 through Fig. 4.15. In model 1, the deflections at the connectors are obtained by interpolation from the end displacements of the beam (see Eq. (3.25)) while in model 2, the connector displacements are obtained directly from the displacements of the nodes to which each connector is joined. The reaction at the connector support in model 1 is calculated as the connector displacement times the connector stiffness. For each test problem, the percentage difference between the reaction at each support (including connector supports) in model 1 and the reaction at the corresponding support in model 2 is computed. Only the maximum percentage difference for each test problem is shown in the second to last column of Table 4.2. The percentage difference between the torsional rotations at the beam supports in model 1 and those in model 2 for each test problem is computed and shown in the last column of Table.4.2.

In test problem 1, there is no difference in reactions between models 1 and 2 because of the geometric properties of the assembly. However, the difference in end rotations implies that model 1 and model 2 are different in response because of the interpolation for the connector displacements. The connector displacements in model 1 for each test problem are the same because the displacements are obtained from the linear interpolation of the end rotations of the beam.



(a)

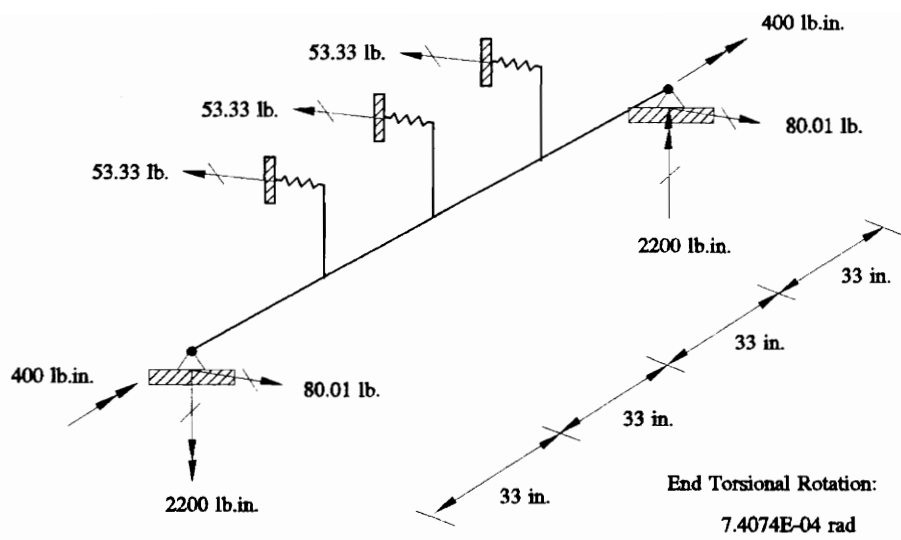


(b)

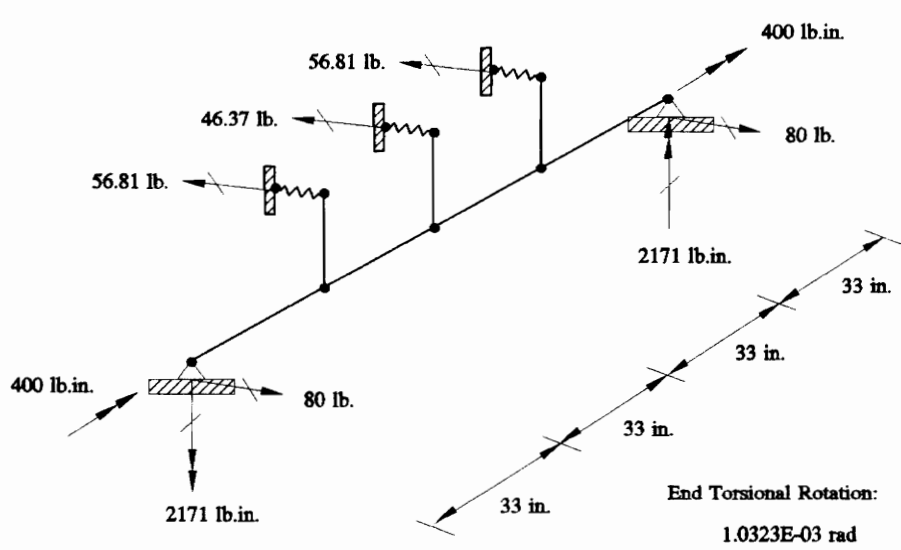
Fig. 4.12 Results of test problem 1 in Table 4.2.

(connector stiffness = 14400 lb./in.)

(a) Model 1; (b) Model 2.



(a)

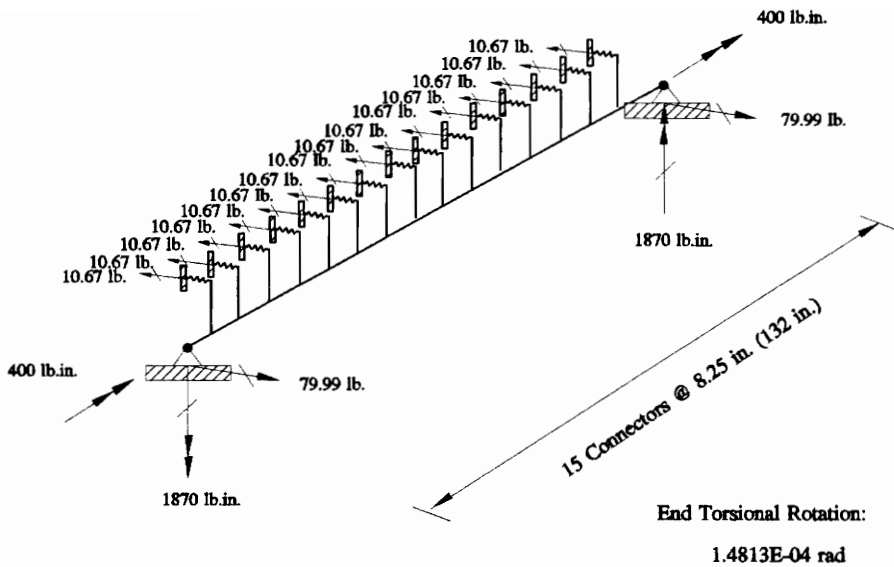


(b)

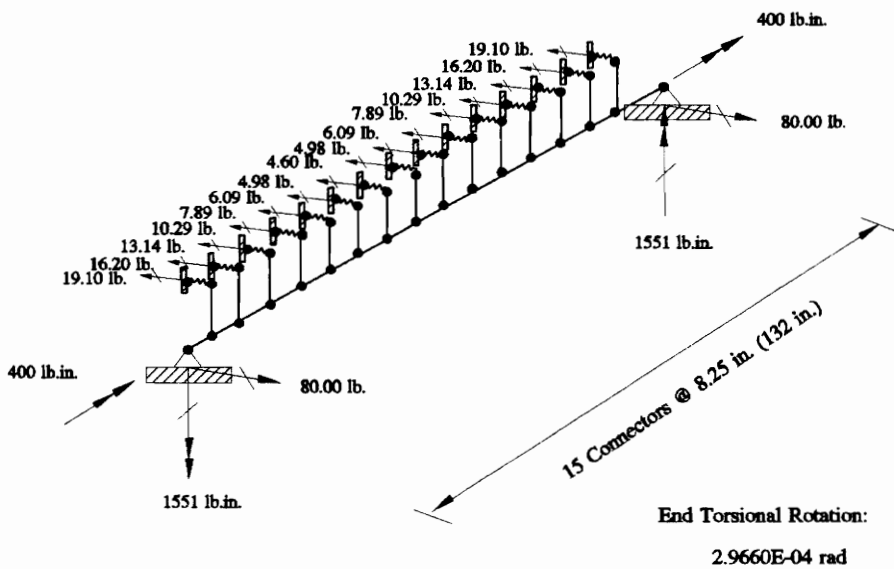
Fig. 4.13 Results of test problem 2 in Table 4.2.

(connector stiffness = 14400 lb./in.)

(a) Model 1; (b) Model 2.



(a)

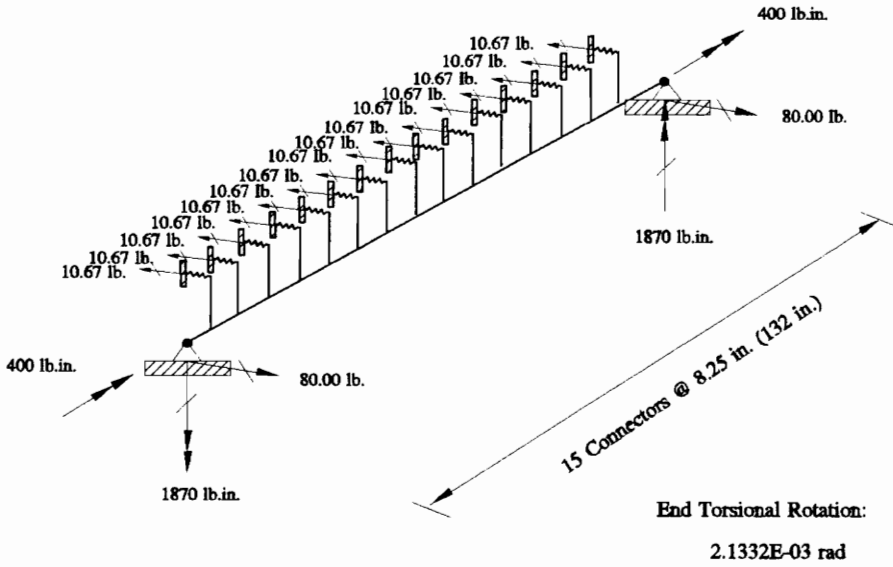


(b)

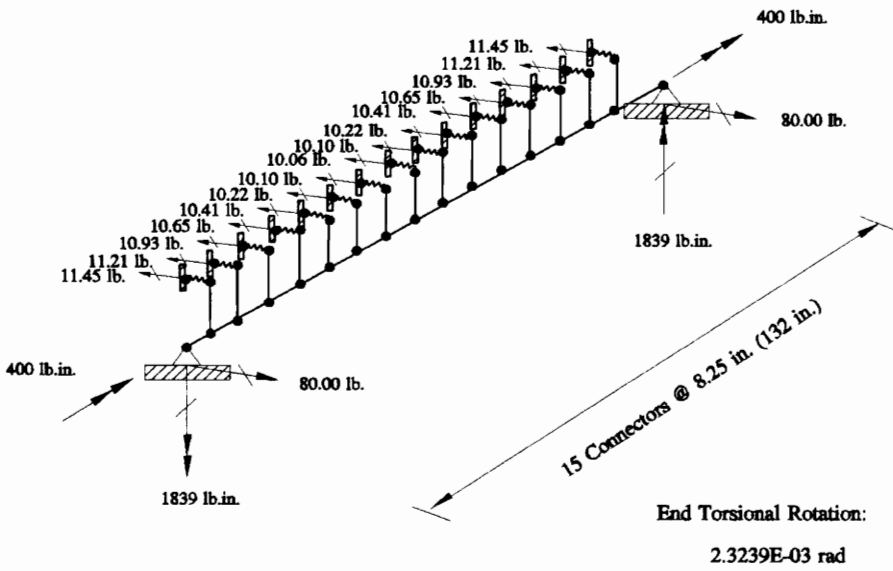
Fig. 4.14 Results of test problem 3 in Table 4.2.

(connector stiffness = 14400 lb./in.)

(a) Model 1; (b) Model 2.



(a)



(b)

Fig. 4.15 Results of test problem 4 in Table 4.2.

(connector stiffness = 1000 lb./in.)

(a) Model 1; (b) Model 2.

Test problems 1, 2, and 3 indicate that an increase in the number of connectors increases the percentage difference between model 1 and model 2. The reason is similar to that mentioned in Section 4.2.3. In model 1, the deflections at the connectors are obtained by interpolation from the end displacements of the beam. Since the interpolation functions are approximate functions, the connector displacements in models 1 and 2 are different. When there are more connectors attached to a beam, more approximations from the interpolation are involved to obtain the connector displacements in model 1. As the reactions at the connector supports (fixed ends) depend on the connector displacements, an increase in the number of connectors increases the difference in reactions between the two models.

On the basis of test problems 3 and 4, one can observe that a decrease in connector stiffness results in a decrease in percentage difference between two models. This is because when the connector is much stiffer than the beam, it is not a realistic beam/connector assembly (Section 4.2.3). Therefore, when the connector stiffness decreases relative to the beam stiffness, the two models simulate the real beam/connector assembly so that their differences are small.

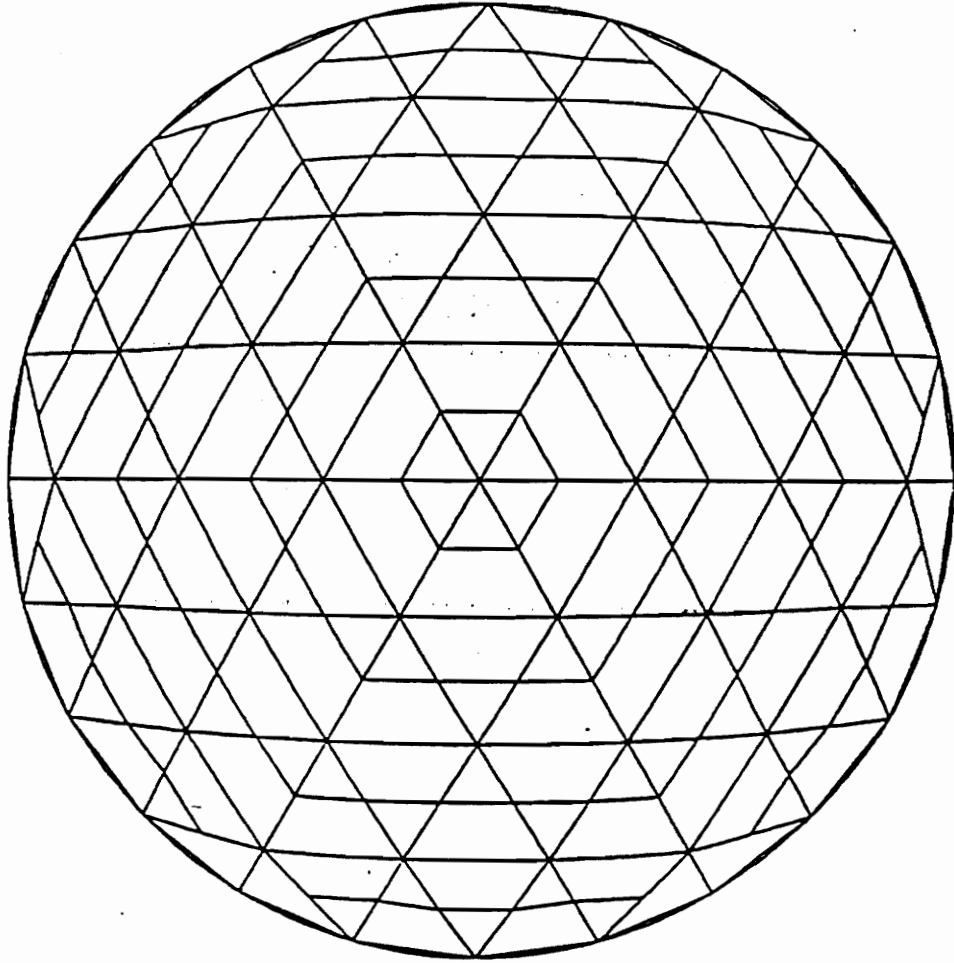
Chapter 5

DOME CAP MODEL

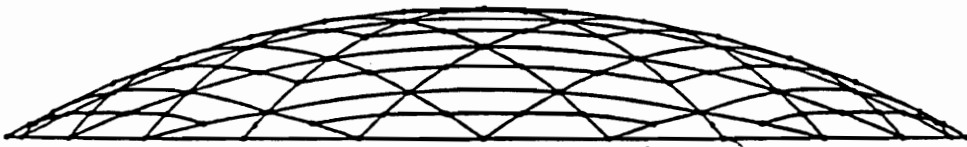
5.1 Introduction

In this study, the finite element modeling is limited to a dome cap whose geometry is based on the Crafts Pavilion Triax dome built in Raleigh, North Carolina, in 1975. The dome has a span of 1595 inches (132.92 feet) and a rise of 212.35 inches (17.70 feet). The members of the dome lie on the surface of a sphere which has a radius of 1600 inches (133.33 feet). In addition, all members lie in great circle planes. The dome is composed of curved beams, purlins, a 2" tongue-and-groove wood decking fastened to the beams and purlins with nails, and a steel tension ring. It is cyclically symmetric and composed of six identical sectors. The plan of the dome is shown in Fig. 5.1.

The dome model is created by defining its geometry on a horizontal plane which is



PLAN VIEW



Span = 133 ft
Height = 18 ft

ELEVATION

Fig. 5.1 Plan of dome.

1387.66 inches (115.64 feet) above the center of the sphere. The geometry of the dome is a grid of equilateral triangles on this horizontal plane. A network of the equilateral triangles is projected onto the spherical surface of the dome by rays originating from the sphere center.

The objectives of this chapter are to present a finite element model of the dome cap for analysis (Section 5.2), to define the boundary conditions (Section 5.3), and to specify the required material properties (Section 5.4). Besides, the design loads for analysis and creation of an ABAQUS input file are presented in Sections 5.5 and 5.6, respectively.

5.2 Finite Element Modeling of Dome Cap

The dome cap model consists of the main beams, edge beams, purlins and tension ring. The main beams are considered to be a set of beams forming the first ring around the apex of the dome. The dome cap model is created because it is much smaller than the whole dome and is cheaper for analysis in terms of computer costs and time. Since the dome cap model is derived from the complete dome model, its behavior is similar to that of the complete dome. Therefore, after the dome cap model is analyzed, potential modeling and analysis problems for the complete dome model can be identified (Telang, 1992, p.78).

However, there is a potential problem with analyzing only the dome cap rather

than the complete dome. In the dome cap, all the beams (meridional and circumferential beams) are vertical, while in the complete dome, the circumferential beams are inclined (meridional beams are vertical). Therefore, in the dome cap, the decking is not greatly activated because the beams, which are vertical, have enough lateral stiffness to suppress lateral buckling. As mentioned previously, the circumferential beams in the complete dome are inclined so that the decking is greatly activated to provide lateral resistance to the beams. Since the scope of this study is limited to the analyses of various dome cap models, an analysis of the complete dome with the beam/connector elements is suggested for future research.

The following subsections will present the modeling of the components of the dome cap: modeling of the beams, purlins, and tension ring (Section 5.2.1) and modeling of the decking (Section 5.2.2).

5.2.1 Modeling of Beams, Purlins and Tension Ring

For the complete dome, the beams are divided into three categories. The set of beams forming the first ring around the apex of the dome is main beam I. The beams at the base or perimeter of the dome are called edge beams and the remaining beams belong to main beam II. All the members are shown in Fig. 5.2 and their dimensions are given below (Holzer, Wu, and Tissaoui, 1991):

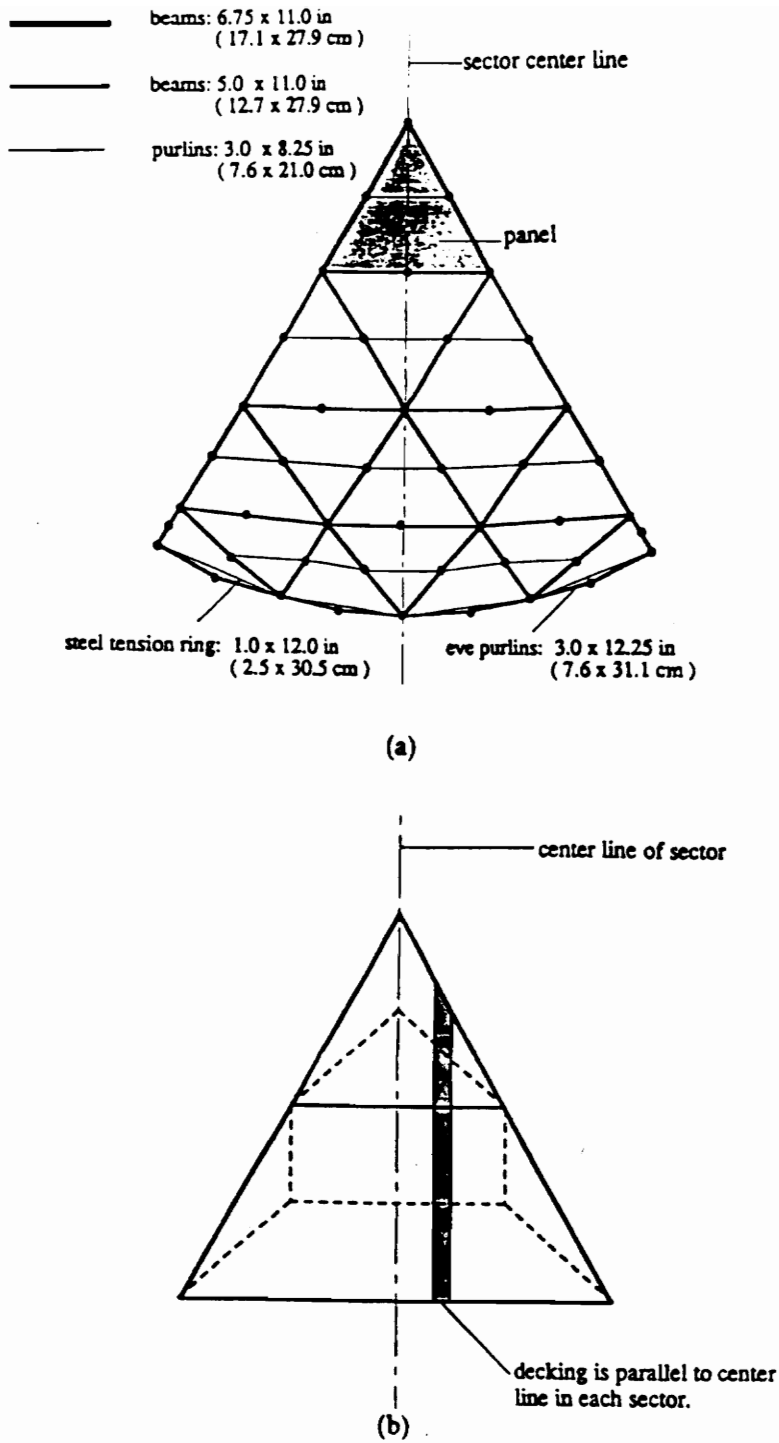


Fig. 5.2 Members of dome model.

1. Main Beam I : 6.75 in. x 11.0 in.
2. Main Beam II : 5.0 in. x 11.0 in.
3. Edge Beam : 3.0 in. x 12.25 in.
4. Purlins : 3.0 in. x 8.25 in.
5. Steel Tension Ring : 1.0 in. x 12.0 in.

For the dome cap model, all of the above elements are present except main beam II. The edge beams for the dome cap are defined as those beams located at the perimeter of the dome cap.

The finite element model of the dome cap is shown in Fig. 5.3. Each physical beam is divided into two beam elements. All the beams are modeled by B33, which are the two noded Bernoulli-Euler elements in ABAQUS, and the purlins and the tension ring are modeled with C1D2, which are the two node isoparametric truss elements in the ABAQUS element library (ABAQUS 4.8 User's Manual, 1991). The choice of the elements is based on the studies conducted by Wu (1991).

The main function of the tension ring is to absorb the individual tensile forces along the base ring of the dome. The tension ring is placed along the first ring of the dome cap. Since the function of the tension ring is to carry the axial force, the tension ring can be modeled with the C1D2 truss elements. The area of the truss element can be defined by the keyword *SOLID SECTION. The element stress of a C1D2 element is given at the Gauss point of the element (Mohammad, 1991, p.51).

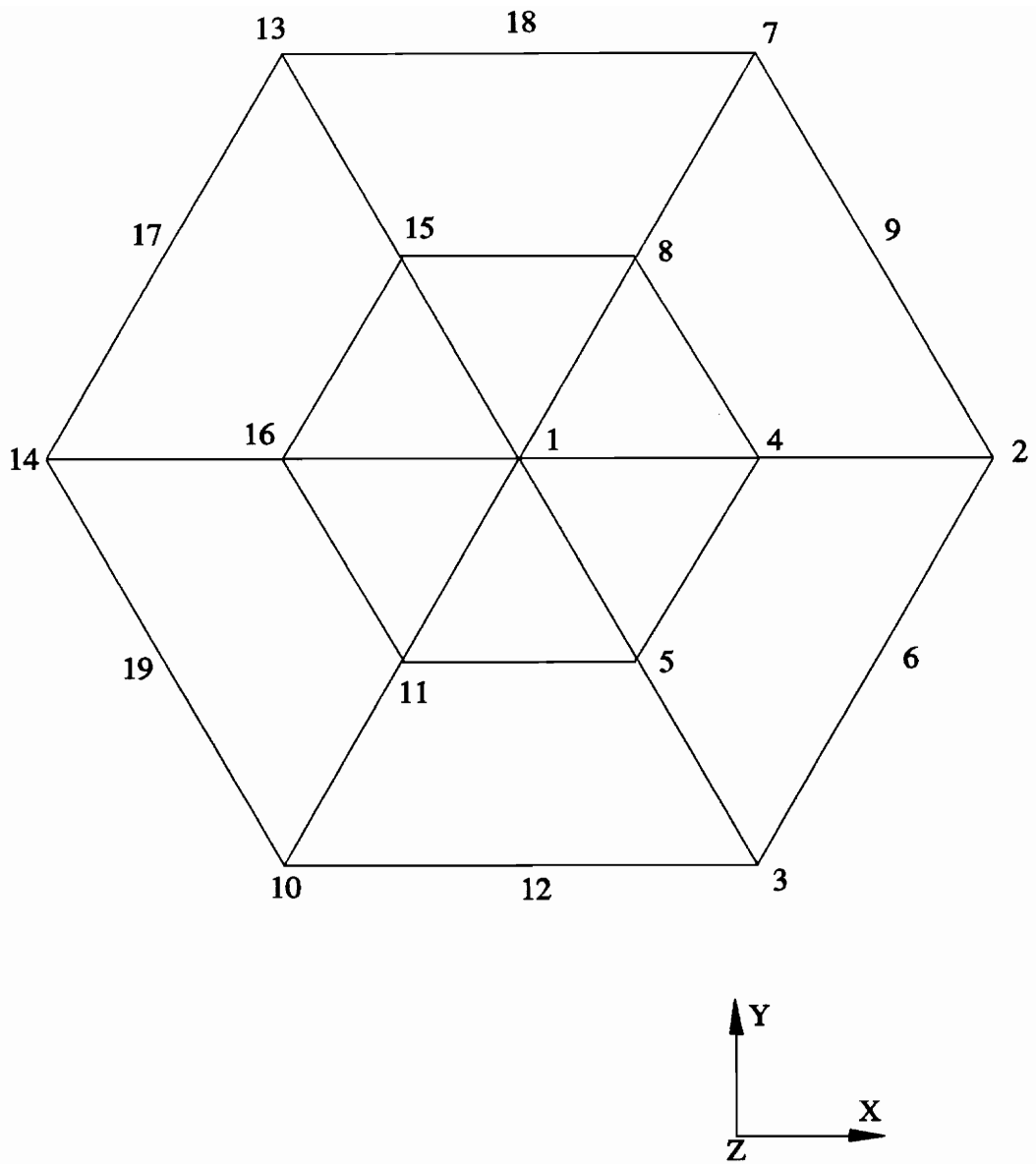


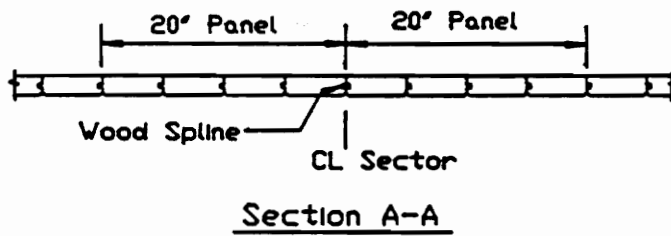
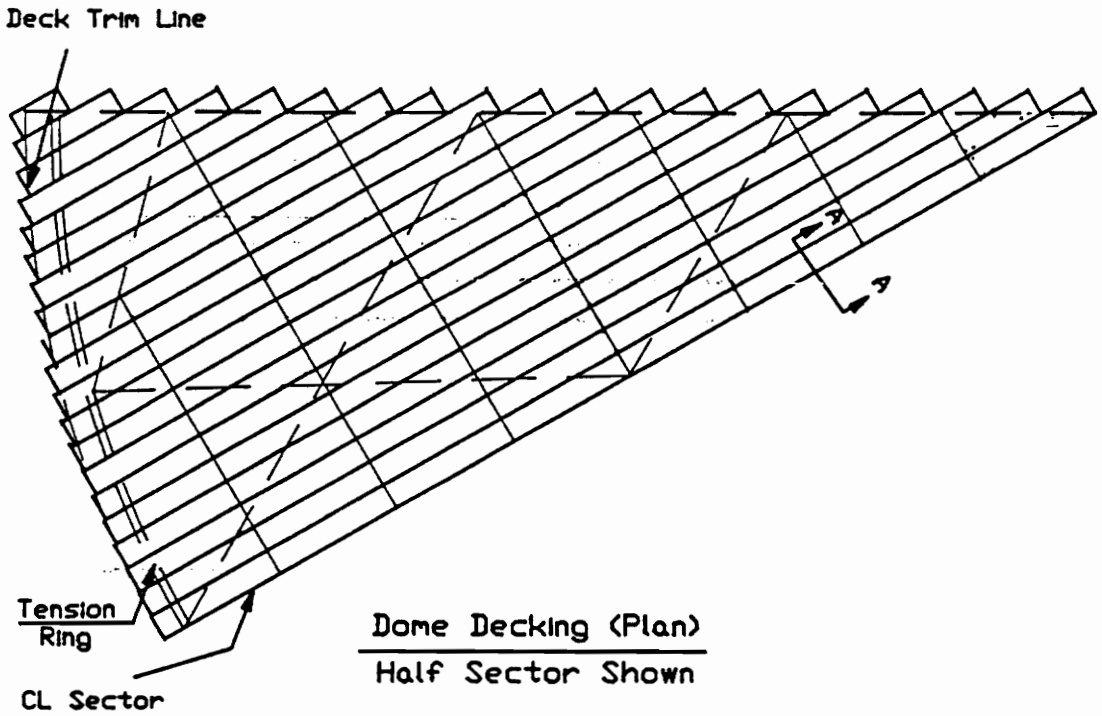
Fig. 5.3 Dome cap model.

5.2.2 Modeling of Decking

As mentioned earlier, the dome is covered with a 2" tongue-and-groove wood decking fastened to the beams and purlins with nails (Fig. 5.4). In the previous studies of Wu (1991) and Telang (1992), the decking was modeled by bracings to take the stabilizing effects of decking on the beams into consideration. However, there are no bracings in the real dome. In order to model the decking in a more realistic way, the 3-D beam/connector element model (Section 3.3) is used to simulate the beam/decking connectors. Results from the stability analysis of the model with the beam/connector elements are compared with those from the model with bracings. The results will be presented and discussed in Chapter 6. In the following paragraphs, the beam/decking connectors are modeled by the beam/connector model, and the parameters necessary for the model are computed.

In the beam/connector element, the linear spring models the lateral load-slip behavior of the nailed joint. The load-slip curve of the nailed joint should be obtained before we linearize the load-slip relationship by a constant stiffness for the spring.

In order to obtain the load-slip curve of the nailed joint, the first step is to compute a point on the curve by Wilkinson's formula (Eq. (2.1)). The Young's



Note: 2-16d face nails thru each 2x6 within the panel @ each support.
1-16d toe nail on the tongue edge of each support.

Fig. 5.4 Plan of dome decking.

modulus E of 3×10^7 psi was suggested by Wilkinson (1971) for common nails. The bearing constant k_o is taken as 1,280,000 G (See Section 2.3.1) because we assume that the grain of the beam is parallel to the beam longitudinal axis, and the load direction is perpendicular to the grain. For E-rated southern pine, the specific gravity G is 0.52 (Timber Construction Manual, 1985) and the elastic bearing constant is

$$\begin{aligned} k_o &= 1,280,000 \times 0.52 \\ &= 665600 \text{ lb/in.}^3 \end{aligned} \quad (5.1)$$

The diameter of a 16-d common nail is taken as $d=0.162$ in. and the joint slip Δ is suggested to be 0.015 in. (Pellicane, Stone, and Vanderbilt, 1991, p.62). By the substitutions of above values of E , k_o , d and Δ into Eq. (2.1), the lateral load at a joint slip of 0.015 in. is

$$\begin{aligned} P &= 0.1667 (30 \times 10^6)^{1/4} (665600)^{3/4} (0.162)^{7/4} (0.015) \\ &= 178.35 \text{ lb.} \end{aligned} \quad (5.2)$$

The second step is to calculate the parameters A and B in Eq. (2.2). Since only solid wood members (southern pine) are used in the dome, Eq. (2.5) is chosen to compute parameter A . The specific gravity (lb/in.^3) of the main and holding members is 0.52 ($\text{SGS} = \text{SGM} = 0.52$) and the parameter A is computed as follows:

$$A = 205.3 + \frac{232.2}{0.52} - \frac{32.4}{0.52 \times 0.52}$$

$$A = 532.02 \quad (5.3)$$

By substituting Eqs. (5.2), (5.3) and $\Delta = 0.015$ in. into Eq. (2.6), one obtains

$$\begin{aligned} B &= \frac{10^{178.25/532.02} - 1}{0.015} \\ &= 77.59 \end{aligned} \quad (5.4)$$

The last step is to compute several correction factors for the parameters A and B. For the interlayer gap effect, the gap g is taken as zero because we assume that there is no gap between the decking and the beams. Since the dome decking is a nominal 2" x 6" tongue-and-groove, kiln dried solid timber decking (moisture content less than 15%), we can assume that there is no significant shrinkage occurred in the decking so the value of g is taken as zero (Timber Construction Manual, 1985, pp. 735-757). The correction factors for the interlayer gap effect are (Eqs. (2.9) and (2.10))

$$C_{Ag} = 1.223 \quad (5.5)$$

and

$$\begin{aligned} C_{Bg} &= 10^{(0.284 - 8.05 \times 0)} \\ C_{Bg} &= 1.92 \end{aligned} \quad (5.6)$$

For the member thickness effect, the side member thickness t is greater than 0.822 in. because the side member (decking) in the dome is 2 in. thick. As a result, the correction factors are taken as (Eqs. (2.11) - (2.13))

$$C_{At} = 1.02 \quad (5.7)$$

and

$$C_{Bt} = 1.0 \quad (5.8)$$

For the nail diameter effect, the nail diameter d is equal to 0.162 in. The correction factors are expressed as (Eqs. (2.14) - (2.16)):

$$\begin{aligned} C_{Ad} &= -2.21 + 39.3 (0.162) - 113.0 (0.162)^2 \\ &= 1.191 \end{aligned} \quad (5.9)$$

and

$$\begin{aligned} C_{Bd} &= 2.83 - 14.6 (0.162) \\ &= 0.465 \end{aligned} \quad (5.10)$$

By substituting Eqs. (5.5) - (5.10), $A' = 532.02$ (Eq. (5.3)), and $B' = 77.59$ (Eq. (5.4)) into Eqs. (2.7) and (2.8), one obtains the predicted parameters A_p and B_p as

$$\begin{aligned} A_p &= 532.02 \times 1.223 \times 1.02 \times 1.191 \\ A_p &= 790.45 \end{aligned} \quad (5.11)$$

and

$$\begin{aligned} B_p &= 77.59 \times 1.92 \times 1.0 \times 0.465 \\ B_p &= 69.36 \end{aligned} \quad (5.12)$$

The empirical equation to predict the load-slip curve for the nailed joints in the dome is obtained by substituting Eqs. (5.11) and (5.12) into Eq. (2.17):

$$P = 790.45 \log_{10} (1 + 69.36 \Delta) \quad (5.13)$$

This equation can predict the load-slip curve up to the joint slip of 0.1 in. and the load-slip curve is shown in Fig. 5.5. A constant stiffness of a nailed joint can be obtained by drawing a straight line from the origin to a point on the curve at a particular joint slip of interest. The slope of this line is the constant stiffness of the nailed joint and can be used as the connector stiffness of the beam/connector element.

In the dome, the spacing of nailed joints on the beams is assumed to be around 8 to 9 in. Therefore, there are about 16 nailed joints on each beam element (132 in.) in the dome cap model with unrefined mesh (Section 5.2.1). The location of each nailed joint on the beam is represented by a nail in Fig. 5.6. It is important to note that each nailed joint is assumed to be composed of two identical nails. Thus, the connector stiffness of the beam/connector element for each joint is equal to two times the constant stiffness of a single joint. The connector stiffness matrices of the nailed joints for each main beam and edge beam are computed by the FORTRAN programs MKS1 and MKS3 in Appendix A and Appendix B, respectively. These programs combine the connector stiffness matrices of each beam element (one connector stiffness matrix for one nailed joint) into one matrix so that the input file for the model with beam/connector elements is more concise. It should be noted that the programs compute the connector stiffness matrices according to the locations of nailed joints. The nailed joints are uniformly located (see Fig. 5.6), and their locations are automatically generated in the programs and depend on how the beam is directed. For example, if a beam is directed from node

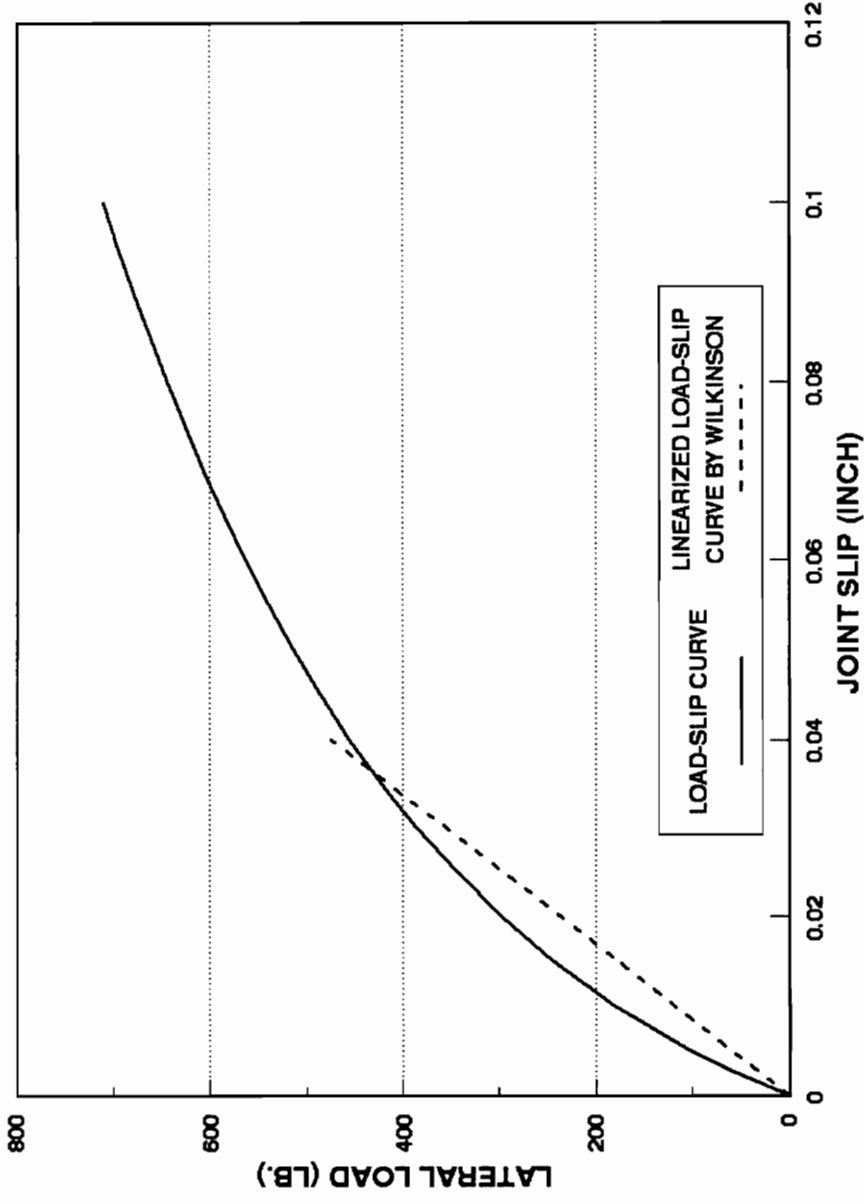


Fig. 5.5 Load-slip curve of nailed joint.

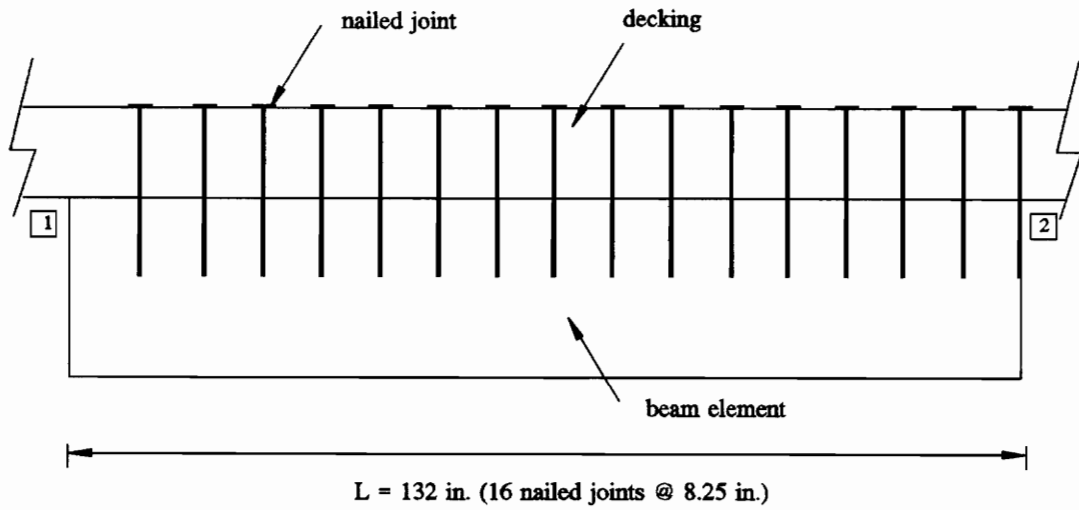


Fig. 5.6 Location of nailed joints on beam element (unrefined mesh).

1 to node 2 (Fig. 5.6), the locations of nailed joints are the same as those in Fig. 5.6. However, if the beam is directed from node 2 to node 1, the locations of nailed joints are similar to those in Fig. 5.6 except there is no nailed joint at node 2, but there is at node 1. Thus, the user should be aware of whether the locations of nailed joints in the models are appropriate or not (see Appendices A and B).

5.3 Boundary Conditions

The boundary constraints used in the dome cap model are similar to those used by Telang (1992). The selected constraints must eliminate the rigid body motion of the model but at the same time must allow the tension ring to move freely in the radial direction (Davalos, 1989).

The boundary constraints are applied to the perimeter nodes (nodes 2, 3, 7, 10, 13, 14). All the perimeter nodes are constrained in the Z-direction to eliminate the vertical rigid body motion. To remove the rigid body rotation of the dome about the Z-axis and the rigid body translation in X and Y-directions, nodes 2 and 14 are constrained in the Y-direction, and nodes 12 and 18 are constrained in the X-direction (see Fig. 5.3).

5.4 Material Properties

The glulam beams and purlins are classified as E-rated 56 southern pine (NDS, 1986) and their Young's modulus is taken as $E=1.8 \times 10^6$ psi. The shear modulus is taken as $G=1.6 \times 10^5$ psi and is obtained from torsion tests of small glulam samples (Davalos, 1989).

In order to input the value of the shear modulus, ABAQUS requires the user to specify values for Young's modulus E and Poisson's ratio ν in the input file. The equation used by ABAQUS to compute Poisson's ratio is

$$G = \frac{E}{2(1+\nu)} \quad (5.14)$$

By rearranging Eq. (5.14), Poisson's ratio can be expressed as

$$\nu = \frac{E}{2G} - 1 \quad (5.15)$$

The only way of specifying the shear modulus of 1.6×10^5 psi along with the Young's modulus of 1.8×10^6 psi is by using the user subroutine option (Telang, 1992, p.51). The user subroutine is included in the input file given in Appendix D.

The maximum parallel to grain stresses for longleaf pine (southern pine) can be obtained from the Wood Handbook (1987). The values are used to check the maximum stresses of the members from the analysis of the dome cap model

(linear material law model) and they are shown below (Wu, 1991, p.14):

1. Proportional limit for compression (linear material) : 5900 psi
2. Proportional limit for tension (linear material) : 8790 psi
3. Ultimate compressive stress (linear material) : 8470 psi
4. Ultimate tensile stress (linear material) : 14500 psi
5. Ultimate shearing stress (linear material) : 1510 psi

So far the material properties for linear material law of wood ($E=1.8 \times 10^6$ psi; $G=1.6 \times 10^5$ psi) are presented. However, wood has a nonlinear stress-strain law, where the behavior in tension is different from that in compression (Telang, 1992, p. 7). The details concerning the stress-strain curve for wood and the nonlinear material law may be found in Telang (1992, pp. 8-16). The stress-strain curve for wood (nonlinear material law) is shown in Fig. 5.7 (Telang, 1992, p.15). According to Telang (1992, p.76), the proportional limit and the ultimate stresses are different for the linear and the nonlinear material laws. The values for the proportional limit and the ultimate stresses for the nonlinear material law are shown below (Telang, 1992, p.78):

1. Proportional limit in compression (nonlinear material) : 4873 psi
2. Proportional limit in tension (nonlinear material) : 2578 psi
3. Ultimate compressive stress (nonlinear material) : 10496 psi
4. Ultimate tensile stress (nonlinear material) : 14500 psi

The ABAQUS user subroutine written by Telang (1992, pp. 141-143) for the

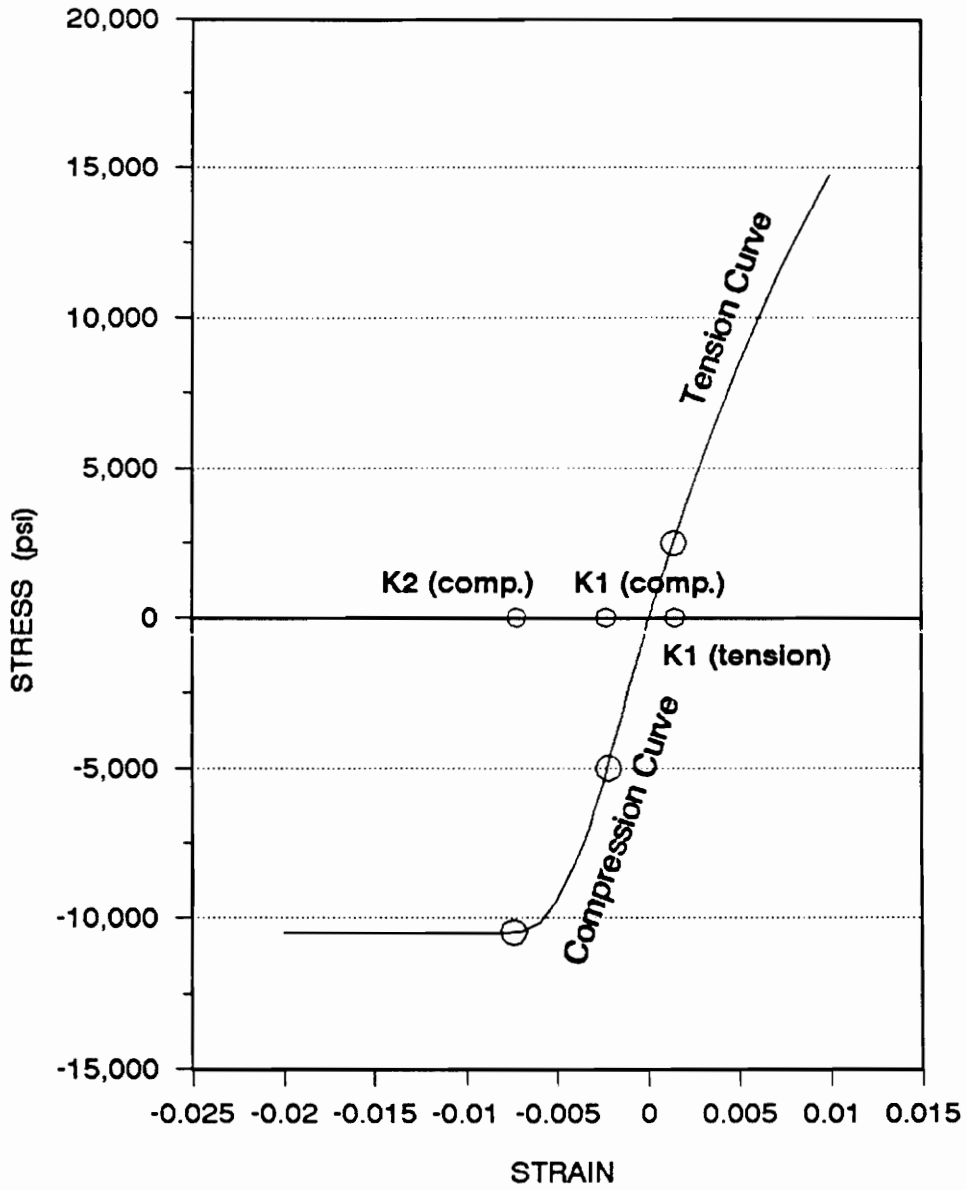


Fig. 5.7 Stress-strain curve for wood (nonlinear material law).

nonlinear material law is included in the input file given in Appendix E.

A Young's modulus of 2.9×10^7 psi and a Poisson's ratio of 0.3 are provided for the steel tension ring.

5.5 Design Loads

The design load is divided into dead load and live load. The design dead load pressure is 16 psf and the live load pressure is 20 psf. The design dead load pressure is due to the selfweight of the following components of the dome (Telang, 1992; Wu, 1991; Davalos, 1989):

1.Beams and purlins	: 2.0 psf
2.Tongue and groove decking	: 5.0 psf
3.Connectors, roofing and insulator	: 9.0 psf
Total dead load	: <u>16.0 psf</u>

The design live load pressure is mainly due to the snow over the dome cap. The value of the snow load pressure is the same as that used by Wu (1991) and Telang (1992). According to the study conducted by Telang (1992, p.66), the snow load is considered to be distributed on the plan area of the dome cap. Only uniform snow load over the dome cap is considered in this study.

5.6 Creation of ABAQUS Input File

The ABAQUS input file for the dome cap model is created in three steps. In the first step, the model is generated graphically with I-DEAS (Integrated Design and Engineering Analyses Software) and translated into an input file with ABAQUS format. Secondly, nodal loads, beam orientations, and beam/connector element properties are computed and written to a file in the required ABAQUS input format. Lastly, the input file is modified by adding the boundary conditions, the beam orientations, the beam/connector element properties, the step definition, the nodal loadings, and the output request cards. Details concerning the use of I-DEAS and input file modifications may be found in Telang (1992, pp. 67-73). The following three subsections will briefly present how the nodal loads (Section 5.6.1), the beam orientations (Section 5.6.2), and the beam/connector element properties (Section 5.6.3) are computed.

5.6.1 Nodal Loads

A linear analysis is conducted in ABAQUS to obtain the nodal loads. The nodal loads are computed by using triangular shell elements, STRI3, which are formed by connecting three nodes with I-DEAS. In the analysis, all the nodes of the dome

cap are fixed and the distributed load due to dead load or snow load is applied over the shell elements in the positive Z-direction (vertical). The reaction forces obtained at all the nodes are the nodal loads because the shell elements discretize the distributed loads to the nodes. Since there are no shell elements in the dome analysis, the nodal loads are applied instead of distributed loads.

5.6.2 Beam Orientations

All the beams except the edge beams in the dome cap are oriented such that each beam lies in a plane passing through the center of the sphere. The edge beams are vertical. More details about the beam orientations may be found in Telang (1992, pp.71-72). The concepts used to compute the beam orientations may be found in Appendix C of Holzer (1985, pp.391-403).

5.6.3 Beam/Connector Element Properties

The beam/connector element properties are based on the space beam stiffness matrix and the connector stiffness matrix (Section 3.3). For the dome cap models with the beam/connector elements, the global connector stiffness matrix for each main beam element is computed by the FORTRAN program MKS1 (Appendix A), while the connector stiffness matrix for each edge beam element is computed

by the program MKS3 (Appendix B). The programs write the user element definition cards and the connector stiffness matrix in the required format for the ABAQUS input file.

The local beam stiffness matrix is transformed into the global beam stiffness matrix by the rotation matrix (Holzer, 1985, Appendix C). The rotation matrix is obtained based on the directions of the local axes and the global axes of the beam. If the rotation matrix used in the beam is applied to the transformation of the local into the global connector stiffness matrix, the connector element should have the same local axes as those of the beam.

The connector element has the same local axes as that of the beam shown in Fig. 3.5 because its connector stiffness matrix is formulated based on the beam interpolation functions. On the basis of the ABAQUS input file for the dome cap (Appendix D), one observes that the local axes of the connector element (see Fig. 3.5) coincide with those of the edge beams (see the direction cosines of the edge beams and Fig. 5.8a). Thus, for the connector elements on the edge beams, the local connector stiffness matrix is the same as that shown in Eq. (3.33). This matrix is transformed into the global connector stiffness matrix by using the rotation matrix for the edge beams.

However, the local axes of the connector element do not coincide with those of the main beams (Fig. 5.8b). Therefore, the connector element should be transformed such that its local axes are compatible with those of the main beams. The objective of this section is to obtain the local connector stiffness matrix whose

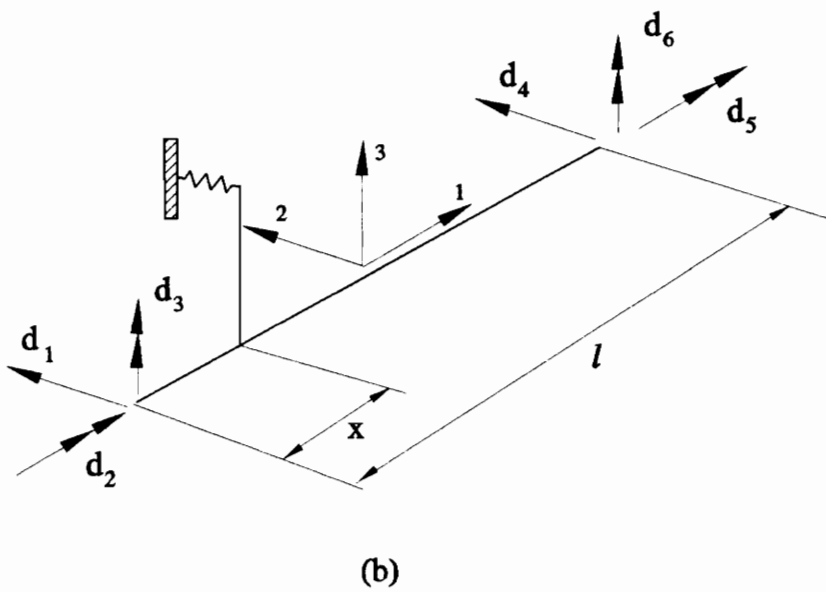
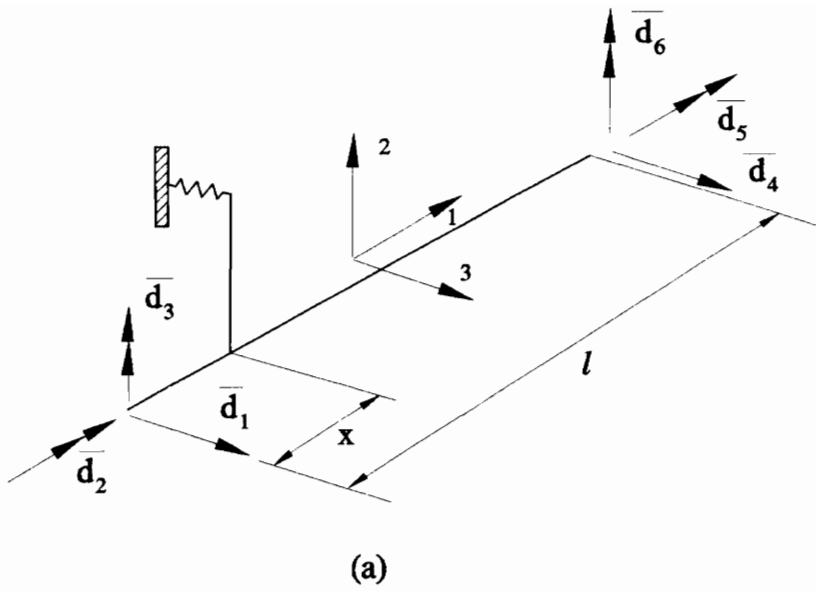


Fig. 5.8 Local axes of beam/connector models.

(a) Edge beam and connector model; (b) main beam and connector model.

local axes coincide with those of the main beams.

The beam/connector model for the edge beams is shown in Fig. 5.8a (similar to Fig. 3.5) while the beam/connector model for the main beams is shown in Fig. 5.8b. Only the beam displacements that activate the connector element are shown in these two diagrams. By comparing Fig. 5.8a and Fig. 5.8b, one obtains the relationship between the two sets of displacements (in matrix form):

$$\begin{bmatrix} \bar{d}_1 \\ \bar{d}_2 \\ \bar{d}_3 \\ \bar{d}_4 \\ \bar{d}_5 \\ \bar{d}_6 \end{bmatrix} = \begin{bmatrix} -1 & 0 & 0 & 0 & 0 & 0 \\ & 1 & 0 & 0 & 0 & 0 \\ & & 1 & 0 & 0 & 0 \\ & & & -1 & 0 & 0 \\ & & & & 1 & 0 \\ & & & & & 1 \end{bmatrix} \begin{bmatrix} d_1 \\ d_2 \\ d_3 \\ d_4 \\ d_5 \\ d_6 \end{bmatrix} \quad (5.16)$$

sym.

or

$$\bar{d} = T d \quad (5.17)$$

where

$$\bar{d} = \begin{bmatrix} \bar{d}_1 \\ \bar{d}_2 \\ \bar{d}_3 \\ \bar{d}_4 \\ \bar{d}_5 \\ \bar{d}_6 \end{bmatrix} \quad (5.18)$$

and

$$\mathbf{T} = \begin{bmatrix} -1 & 0 & 0 & 0 & 0 & 0 \\ & 1 & 0 & 0 & 0 & 0 \\ & & 1 & 0 & 0 & 0 \\ & & & -1 & 0 & 0 \\ & & & & 1 & 0 \\ \text{sym.} & & & & & 1 \end{bmatrix} \quad (5.19)$$

The spring energy U_s in Fig. 5.8a is expressed as

$$U_s = \frac{1}{2} \bar{\mathbf{d}}^T \bar{\mathbf{k}}_s \bar{\mathbf{d}} \quad (5.20)$$

where $\bar{\mathbf{k}}_s$ is defined in Eq. (3.30).

Substituting Eq. (5.17) into Eq. (5.20) yields

$$U_s = \frac{1}{2} \mathbf{d}^T \mathbf{T}^T \bar{\mathbf{k}}_s \mathbf{T} \mathbf{d} \quad (5.21)$$

or

$$U_s = \frac{1}{2} \mathbf{d}^T \mathbf{k}_s \mathbf{d} \quad (5.22)$$

where

$$\mathbf{k}_s = \mathbf{T}^T \bar{\mathbf{k}}_s \mathbf{T} \quad (5.23)$$

The spring energy of the connector element in Fig. 5.8b is expressed in Eq. (5.22).

The connector element has the connector stiffness matrix \mathbf{k}_s . After being

expanded, the connector stiffness matrix k_s (Eq. (5.23)) for Fig. 5.8b is obtained as below:

$$k_s = \begin{bmatrix} g_1 & -g_2 & -g_4 & g_7 & -g_{11} & -g_{16} \\ & g_3 & g_5 & -g_8 & g_{12} & g_{17} \\ & & g_6 & -g_9 & g_{13} & g_{18} \\ & & & g_{10} & -g_{14} & -g_{19} \\ & & & & g_{15} & g_{20} \\ \text{sym.} & & & & & g_{21} \end{bmatrix} \quad (5.24)$$

where g_i 's are defined in Eq. (3.31).

In order to extend the connector stiffness matrix (6 x 6) in Eq. (5.24) to a 12 x 12 matrix, which is compatible with the space frame element matrix in ABAQUS, the member code matrix is used and obtained by comparing Fig. 5.8b with Fig. 5.9:

$$M = \begin{bmatrix} 2 \\ 4 \\ 6 \\ 8 \\ 10 \\ 12 \end{bmatrix} \quad (5.25)$$

Fig. 5.9 is the local main beam element of the dome cap with displacements based on the local axes defined in Fig. 5.8b. The member code matrix is then assigned to

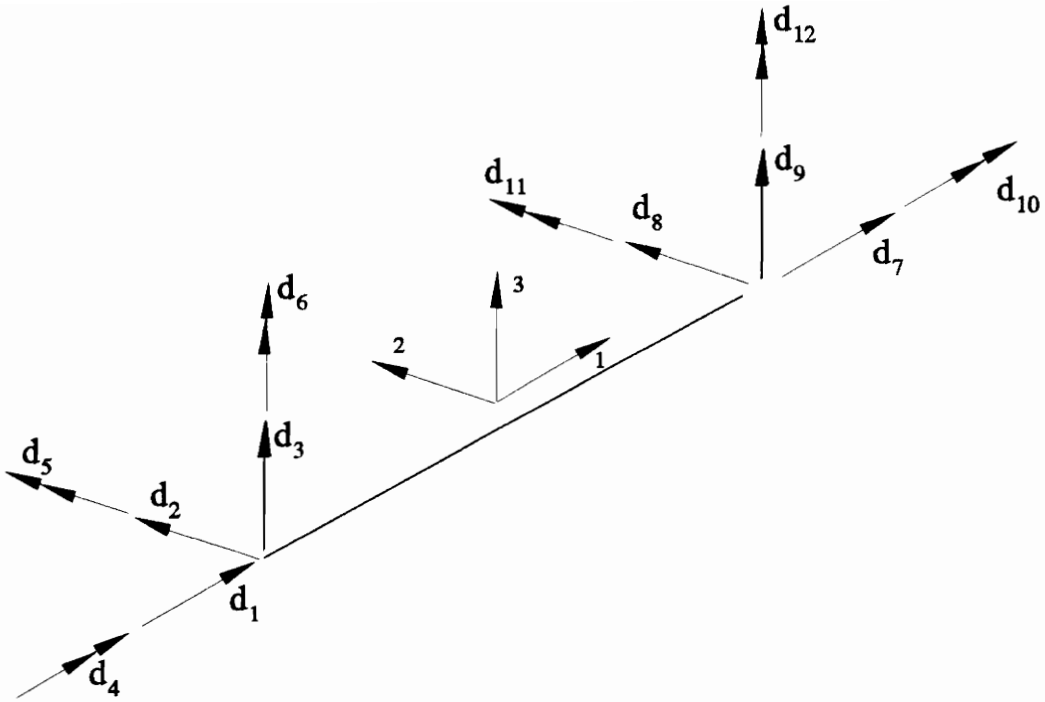


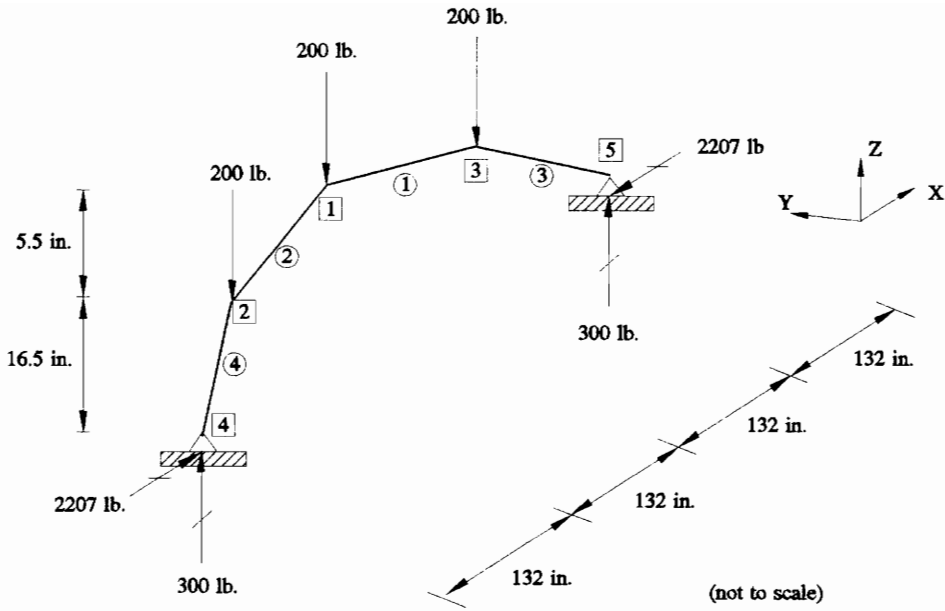
Fig. 5.9 Local main beam element of dome cap model.

the matrix in Eq. (5.24), and the 3-D connector stiffness matrix for the main beams is

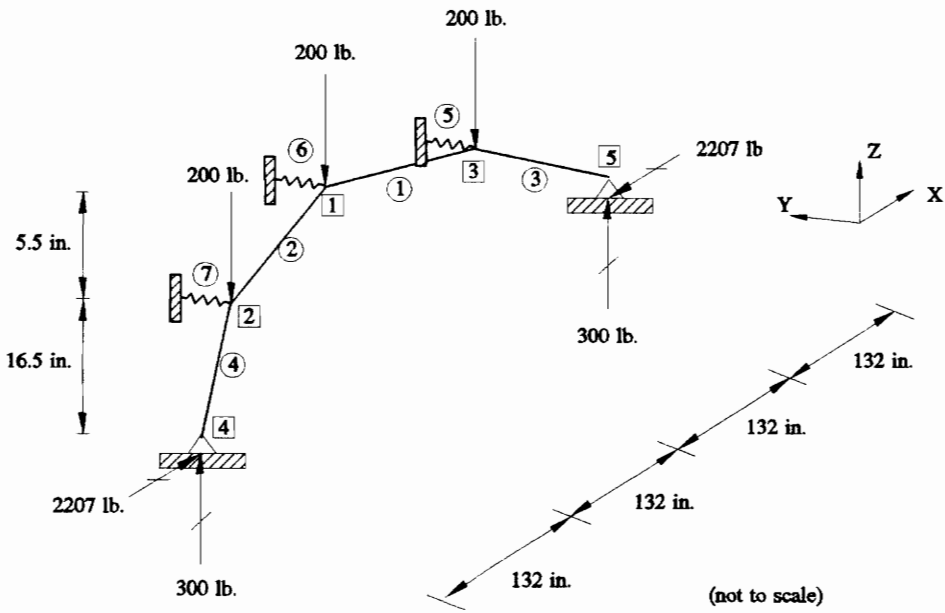
$$\mathbf{k}_s = \begin{bmatrix}
 0 & 0 & 0 & 0 & 0 & 0 & 0 & 0 & 0 & 0 & 0 & 0 \\
 g_1 & 0 & -g_2 & 0 & -g_4 & 0 & g_7 & 0 & -g_{11} & 0 & -g_{16} & \\
 0 & 0 & 0 & 0 & 0 & 0 & 0 & 0 & 0 & 0 & 0 & \\
 g_3 & 0 & g_5 & 0 & -g_8 & 0 & g_{12} & 0 & g_{17} & & & \\
 0 & 0 & 0 & 0 & 0 & 0 & 0 & 0 & 0 & & & \\
 g_6 & 0 & -g_9 & 0 & g_{13} & 0 & g_{18} & & & & & \\
 0 & 0 & 0 & 0 & 0 & 0 & 0 & & & & & \\
 g_{10} & 0 & -g_{14} & 0 & -g_{19} & & & & & & & \\
 0 & 0 & 0 & 0 & 0 & & & & & & & \\
 g_{15} & 0 & g_{20} & & & & & & & & & \\
 0 & 0 & & & & & & & & & & \\
 \text{sym.} & & & & & & & & & & & g_{21}
 \end{bmatrix} \quad (5.26)$$

It is important to test that the connector element is attached laterally to the beam because the element is assumed to provide lateral resistance only to the beam. A cap rib model is used for this purpose (Fig. 5.10). The model consists of four main beams which lie on the meridian line of the dome cap. All the nodes are constrained in the Y- direction to prevent the lateral instability of the model. Concentrated loads are applied in the negative Z-direction at the nodes. The ABAQUS input file of the cap rib is presented in Appendix C.

Linear analysis with ABAQUS is conducted on the cap rib model. The cap rib model is then modified by adding the connector elements to the nodes 1, 2, and 3. The connector stiffness of the elements is taken as 32600 lb/in. The global



(a)



(b)

Fig. 5.10 Reactions of cap rib models.
(a) Cap rib model without connector elements;
(b) cap rib model with connector elements.

connector stiffness matrices for the connector elements are generated by the MKS1 program (Appendix A) based on the local stiffness matrix defined in Eq. (5.26). If the connector elements are not attached laterally to the beams, the elements will be activated to carry some of the loads. This modified model is also analyzed with ABAQUS. The reactions for both models are shown in Fig. 5.10. The reactions are the same for both models, which indicates that the connector elements are attached laterally to the beam.

Chapter 6

DOME CAP ANALYSIS

6.1 Introduction

The objective of this chapter is to present the results of stability analyses of various dome cap models with the beam/connector elements (Chapter 5) in order to find out whether the beam/connector model is a potential model to simulate the decking. The beam/connector elements are activated due to twisting or lateral bending of beams.

In Section 6.2, nonlinear analysis procedures in ABAQUS are presented. Nonlinear analyses of various dome cap models with the nailed joints only at the bracing points are conducted. Their test results are compared with those of the truss bracing model (Section 6.3). Similarly, the nonlinear analyses are performed for various dome cap models with 16 nailed joints on each beam element. The results

are compared with those of the model with the truss bracings (Section 6.4). The nailed joints on the beam are modeled by the spring elements of the beam/connector model.

6.2 Nonlinear Analysis Procedures

Nonlinearity in structures can be classified as material nonlinearity, which relates to a nonlinear stress-strain relationship, or as geometric nonlinearity, in which the strain-displacement relationship is nonlinear and equilibrium is satisfied for the deformed state (Cook, 1989, p.501). In this study, both material and geometric nonlinearity are considered.

The two nonlinear analysis methods used in this study are the Newton-Raphson method and the modified Riks-Wempner Method. The Newton-Raphson method (Bathe, 1982) starts with a known equilibrium point, and then uses iterative procedures to find the next equilibrium point at an increment of load $\Delta\lambda$. This procedure is repeated again and again until the load reaches a limit point, where convergence becomes increasingly difficult. Unlike the Newton-Raphson method, the modified Riks-Wempner method (Ramm, 1980; Ramm and Stegmuller, 1982) is able to trace the equilibrium path beyond a limit point, which is defined as a turning point on the load deflection curve. The load deflection curve is the projection of the equilibrium path onto a load-deflection plane.

The loading on the dome is applied in two steps with ABAQUS, which are given below (ABAQUS 4.8 User's Manual, 1990):

1. The Newton-Raphson method is used in the first step to load the dome up to its full dead load (16 psf).

2. The Riks method (ABAQUS 4.6 Theory Manual, 1987, p. 3.10.1) is used in the second step to apply the snow load up to the limit load and trace the equilibrium path beyond the limit point.

The total load pressure at any instant is given by (Holzer, Wu, and Tissaoui, 1991)

$$p = p_D + \lambda p_L$$

where

p = total load pressure

p_D = dead load pressure (16 psf)

p_L = live load pressure (20 psf)

λ = load proportionality factor

In the following sections, the critical load factor represents the load proportionality factor at the limit point.

Before embarking on the nonlinear analyses, linear analyses of the dome cap models are carried out to make sure that there are no major defects or

imperfections in the finite element models. In the linear analyses, the dome models are subjected to cyclically symmetric loads (dead load), and the reactions at all the supports and the displacements at the nodes are found to be symmetric.

6.3 Dome Cap Analysis with Nailed Joints at Bracing Points

The dome cap models are created because they are much smaller than the complete dome models, and they are cheaper to analyze in terms of computer cost and time. Since the dome cap models are derived from the complete dome model, their behavior should be similar to that of the complete dome. Thus, after analyzing the dome cap models, potential modeling and analysis problems for the complete dome models can be identified.

The dome cap model consists of six identical sectors, and its geometry exhibits cyclic symmetry. The details concerning the modeling and the boundary conditions of the dome cap may be found in Chapter 5. In order to simulate the dome behavior, the geometric properties and orientations of the edge beams (at the base of the dome cap) for the dome cap are the same as those of the edge beams for the complete dome. The edge beams have a cross section of 3.0 in. x 12.25 in. and are oriented vertically (see Sections 5.2 and 5.6.2). Only uniform snow load (live load) over the dome cap is considered in this study (Section 5.5).

This section is divided into two subsections: (1) rigid link length $h=0$ (Section

6.3.1), and (2) rigid link length $h>0$ (Section 6.3.2).

6.3.1 Rigid Link Length $h=0$

A dome cap model with truss bracings is the simplest model to simulate the decking effects (Fig. 6.1). However, the truss bracing does not simulate the closely spaced nail connections; therefore, the beam/connector model was created (Chapter 3).

Aside from the connection spacing, there is another difference between the truss bracing model and the beam/connector model. In the truss bracing model, the bracings move with the beams, while in the beam/connector model, one end of the spring is attached to a fixed support (see Fig. 3.5). Since the decking is very stiff in membrane action, this was a logical first step in modeling the beam-decking connectors; i.e. the basic assumption is that the decking does not move, and the nails, which are attached to the decking, restrain the lateral displacements of the beams.

The objective of this section is to present the results of various dome cap models in order to study the behavior of the beam/connector model. Six different dome cap models, which are outlined in Table 6.1, are analyzed with ABAQUS. Models 1 and 4 are the dome cap models with the truss bracings (see Fig. 6.1), and they have different material laws. These models are the simplest models to simulate

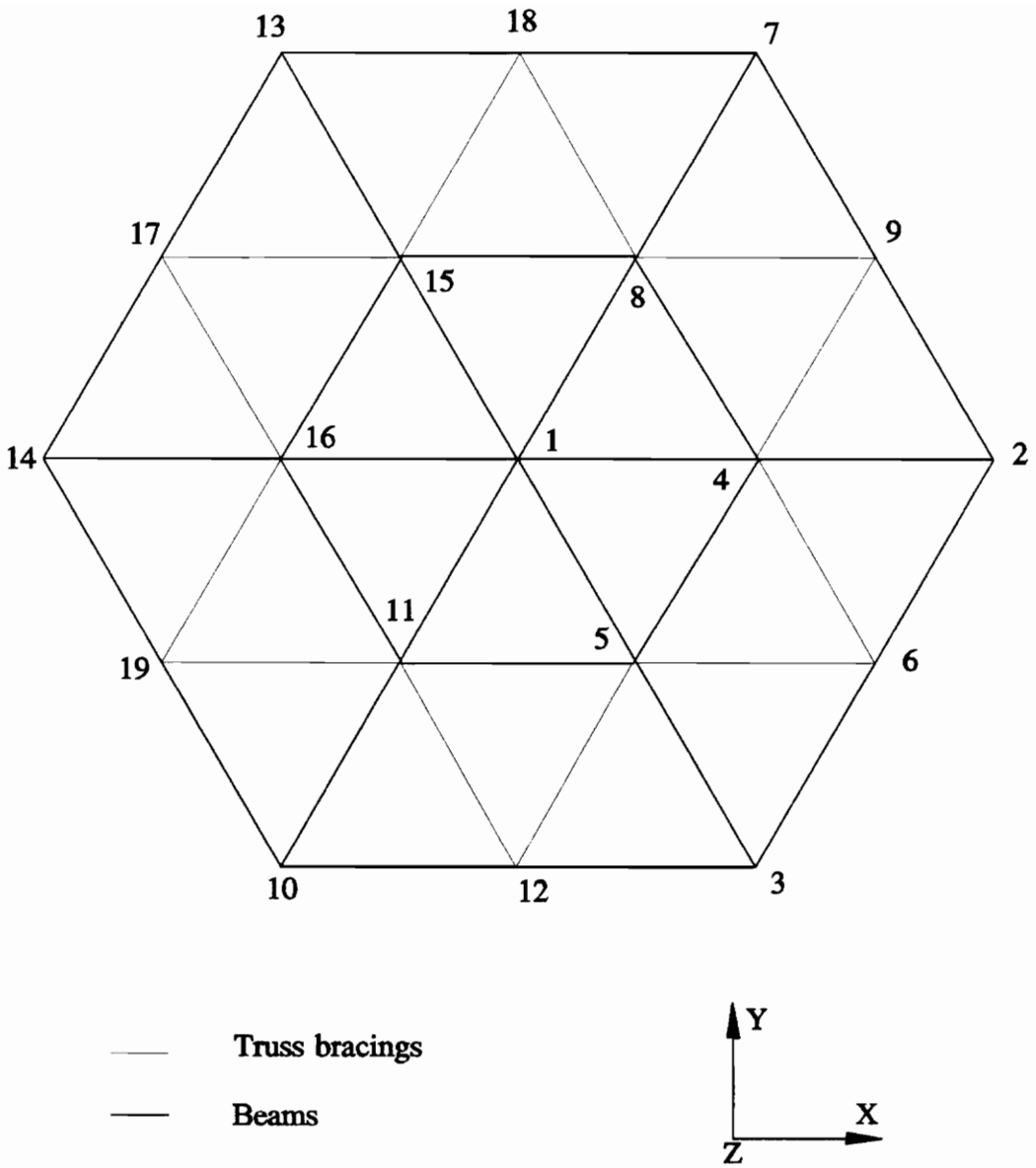


Fig. 6.1 Dome cap model with truss bracings.

Table 6.1 Nonlinear analysis results of dome cap models with truss bracing and nailed joints at bracing points (h=0).

Model No.	Material Law	Connector Stiffness (lb./in.)	Critical Load ** Factor	Max. Stress/psi. *** (Element no.)	Apex Deflection (in.)	Max. Nail Deflection/in. (node no.)
1 (Truss Bracings)	Linear	-	9.743	8303 (5)	-8.315	-
2 (Nailed Joints)*	Linear	32600 (h=0)	9.736	8229 (5)	-8.33	0.032 (6)
3 (Nailed Joints)*	Linear	14200 (h=0)	9.734	8260 (5)	-8.329	0.07 (6)
4 (Truss Bracings)	Nonlinear	-	10.72	-8375 (5)	-7.101	-
5 (Nailed Joints)*	Nonlinear	32600 (h=0)	11.18	-9023 (5)	-9.497	0.04 (6)
6 (Nailed Joints)*	Nonlinear	14200 (h=0)	10.81	-8566 (5)	-7.191	0.16 (6)

* nailed joints at bracing points (h=0)

** at limit point

*** + : tensile stress; - : compressive stress

the decking (Wu, 1991, pp.42-48). The wood truss bracings are modeled by the truss elements C1D2 and have a cross section of 0.3 in.

The rest of the models in Table 6.1 are the dome cap models with the nailed joints at the bracing points (Fig. 6.2). These models are created because we need some models that are very similar to the truss bracing models in order to test the fixed support effects. The nailed joints are modeled by the springs in the beam/connector model, and the connector stiffness matrices are generated by the FORTRAN programs MKS1 and MKS3 in Appendix A and Appendix B, respectively. According to the design of the programs, there is only one nailed joint attached to the end of each of the following elements in the ABAQUS input file: elements 1, 3, 5, 15, 19, 31, 33, 43, 45, 47, 59, 71. Thus, there are only 12 nailed joints in each model (see Fig. 6.2). The user of these programs should be aware of whether the locations of the nailed joints are appropriate (see Appendices A and B). Since the truss bracing is applied at the centroid of the beam cross section, the rigid link length of the beam/connector model is taken as $h=0$ to simulate the truss bracing.

Models 1 to 3 are the models with linear material law for wood. In these models, Young's modulus E is taken as 1.8×10^6 psi and the shear modulus G is 1.6×10^5 psi. The input file for model 2 is presented in Appendix D. Models 4 to 6 are the models with nonlinear material law for wood. The stress-strain curve for nonlinear material law and the details concerning nonlinear material law can be found in Telang (1992, pp. 6-16). According to the studies by Telang (1992, pp. 63-65), the

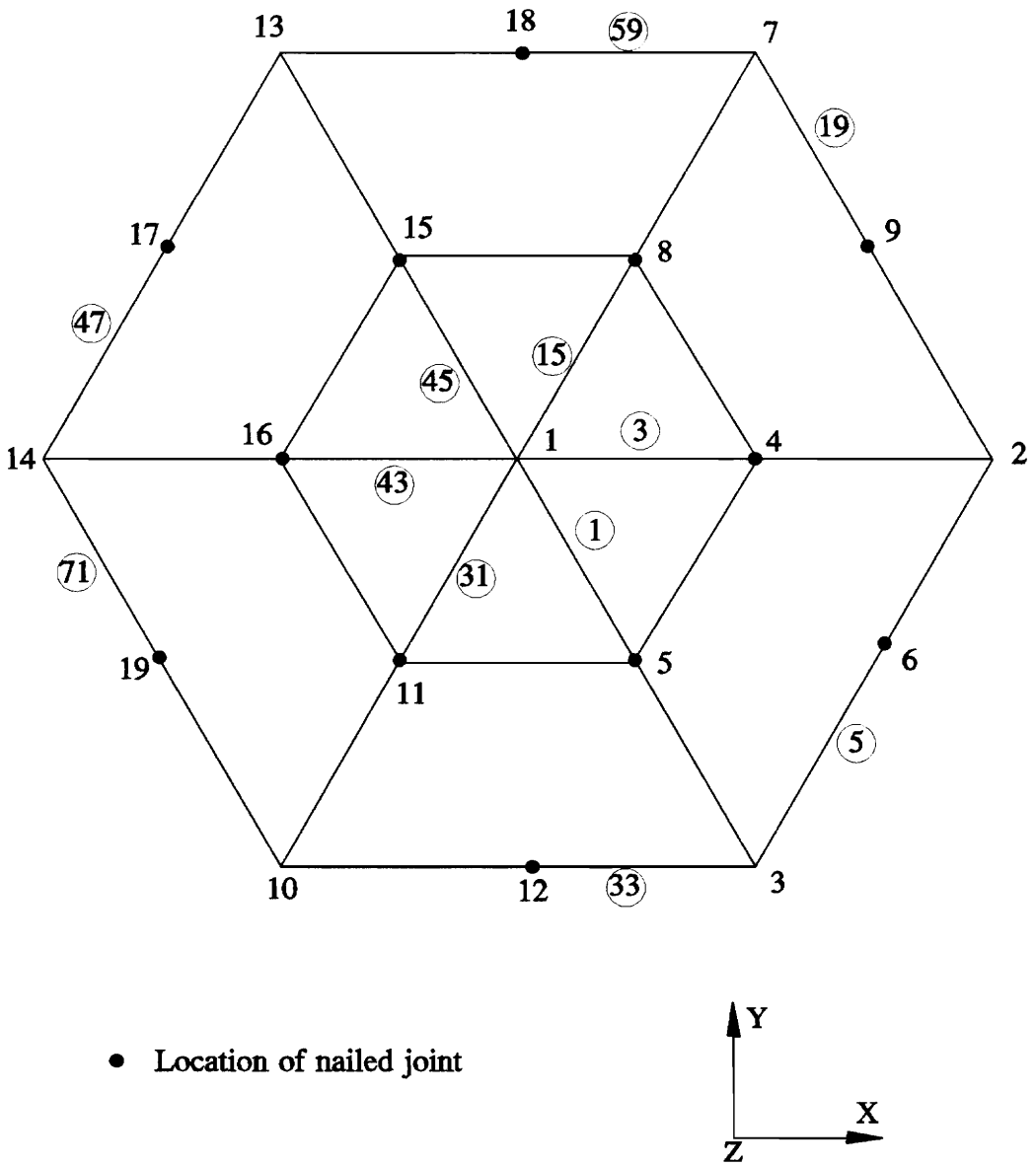


Fig. 6.2 Location of nailed joints (at bracing points) in dome cap model.

initial longitudinal modulus of wood in tension $E_{(tension)} = 1.81 \times 10^6$ psi and in compression $E_{(compression)} = 2.19 \times 10^6$ psi. The shear modulus is taken as $G = 1.6 \times 10^5$ psi.

The choice of the connector stiffnesses for the models is based on the load-slip curve in Fig. 5.5. As mentioned in Section 5.2.2, our goal is to linearize the load-slip curve in Fig. 5.5 in order to obtain a constant value of connector stiffness. On the basis of Fig. 5.5, suppose the joint slip of the nail is 0.015 in. The joint slip up to 0.015 in. is considered as the linear range of the load-slip curve (Hoyle, 1973, p.140). By substituting $\Delta = 0.015$ in. into Eq. 5.13, one obtains the lateral load of the nail as 245 lb. Therefore, the nail stiffness in this linear range is $245/0.015 = 16300$ lb./in. As a nailed joint consists of two identical nails in this study (see Section 5.2.2), the connector stiffness of the nailed joint is $16300 \times 2 = 32600$ lb./in. Similarly, the constant nail stiffness at the joint slip of 0.1 in. (max. joint slip of the load-slip curve by McLain's formula) is calculated as 7100 lb./in., and the connector stiffness of the nailed joint is taken as $7100 \times 2 = 14200$ lb./in. (Fig. 6.3).

The values of the connector stiffnesses for the models are roundoff values. In the analyses, the actual input values for stiffnesses 32600 lb/in and 14200 lb/in are 32642 lb/in and 14222 lb/in, respectively. The limit nail deflections (joint slip limit) for stiffnesses 32600 lb/in and 14200 lb/in are 0.015 in. and 0.1 in. respectively.

Selective results from the nonlinear analysis for each model are presented in Table

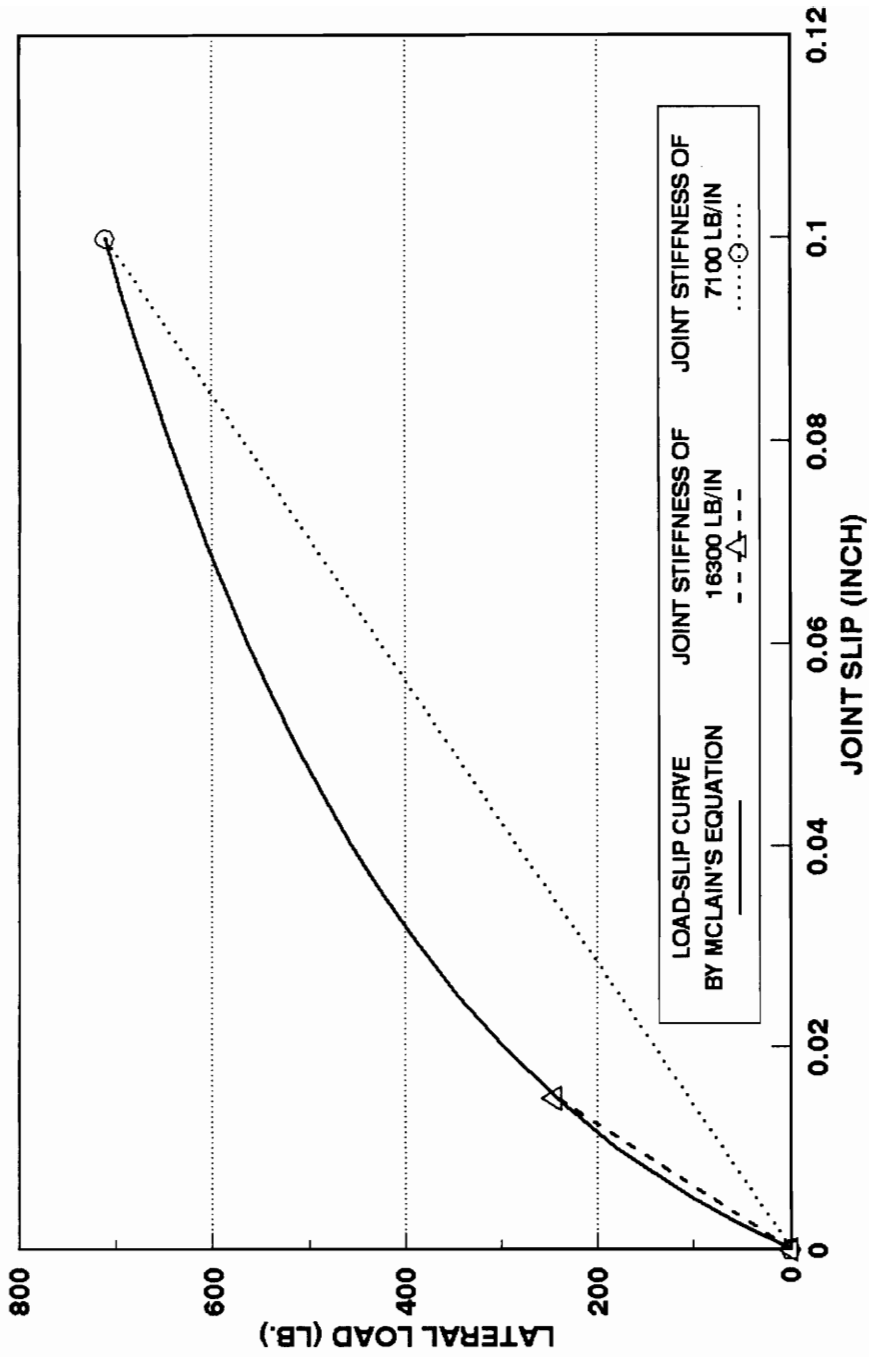


Fig. 6.3 Load-slip curve with constant nail stiffnesses.

6.1. These results include the critical load factor (load factor at limit point), maximum element stress, apex deflection (deflection of node 1), and maximum nail deflection. The nail deflections of each model are computed by the FORTRAN programs MDISP1 and MDISP3 presented in Appendix F and Appendix G, respectively. The nail deflections of the main beams are computed by MDISP1, while the nail deflections of the edge beams are computed by MDISP3. The results from models 2 and 3 are compared with those of model 1 while the results from models 5 and 6 are compared with those of model 4. The load deflection paths (apex deflection) of models 1 to 3 are shown in Fig. 6.4, while the load deflection paths of models 4 to 6 are shown in Fig. 6.5. The downward apex deflection is taken as positive on these load deflection paths.

On the basis of Figs. 6.4 and 6.5, one can observe that the response of the beam/connector models is similar to that of the corresponding truss bracing model. Thus, the fixed support of the beam/connector model does not cause a large difference in response between the truss bracing model and the beam/connector models for this test case.

The models with nonlinear material law have higher critical load factors than the models with linear material law. Thus, the models with nonlinear material law have stiffer response because the models have the longitudinal modulus in compression of $E_{(compression)} = 2.19 \times 10^6$ psi, which is higher than Young's modulus ($E=1.8 \times 10^6$ psi) of linear material models (Telang, 1992, pp. 87-92). The response of the models is not sensitive to the change of connector stiffness because the cross sections of the beams are vertical. For model 2, the maximum

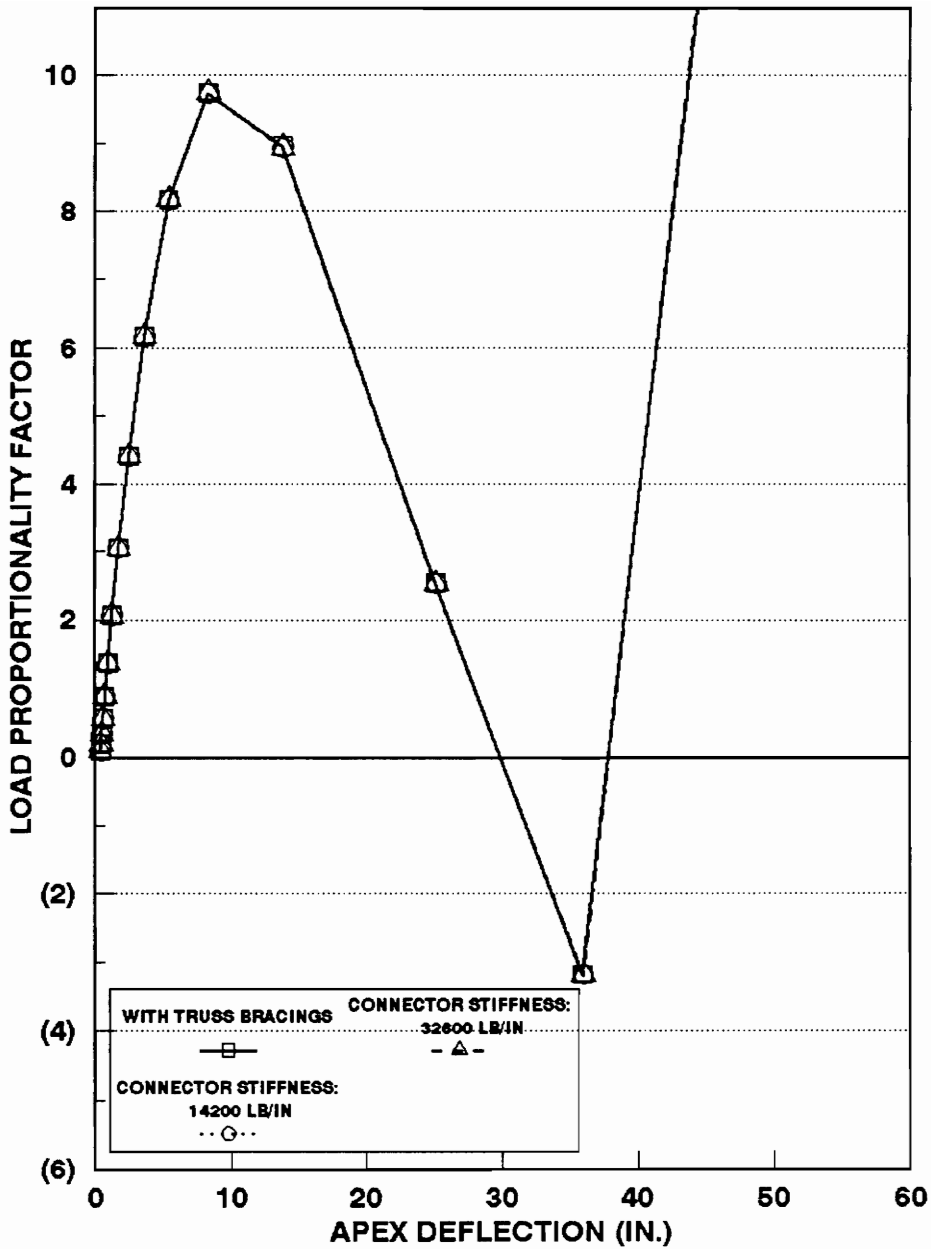


FIG. 6.4 LOAD DEFLECTION PATHS OF DOME CAP MODELS WITH NAILED JOINTS AT BRACING POINTS ($h=0$) (LINEAR MATERIAL LAW; $E=1.8E+06$ psi)

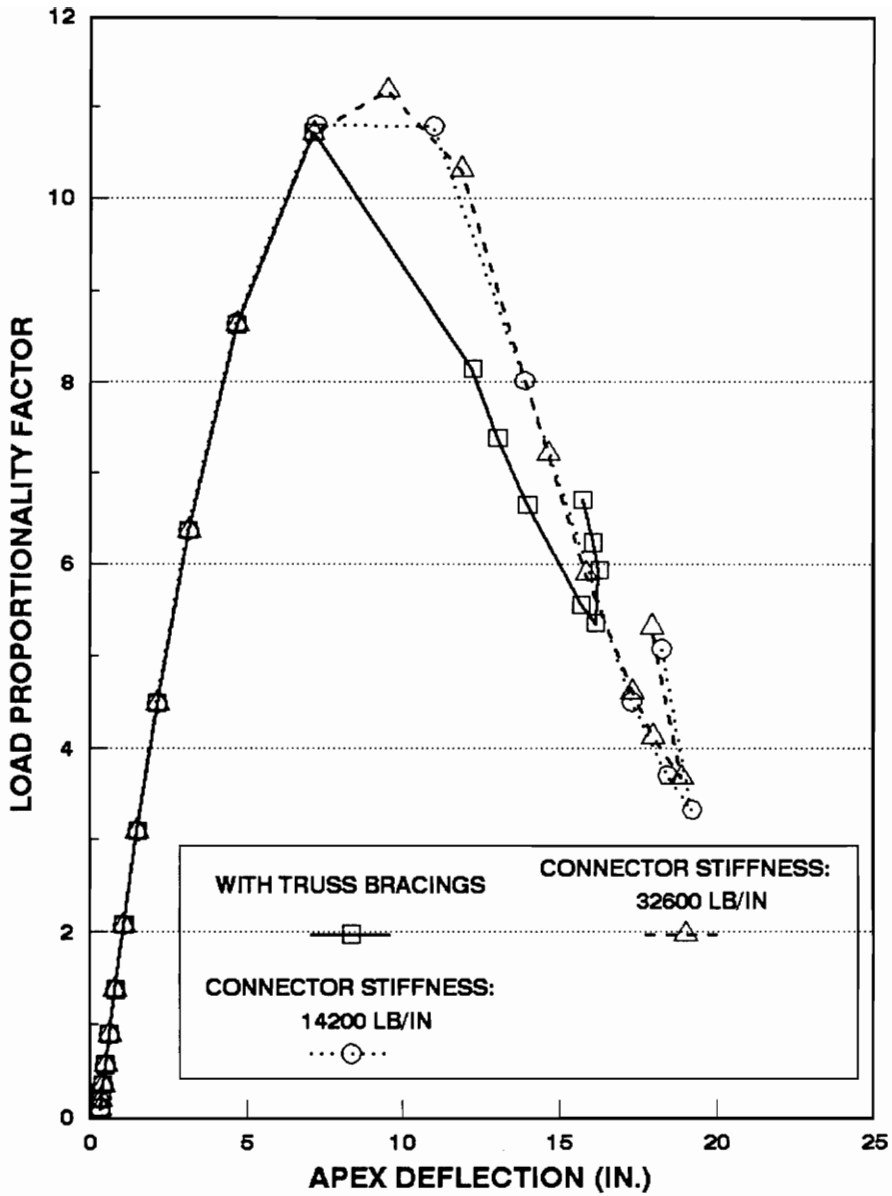


FIG. 6.5 LOAD DEFLECTION PATHS OF DOME CAP MODELS WITH NAILED JOINTS AT BRACING POINTS ($h=0$) (NONLINEAR MATERIAL LAW)

nail deflection (0.032 in.) is not within the nail deflection limit (0.015 in.) of the connector stiffness 32600 lb./in. The same happens in models 5 and 6.

6.3.2 Rigid Link Length $h > 0$

Section 6.3.1 indicates that the response of the dome cap models with the beam/connector elements is similar to that with truss bracings. The spring of the beam/connector model is attached to the centroid of the beam (Section 6.3.1). However, it is unrealistic to attach the spring to the beam centroid (Zahn, 1972). In order to simulate a realistic nail model, the rigid link is used to connect the spring to the top of the beam. This model is able to resist torsion from the beams (see Section 3.3). The objective of this section is to analyze various dome cap models with nailed joints at bracing points ($h > 0$) in order to study the rigid link effects on the beam/connector model.

Six different dome cap models, which are outlined in Table 6.2, are analyzed with ABAQUS. Models 1 and 4 are the dome cap models with the truss bracings. The rest of the models are the dome cap models with nailed joints at bracing points. The rigid link h is taken as 5.5 in. for the main beams, and h is taken as 6.125 in. for the edge beams (see Fig. 3.5). Linear material law ($E = 1.8 \times 10^6$ psi) is applied to models 1 to 3, while nonlinear material law is applied to models 4 to 6.

Selective results from the nonlinear analysis for each model are presented in Table

Table 6.2 Nonlinear analysis results of dome cap models with truss bracing and nailed joints at bracing points ($h > 0$).

Model No.	Material Law	Connector Stiffness (lb./in.)	Critical Load ** Factor	Max. Stress/psi *** (Element no.)	Apex Deflection (in.)	Max. Nail Deflection/in. (node no.)
1 (Truss Bracings)	Linear	-	9.743	8303 (5)	-8.315	-
2 (Nailed Joints)*	Linear	32600 ($h > 0$)	9.736	8431 (5)	-8.326	0.035 (6)
3 (Nailed Joints)*	Linear	14200 ($h > 0$)	9.734	8388 (5)	-8.325	0.078 (6)
4 (Truss Bracings)	Nonlinear	-	10.72	-8375 (5)	-7.101	-
5 (Nailed Joints)*	Nonlinear	32600 ($h > 0$)	10.84	9491 (5)	-10.85	0.049 (6)
6 (Nailed Joints)*	Nonlinear	14200 ($h > 0$)	10.83	9445 (5)	-10.84	0.11 (6)

* nailed joints at bracing points ($h = 5.5$ in. for main beams and $h = 6.125$ in. for edge beams)

** at limit point

*** + : tensile stress; - : compressive stress

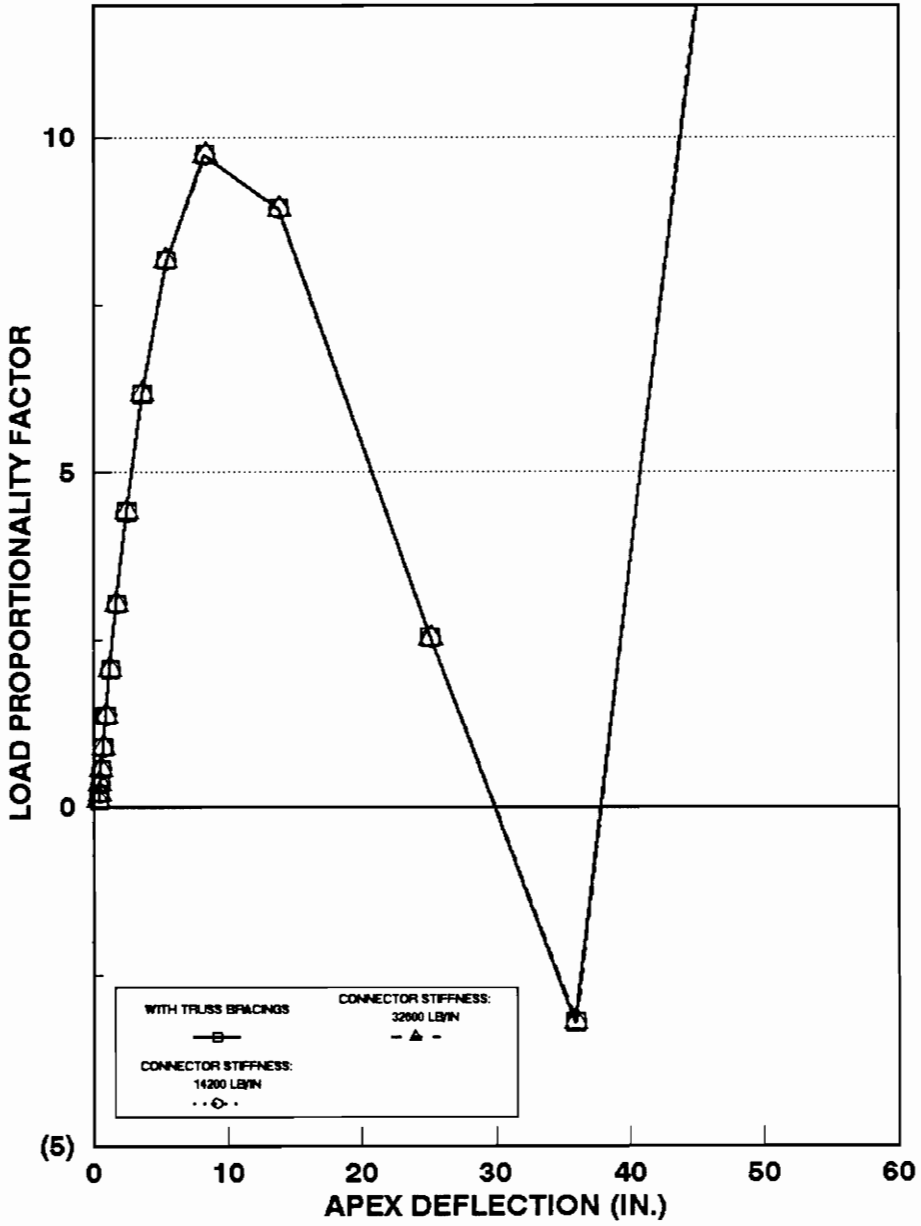


FIG. 6.6 LOAD DEFLECTION PATHS OF DOME CAP MODELS WITH NAILED JOINT AT BRACING POINTS ($h > 0$) (LINEAR MATERIAL LAW; $E = 1.8E + 06$ psi)

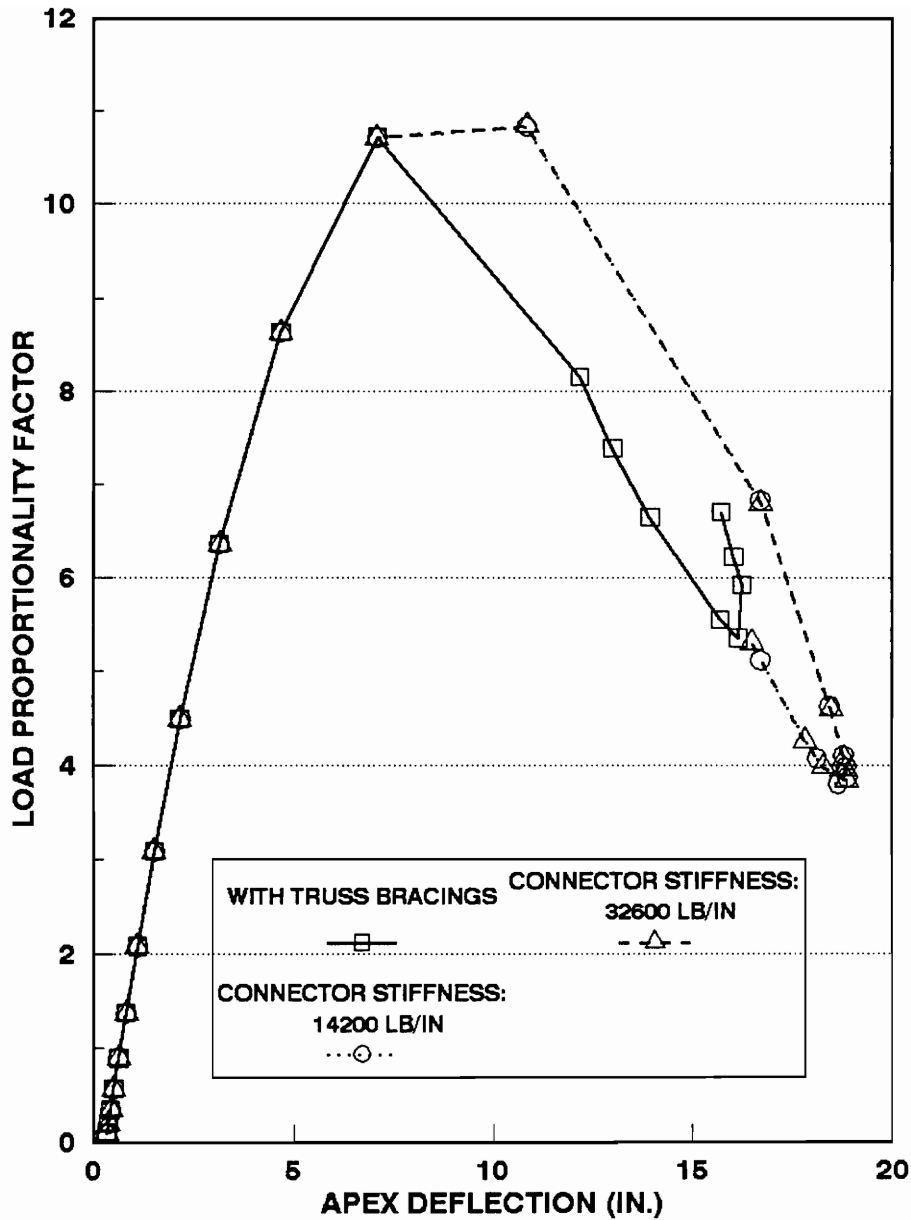


FIG. 6.7 LOAD DEFLECTION PATHS OF DOME CAP MODELS WITH NAILED JOINTS AT BRACING POINTS ($h > 0$) (NONLINEAR MATERIAL LAW)

6.2. The load deflection paths of models 1 to 3 are shown in Fig. 6.6, while the load deflection paths of models 4 to 6 are shown in Fig. 6.7.

On the basis of Figs. 6.6 and 6.7, one can see that the response of the beam/connector models is similar to that of the corresponding truss bracing model. For models 2 and 3, the critical load factor of each model is the same as that of the corresponding model in Table 6.1. Therefore, the response of the beam/connector models is not sensitive to the rigid link effect for this case because there is negligible torsion in the beams for the uniform snow load case (Telang, 1992, p.84).

For models 5 and 6, the critical load factor of each model is a little less than that of the corresponding model in Table 6.1. This does not make sense because the models with $h > 0$ are able to resist torsion from the beams so that they should be stiffer than the models with $h = 0$. Therefore, the initial time increment in nonlinear analysis should be refined in order to obtain more accurate results around the limit point region. "Time" is interpreted by the algorithm as arc length along the equilibrium solution path in a load-deflection plot (ABAQUS 4.8 User's Manual p. 7.3.12-3). The maximum nail deflections of models 2, 5, and 6 exceed the nail deflection limit of the corresponding connector stiffness. However, we need to model the actual nail distribution to assess the quality of the spring element.

6.4 Dome Cap Analysis with 16 Nailed Joints per Beam Element

On the basis of Section 6.3, we can conclude that the behavior of the dome cap models with the beam/connector elements is similar to that of the truss bracing model. Since the spring element of the beam/connector model is created to simulate the nailed joint (not bracing), it is more realistic to put the nailed joints along the beams instead of putting the joints at the bracing points only. The objective of this section is to analyze various dome cap models with 16 nailed joints per beam element to study the response of the beam/connector model. The nailed joints are modeled by the spring elements of the beam/connector model. This section is divided into two subsections: (1) rigid link length $h=0$ (Section 6.4.1), and (2) rigid link length $h>0$ (Section 6.4.2).

6.4.1 Rigid Link Length $h=0$

As mentioned previously in Section 5.2, the spacing of the nailed joints on the beams was assumed to be 8 to 9 in. In this study, we assumed that there are 16 nailed joints (spacing of joints = 8.25 in.) on each beam element, which has the length of 132 in. The rigid link length h is taken as zero in this section.

Six different dome cap models, which are outlined in Table 6.3, are analyzed with

ABAQUS. Models 1 and 4 are the dome cap models with the truss bracings. The other models are the dome cap models with 16 nailed joints on each beam element. The details concerning the locations of the nailed joints can be found in Section 5.2.2.

Selective results of the nonlinear analysis for each model are presented in Table 6.3. The load deflection paths of models 1 to 3 are shown in Fig. 6.8, while the load deflection paths of models 4 to 6 are shown in Fig. 6.9.

On the basis of Figs. 6.8 and 6.9, one can observe that the response of the beam/connector models is similar to that of the corresponding truss bracing model. For models 2 and 3, the critical load factors are higher than those of the corresponding models in Table 6.1 (nailed joints at bracing points) because more lateral stiffness is provided by the models with 16 nailed joints per beam element. Besides, the response of the beam/connector models is not sensitive to the number of nailed joints and the connector stiffness in this case. For models 5 and 6, the critical load factors are less than those of the corresponding models in Table 6.1 (nailed joints at bracing points). Therefore, the refinement of the initial time increment in the nonlinear analysis is needed to obtain more accurate results over the limit point region. The maximum nail deflection for each beam/connector model exceeds the nail deflection limit of the corresponding connector stiffness. As a result, a nonlinear spring element will be needed to simulate the realistic nail behavior. In addition, the load-slip curve up to ultimate load (about joint slip of 0.3 in.) should be obtained from experiments because McLain's formula can only be used to predict the load-slip curve up to the joint slip of 0.1 in. (see Fig. 6.3).

Table 6.3 Nonlinear analysis results of dome cap models with truss bracing and 16 nailed joints per beam element (h=0).

Model No.	Material Law	Connector Stiffness (lb./in.)	Critical Load **	Max. Stress/psi *** (Element no.)	Apex Deflection (in.)	Max. Nail Deflection/in. (node no.)
1 (Truss Bracings)	Linear	-	9.743	8303 (5)	-8.315	-
2 (Nailed Joints)*	Linear	32600 (h=0)	9.88	8117 (5)	-7.906	0.1656 (2)
3 (Nailed Joints)*	Linear	14200 (h=0)	9.803	8196 (5)	-8.127	0.1790 (2)
4 (Truss Bracings)	Nonlinear	-	10.72	-8375 (5)	-7.101	-
5 (Nailed Joints)*	Nonlinear	32600 (h=0)	10.61	-7823 (5)	-6.659	0.1448 (8.25 in from node 3 to node 6)
6 (Nailed Joints)*	Nonlinear	14200 (h=0)	10.90	9374 (5)	-10.65	0.2388 (2)

* 16 nailed joints per beam element (h=0)

** at limit point

*** + : tensile stress; - : compressive stress

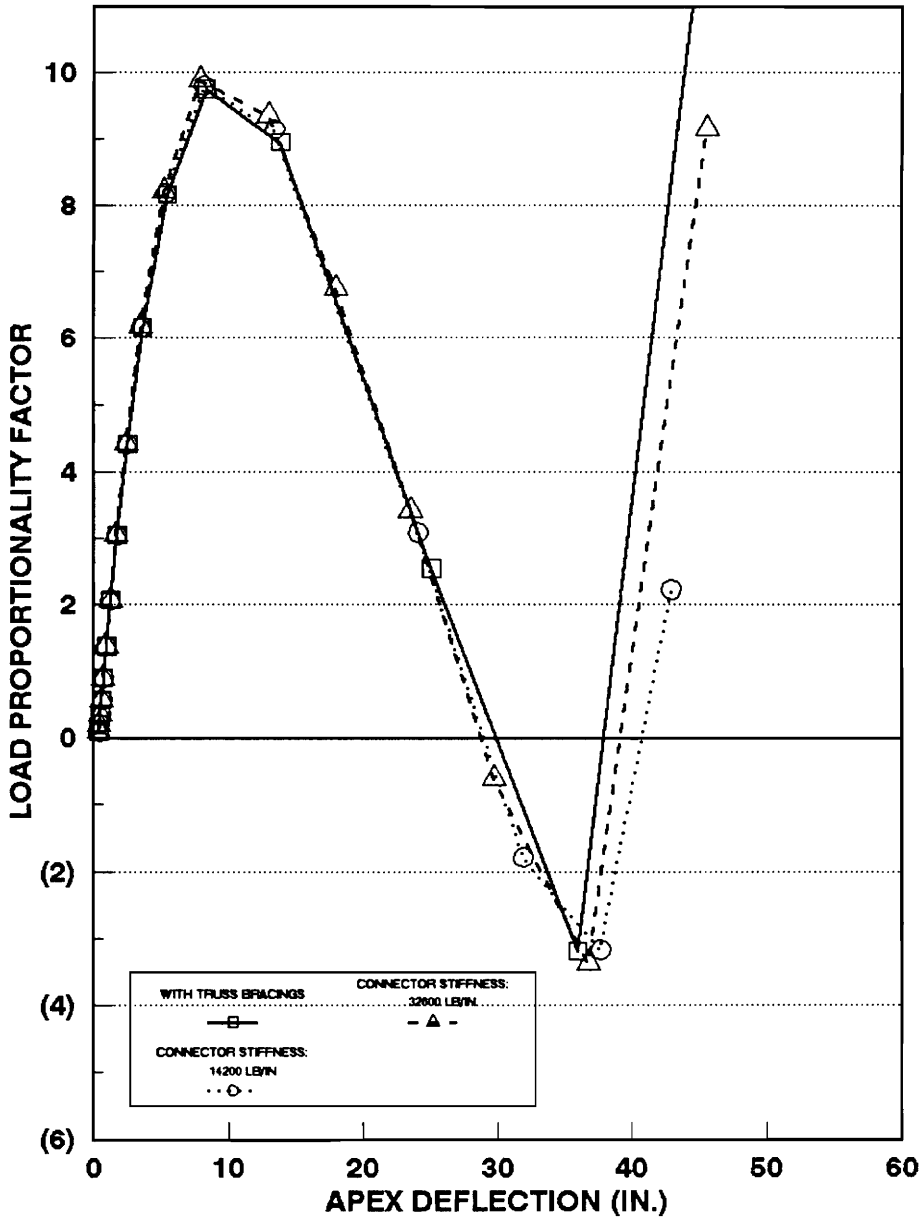


FIG 6.8 LOAD DEFLECTION PATHS OF DOME CAP MODELS WITH 16 NAILED JOINTS PER BEAM ELEMENT (h=0) (LINEAR MATERIAL LAW; E=1.8E+06 psi)

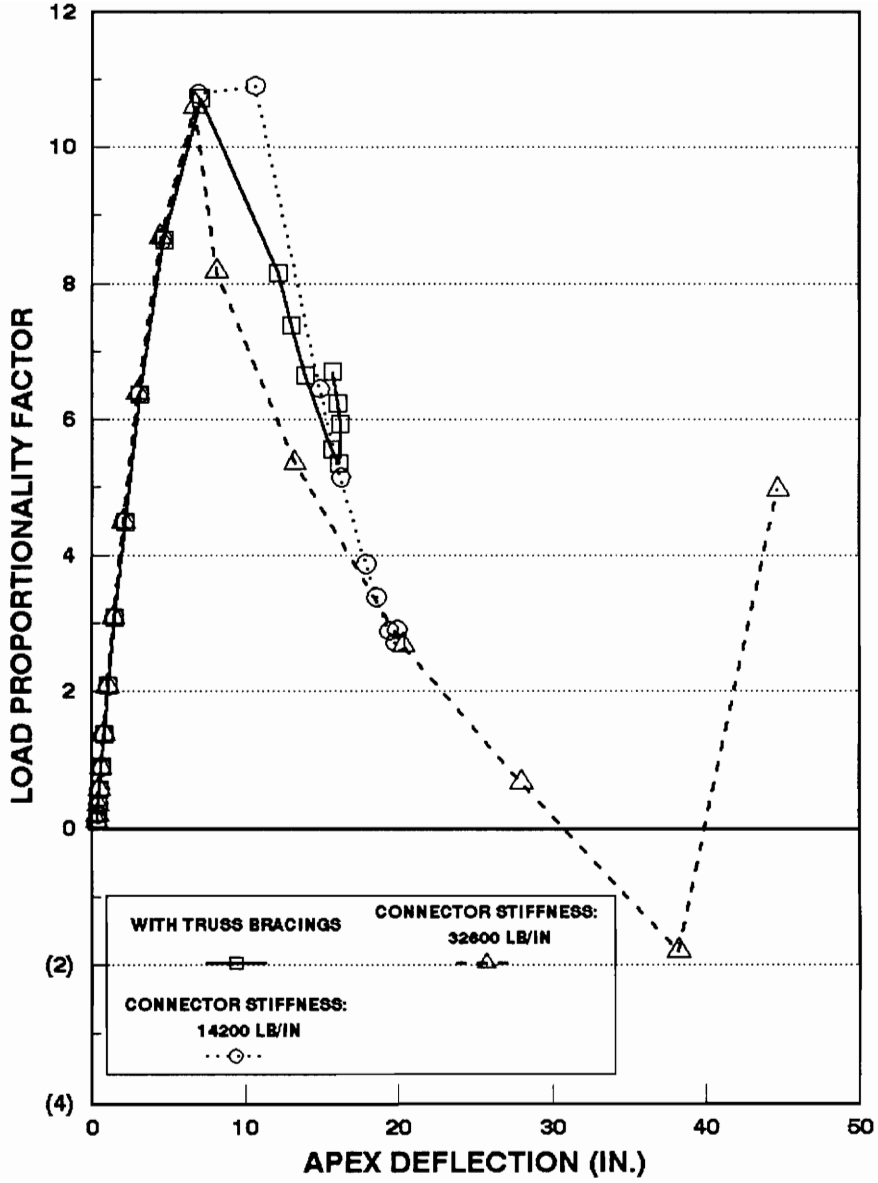


FIG. 6.9 LOAD DEFLECTION PATHS OF DOME CAP MODELS WITH 16 NAILED JOINTS PER BEAM ELEMENT ($h=0$) (NONLINEAR MATERIAL LAW)

6.4.2 Rigid Link Length $h > 0$

The response of the beam/connector models with 16 nailed joints on each beam element ($h=0$) is similar to that of the truss bracing model (Section 6.4.1). If the rigid link length is zero, it implies that the spring is attached to the centroid of the beam cross section. It is more realistic to attach the spring to the top of the beam cross section to model the nail (Zahn, 1972). The objective of this section is to analyze several dome cap models with 16 nailed joints on each beam element, and to study the rigid link effect on the response of the beam/connector models. The rigid link length h is taken as 5.5 in. for the main beams, and h is 6.125 in. for the edge beams.

Six different dome cap models, which are outlined in Table 6.4, are analyzed with ABAQUS. The ABAQUS input file for model 5 is presented in Appendix E. Selective results from the nonlinear analysis for each model are presented in Table 6.4. The load deflection paths of models 1 to 3 are shown in Fig. 6.10, while the load deflection paths of models 4 to 6 are shown in Fig. 6.11.

On the basis of Figs. 6.10 and 6.11, one can observe that the response of the beam/connector models is similar to that of the corresponding truss bracing model. Since the beam/connector model simulates the beam/decking connectors and its response is comparable to that of the truss bracing model, the beam/connector model is a potential model to simulate the decking. The critical load factor of each model is higher than that of the corresponding model in Table

Table 6.4 Nonlinear analysis results of dome cap models with truss bracing and 16 nailed joints per beam element ($h > 0$).

Model No.	Material Law	Connector Stiffness (lb./in.)	Critical Load ** Factor	Max. Stress/psi *** (Element no.)	Apex Deflection (in.)	Max. Nail Deflection/in. (node no.)
1 (Truss Bracings)	Linear	-	9.743	8303 (5)	-8.315	-
2 (Nailed Joints)*	Linear	32600 ($h > 0$)	10.39	7388 (5)	-8.086	0.1818 (2)
3 (Nailed Joints)*	Linear	14200 ($h > 0$)	10.12	7706 (5)	-8.196	0.1877 (2)
4 (Truss Bracings)	Nonlinear	-	10.72	-8375 (5)	-7.101	-
5 (Nailed Joints)*	Nonlinear	32600 ($h > 0$)	11.73	8352 (5)	-10.66	0.2126 (8.25 in from node 3 to node 6)
6 (Nailed Joints)*	Nonlinear	14200 ($h > 0$)	11.20	-8788 (6)	-10.51	0.2369 (8.25 in from node 3 to node 6)

* 16 nailed joints per beam element ($h = 5.5$ in. for main beams and $h = 6.125$ in. for edge beams)

** at limit point

*** + : tensile stress; - : compressive stress

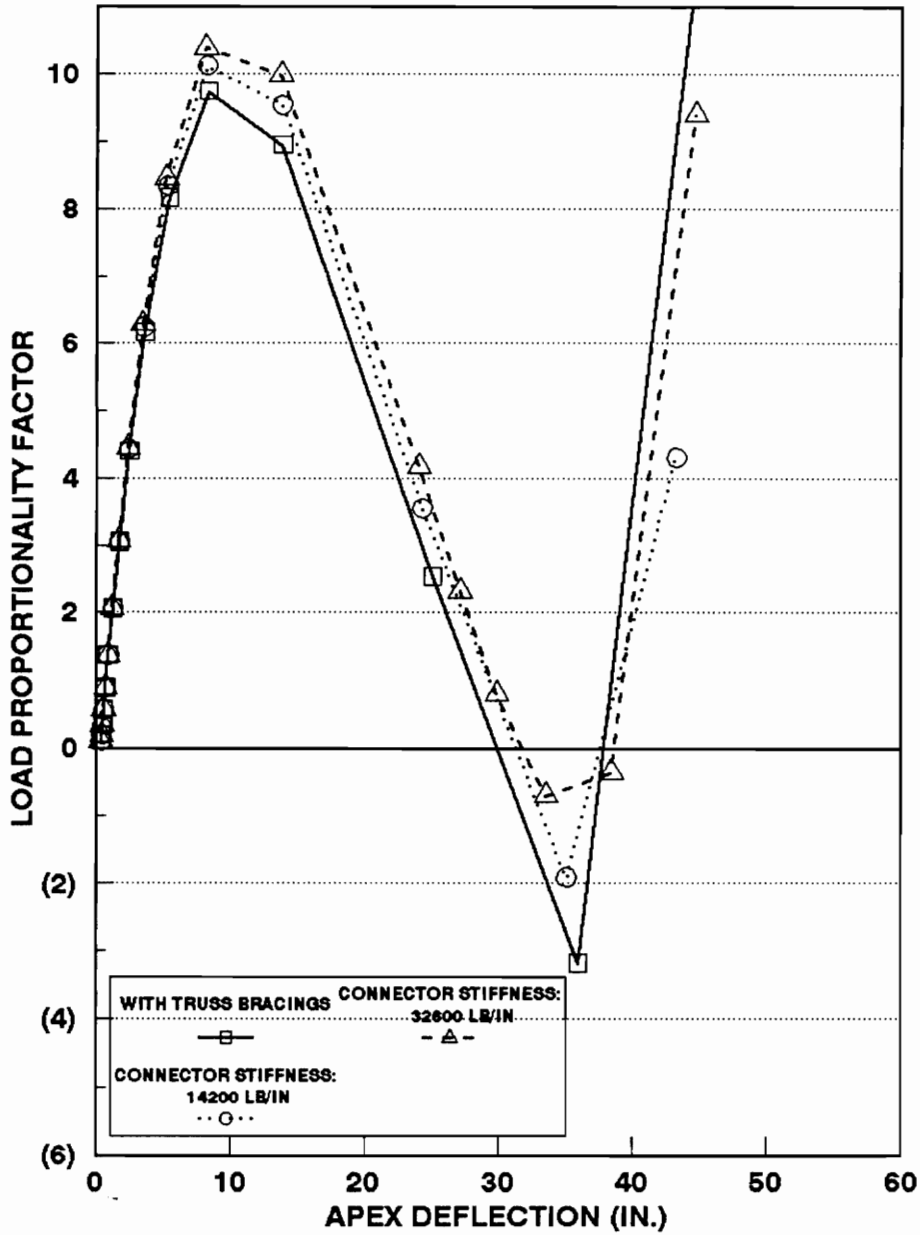


FIG. 6.10 LOAD DEFLECTION PATHS OF DOME CAP MODELS WITH 16 NAILED JOINTS PER BEAM ELEMENT ($h > 0$) (LINEAR MATERIAL LAW; $E = 1.8E+06$ psi)

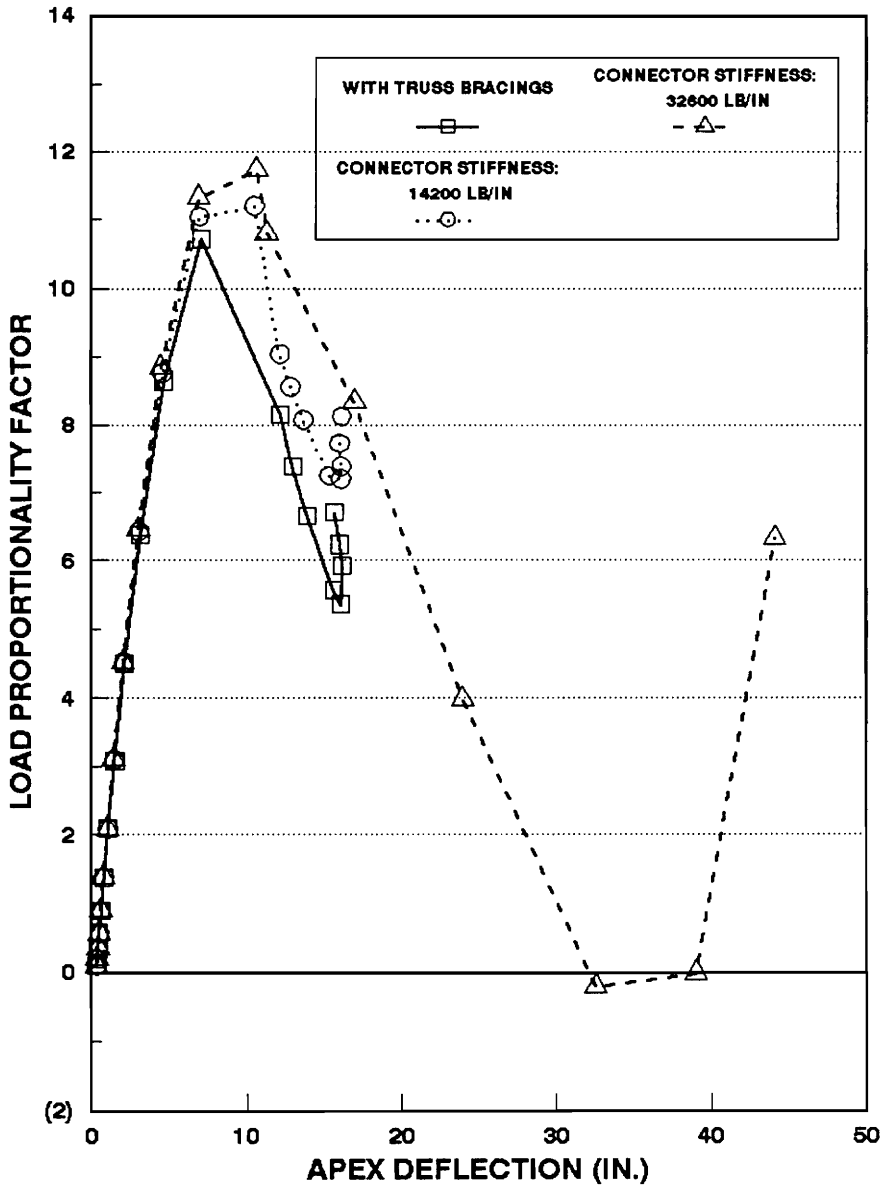


FIG. 6.11 LOAD DEFLECTION PATHS OF DOME CAP MODELS WITH 16 NAILED JOINT PER BEAM ELEMENT ($h > 0$) (NONLINEAR MATERIAL LAW)

6.3 because the models with $h > 0$ are able to resist the torsion from the beams. On the basis of the maximum nail deflection of each model, one can observe that the nonlinear spring element of the beam/connector model should be developed to model the nail behavior in a better way. The real test will come with the complete dome which includes beams whose cross sections are inclined relative to the vertical axis.

Chapter 7

CONCLUSIONS AND RECOMMENDATIONS

7.1 Conclusions

From the limited studies conducted in this research, it is found that:

1. The beam/connector elements can be successfully incorporated in the finite element program ABAQUS by the USER ELEMENT option.
2. Tests of 2-D and 3-D beam/connector elements indicate that an increase in the number of connectors and the connector stiffness increases the percentage difference in reactions between model 1 (beam/connector elements) and model 2 (beam and spring elements) in Tables 4.1 and 4.2.
3. The response of the beam/connector models with the nailed joints at the

bracing points is similar to that of the truss bracing model.

4. The fixed support of the springs in the beam/connector model does not cause large differences in response between the truss bracing model and the beam/connector model.
5. The response of the beam/connector model is not sensitive to the number of nailed joints and the connector stiffness in the dome cap examples.
6. Generally, the maximum nail deflection of each beam/connector model exceeds the nail deflection limit of the corresponding connector stiffness.
7. The response of the beam/connector model is not sensitive to the rigid link effect because there is negligible torsion in the beams of the dome cap for the uniform snow load case.
8. Unexpected response of some of the beam/connector models is due to the initial time increment in the nonlinear analysis being not small enough to obtain more accurate results around the limit point region.
9. The beam/connector models with 16 nailed joints on each beam are stiffer than the models with the nailed joints at the bracing points.
10. The beam/connector model with 16 nailed joints on each beam element ($h > 0$) is a potential model to simulate the decking effects for the complete dome.

7.2 Recommendations

1. Experimental tests should be conducted to obtain the actual lateral load-slip curve of the nailed joint in the dome.
2. Other loading conditions (e.g., half snow load) should be applied to the dome cap models to study their effects on the response of the beam/connector elements.
3. Two element mesh per beam is used for this study. The mesh should be refined to obtain more accurate results of the dome cap models.
4. The initial time increment in the nonlinear analysis should be refined to obtain more accurate results around the limit point region.
5. A nonlinear spring element should be formulated according to the load-slip curve in order to model the actual behavior of the nailed joint.
6. Analyses of the complete dome models with the beam/connector elements should be conducted.
7. Results of the finite element analyses should be verified by experimental tests of scaled dome cap models.

REFERENCES

1. ABAQUS, **General-Purpose Finite Element System**, Hibbitt, Karlsson and Sorensen, Inc., 100 Medway Street, Providence, RI 02906, U.S.A.
2. American Institute of Timber Construction. (1985). **Timber Construction Manual**, John Wiley and Sons, New York.
3. Breyer, D. E. (1980). **Design of Wood Structures**, McGraw-Hill Book Company, New York.
4. Bathe, K. J. (1982). **Finite Element Procedures in Engineering Analysis**, Prentice-Hall, Englewood Cliffs, NJ.
5. Cook, R. D., D. S. Malkus, and M. E. Plesha. (1989). **Concepts and Applications of Finite Element Analysis**, John Wiley & Sons, Inc., New York.
6. Davalos, J. F. (1989). **Geometrically Nonlinear Finite Element Analysis of a Glulam Timber Dome**, Ph. D. Dissertation, Virginia Polytechnic Institute and State University, Blacksburg, Virginia.

7. Dolan, J. D. (1989). **The Dynamic Response of Timber Shear Walls**, Ph. D. Thesis, University of British Columbia, Vancouver, Canada.
8. Ehlbeck, J. (1979). **Nailed Joints in Wood Structures**, Wood Research and Wood Construction Laboratory, Virginia Polytechnic Institute and State University, Blacksburg, Virginia.
9. Foschi, R. O. (1969). **The Load-Slip Characteristics of Nails**. Dept. of the Environment, Canadian Forestry Service, Western Forest Products Lab., Vancouver, British Columbia.
10. Goodman, J. R. (1967). **Layered Wood Systems with Interlayer Slip**, Ph.D. Dissertation, University of California in Berkeley, Berkeley, California.
11. Holzer, S. M. (1985). **Computer Analysis of Structures**, Elsevier Science Publishing Co., Inc., New York.
12. Holzer, S. M. (1991). **Finite Element Analysis of Structures**, Course Notes for CE 5414, Virginia Polytechnic Institute and State University, Blacksburg, Virginia.
13. Holzer, S. M., C. H. Wu, and J. Tissaoui. (1991). **Finite Element Stability Analysis of a Glulam Dome**. International Journal of Space Structures, to appear.
14. Hoyle, R. J. (1973). **Wood Technology in the Design of Structures**,

Mountain Press Publishing Company, Missoula, Montana.

15. Jansson, I. (1955). **Effect of Nail Characteristics on the Load-Carrying Capacity of a Nailed Joint**, M. S. thesis, Iowa State College, Ames, Iowa.
16. Jenkinson, P. M., and J. J. Zahn. (1972). **Lateral Stability of Beam and Deck Structure**. Journal of the Structural Division, ASCE, Vol. 98 (ST3), pp. 599-609.
17. Kuenzi, E. W. (1955). **Theoretical Design of a Nailed or Bolted Joint under Lateral Load**. Report no. D1951, U. S. Dept. of Agriculture, Forest Service Production Laboratory, Madison, Wisconsin.
18. Lantos, G. (1969). **Load Distribution in a Row of Fasteners Subjected to Lateral Load**, Wood Science, Vol. 1, No.3, pp. 129-136.
19. Mack, J. J. (1977). **The Load- Displacement Curve for Nailed Joints**. Journal of Institute of Wood Science, Vol. 7, No. 6, pp. 34-36.
20. McLain, T. E. (1975). **Curvilinear Load-Slip Relations in Laterally Loaded Nailed Joints**, Ph. D. Dissertation, Colorado State University, Fort Collins, Colorado.
21. Mohammad, H. (1990). **Modeling the Roof Deck and Determining its Effect on the Stability of a Glulam Timber Dome**, M. E. Project, Virginia Polytechnic

Institute and State University, Blacksburg, Virginia.

22. Morris, E. N. (1967). **The Rotational Rigidity of Nailed Joints in Double Shear and Subjected to Short Term Loading**, TRADA Research Report E/RR/25, Timber Research and Development Association, England.
23. National Forest Products Association. (1986). **National Design Specification (NDS) for Wood Construction**. NFPA, Washington, D. C.
24. Pellicane, P. J., J. L. Stone and M. D. Vanderbilt. (1991). **Generalized Model for Lateral Load Slip of Nailed Joints**, Journal of Materials in Civil Engineering, Vol. 3, No.1, pp. 60-77.
25. Ramm, E. (1980). **Strategies for Tracing Nonlinear Response near Limit Points**, Europe-US Workshop, Nonlinear Finite Element Analysis in Structural Mechanics, Bochum, G.F.R.
26. Ramm, E., and H. Stegmuller. (1982). **The Displacement Finite Element Method in Nonlinear Buckling Analysis of Shells**, Proceedings of a State-of-the-Art Colloquium in Buckling of Shells, Universitat Stuttgart, Germany, pp. 201-235.
27. Smith, I. (1980). **A Review of Analytical and Empirical Models Used to Predict the Strength and Stiffness Characteristics of Timber Joint with Dowel Type Connectors**. TRADA Research Rpt. No. 1/80. Timber Research and

Development Association, England.

28. Telang, N. M. (1992). **Stability Analysis of a Glulam Dome with Nonlinear Material Law**, M. S. Thesis, Virginia Polytechnic Institute and State University. Blacksburg, Virginia.
29. Thomas, B., and S. K. Malhotra. (1985). **Behavior of Timber Joints with Multiple Nails**, Journal of the Structural Engineering Division, ASCE, Vol. 111 (ST5), pp. 973-991.
30. USDA Forest Service. (1987). **Wood Handbook**. Forest Products Laboratory, Hemisphere Publishing Corporation, New York.
31. Wilkinson, T. L. (1971). **Theoretical Lateral Resistance of Nailed Joints**, Journal of the Structural Division, ASCE, Vol. 97 (ST5), pp. 1381-1398.
32. Wilkinson, T. L. (1972a). **Effect of Deformed Shanks, Prebored Lead Holes and Grain Orientation on the Elastic Bearing Constant for Laterally Loaded Nailed Joints**. Research Paper FPL 192, U.S.D.A. Forest Service, Forest Products Lab., Madison, Wisconsin.
33. Wilkinson, T. L. (1972b). **Analysis of Nailed Joints with Dissimilar Members**, Journal of the Structural Division, ASCE, Vol. 98 (ST9), pp. 2005 - 2013.

34. Wilkinson, T. L. (1974a). **Elastic Bearing Constants for Sheathing Materials**, Research Paper FPL 224, U.S.D.A. Forest Service, Forest Products Lab., Madison, Wisconsin.

35. Wilkinson, T. L. (1974b). **Elastic Bearing Constant of Wood: Effects of Moisture Content Conditions**. Research Paper FPL 235, U.S.D.A. Forest Service, Forest Products Lab., Madison, Wisconsin.

36. Wu, C. H. (1991). **Modeling and Stability Investigation of a Glulam Dome**, M. S. Thesis, Virginia Polytechnic Institute and State University, Blacksburg, Virginia.

37. Zahn, J. J. (1972). **Shear Stiffness of Two-Inch Wood Decks for Roof Systems**. USDA, Forest Service Research Paper FPL 115, Forest Products Laboratory, Madison, Wisconsin.

APPENDIX A

```

C*****
C PROGRAM TO COMPUTE THE CONNECTOR STIFFNESS MATRIX OF EACH
C SPRING ON A BEAM, COMBINE ALL THE MATRICES INTO ONE MATRIX FOR
C INPUT AND WRITE COMMAND LINES FOR ABAQUS INPUT FILE.
C ** MAIN BEAMS 1 **
C BY MOSES TSANG ..... (703) 552 - 2801
C SANDEEP KAVI ..... (703) 953 - 0409
C THE PROGRAM REQUIRES SBEM1 DAT, MKS1 DAT,SNODE DAT AND
C MKS1 EXEC FILES
C
C THE OUTPUT IS WRITTEN TO MKS1 OUT FILE
C
C SEPT. 3, 1992.
C
C*****

REAL S11,S21,S12,S22,S32,S42
REAL XCOS(1700),YCOS(1700),ZCOS(1700),XC(2700),YC(2700),ZC(2700),
1 XCC(2700),YCC(2700),ZCC(2700),ZCOS1(1700),
2 SM(12,12),SM1(12,12),SM2(12,12),R(12,12),TR(12,12),
3 T1(1700),T2(1700),T3(1700),N11(1700),N12(1700),N13(1700),
4 N21(1700),N22(1700),N23(1700)
OPEN(UNIT=10,STATUS='OLD')
OPEN(UNIT=20,STATUS='OLD')
OPEN(UNIT=25,STATUS='OLD')
OPEN(UNIT=30,STATUS='UNKNOWN')
C
C **THE BEAM TYPE.
WRITE(30,105)
C
CC #####READ FROM MKS1 DAT
READ (25,*) S,H,NS,NMAX,NNODE,NELEM
C
C***** READ FROM MKS1 DAT *****
C S=SPRING STIFFNESS, H=RIGID BEAM LENGTH,
C NS=NUMBER OF SPRINGS,
C NMAX=MAX. NUMBER OF ELEMENTS IN THE STRUCTURE
C NNODE=TOTAL NO. OF NODES, NELEM= TOTAL NO. OF ELEMENTS
C
CC #####READ NODES FROM, SNODE DAT A
DO 10 I=1,NNODE
READ (10,*) N, X, Y, Z
XCOS(I) = X
YCOS(I) = Y

```

```

        ZCOS(I) = Z+1387.66
10  CONTINUE
CC
CC ##### MAIN BEAMS1 6.75X11, SBEM1 DAT A
C
        DO 100 N=1,NELEM
            READ (20,*) NE, N1, N2
C
C***** READ FROM SBEM1 DAT *****
C        NE = THE ELEMENT NUMBER.
C        N1,N2=TO WHICH NODES THE BEAM ATTACHED.
C*****
C
C THE STIFFNESS MATRIX IS IN THE LOCAL FRAME OF REFERENCE. TO USE IT
C IN THE INPUT FILE FOR ABAQUS IN THE DOME CAP/DOME ANALYSIS, WE NEED
C TO FIND THE GLOBAL STIFFNESS MATRIX. TO DO THIS THE ROTATION MATRIX
C FOR THE BEAMS AND ITS TRANSPOSE IS CALCULATED.
C THE TRANSFORMATION FROM THE LOCAL TO THE GLOBAL IS OBTAINED BY
C PRE-MULTIPLYING THE LOCAL STIFFNESS MATRIX BY THE TRANSPOSE OF
C ROTATION MATRIX AND THEN POST-MULTIPLYING THE PRODUCT BY THE
C ROTATION MATRIX.
C
C INITIALIZE THE ROTATION & TRANSPOSE ROTATION MATRICES.
C
        DO 40 I=1,12
            DO 45 J=1,12
                R(I,J) = 0.0
                TR(I,J) = 0.0
                SM1(I,J)=0.0
                SM2(I,J)=0.0
45     CONTINUE
40     CONTINUE
C
C DEFINING THE ROTATION MATRIX.
C
        T1(NE) = XCOS(N2) - XCOS(N1)
        T2(NE) = YCOS(N2) - YCOS(N1)
        T3(NE) = ZCOS(N2) - ZCOS(N1)
        TNORM = (T1(NE)**2+T2(NE)**2+T3(NE)**2)**0.5
C
        N11(NE) = YCOS(N1) * ZCOS(N2) - ZCOS(N1) * YCOS(N2)
        N12(NE) = -(XCOS(N1) * ZCOS(N2) - ZCOS(N1) * XCOS(N2))
        N13(NE) = XCOS(N1) * YCOS(N2) - YCOS(N1) * XCOS(N2)
        N1NORM = (N11(NE)**2+N12(NE)**2+N13(NE)**2) ** 0.5
C
        DO 50 I=1,10,3
            R(I,I) = T1(NE)/TNORM
            R(I,I+1)=T2(NE)/TNORM
            R(I,I+2)=T3(NE)/TNORM
            R(I+1,I)=N11(NE) / N1NORM
            R(I+1,I+1)=N12(NE) / N1NORM

```

```

R(I+1,I+2)=N13(NE) / N1NORM
R(I+2,I)=R(1,2)*R(2,3)-R(2,2)*R(1,3)
R(I+2,I+1)=R(2,1)*R(1,3)-R(1,1)*R(2,3)
R(I+2,I+2)=R(1,1)*R(2,2)-R(1,2)*R(2,1)
50 CONTINUE
C
C THE TRANSPOSE OF THE ROTATION MATRIX.
C
DO 60 I=1,12
DO 65 J=1,12
TR(I,J) = R(J,I)
65 CONTINUE
60 CONTINUE
C
C***** SET EACH ENTRY IN SM(12,12) TO BE ZERO *****
C
DO 20 J=1,12
DO 25 I=1,12
SM(I,J)=0.0
25 CONTINUE
20 CONTINUE
C
C***** READ THE LOCATION OF SPRING AND DEFINE *****
C INTERPOLATION FUNCTIONS
C
C ##### SPACE=SPACING BETWEEN EACH SPRING
SPACE=TNORM/NS
DO 30 L=1,NS
XI=SPACE*L/TNORM
S11=-(1.-XI)
S21=-XI
S12=1.-3.*XI**2.+2.*XI**3.
S22=(XI-2.*XI**2.+XI**3.)*TNORM
S32=3.*XI**2.-2.*XI**3.
S42=(XI**3.-XI**2.)*TNORM
C
C***** ASSIGN VALUES TO UPPER TRIANGLE MATRIX ENTRIES *****
C***** MATRIX IS THE SAME AS THAT IN EQ.(5.26) OF TSANG (1992) *****
C
SM(2,2)=SM(2,2)+S*S12*S12
SM(2,4)=SM(2,4)+(S*H*S12*S11)
SM(4,4)=SM(4,4)+S*H*H*S11*S11
SM(2,6)=SM(2,6)+(S*S12*S22)
SM(4,6)=SM(4,6)+S*H*S11*S22
SM(6,6)=SM(6,6)+S*S22*S22
SM(2,8)=SM(2,8)+S*S12*S32
SM(4,8)=SM(4,8)+(S*H*S11*S32)
SM(6,8)=SM(6,8)+(S*S22*S32)
SM(8,8)=SM(8,8)+S*S32*S32
SM(2,10)=SM(2,10)+(S*H*S12*S21)
SM(4,10)=SM(4,10)+S*H*H*S11*S21

```

```

SM(6,10)=SM(6,10)+S*H*S22*S21
SM(8,10)=SM(8,10)+(S*H*S32*S21)
SM(10,10)=SM(10,10)+S*H*H*S21*S21
SM(2,12)=SM(2,12)+(S*S12*S42)
SM(4,12)=SM(4,12)+S*H*S11*S42
SM(6,12)=SM(6,12)+S*S22*S42
SM(8,12)=SM(8,12)+(S*S32*S42)
SM(10,12)=SM(10,12)+S*H*S21*S42
SM(12,12)=SM(12,12)+S*S42*S42
30 CONTINUE
C
C ***** ASSIGN VALUES TO THE LOWER TRIANGLE ENTRIES IN MATRIX *****
SM(4,2)=SM(2,4)
SM(6,2)=SM(2,6)
SM(6,4)=SM(4,6)
SM(8,2)=SM(2,8)
SM(8,4)=SM(4,8)
SM(8,6)=SM(6,8)
SM(10,2)=SM(2,10)
SM(10,4)=SM(4,10)
SM(10,6)=SM(6,10)
SM(10,8)=SM(8,10)
SM(12,2)=SM(2,12)
SM(12,4)=SM(4,12)
SM(12,6)=SM(6,12)
SM(12,8)=SM(8,12)
SM(12,10)=SM(10,12)
C
C PRE-MULTIPLYING STIFFNESS MATRIX FOR THE USER ELEMENT BY THE
C TRANSPOSE OF THE ROTATION MATRIX.(TR X SM = SM1)
C
DO 70 I=1,12
DO 75 J=1,12
DO 80 K=1,12
SM1(I,J) = SM(I,J) + TR(I,K)*SM(K,J)
80 CONTINUE
75 CONTINUE
70 CONTINUE
C
C POST-MULTIPLYING THE ABOVE OBTAINED MATRIX BY
C THE ROTATION MATRIX.(SM1 X R = SM2).
C THIS (SM2) MATRIX WILL BE USED IN THE INPUT FILE FOR ABAQUS.
C
DO 85 I=1,12
DO 90 J=1,12
DO 95 K=1,12
SM2(I,J) = SM1(I,J) + SM1(I,K)*R(K,J)
95 CONTINUE
90 CONTINUE
85 CONTINUE
C

```

```

C***** WRITE ABAQUS COMMAND LINES TO MKS1 OUT *****
C
C **COMMAND LINES.
  WRITE(30,110) NE
  WRITE(30,115)
  WRITE(30,120) NE,NE
  WRITE(30,125)NE+NMAX,N1,N2
  WRITE(30,130)
C **THE GLOBAL STIFFNESS MATRIX.
  WRITE(30,135) SM2(1,1)
  WRITE(30,140) SM2(1,2),SM2(2,2)
  WRITE(30,145) SM2(1,3),SM2(2,3),SM2(3,3)
  WRITE(30,150) SM2(1,4),SM2(2,4),SM2(3,4),SM2(4,4)
  WRITE(30,150) SM2(1,5),SM2(2,5),SM2(3,5),SM2(4,5)
  WRITE(30,135) SM2(5,5)
  WRITE(30,150) SM2(1,6),SM2(2,6),SM2(3,6),SM2(4,6)
  WRITE(30,140) SM2(5,6),SM2(6,6)
  WRITE(30,150) SM2(1,7),SM2(2,7),SM2(3,7),SM2(4,7)
  WRITE(30,145) SM2(5,7),SM2(6,7),SM2(7,7)
  WRITE(30,150) SM2(1,8),SM2(2,8),SM2(3,8),SM2(4,8)
  WRITE(30,150) SM2(5,8),SM2(6,8),SM2(7,8),SM2(8,8)
  WRITE(30,150) SM2(1,9),SM2(2,9),SM2(3,9),SM2(4,9)
  WRITE(30,150) SM2(5,9),SM2(6,9),SM2(7,9),SM2(8,9)
  WRITE(30,135) SM2(9,9)
  WRITE(30,150) SM2(1,10),SM2(2,10),SM2(3,10),SM2(4,10)
  WRITE(30,150) SM2(5,10),SM2(6,10),SM2(7,10),SM2(8,10)
  WRITE(30,140) SM2(9,10),SM2(10,10)
  WRITE(30,150) SM2(1,11),SM2(2,11),SM2(3,11),SM2(4,11)
  WRITE(30,150) SM2(5,11),SM2(6,11),SM2(7,11),SM2(8,11)
  WRITE(30,145) SM2(9,11),SM2(10,11),SM2(11,11)
  WRITE(30,150) SM2(1,12),SM2(2,12),SM2(3,12),SM2(4,12)
  WRITE(30,150) SM2(5,12),SM2(6,12),SM2(7,12),SM2(8,12)
  WRITE(30,150) SM2(9,12),SM2(10,12),SM2(11,12),SM2(12,12)
C **COMMAND LINE.
  WRITE(30,160) NE
100 CONTINUE
CC#####
#####
105  FORMAT ('**',35('-'),'MAIN BEAMS 1/USER ELEMENTS')
C
110  FORMAT ('*USER ELEMENT,NODES=2,TYPE=U',I4,',LINEAR')
115  FORMAT ('1,2,3,4,5,6')
120  FORMAT ('*ELEMENT,TYPE=U',I4,',ELSET=C',I4)
125  FORMAT (I4,',',I4,',',I4)
130  FORMAT ('*MATRIX,TYPE=STIFFNESS')
135  FORMAT(G12.4)
140  FORMAT(G12.4,',',G12.4)
145  FORMAT(G12.4,',',G12.4,',',G12.4)
150  FORMAT(G12.4,',',G12.4,',',G12.4,',',G12.4)
160  FORMAT ('*UEL PROPERTY,ELSET=C',I4)
  END

```

APPENDIX B

```

C*****
C PROGRAM TO COMPUTE THE CONNECTOR STIFFNESS MATRIX OF EACH
C SPRING ON A BEAM, COMBINE ALL THE MATRICES INTO ONE MATRIX FOR
C INPUT AND WRITE COMMAND LINES FOR ABAQUS INPUT FILE.
C ** EDGE BEAMS **
C BY MOSES TSANG ..... (703) 552 - 2801
C SANDEEP KAVI ..... (703) 953 - 0409
C THE PROGRAM REQUIRES SEBEM DAT,MKS3 DAT,MKS3 EXEC FILES, AND
C SNODE DAT
C THE OUTPUT IS WRITTEN TO MKS3 OUT FILE
C
C SEPT. 3, 1992.
C
C*****

REAL S11,S21,S12,S22,S32,S42
REAL XCOS(1700),YCOS(1700),ZCOS(1700),XC(2700),YC(2700),ZC(2700),
1 XCC(2700),YCC(2700),ZCC(2700),ZCOS1(1700),
2 SM(12,12),SM1(12,12),SM2(12,12),R(12,12),TR(12,12),
3 T1(1700),T2(1700),T3(1700),N11(1700),N12(1700),N13(1700),
4 N21(1700),N22(1700),N23(1700)
OPEN(UNIT=10,STATUS='OLD')
OPEN(UNIT=20,STATUS='OLD')
OPEN(UNIT=25,STATUS='OLD')
OPEN(UNIT=30,STATUS='UNKNOWN')

C
C **THE BEAM TYPE.
WRITE(30,105)

C
CC ##### READ FROM MKS3 DAT
READ (25,*) S,H,NS,NMAX,NNODE,NELEM

C
C***** READ FROM MKS3 DAT *****
C S=SPRING STIFFNESS, H=RIGID BEAM LENGTH,
C NS=NUMBER OF SPRINGS.
C NMAX=MAX. NUMBER OF ELEMENTS IN THE STRUCTURE
C NNODE=TOTAL NO. OF NODES.
C NELEM=TOTAL NO. OF ELEMENTS.
C*****
CC ##### READ NODES FROM, SNODE DAT A
DO 10 I=1,NNODE
READ (10,*) N, X, Y, Z
XCOS(I) = X
YCOS(I) = Y

```

```

CC ###ZCOS1 = Z-190.46 FOR EDGE BEAMS NOT ON THE GREAT CIRCLE.
CC ###ZCOS1 = Z+1387.66 FOR EDGE BEAMS ON THE GREAT CIRCLE.
    ZCOS1(I) = Z-190.46
10  CONTINUE
CC##### READ EDGE BEAMS 12.25X3.0, SEBEM DAT A
C
    DO 100 N=1,NELEM
        READ (20,*) NE, N1, N2
C
C***** READ FROM SEBEM DAT *****
C    NE = THE ELEMENT NUMBER.
C    N1,N2=TO WHICH NODES THE BEAM ATTACHED.
C
C THE STIFFNESS MATRIX IS IN THE LOCAL FRAME OF REFERENCE. TO USE IT
C IN THE INPUT FILE FOR ABAQUS IN THE DOME CAP/DOME ANALYSIS, WE NEED
C TO FIND THE GLOBAL STIFFNESS MATRIX. TO DO THIS THE ROTATION MATRIX
C FOR THE BEAMS AND ITS TRANSPOSE IS CALCULATED.
C THE TRANSFORMATION FROM THE LOCAL TO THE GLOBAL IS OBTAINED BY
C PRE-MULTIPLYING THE LOCAL STIFFNESS MATRIX BY THE TRANSPOSE OF
C ROTATION MATRIX AND THEN POST-MULTIPLYING THE PRODUCT BY THE
C ROTATION MATRIX.
C
C INITIALIZE THE ROTATION & TRANSPOSE ROTATION MATRICES.
C
    DO 40 I=1,12
        DO 45 J=1,12
            R(I,J) = 0.0
            TR(I,J) = 0.0
            SM1(I,J)=0.0
            SM2(I,J)=0.0
45    CONTINUE
40    CONTINUE
C
    T1(NE) = XCOS(N2) - XCOS(N1)
    T2(NE) = YCOS(N2) - YCOS(N1)
    T3(NE) = ZCOS1(N2) - ZCOS1(N1)
    TNORM = (T1(NE)**2+T2(NE)**2+T3(NE)**2)**0.5
C
    N11(NE) = YCOS(N1) * ZCOS1(N2) - ZCOS1(N1) * YCOS(N2)
    N12(NE) = -(XCOS(N1) * ZCOS1(N2) - ZCOS1(N1) * XCOS(N2))
    N13(NE) = XCOS(N1) * YCOS(N2) - YCOS(N1) * XCOS(N2)
    N1NORM = (N11(NE)**2+N12(NE)**2+N13(NE)**2) ** 0.5
C
    N21(NE) = T2(NE)*N13(NE)-T3(NE)*N12(NE)
    N22(NE) = T3(NE)*N11(NE)-T1(NE)*N13(NE)
    N23(NE) = T1(NE)*N12(NE)-T2(NE)*N11(NE)
    N2NORM = (N21(NE)**2+N22(NE)**2+N23(NE)**2) ** 0.5
CC
    DO 50 I=1,10,3
        R(I,I) = T1(NE)/TNORM
        R(I,I+1)=T2(NE)/TNORM

```

```

R(I,I+2)=T3(NE)/TNORM
R(I+1,I)=N11(NE)/N1NORM
R(I+1,I+1)=N12(NE)/N1NORM
R(I+1,I+2)=N13(NE)/N1NORM
R(I+2,I)=N21(NE)/N2NORM
R(I+2,I+1)=N22(NE)/N2NORM
R(I+2,I+2)=N23(NE)/N2NORM
C ALTERNATIVELY >>
C   R(I+2,I)=R(1,2)*R(2,3)-R(2,2)*R(1,3)
C   R(I+2,I+1)=R(2,1)*R(1,3)-R(1,1)*R(2,3)
C   R(I+2,I+2)=R(1,1)*R(2,2)-R(1,2)*R(2,1)
50  CONTINUE
C
C THE TRANSPOSE OF THE ROTATION MATRIX.
C
DO 60 I=1,12
DO 65 J=1,12
TR(I,J) = R(J,I)
65  CONTINUE
60  CONTINUE
C
C
C***** SET EACH ENTRY IN SM(12,12) TO BE ZERO *****
C
DO 20 J=1,12
DO 25 I=1,12
SM(I,J)=0.0
25  CONTINUE
20  CONTINUE
C
C
C***** READ THE LOCATION OF SPRING AND DEFINE *****
C INTERPOLATION FUNCTIONS
C ***** ORIGINAL MATRIX WITH LOCAL AXIS FROM HOLZER'S BOOK *****
C ***** COMPATIBLE WITH LOCAL AXIS DIRECTION OF EDGE BEAMS *****
C
SPACE=TNORM/NS
C ##### SPACE=SPACING BETWEEN EACH SPRING
DO 30 L=1,NS
XI=SPACE*L/TNORM
S11=1.-XI
S21=XI
S12=1.-3.*XI**2.+2.*XI**3.
S22=-(XI-2.*XI**2.+XI**3.)*TNORM
S32=3.*XI**2.-2.*XI**3.
S42=(XI**2.-XI**3.)*TNORM
C
C ***** ASSIGN VALUES TO THE UPPER TRIANGLE ENTRIES IN MATRIX *****
C
SM(3,3)=SM(3,3)+S*S12*S12
SM(3,4)=SM(3,4)+S*H*S12*S11

```

```

SM(4,4)=SM(4,4)+S*H*H*S11*S11
SM(3,5)=SM(3,5)+S*S12*S22
SM(4,5)=SM(4,5)+S*H*S11*S22
SM(5,5)=SM(5,5)+S*S22*S22
SM(3,9)=SM(3,9)+S*S12*S32
SM(4,9)=SM(4,9)+S*H*S11*S32
SM(5,9)=SM(5,9)+S*S22*S32
SM(9,9)=SM(9,9)+S*S32*S32
SM(3,10)=SM(3,10)+S*H*S12*S21
SM(4,10)=SM(4,10)+S*H*H*S11*S21
SM(5,10)=SM(5,10)+S*H*S22*S21
SM(9,10)=SM(9,10)+S*H*S32*S21
SM(10,10)=SM(10,10)+S*H*H*S21*S21
SM(3,11)=SM(3,11)+S*S12*S42
SM(4,11)=SM(4,11)+S*H*S11*S42
SM(5,11)=SM(5,11)+S*S22*S42
SM(9,11)=SM(9,11)+S*S32*S42
SM(10,11)=SM(10,11)+S*H*S21*S42
SM(11,11)=SM(11,11)+S*S42*S42
30 CONTINUE
C
C ***** ASSIGN VALUES TO THE LOWER TRIANGLE ENTRIES IN MATRIX *****
SM(4,3)=SM(3,4)
SM(5,3)=SM(3,5)
SM(5,4)=SM(4,5)
SM(9,3)=SM(3,9)
SM(9,4)=SM(4,9)
SM(9,5)=SM(5,9)
SM(10,3)=SM(3,10)
SM(10,4)=SM(4,10)
SM(10,5)=SM(5,10)
SM(10,9)=SM(9,10)
SM(11,3)=SM(3,11)
SM(11,4)=SM(4,11)
SM(11,5)=SM(5,11)
SM(11,9)=SM(9,11)
SM(11,10)=SM(10,11)
C
C PRE-MULTIPLYING STIFFNESS MATRIX FOR THE USER ELEMENT BY THE
C TRANSPOSE OF THE ROTATION MATRIX.(TR X SM = SM1)
C
DO 70 I=1,12
DO 75 J=1,12
DO 80 K=1,12
SM1(I,J) = SM(I,J) + TR(I,K)*SM(K,J)
80 CONTINUE
75 CONTINUE
70 CONTINUE
C
C POST-MULTIPLYING THE ABOVE OBTAINED MATRIX BY
C THE ROTATION MATRIX.(SM1 X R = SM2).

```

```

C THIS (SM2) MATRIX WILL BE USED IN THE INPUT FILE FOR ABAQUS.
C
  DO 85 I=1,12
    DO 90 J=1,12
      DO 95 K=1,12
        SM2(I,J) = SM2(I,J) + SM1(I,K)*R(K,J)
95      CONTINUE
90      CONTINUE
85      CONTINUE
C
C
C***** WRITE ABAQUS COMMAND LINES TO MKS3 OUT *****
C
C **COMMAND LINES.
  WRITE(30,110) NE
  WRITE(30,115)
  WRITE(30,120) NE,NE
  WRITE(30,125)NE+NMAX,N1,N2
  WRITE(30,130)
C **THE GLOBAL STIFFNESS MATRIX.
  WRITE(30,135) SM2(1,1)
  WRITE(30,140) SM2(1,2),SM2(2,2)
  WRITE(30,145) SM2(1,3),SM2(2,3),SM2(3,3)
  WRITE(30,150) SM2(1,4),SM2(2,4),SM2(3,4),SM2(4,4)
  WRITE(30,150) SM2(1,5),SM2(2,5),SM2(3,5),SM2(4,5)
  WRITE(30,135) SM2(5,5)
  WRITE(30,150) SM2(1,6),SM2(2,6),SM2(3,6),SM2(4,6)
  WRITE(30,140) SM2(5,6),SM2(6,6)
  WRITE(30,150) SM2(1,7),SM2(2,7),SM2(3,7),SM2(4,7)
  WRITE(30,145) SM2(5,7),SM2(6,7),SM2(7,7)
  WRITE(30,150) SM2(1,8),SM2(2,8),SM2(3,8),SM2(4,8)
  WRITE(30,150) SM2(5,8),SM2(6,8),SM2(7,8),SM2(8,8)
  WRITE(30,150) SM2(1,9),SM2(2,9),SM2(3,9),SM2(4,9)
  WRITE(30,150) SM2(5,9),SM2(6,9),SM2(7,9),SM2(8,9)
  WRITE(30,135) SM2(9,9)
  WRITE(30,150) SM2(1,10),SM2(2,10),SM2(3,10),SM2(4,10)
  WRITE(30,150) SM2(5,10),SM2(6,10),SM2(7,10),SM2(8,10)
  WRITE(30,140) SM2(9,10),SM2(10,10)
  WRITE(30,150) SM2(1,11),SM2(2,11),SM2(3,11),SM2(4,11)
  WRITE(30,150) SM2(5,11),SM2(6,11),SM2(7,11),SM2(8,11)
  WRITE(30,145) SM2(9,11),SM2(10,11),SM2(11,11)
  WRITE(30,150) SM2(1,12),SM2(2,12),SM2(3,12),SM2(4,12)
  WRITE(30,150) SM2(5,12),SM2(6,12),SM2(7,12),SM2(8,12)
  WRITE(30,150) SM2(9,12),SM2(10,12),SM2(11,12),SM2(12,12)
C **COMMAND LINE.
  WRITE(30,160) NE
100 CONTINUE
CC#####
#####
105 FORMAT ('**',35('-'),'EDGE BEAMS/USER ELEMENTS')
C

```

```
110 FORMAT ('*USER ELEMENT,NODES=2,TYPE=U',I4,',LINEAR')
115 FORMAT ('1,2,3,4,5,6')
120 FORMAT ('*ELEMENT,TYPE=U',I4,',ELSET=C',I4)
125 FORMAT (I4,',',I4,',',I4)
130 FORMAT ('*MATRIX,TYPE=STIFFNESS')
CC
135 FORMAT(G12.4)
140 FORMAT(G12.4,',',G12.4)
145 FORMAT(G12.4,',',G12.4,',',G12.4)
150 FORMAT(G12.4,',',G12.4,',',G12.4,',',G12.4)
160 FORMAT ('*UEL PROPERTY,ELSET=C',I4)
END
```

APPENDIX C

```
*HEADING
SDRC I-DEAS ABAQUS FILE TRANSLATOR 30-JUL-92 20:59:28
**USER: MOSES TSANG (703) 552-2801
**DOME CAP RIB/ UNREFINED MESH
**LINEAR ANALYSIS
**LINEAR MATERIAL LAW ( G = 6.0E+05 PSI)
**-----NODES
*NODE, SYSTEM=R,NSET=NALL
      1, 0.00000E+00, 0.00000E+00, 0.21234E+03
      2,-0.13232E+03, 0.00000E+00, 0.20686E+03
      3, 0.13232E+03, 0.00000E+00, 0.20686E+03
      4,-0.26374E+03, 0.00000E+00, 0.19046E+03
      5, 0.26374E+03, 0.00000E+00, 0.19046E+03
*NSET,NSET=SUPPORT
4, 5
**-----ELEMENT INCIDENCES
**-----BEAM ELEMENTS
**-----MAIN BEAMS
*ELEMENT,TYPE=B33,ELSET=E 1
      1, 1, 3
*ELEMENT,TYPE=B33,ELSET=E 2
      2, 1, 2
*ELEMENT,TYPE=B33,ELSET=E 3
      3, 3, 5
*ELEMENT,TYPE=B33,ELSET=E 4
      4, 2, 4
**-----SECTION PROPERTIES
**-----BEAM ELEMENTS
*BEAM SECTION,SECTION=RECT,MATERIAL=WOOD,ELSET=E 1
      6.75, 11.0
      0.0000, 1.0000, 0.0000
*TRANSVERSE SHEAR STIFFNESS
      37594518., 37594518.
*BEAM SECTION,SECTION=RECT,MATERIAL=WOOD,ELSET=E 2
      6.75, 11.0
      0.0000, -1.0000, 0.0000
*TRANSVERSE SHEAR STIFFNESS
      37594518., 37594518.
*BEAM SECTION,SECTION=RECT,MATERIAL=WOOD,ELSET=E 3
      6.75, 11.0
      0.0000, 1.0000, 0.0000
*TRANSVERSE SHEAR STIFFNESS
      37594518., 37594518.
*BEAM SECTION,SECTION=RECT,MATERIAL=WOOD,ELSET=E 4
```

```

6.75, 11.0
0.0000, -1.0000, 0.0000
*TRANSVERSE SHEAR STIFFNESS
37594518., 37594518.
**-----MATERIAL PROPERTIES
*MATERIAL,NAME=WOOD
*ELASTIC
1.8E+06,4.625
**-----BOUNDRY CONDITION
*BOUNDARY
4,1,3
5,1,3
1,2
2,2
3,2
*STEP,LINEAR
*STATIC
**-----DEAD LOAD + SNOW LOAD
*CLOAD
1, 3, -1.0E+2
2, 3, -1.0E+2
3, 3, -1.0E+2
1, 3, -1.0E+2
2, 3, -1.0E+2
3, 3, -1.0E+2
**-----OUTPUT REQUEST
*EL PRINT
S
*NODE PRINT,NSET=NALL,SUMMARY=NO
U
*NODE PRINT,NSET=NALL,SUMMARY=NO
CF
*NODE PRINT,NSET=SUPPORT,SUMMARY=NO
RF
*END STEP

```

APPENDIX D

```
**-----
*HEADING
SDRC I-DEAS ABAQUS FILE TRANSLATOR 10-JUL-92 02:05:58
*** USER ELEMENTS USED IN PLACE OF THE TRUSS BRACING. ***
**USER:MOSES TSANG (703) 552-2801 GAMMA = 32642 LB/IN.
**NAILED JOINTS AT BRACING POINTS H=0
**DOME CAP / UNREFINED MESH / FULL SNOW LOAD
**NON-LINEAR RIKS ANALYSIS\FULL SNOW LOAD\USER MATERIAL ALL BEAMS
**LINEAR MATERIAL LAW ( E = 1.8E+06 PSI G = 1.6E+05 PSI)
**-----NODES
*NODE, SYSTEM=R,NSET=NALL
  1, 0.0000E+00, 0.0000E+00, 2.1234E+02
  2, 2.6374E+02, 0.0000E+00, 1.9046E+02
  3, 1.3187E+02,-2.2840E+02, 1.9046E+02
  4, 1.3232E+02, 0.0000E+00, 2.0686E+02
  5, 6.6161E+01,-1.1459E+02, 2.0686E+02
  6, 1.9848E+02,-1.1459E+02, 1.9584E+02
  7, 1.3187E+02, 2.2840E+02, 1.9046E+02
  8, 6.6161E+01, 1.1459E+02, 2.0686E+02
  9, 1.9848E+02, 1.1459E+02, 1.9584E+02
 10,-1.3187E+02,-2.2840E+02, 1.9046E+02
 11,-6.6162E+01,-1.1460E+02, 2.0686E+02
 12, 9.0111E-04,-2.2918E+02, 1.9584E+02
 13,-1.3187E+02, 2.2840E+02, 1.9046E+02
 14,-2.6374E+02, 7.5092E-05, 1.9046E+02
 15,-6.6162E+01, 1.1460E+02, 2.0686E+02
 16,-1.3232E+02,-1.5018E-04, 2.0686E+02
 17,-1.9848E+02, 1.1459E+02, 1.9584E+02
 18, 8.2602E-04, 2.2918E+02, 1.9584E+02
 19,-1.9848E+02,-1.1459E+02, 1.9584E+02
**-----BOUNDRY NODES
*NSET,NSET=SUPPORT
3, 2, 7, 13, 14, 10
**-----ELEMENT INCIDENCES
**-----BEAM ELEMENTS
**-----MAIN BEAMS 1
*ELEMENT,TYPE=B33,ELSET=E 1
  1, 1, 5
*ELEMENT,TYPE=B33,ELSET=E 2
  2, 5, 3
*ELEMENT,TYPE=B33,ELSET=E 3
  3, 1, 4
*ELEMENT,TYPE=B33,ELSET=E 4
  4, 4, 2
```

```

*ELEMENT,TYPE=B33,ELSET=E 46
  46, 15, 13
*ELEMENT,TYPE=B33,ELSET=E 45
  45, 1, 15
*ELEMENT,TYPE=B33,ELSET=E 32
  32, 11, 10
*ELEMENT,TYPE=B33,ELSET=E 31
  31, 1, 11
*ELEMENT,TYPE=B33,ELSET=E 16
  16, 8, 7
*ELEMENT,TYPE=B33,ELSET=E 43
  43, 1, 16
*ELEMENT,TYPE=B33,ELSET=E 44
  44, 16, 14
*ELEMENT,TYPE=B33,ELSET=E 15
  15, 1, 8
**-----EDGE BEAMS
*ELEMENT,TYPE=B33,ELSET=E 5
  5, 3, 6
*ELEMENT,TYPE=B33,ELSET=E 6
  6, 6, 2
*ELEMENT,TYPE=B33,ELSET=E 48
  48, 17, 13
*ELEMENT,TYPE=B33,ELSET=E 60
  60, 18, 13
*ELEMENT,TYPE=B33,ELSET=E 19
  19, 7, 9
*ELEMENT,TYPE=B33,ELSET=E 20
  20, 9, 2
*ELEMENT,TYPE=B33,ELSET=E 34
  34, 12, 10
*ELEMENT,TYPE=B33,ELSET=E 59
  59, 7, 18
*ELEMENT,TYPE=B33,ELSET=E 47
  47, 14, 17
*ELEMENT,TYPE=B33,ELSET=E 33
  33, 3, 12
*ELEMENT,TYPE=B33,ELSET=E 72
  72, 19, 10
*ELEMENT,TYPE=B33,ELSET=E 71
  71, 14, 19
**-----TENSION RING
*ELEMENT,TYPE=C1D2,ELSET=RING
  64 7 13
  24 7 2
  10 3 2
  38 3 10
  76 14 10
  52 14 13
**-----PURLINS
*ELEMENT,TYPE=C1D2,ELSET=PURLIN

```

```

73 16 11
21 8 4
49 16 15
35 5 11
7 5 4
61 8 15
**-----TRUSS BRACING
**ELEMENT,TYPE=C1D2,ELSET=BRACE
** 37 11 12
** 75 11 19
** 9 4 6
** 51 15 17
** 62 8 18
** 8 5 6
** 74 16 19
** 50 16 17
** 63 15 18
** 23 4 9
** 22 8 9
** 36 5 12
**-----SECTION PROPERTIES
**-----TRUSS ELEMENTS
*SOLID SECTION,ELSET=RING,MATERIAL=STEEL
12.
*SOLID SECTION,ELSET=PURLIN,MATERIAL=UWOOD
24.75
**SOLID SECTION,ELSET=BRACE,MATERIAL=UWOOD
**0.3
**-----BEAM ELEMENTS
**-----MAIN BEAMS 1
*BEAM SECTION,SECTION=RECT,MATERIAL=UWOOD,ELSET=E 1
6.75, 11.0
0.8660, 0.5000, 0.0000
*TRANSVERSE SHEAR STIFFNESS
9972128.26, 9972128.26
*BEAM SECTION,SECTION=RECT,MATERIAL=UWOOD,ELSET=E 2
6.75, 11.0
0.8660, 0.5000, 0.0000
*TRANSVERSE SHEAR STIFFNESS
9972128.26, 9972128.26
*BEAM SECTION,SECTION=RECT,MATERIAL=UWOOD,ELSET=E 3
6.75, 11.0
0.0000, 1.0000, 0.0000
*TRANSVERSE SHEAR STIFFNESS
9972128.26, 9972128.26
*BEAM SECTION,SECTION=RECT,MATERIAL=UWOOD,ELSET=E 4
6.75, 11.0
0.0000, 1.0000, 0.0000
*TRANSVERSE SHEAR STIFFNESS
9972128.26, 9972128.26
*BEAM SECTION,SECTION=RECT,MATERIAL=UWOOD,ELSET=E 46

```

```

6.75, 11.0
-0.8660, -0.5000, 0.0000
*TRANSVERSE SHEAR STIFFNESS
9972128.26, 9972128.26
*BEAM SECTION,SECTION=RECT,MATERIAL=UWOOD,ELSET=E 45
6.75, 11.0
-0.8660, -0.5000, 0.0000
*TRANSVERSE SHEAR STIFFNESS
9972128.26, 9972128.26
*BEAM SECTION,SECTION=RECT,MATERIAL=UWOOD,ELSET=E 32
6.75, 11.0
0.8660, -0.5000, 0.0000
*TRANSVERSE SHEAR STIFFNESS
9972128.26, 9972128.26
*BEAM SECTION,SECTION=RECT,MATERIAL=UWOOD,ELSET=E 31
6.75, 11.0
0.8660, -0.5000, 0.0000
*TRANSVERSE SHEAR STIFFNESS
9972128.26, 9972128.26
*BEAM SECTION,SECTION=RECT,MATERIAL=UWOOD,ELSET=E 16
6.75, 11.0
-0.8660, 0.5000, 0.0000
*TRANSVERSE SHEAR STIFFNESS
9972128.26, 9972128.26
*BEAM SECTION,SECTION=RECT,MATERIAL=UWOOD,ELSET=E 43
6.75, 11.0
0.0000, -1.0000, 0.0000
*TRANSVERSE SHEAR STIFFNESS
9972128.26, 9972128.26
*BEAM SECTION,SECTION=RECT,MATERIAL=UWOOD,ELSET=E 44
6.75, 11.0
0.0000, -1.0000, 0.0000
*TRANSVERSE SHEAR STIFFNESS
9972128.26, 9972128.26
*BEAM SECTION,SECTION=RECT,MATERIAL=UWOOD,ELSET=E 15
6.75, 11.0
-0.8660, 0.5000, 0.0000
*TRANSVERSE SHEAR STIFFNESS
9972128.26, 9972128.26
**-----MAIN BEAMS 1/USER ELEMENTS
*USER ELEMENT,NODES=2,TYPE=U 1,LINEAR
1,2,3,4,5,6
*ELEMENT,TYPE=U 1,ELSET=C 1
77, 1, 5
*MATRIX,TYPE=STIFFNESS
0.0000E+00
0.0000E+00, 0.0000E+00
0.0000E+00, 0.0000E+00, 0.0000E+00
0.0000E+00, 0.0000E+00, 0.0000E+00, 0.0000E+00
0.0000E+00, 0.0000E+00, 0.0000E+00, 0.0000E+00
0.0000E+00

```



```

*ELEMENT,TYPE=U 45,ELSET=C 45
121, 1, 15
*MATRIX,TYPE=STIFFNESS
0.0000E+00
0.0000E+00, 0.0000E+00
0.0000E+00, 0.0000E+00, 0.0000E+00
0.0000E+00, 0.0000E+00, 0.0000E+00, 0.0000E+00
0.0000E+00, 0.0000E+00, 0.0000E+00, 0.0000E+00
0.0000E+00
0.0000E+00, 0.0000E+00, 0.0000E+00, 0.0000E+00
0.0000E+00, 0.0000E+00
0.0000E+00, 0.0000E+00, 0.0000E+00, 0.0000E+00
0.0000E+00, 0.0000E+00, 0.2448E+05
0.0000E+00, 0.0000E+00, 0.0000E+00, 0.0000E+00
0.0000E+00, 0.0000E+00, 0.1413E+05, 8160.
0.0000E+00, 0.0000E+00, 0.0000E+00, 0.0000E+00
0.0000E+00, 0.0000E+00, 0.0000E+00, 0.0000E+00
0.0000E+00
0.0000E+00, 0.0000E+00, 0.0000E+00, 0.0000E+00
0.0000E+00, 0.0000E+00, 0.0000E+00, 0.0000E+00
0.0000E+00, 0.0000E+00
0.0000E+00, 0.0000E+00, 0.0000E+00, 0.0000E+00
0.0000E+00, 0.0000E+00, 0.0000E+00, 0.0000E+00
0.0000E+00, 0.0000E+00, 0.0000E+00, 0.0000E+00
0.0000E+00, 0.0000E+00, 0.0000E+00, 0.0000E+00
0.0000E+00, 0.0000E+00, 0.0000E+00, 0.0000E+00
0.0000E+00
0.0000E+00, 0.0000E+00, 0.0000E+00, 0.0000E+00
0.0000E+00, 0.0000E+00, 0.0000E+00, 0.0000E+00
0.0000E+00, 0.0000E+00, 0.0000E+00, 0.0000E+00
0.0000E+00, 0.0000E+00, 0.0000E+00, 0.0000E+00
0.0000E+00
0.0000E+00, 0.0000E+00, 0.0000E+00, 0.0000E+00
0.0000E+00, 0.0000E+00, 0.2448E+05
0.0000E+00, 0.0000E+00, 0.0000E+00, 0.0000E+00
0.0000E+00, 0.0000E+00, -0.1413E+05, 8160.
0.0000E+00, 0.0000E+00, 0.0000E+00, 0.0000E+00
0.0000E+00, 0.0000E+00, 0.0000E+00, 0.0000E+00
0.0000E+00
0.0000E+00, 0.0000E+00, 0.0000E+00, 0.0000E+00
0.0000E+00, 0.0000E+00, 0.0000E+00, 0.0000E+00
0.0000E+00, 0.0000E+00

```

```

0.0000E+00, 0.0000E+00, 0.0000E+00, 0.0000E+00
0.0000E+00, 0.0000E+00, 0.0000E+00, 0.0000E+00
0.0000E+00, 0.0000E+00, 0.0000E+00
0.0000E+00, 0.0000E+00, 0.0000E+00, 0.0000E+00
0.0000E+00, 0.0000E+00, 0.0000E+00, 0.0000E+00
0.0000E+00, 0.0000E+00, 0.0000E+00, 0.0000E+00
*UEL PROPERTY,ELSET=C 31
*USER ELEMENT,NODES=2,TYPE=U 43,LINEAR
1,2,3,4,5,6
*ELEMENT,TYPE=U 43,ELSET=C 43
119, 1, 16
*MATRIX,TYPE=STIFFNESS
0.0000E+00
0.0000E+00, 0.0000E+00
0.0000E+00, 0.0000E+00, 0.0000E+00
0.0000E+00, 0.0000E+00, 0.0000E+00, 0.0000E+00
0.0000E+00, 0.0000E+00, 0.0000E+00, 0.0000E+00
0.0000E+00
0.0000E+00, 0.0000E+00, 0.0000E+00, 0.0000E+00
0.0000E+00, 0.0000E+00
0.0000E+00, 0.0000E+00, 0.0000E+00, 0.0000E+00
0.0000E+00, 0.0000E+00, 0.4205E-07
0.0000E+00, 0.0000E+00, 0.0000E+00, 0.0000E+00
0.0000E+00, 0.0000E+00, -0.3705E-01, 0.3264E+05
0.0000E+00, 0.0000E+00, 0.0000E+00, 0.0000E+00
0.0000E+00, 0.0000E+00, 0.0000E+00, 0.0000E+00
0.0000E+00
0.0000E+00, 0.0000E+00, 0.0000E+00, 0.0000E+00
0.0000E+00, 0.0000E+00, 0.0000E+00, 0.0000E+00
0.0000E+00, 0.0000E+00
0.0000E+00, 0.0000E+00, 0.0000E+00, 0.0000E+00
0.0000E+00, 0.0000E+00, 0.0000E+00, 0.0000E+00
0.0000E+00, 0.0000E+00, 0.0000E+00
0.0000E+00, 0.0000E+00, 0.0000E+00, 0.0000E+00
0.0000E+00, 0.0000E+00, 0.0000E+00, 0.0000E+00
0.0000E+00, 0.0000E+00, 0.0000E+00, 0.0000E+00
*UEL PROPERTY,ELSET=C 43
*USER ELEMENT,NODES=2,TYPE=U 15,LINEAR
1,2,3,4,5,6
*ELEMENT,TYPE=U 15,ELSET=C 15
91, 1, 8
*MATRIX,TYPE=STIFFNESS
0.0000E+00
0.0000E+00, 0.0000E+00
0.0000E+00, 0.0000E+00, 0.0000E+00
0.0000E+00, 0.0000E+00, 0.0000E+00, 0.0000E+00
0.0000E+00, 0.0000E+00, 0.0000E+00, 0.0000E+00
0.0000E+00
0.0000E+00, 0.0000E+00, 0.0000E+00, 0.0000E+00
0.0000E+00, 0.0000E+00
0.0000E+00, 0.0000E+00, 0.0000E+00, 0.0000E+00

```

```

0.0000E+00, 0.0000E+00, 0.2448E+05
0.0000E+00, 0.0000E+00, 0.0000E+00, 0.0000E+00
0.0000E+00, 0.0000E+00, -0.1413E+05, 8161.
0.0000E+00, 0.0000E+00, 0.0000E+00, 0.0000E+00
0.0000E+00, 0.0000E+00, 0.0000E+00, 0.0000E+00
0.0000E+00
0.0000E+00, 0.0000E+00, 0.0000E+00, 0.0000E+00
0.0000E+00, 0.0000E+00, 0.0000E+00, 0.0000E+00
0.0000E+00, 0.0000E+00
0.0000E+00, 0.0000E+00, 0.0000E+00, 0.0000E+00
0.0000E+00, 0.0000E+00, 0.0000E+00, 0.0000E+00
0.0000E+00, 0.0000E+00, 0.0000E+00
0.0000E+00, 0.0000E+00, 0.0000E+00, 0.0000E+00
0.0000E+00, 0.0000E+00, 0.0000E+00, 0.0000E+00
0.0000E+00, 0.0000E+00, 0.0000E+00, 0.0000E+00
*UEL PROPERTY,ELSET=C 15
**-----EDGE BEAMS
*BEAM SECTION,SECTION=RECT,MATERIAL=UWOOD,ELSET=E 5
12.25, 3.0
-0.0406, -0.0234, 0.9989
*TRANSVERSE SHEAR STIFFNESS
9972128.26, 9972128.26
*BEAM SECTION,SECTION=RECT,MATERIAL=UWOOD,ELSET=E 6
12.25, 3.0
0.0000, 0.0469, 0.9989
*TRANSVERSE SHEAR STIFFNESS
9972128.26, 9972128.26
*BEAM SECTION,SECTION=RECT,MATERIAL=UWOOD,ELSET=E 48
12.25, 3.0
-0.0406, -0.0234, -0.9989
*TRANSVERSE SHEAR STIFFNESS
9972128.26, 9972128.26
*BEAM SECTION,SECTION=RECT,MATERIAL=UWOOD,ELSET=E 60
12.25, 3.0
-0.0406, -0.0234, 0.9989
*TRANSVERSE SHEAR STIFFNESS
9972128.26, 9972128.26
*BEAM SECTION,SECTION=RECT,MATERIAL=UWOOD,ELSET=E 19
12.25, 3.0
0.0406, -0.0234, -0.9989
*TRANSVERSE SHEAR STIFFNESS
9972128.26, 9972128.26
*BEAM SECTION,SECTION=RECT,MATERIAL=UWOOD,ELSET=E 20
12.25, 3.0
0.0000, 0.0469, -0.9989
*TRANSVERSE SHEAR STIFFNESS
9972128.26, 9972128.26
*BEAM SECTION,SECTION=RECT,MATERIAL=UWOOD,ELSET=E 34
12.25, 3.0
0.0406, -0.0234, -0.9989
*TRANSVERSE SHEAR STIFFNESS

```

```

9972128.26, 9972128.26
*BEAM SECTION,SECTION=RECT,MATERIAL=UWOOD,ELSET=E 59
12.25, 3.0
0.0406, -0.0234, 0.9989
*TRANSVERSE SHEAR STIFFNESS
9972128.26, 9972128.26
*BEAM SECTION,SECTION=RECT,MATERIAL=UWOOD,ELSET=E 47
12.25, 3.0
0.0000, 0.0469, -0.9989
*TRANSVERSE SHEAR STIFFNESS
9972128.26, 9972128.26
*BEAM SECTION,SECTION=RECT,MATERIAL=UWOOD,ELSET=E 33
12.25, 3.0
-0.0406, -0.0234, -0.9989
*TRANSVERSE SHEAR STIFFNESS
9972128.26, 9972128.26
*BEAM SECTION,SECTION=RECT,MATERIAL=UWOOD,ELSET=E 72
12.25, 3.0
0.0406, -0.0234, 0.9989
*TRANSVERSE SHEAR STIFFNESS
9972128.26, 9972128.26
*BEAM SECTION,SECTION=RECT,MATERIAL=UWOOD,ELSET=E 71
12.25, 3.0
0.0000, 0.0469, 0.9989
*TRANSVERSE SHEAR STIFFNESS
9972128.26, 9972128.26
**-----EDGE BEAMS/USER ELEMENTS
*USER ELEMENT,NODES=2,TYPE=U 5,LINEAR
1,2,3,4,5,6
*ELEMENT,TYPE=U 5,ELSET=C 5
81, 3, 6
*MATRIX,TYPE=STIFFNESS
0.0000E+00
0.0000E+00, 0.0000E+00
0.0000E+00, 0.0000E+00, 0.0000E+00
0.0000E+00, 0.0000E+00, 0.0000E+00, 0.0000E+00
0.0000E+00, 0.0000E+00, 0.0000E+00, 0.0000E+00
0.0000E+00
0.0000E+00, 0.0000E+00, 0.0000E+00, 0.0000E+00
0.0000E+00, 0.0000E+00
0.0000E+00, 0.0000E+00, 0.0000E+00, 0.0000E+00
0.0000E+00, 0.0000E+00, 0.2427E+05
0.0000E+00, 0.0000E+00, 0.0000E+00, 0.0000E+00
0.0000E+00, 0.0000E+00, -0.1424E+05, 8351.
0.0000E+00, 0.0000E+00, 0.0000E+00, 0.0000E+00
0.0000E+00, 0.0000E+00, 652.7 , -382.8
17.55
0.0000E+00, 0.0000E+00, 0.0000E+00, 0.0000E+00
0.0000E+00, 0.0000E+00, 0.0000E+00, 0.0000E+00
0.0000E+00, 0.0000E+00
0.0000E+00, 0.0000E+00, 0.0000E+00, 0.0000E+00

```

```

0.0000E+00, 0.0000E+00, 0.0000E+00, 0.0000E+00
0.0000E+00, 0.0000E+00, 0.0000E+00
0.0000E+00, 0.0000E+00, 0.0000E+00, 0.0000E+00
0.0000E+00, 0.0000E+00, 0.0000E+00, 0.0000E+00
0.0000E+00, 0.0000E+00, 0.0000E+00, 0.0000E+00
*UEL PROPERTY,ELSET=C 5
*USER ELEMENT,NODES=2,TYPE=U 19,LINEAR
1,2,3,4,5,6
*ELEMENT,TYPE=U 19,ELSET=C 19
95, 7, 9
*MATRIX,TYPE=STIFFNESS
0.0000E+00
0.0000E+00, 0.0000E+00
0.0000E+00, 0.0000E+00, 0.0000E+00
0.0000E+00, 0.0000E+00, 0.0000E+00, 0.0000E+00
0.0000E+00, 0.0000E+00, 0.0000E+00, 0.0000E+00
0.0000E+00
0.0000E+00, 0.0000E+00, 0.0000E+00, 0.0000E+00
0.0000E+00, 0.0000E+00
0.0000E+00, 0.0000E+00, 0.0000E+00, 0.0000E+00
0.0000E+00, 0.0000E+00, 0.2427E+05
0.0000E+00, 0.0000E+00, 0.0000E+00, 0.0000E+00
0.0000E+00, 0.0000E+00, 0.1424E+05, 8351.
0.0000E+00, 0.0000E+00, 0.0000E+00, 0.0000E+00
0.0000E+00, 0.0000E+00, 652.7 , 382.8
17.55
0.0000E+00, 0.0000E+00, 0.0000E+00, 0.0000E+00
0.0000E+00, 0.0000E+00, 0.0000E+00, 0.0000E+00
0.0000E+00, 0.0000E+00
0.0000E+00, 0.0000E+00, 0.0000E+00, 0.0000E+00
0.0000E+00, 0.0000E+00, 0.0000E+00, 0.0000E+00
0.0000E+00, 0.0000E+00, 0.0000E+00
0.0000E+00, 0.0000E+00, 0.0000E+00, 0.0000E+00
0.0000E+00, 0.0000E+00, 0.0000E+00, 0.0000E+00
0.0000E+00, 0.0000E+00, 0.0000E+00, 0.0000E+00
0.0000E+00, 0.0000E+00, 0.0000E+00, 0.0000E+00
0.0000E+00, 0.0000E+00, 0.0000E+00, 0.0000E+00
*UEL PROPERTY,ELSET=C 19
*USER ELEMENT,NODES=2,TYPE=U 59,LINEAR
1,2,3,4,5,6
*ELEMENT,TYPE=U 59,ELSET=C 59
135, 7, 18
*MATRIX,TYPE=STIFFNESS
0.0000E+00
0.0000E+00, 0.0000E+00
0.0000E+00, 0.0000E+00, 0.0000E+00
0.0000E+00, 0.0000E+00, 0.0000E+00, 0.0000E+00
0.0000E+00, 0.0000E+00, 0.0000E+00, 0.0000E+00
0.0000E+00
0.0000E+00, 0.0000E+00, 0.0000E+00, 0.0000E+00
0.0000E+00, 0.0000E+00
0.0000E+00, 0.0000E+00, 0.0000E+00, 0.0000E+00
0.0000E+00, 0.0000E+00, 1.536

```

```

0.0000E+00, 0.0000E+00, 0.0000E+00, 0.0000E+00
0.0000E+00, 0.0000E+00, 223.8 , 0.3262E+05
0.0000E+00, 0.0000E+00, 0.0000E+00, 0.0000E+00
0.0000E+00, 0.0000E+00, 5.192 , 756.7
17.55
0.0000E+00, 0.0000E+00, 0.0000E+00, 0.0000E+00
0.0000E+00, 0.0000E+00, 0.0000E+00, 0.0000E+00
0.0000E+00, 0.0000E+00
0.0000E+00, 0.0000E+00, 0.0000E+00, 0.0000E+00
0.0000E+00, 0.0000E+00, 0.0000E+00, 0.0000E+00
0.0000E+00, 0.0000E+00, 0.0000E+00
0.0000E+00, 0.0000E+00, 0.0000E+00, 0.0000E+00
0.0000E+00, 0.0000E+00, 0.0000E+00, 0.0000E+00
0.0000E+00, 0.0000E+00, 0.0000E+00, 0.0000E+00
*UEL PROPERTY,ELSET=C 59
*USER ELEMENT,NODES=2,TYPE=U 47,LINEAR
1,2,3,4,5,6
*ELEMENT,TYPE=U 47,ELSET=C 47
123, 14, 17
*MATRIX,TYPE=STIFFNESS
0.0000E+00
0.0000E+00, 0.0000E+00
0.0000E+00, 0.0000E+00, 0.0000E+00
0.0000E+00, 0.0000E+00, 0.0000E+00, 0.0000E+00
0.0000E+00, 0.0000E+00, 0.0000E+00, 0.0000E+00
0.0000E+00
0.0000E+00, 0.0000E+00, 0.0000E+00, 0.0000E+00
0.0000E+00, 0.0000E+00
0.0000E+00, 0.0000E+00, 0.0000E+00, 0.0000E+00
0.0000E+00, 0.0000E+00, 0.2466E+05
0.0000E+00, 0.0000E+00, 0.0000E+00, 0.0000E+00
0.0000E+00, 0.0000E+00, -0.1401E+05, 7963.
0.0000E+00, 0.0000E+00, 0.0000E+00, 0.0000E+00
0.0000E+00, 0.0000E+00, -657.9 , 373.9
17.55
0.0000E+00, 0.0000E+00, 0.0000E+00, 0.0000E+00
0.0000E+00, 0.0000E+00, 0.0000E+00, 0.0000E+00
0.0000E+00, 0.0000E+00
0.0000E+00, 0.0000E+00, 0.0000E+00, 0.0000E+00
0.0000E+00, 0.0000E+00, 0.0000E+00, 0.0000E+00
0.0000E+00, 0.0000E+00, 0.0000E+00
0.0000E+00, 0.0000E+00, 0.0000E+00, 0.0000E+00
0.0000E+00, 0.0000E+00, 0.0000E+00, 0.0000E+00
0.0000E+00, 0.0000E+00, 0.0000E+00, 0.0000E+00
0.0000E+00, 0.0000E+00, 0.0000E+00, 0.0000E+00
*UEL PROPERTY,ELSET=C 47
*USER ELEMENT,NODES=2,TYPE=U 33,LINEAR
1,2,3,4,5,6
*ELEMENT,TYPE=U 33,ELSET=C 33
109, 3, 12
*MATRIX,TYPE=STIFFNESS
0.0000E+00

```



```

0.0000E+00, 0.0000E+00, 0.0000E+00, 0.0000E+00
0.0000E+00, 0.0000E+00, 0.0000E+00, 0.0000E+00
*UEL PROPERTY,ELSET=C 71
**-----MATERIAL PROPERTIES
*MATERIAL,NAME=WOOD
*ELASTIC
1.8E+06,4.625
*MATERIAL,NAME=UWOOD
*USER MATERIAL, CONSTANT=3
12.00,0.52,4.625
*MATERIAL,NAME=STEEL
*ELASTIC
2.9E+07,0.3
**-----BOUNDARY CONDITION
*BOUNDARY
SUPPORT,3
14,2
2,2
12,1
18,1
**-----APPLICATION OF DEAD LOAD
**-----NEWTON-RAPHSON STEP
*STEP,NLGEOM,INC=100,CYCLE=12
*STATIC,PTOL=20.,MTOL=2000.
0.1,1.,0.0, ,
**-----DEAD LOAD
*CLOAD
1, 3, -0.1687E+04
2, 3, -0.5581E+03
3, 3, -0.5581E+03
4, 3, -0.1682E+04
5, 3, -0.1682E+04
6, 3, -0.8391E+03
7, 3, -0.5581E+03
8, 3, -0.1682E+04
9, 3, -0.8391E+03
10, 3, -0.5581E+03
11, 3, -0.1682E+04
12, 3, -0.8391E+03
13, 3, -0.5581E+03
14, 3, -0.5581E+03
15, 3, -0.1682E+04
16, 3, -0.1682E+04
17, 3, -0.8391E+03
18, 3, -0.8391E+03
19, 3, -0.8391E+03
**-----NODE,ELEMENT SETS AND OUTPUTS
*NSET,NSET=APEX1
1
*ELSET,ELSET=ELE1
4

```

```

**-----OUTPUT REQUEST
*PRINT,RESIDUAL=NO
*NODE PRINT,NSET=APEX1,SUMMARY=NO,FREQUENCY=5
U
*NODE PRINT,NSET=APEX1,SUMMARY=NO,FREQUENCY=5
CF
*EL PRINT,ELSET=ELE1,SUMMARY=NO,FREQUENCY=20
3,23
S
*END STEP
**-----APPLICATION OF LIVE LOAD
**-----RIKS STEP
*STEP,NLGEOM,INC=30,CYCLE=12
*STATIC,PTOL=20.,MTOL=2000.,RIKS
0.1,1.,0.0, ,
**-----DEAD LOAD + SNOW LOAD
*CLOAD
  1, 3, -0.1687E+04
  2, 3, -0.5581E+03
  3, 3, -0.5581E+03
  4, 3, -0.1682E+04
  5, 3, -0.1682E+04
  6, 3, -0.8391E+03
  7, 3, -0.5581E+03
  8, 3, -0.1682E+04
  9, 3, -0.8391E+03
 10, 3, -0.5581E+03
 11, 3, -0.1682E+04
 12, 3, -0.8391E+03
 13, 3, -0.5581E+03
 14, 3, -0.5581E+03
 15, 3, -0.1682E+04
 16, 3, -0.1682E+04
 17, 3, -0.8391E+03
 18, 3, -0.8391E+03
 19, 3, -0.8391E+03
  1, 3, -0.2106E+04
  2, 3, -0.6972E+03
  3, 3, -0.6972E+03
  4, 3, -0.2101E+04
  5, 3, -0.2101E+04
  6, 3, -0.1048E+04
  7, 3, -0.6972E+03
  8, 3, -0.2101E+04
  9, 3, -0.1048E+04
 10, 3, -0.6971E+03
 11, 3, -0.2101E+04
 12, 3, -0.1048E+04
 13, 3, -0.6971E+03
 14, 3, -0.6972E+03
 15, 3, -0.2101E+04

```

```

16, 3, -0.2101E+04
17, 3, -0.1048E+04
18, 3, -0.1048E+04
19, 3, -0.1048E+04
**-----NODE,ELEMENT SETS AND OUTPUTS
*NSET,NSET=APEX
1
*NSET,NSET=NWATCH
1,2,3,4,5,6
*ELSET,ELSET=EWATCH
5,6
**5,6,19,20,33,34,47,48,59,60,71,72
**-----OUTPUT REQUEST
*PRINT,RESIDUAL=NO
*EL PRINT,ELSET=EWATCH,POSITION=NODES
S
*NODE PRINT,NSET=NWATCH
U
*NODE PRINT,NSET=APEX,SUMMARY=NO
U
*NODE PRINT,NSET=APEX,SUMMARY=NO
CF
*NODE FILE,NSET=NALL
U
*END STEP

*USER SUBROUTINE

*****
*****      SUBROUTINE TO TEST USER SUBROUTINE UMAT      *****
*****                               *****
*****      NIKET M. TELANG .....10 APRIL'91      *****
*****
SUBROUTINE UMAT(STRESS,STATEV,DDSDDE,SSE,SPD,SCD,
1 RPL,DDSDDT,DRPLDE,DRPLDT,
2 STRAN,DSTRAN,TIME,DTIME,TEMP,DTEMP,PREDEF,DPRED,CMNAME,
3 NDI,NSHR,NTENS,NSTATV,PROPS,NPROPS,COORDS,DROT)
C
C      IMPLICIT REAL*8(A-H,O-Z)
C
C      CHARACTER*8 CMNAME
C
C
C      DIMENSION STRESS(NTENS),STATEV(NSTATV),
1 DDSDDE(NTENS,NTENS),
2 DDSDDT(NTENS),DRPLDE(NTENS),
3 STRAN(NTENS),DSTRAN(NTENS),PREDEF(1),DPRED(1),
4 PROPS(NPROPS),COORDS(3),DROT(3,3)

```

```

C   DIMENSION DSTRES(2)
C
C
C   DO 20 I=1,NTENS
C     DO 10 J=1,NTENS
C       DDSDDDE(I,J)=0.0
10    CONTINUE
20    CONTINUE
C
C     *LONGITUDINAL STRESS*
C
C
C
C   TS=0.0
C   TS=STRAN(1) + DSTRAN(1)
C
C     *TENSION ZONE*
C
C   DDSDDDE(1,1)=1.805365E+06
C   STRESS(1)=DDSDDDE(1,1)*TS
C
C     *TORSIONAL SHEAR STRESS*
C
C
C   TT=0.0
C   TT=STRAN(2) + DSTRAN(2)
C
C   DDSDDDE(2,2)=(1.6000E+05)
C   STRESS(2)=DDSDDDE(2,2)*TT
C
C   RETURN
C   END

```

APPENDIX E

```
**-----
*HEADING
SDRC I-DEAS ABAQUS FILE TRANSLATOR 10-JUL-92 02:05:58
****USER ELEMENTS USED IN PLACE OF THE TRUSS BRACING. ****
**USER:MOSES TSANG 552-2801
**16 NAILED JOINTS PER BEAM ELEMENT; H>0, GAMMA=32642 LB/IN.
**DOME CAP / UNREFINED MESH / FULL SNOW LOAD
**NON-LINEAR RIKS ANALYSIS\FULL SNOW LOAD\USER MATERIAL ALL BEAMS
**NON-LINEAR MATERIAL LAW ( G = 1.6E+05 PSI)
**-----NODES
*NODE, SYSTEM=R,NSET=NALL
  1, 0.0000E+00, 0.0000E+00, 2.1234E+02
  2, 2.6374E+02, 0.0000E+00, 1.9046E+02
  3, 1.3187E+02,-2.2840E+02, 1.9046E+02
  4, 1.3232E+02, 0.0000E+00, 2.0686E+02
  5, 6.6161E+01,-1.1459E+02, 2.0686E+02
  6, 1.9848E+02,-1.1459E+02, 1.9584E+02
  7, 1.3187E+02, 2.2840E+02, 1.9046E+02
  8, 6.6161E+01, 1.1459E+02, 2.0686E+02
  9, 1.9848E+02, 1.1459E+02, 1.9584E+02
 10,-1.3187E+02,-2.2840E+02, 1.9046E+02
 11,-6.6162E+01,-1.1460E+02, 2.0686E+02
 12, 9.0111E-04,-2.2918E+02, 1.9584E+02
 13,-1.3187E+02, 2.2840E+02, 1.9046E+02
 14,-2.6374E+02, 7.5092E-05, 1.9046E+02
 15,-6.6162E+01, 1.1460E+02, 2.0686E+02
 16,-1.3232E+02,-1.5018E-04, 2.0686E+02
 17,-1.9848E+02, 1.1459E+02, 1.9584E+02
 18, 8.2602E-04, 2.2918E+02, 1.9584E+02
 19,-1.9848E+02,-1.1459E+02, 1.9584E+02
**-----BOUNDRY NODES
*NSET,NSET=SUPPORT
3, 2, 7, 13, 14, 10
**-----ELEMENT INCIDENCES
**-----BEAM ELEMENTS
**-----MAIN BEAMS 1
*ELEMENT,TYPE=B33,ELSET=E 1
  1, 1, 5
*ELEMENT,TYPE=B33,ELSET=E 2
  2, 5, 3
*ELEMENT,TYPE=B33,ELSET=E 3
  3, 1, 4
*ELEMENT,TYPE=B33,ELSET=E 4
  4, 4, 2
```

```

*ELEMENT,TYPE=B33,ELSET=E 46
  46, 15, 13
*ELEMENT,TYPE=B33,ELSET=E 45
  45, 1, 15
*ELEMENT,TYPE=B33,ELSET=E 32
  32, 11, 10
*ELEMENT,TYPE=B33,ELSET=E 31
  31, 1, 11
*ELEMENT,TYPE=B33,ELSET=E 16
  16, 8, 7
*ELEMENT,TYPE=B33,ELSET=E 43
  43, 1, 16
*ELEMENT,TYPE=B33,ELSET=E 44
  44, 16, 14
*ELEMENT,TYPE=B33,ELSET=E 15
  15, 1, 8
**-----EDGE BEAMS
*ELEMENT,TYPE=B33,ELSET=E 5
  5, 3, 6
*ELEMENT,TYPE=B33,ELSET=E 6
  6, 6, 2
*ELEMENT,TYPE=B33,ELSET=E 48
  48, 17, 13
*ELEMENT,TYPE=B33,ELSET=E 60
  60, 18, 13
*ELEMENT,TYPE=B33,ELSET=E 19
  19, 7, 9
*ELEMENT,TYPE=B33,ELSET=E 20
  20, 9, 2
*ELEMENT,TYPE=B33,ELSET=E 34
  34, 12, 10
*ELEMENT,TYPE=B33,ELSET=E 59
  59, 7, 18
*ELEMENT,TYPE=B33,ELSET=E 47
  47, 14, 17
*ELEMENT,TYPE=B33,ELSET=E 33
  33, 3, 12
*ELEMENT,TYPE=B33,ELSET=E 72
  72, 19, 10
*ELEMENT,TYPE=B33,ELSET=E 71
  71, 14, 19
**-----TENSION RING
*ELEMENT,TYPE=C1D2,ELSET=RING
  64  7  13
  24  7  2
  10  3  2
  38  3  10
  76 14  10
  52 14  13
**-----PURLINS
*ELEMENT,TYPE=C1D2,ELSET=PURLIN

```

```

73 16 11
21 8 4
49 16 15
35 5 11
7 5 4
61 8 15
**-----TRUSS BRACING
**ELEMENT,TYPE=C1D2,ELSET=BRACE
** 37 11 12
** 75 11 19
** 9 4 6
** 51 15 17
** 62 8 18
** 8 5 6
** 74 16 19
** 50 16 17
** 63 15 18
** 23 4 9
** 22 8 9
** 36 5 12
**-----SECTION PROPERTIES
**-----TRUSS ELEMENTS
*SOLID SECTION,ELSET=RING,MATERIAL=STEEL
12.
*SOLID SECTION,ELSET=PURLIN,MATERIAL=UWOOD
24.75
**SOLID SECTION,ELSET=BRACE,MATERIAL=UWOOD
**0.3
**-----BEAM ELEMENTS
**-----MAIN BEAMS 1
*BEAM SECTION,SECTION=RECT,MATERIAL=UWOOD,ELSET=E 1
6.75, 11.0
0.8660, 0.5000, 0.0000
*TRANSVERSE SHEAR STIFFNESS
9972128.26, 9972128.26
*BEAM SECTION,SECTION=RECT,MATERIAL=UWOOD,ELSET=E 2
6.75, 11.0
0.8660, 0.5000, 0.0000
*TRANSVERSE SHEAR STIFFNESS
9972128.26, 9972128.26
*BEAM SECTION,SECTION=RECT,MATERIAL=UWOOD,ELSET=E 3
6.75, 11.0
0.0000, 1.0000, 0.0000
*TRANSVERSE SHEAR STIFFNESS
9972128.26, 9972128.26
*BEAM SECTION,SECTION=RECT,MATERIAL=UWOOD,ELSET=E 4
6.75, 11.0
0.0000, 1.0000, 0.0000
*TRANSVERSE SHEAR STIFFNESS
9972128.26, 9972128.26
*BEAM SECTION,SECTION=RECT,MATERIAL=UWOOD,ELSET=E 46

```

```

6.75, 11.0
-0.8660, -0.5000, 0.0000
*TRANSVERSE SHEAR STIFFNESS
9972128.26, 9972128.26
*BEAM SECTION,SECTION=RECT,MATERIAL=UWOOD,ELSET=E 45
6.75, 11.0
-0.8660, -0.5000, 0.0000
*TRANSVERSE SHEAR STIFFNESS
9972128.26, 9972128.26
*BEAM SECTION,SECTION=RECT,MATERIAL=UWOOD,ELSET=E 32
6.75, 11.0
0.8660, -0.5000, 0.0000
*TRANSVERSE SHEAR STIFFNESS
9972128.26, 9972128.26
*BEAM SECTION,SECTION=RECT,MATERIAL=UWOOD,ELSET=E 31
6.75, 11.0
0.8660, -0.5000, 0.0000
*TRANSVERSE SHEAR STIFFNESS
9972128.26, 9972128.26
*BEAM SECTION,SECTION=RECT,MATERIAL=UWOOD,ELSET=E 16
6.75, 11.0
-0.8660, 0.5000, 0.0000
*TRANSVERSE SHEAR STIFFNESS
9972128.26, 9972128.26
*BEAM SECTION,SECTION=RECT,MATERIAL=UWOOD,ELSET=E 43
6.75, 11.0
0.0000, -1.0000, 0.0000
*TRANSVERSE SHEAR STIFFNESS
9972128.26, 9972128.26
*BEAM SECTION,SECTION=RECT,MATERIAL=UWOOD,ELSET=E 44
6.75, 11.0
0.0000, -1.0000, 0.0000
*TRANSVERSE SHEAR STIFFNESS
9972128.26, 9972128.26
*BEAM SECTION,SECTION=RECT,MATERIAL=UWOOD,ELSET=E 15
6.75, 11.0
-0.8660, 0.5000, 0.0000
*TRANSVERSE SHEAR STIFFNESS
9972128.26, 9972128.26
**-----MAIN BEAMS 1/USER ELEMENTS
*USER ELEMENT,NODES=2,TYPE=U 1,LINEAR
1,2,3,4,5,6
*ELEMENT,TYPE=U 1,ELSET=C 1
77, 1, 5
*MATRIX,TYPE=STIFFNESS
0.1332E+06
0.7693E+05, 0.4442E+05
0.0000E+00, 0.0000E+00, 0.0000E+00
-0.3320E+06, -0.1917E+06, 0.0000E+00, 0.8404E+06
0.5751E+06, 0.3320E+06, 0.0000E+00, -0.1456E+07
0.2521E+07

```

```

0.3148E+07, 0.1818E+07, 0.0000E+00, -0.7712E+07
0.1336E+08, 0.8865E+08
0.5036E+05, 0.2908E+05, 0.0000E+00, -0.1477E+06
0.2557E+06, 0.1868E+07, 0.1577E+06
0.2908E+05, 0.1679E+05, 0.0000E+00, -0.8525E+05
0.1477E+06, 0.1078E+07, 0.9107E+05, 0.5258E+05
0.0000E+00, 0.0000E+00, 0.0000E+00, 0.0000E+00
0.0000E+00, 0.0000E+00, 0.0000E+00, 0.0000E+00
0.0000E+00
-0.2244E+06, -0.1295E+06, 0.0000E+00, 0.6266E+06
-0.1085E+07, -0.7747E+07, -0.5387E+06, -0.3110E+06
0.0000E+00, 0.1868E+07
0.3886E+06, 0.2244E+06, 0.0000E+00, -0.1085E+07
0.1880E+07, 0.1342E+08, 0.9331E+06, 0.5387E+06
0.0000E+00, -0.3236E+07, 0.5604E+07
-0.1837E+07, -0.1061E+07, 0.0000E+00, 0.4933E+07
-0.8545E+07, -0.6531E+08, -0.3076E+07, -0.1776E+07
0.0000E+00, 0.1110E+08, -0.1923E+08, 0.8553E+08
*UEL PROPERTY,ELSET=C 1
*USER ELEMENT,NODES=2,TYPE=U 2,LINEAR
1,2,3,4,5,6
*ELEMENT,TYPE=U 2,ELSET=C 2
78, 5, 3
*MATRIX,TYPE=STIFFNESS
0.1332E+06
0.7693E+05, 0.4442E+05
-0.1363 , -0.7867E-01, 0.1393E-06
-0.2008E+06, -0.1159E+06, 0.2053 , 0.3507E+06
0.3477E+06, 0.2008E+06, -0.3556 , -0.6075E+06
0.1052E+07
0.3192E+07, 0.1843E+07, -3.265 , -0.4093E+07
0.7089E+07, 0.9062E+08
0.5036E+05, 0.2908E+05, -0.5150E-01, -0.6993E+05
0.1211E+06, 0.1886E+07, 0.1577E+06
0.2908E+05, 0.1679E+05, -0.2973E-01, -0.4038E+05
0.6994E+05, 0.1089E+07, 0.9107E+05, 0.5258E+05
-0.5150E-01, -0.2973E-01, 0.5267E-07, 0.7152E-01
-0.1239 , -1.929 , -0.1613 , -0.9313E-01
0.1649E-06
-0.2995E+06, -0.1729E+06, 0.3063 , 0.3948E+06
-0.6838E+06, -0.1052E+08, -0.6640E+06, -0.3834E+06
0.6791 , 0.2916E+07
0.5188E+06, 0.2995E+06, -0.5305 , -0.6838E+06
0.1184E+07, 0.1822E+08, 0.1150E+07, 0.6640E+06
-1.176 , -0.5051E+07, 0.8748E+07
-0.1794E+07, -0.1036E+07, 1.834 , 0.2159E+07
-0.3739E+07, -0.6439E+08, -0.2977E+07, -0.1719E+07
3.044 , 0.1416E+08, -0.2453E+08, 0.8134E+08
*UEL PROPERTY,ELSET=C 2
*USER ELEMENT,NODES=2,TYPE=U 3,LINEAR
1,2,3,4,5,6

```

```

*ELEMENT,TYPE=U 3,ELSET=C 3
79, 1, 4
*MATRIX,TYPE=STIFFNESS
0.0000E+00
0.0000E+00, 0.1777E+06
0.0000E+00, 0.0000E+00, 0.0000E+00
0.0000E+00, -0.7668E+06, 0.0000E+00, 0.3361E+07
0.0000E+00, 0.0000E+00, 0.0000E+00, 0.0000E+00
0.0000E+00
0.0000E+00, 0.3635E+07, 0.0000E+00, -0.1542E+08
0.0000E+00, 0.8865E+08
0.0000E+00, 0.0000E+00, 0.0000E+00, 0.0000E+00
0.0000E+00, 0.0000E+00, 0.0000E+00
0.0000E+00, 0.6715E+05, 0.0000E+00, -0.3410E+06
0.0000E+00, 0.2157E+07, 0.0000E+00, 0.2103E+06
0.0000E+00, 0.0000E+00, 0.0000E+00, 0.0000E+00
0.0000E+00, 0.0000E+00, 0.0000E+00, 0.0000E+00
0.0000E+00
0.0000E+00, -0.5182E+06, 0.0000E+00, 0.2506E+07
0.0000E+00, -0.1549E+08, 0.0000E+00, -0.1244E+07
0.0000E+00, 0.7472E+07
0.0000E+00, 0.0000E+00, 0.0000E+00, 0.0000E+00
0.0000E+00, 0.0000E+00, 0.0000E+00, 0.0000E+00
0.0000E+00, 0.0000E+00, 0.0000E+00
0.0000E+00, -0.2121E+07, 0.0000E+00, 0.9867E+07
0.0000E+00, -0.6531E+08, 0.0000E+00, -0.3552E+07
0.0000E+00, 0.2220E+08, 0.0000E+00, 0.8553E+08
*UEL PROPERTY,ELSET=C 3
*USER ELEMENT,NODES=2,TYPE=U 4,LINEAR
1,2,3,4,5,6
*ELEMENT,TYPE=U 4,ELSET=C 4
80, 4, 2
*MATRIX,TYPE=STIFFNESS
0.0000E+00
0.0000E+00, 0.1777E+06
0.0000E+00, 0.0000E+00, 0.0000E+00
0.0000E+00, -0.4636E+06, 0.0000E+00, 0.1403E+07
0.0000E+00, 0.0000E+00, 0.0000E+00, 0.0000E+00
0.0000E+00
0.0000E+00, 0.3686E+07, 0.0000E+00, -0.8186E+07
0.0000E+00, 0.9062E+08
0.0000E+00, 0.0000E+00, 0.0000E+00, 0.0000E+00
0.0000E+00, 0.0000E+00, 0.0000E+00
0.0000E+00, 0.6715E+05, 0.0000E+00, -0.1615E+06
0.0000E+00, 0.2178E+07, 0.0000E+00, 0.2103E+06
0.0000E+00, 0.0000E+00, 0.0000E+00, 0.0000E+00
0.0000E+00, 0.0000E+00, 0.0000E+00, 0.0000E+00
0.0000E+00
0.0000E+00, -0.6917E+06, 0.0000E+00, 0.1579E+07
0.0000E+00, -0.2104E+08, 0.0000E+00, -0.1534E+07
0.0000E+00, 0.1166E+08

```

```

0.0000E+00, 0.0000E+00, 0.0000E+00, 0.0000E+00
0.0000E+00, 0.0000E+00, 0.0000E+00, 0.0000E+00
0.0000E+00, 0.0000E+00, 0.0000E+00
0.0000E+00, -0.2071E+07, 0.0000E+00, 0.4318E+07
0.0000E+00, -0.6439E+08, 0.0000E+00, -0.3437E+07
0.0000E+00, 0.2833E+08, 0.0000E+00, 0.8135E+08
*UEL PROPERTY,ELSET=C 4
*USER ELEMENT,NODES=2,TYPE=U 46,LINEAR
1,2,3,4,5,6
*ELEMENT,TYPE=U 46,ELSET=C 46
122, 15, 13
*MATRIX,TYPE=STIFFNESS
0.1332E+06
0.7693E+05, 0.4442E+05
-0.6558 , -0.3787 , 0.3228E-05
-0.2008E+06, -0.1159E+06, 0.9882 , 0.3508E+06
0.3477E+06, 0.2008E+06, -1.711 , -0.6076E+06
0.1052E+07
-0.3192E+07, -0.1843E+07, 15.71 , 0.4093E+07
-0.7088E+07, 0.9060E+08
0.5036E+05, 0.2908E+05, -0.2479 , -0.6995E+05
0.1211E+06, -0.1886E+07, 0.1577E+06
0.2908E+05, 0.1679E+05, -0.1431 , -0.4039E+05
0.6994E+05, -0.1089E+07, 0.9107E+05, 0.5258E+05
-0.2479 , -0.1431 , 0.1220E-05, 0.3443
-0.5961 , 9.281 , -0.7763 , -0.4482
0.3821E-05
-0.2995E+06, -0.1730E+06, 1.474 , 0.3949E+06
-0.6838E+06, 0.1052E+08, -0.6640E+06, -0.3834E+06
3.268 , 0.2916E+07
0.5188E+06, 0.2995E+06, -2.553 , -0.6839E+06
0.1184E+07, -0.1822E+08, 0.1150E+07, 0.6641E+06
-5.661 , -0.5051E+07, 0.8747E+07
0.1794E+07, 0.1036E+07, -8.827 , -0.2159E+07
0.3739E+07, -0.6438E+08, 0.2976E+07, 0.1719E+07
-14.65 , -0.1416E+08, 0.2453E+08, 0.8133E+08
*UEL PROPERTY,ELSET=C 46
*USER ELEMENT,NODES=2,TYPE=U 45,LINEAR
1,2,3,4,5,6
*ELEMENT,TYPE=U 45,ELSET=C 45
121, 1, 15
*MATRIX,TYPE=STIFFNESS
0.1333E+06
0.7693E+05, 0.4441E+05
0.0000E+00, 0.0000E+00, 0.0000E+00
-0.3320E+06, -0.1917E+06, 0.0000E+00, 0.8403E+06
0.5751E+06, 0.3320E+06, 0.0000E+00, -0.1456E+07
0.2521E+07
-0.3148E+07, -0.1818E+07, 0.0000E+00, 0.7712E+07
-0.1336E+08, 0.8866E+08
0.5036E+05, 0.2908E+05, 0.0000E+00, -0.1476E+06

```

```

0.2557E+06, -0.1868E+07, 0.1577E+06
0.2908E+05, 0.1679E+05, 0.0000E+00, -0.8524E+05
0.1476E+06, -0.1078E+07, 0.9107E+05, 0.5257E+05
0.0000E+00, 0.0000E+00, 0.0000E+00, 0.0000E+00
0.0000E+00, 0.0000E+00, 0.0000E+00, 0.0000E+00
0.0000E+00
-0.2244E+06, -0.1295E+06, 0.0000E+00, 0.6265E+06
-0.1085E+07, 0.7747E+07, -0.5387E+06, -0.3110E+06
0.0000E+00, 0.1868E+07
0.3886E+06, 0.2244E+06, 0.0000E+00, -0.1085E+07
0.1880E+07, -0.1342E+08, 0.9331E+06, 0.5387E+06
0.0000E+00, -0.3236E+07, 0.5604E+07
0.1837E+07, 0.1061E+07, 0.0000E+00, -0.4934E+07
0.8545E+07, -0.6532E+08, 0.3076E+07, 0.1776E+07
0.0000E+00, -0.1110E+08, 0.1923E+08, 0.8554E+08
*UEL PROPERTY,ELSET=C 45
*USER ELEMENT,NODES=2,TYPE=U 32,LINEAR
1,2,3,4,5,6
*ELEMENT,TYPE=U 32,ELSET=C 32
108, 11, 10
*MATRIX,TYPE=STIFFNESS
0.1332E+06
-0.7693E+05, 0.4442E+05
-0.6558 , 0.3787 , 0.3228E-05
0.2008E+06, -0.1159E+06, -0.9882 , 0.3508E+06
0.3477E+06, -0.2008E+06, -1.711 , 0.6076E+06
0.1052E+07
0.3192E+07, -0.1843E+07, -15.71 , 0.4093E+07
0.7088E+07, 0.9060E+08
0.5036E+05, -0.2908E+05, -0.2479 , 0.6995E+05
0.1211E+06, 0.1886E+07, 0.1577E+06
-0.2908E+05, 0.1679E+05, 0.1431 , -0.4039E+05
-0.6994E+05, -0.1089E+07, -0.9107E+05, 0.5258E+05
-0.2479 , 0.1431 , 0.1220E-05, -0.3443
-0.5961 , -9.281 , -0.7763 , 0.4482
0.3821E-05
0.2995E+06, -0.1730E+06, -1.474 , 0.3949E+06
0.6838E+06, 0.1052E+08, 0.6640E+06, -0.3834E+06
-3.268 , 0.2916E+07
0.5188E+06, -0.2995E+06, -2.553 , 0.6839E+06
0.1184E+07, 0.1822E+08, 0.1150E+07, -0.6641E+06
-5.661 , 0.5051E+07, 0.8747E+07
-0.1794E+07, 0.1036E+07, 8.827 , -0.2159E+07
-0.3739E+07, -0.6438E+08, -0.2976E+07, 0.1719E+07
14.65 , -0.1416E+08, -0.2453E+08, 0.8133E+08
*UEL PROPERTY,ELSET=C 32
*USER ELEMENT,NODES=2,TYPE=U 31,LINEAR
1,2,3,4,5,6
*ELEMENT,TYPE=U 31,ELSET=C 31
107, 1, 11
*MATRIX,TYPE=STIFFNESS

```

```

0.1333E+06
-0.7693E+05, 0.4441E+05
0.0000E+00, 0.0000E+00, 0.0000E+00
0.3320E+06, -0.1917E+06, 0.0000E+00, 0.8403E+06
0.5751E+06, -0.3320E+06, 0.0000E+00, 0.1456E+07
0.2521E+07
0.3148E+07, -0.1818E+07, 0.0000E+00, 0.7712E+07
0.1336E+08, 0.8866E+08
0.5036E+05, -0.2908E+05, 0.0000E+00, 0.1476E+06
0.2557E+06, 0.1868E+07, 0.1577E+06
-0.2908E+05, 0.1679E+05, 0.0000E+00, -0.8524E+05
-0.1476E+06, -0.1078E+07, -0.9107E+05, 0.5257E+05
0.0000E+00, 0.0000E+00, 0.0000E+00, 0.0000E+00
0.0000E+00, 0.0000E+00, 0.0000E+00, 0.0000E+00
0.0000E+00
0.2244E+06, -0.1295E+06, 0.0000E+00, 0.6265E+06
0.1085E+07, 0.7747E+07, 0.5387E+06, -0.3110E+06
0.0000E+00, 0.1868E+07
0.3886E+06, -0.2244E+06, 0.0000E+00, 0.1085E+07
0.1880E+07, 0.1342E+08, 0.9331E+06, -0.5387E+06
0.0000E+00, 0.3236E+07, 0.5604E+07
-0.1837E+07, 0.1061E+07, 0.0000E+00, -0.4934E+07
-0.8545E+07, -0.6532E+08, -0.3076E+07, 0.1776E+07
0.0000E+00, -0.1110E+08, -0.1923E+08, 0.8554E+08
*UEL PROPERTY,ELSET=C 31
*USER ELEMENT,NODES=2,TYPE=U 16,LINEAR
1,2,3,4,5,6
*ELEMENT,TYPE=U 16,ELSET=C 16
92, 8, 7
*MATRIX,TYPE=STIFFNESS
0.1332E+06
-0.7693E+05, 0.4442E+05
-0.1363 , 0.7867E-01, 0.1393E-06
0.2008E+06, -0.1159E+06, -0.2053 , 0.3507E+06
0.3477E+06, -0.2008E+06, -0.3556 , 0.6075E+06
0.1052E+07
-0.3192E+07, 0.1843E+07, 3.265 , -0.4093E+07
-0.7089E+07, 0.9062E+08
0.5036E+05, -0.2908E+05, -0.5150E-01, 0.6993E+05
0.1211E+06, -0.1886E+07, 0.1577E+06
-0.2908E+05, 0.1679E+05, 0.2973E-01, -0.4038E+05
-0.6994E+05, 0.1089E+07, -0.9107E+05, 0.5258E+05
-0.5150E-01, 0.2973E-01, 0.5267E-07, -0.7152E-01
-0.1239 , 1.929 , -0.1613 , 0.9313E-01
0.1649E-06
0.2995E+06, -0.1729E+06, -0.3063 , 0.3948E+06
0.6838E+06, -0.1052E+08, 0.6640E+06, -0.3834E+06
-0.6791 , 0.2916E+07
0.5188E+06, -0.2995E+06, -0.5305 , 0.6838E+06
0.1184E+07, -0.1822E+08, 0.1150E+07, -0.6640E+06
-1.176 , 0.5051E+07, 0.8748E+07

```

```

0.1794E+07, -0.1036E+07, -1.834 , 0.2159E+07
0.3739E+07, -0.6439E+08, 0.2977E+07, -0.1719E+07
-3.044 , 0.1416E+08, 0.2453E+08, 0.8134E+08
*UEL PROPERTY,ELSET=C 16
*USER ELEMENT,NODES=2,TYPE=U 43,LINEAR
1,2,3,4,5,6
*ELEMENT,TYPE=U 43,ELSET=C 43
119, 1, 16
*MATRIX,TYPE=STIFFNESS
0.2289E-06
-0.2016 , 0.1777E+06
0.0000E+00, 0.0000E+00, 0.0000E+00
0.8703 , -0.7668E+06, 0.0000E+00, 0.3361E+07
0.9877E-06, -0.8703 , 0.0000E+00, 3.815
0.4330E-05
4.126 , -0.3635E+07, 0.0000E+00, 0.1542E+08
17.51 , 0.8865E+08
0.8650E-07, -0.7621E-01, 0.0000E+00, 0.3870
0.4392E-06, 2.448 , 0.2709E-06
-0.7621E-01, 0.6715E+05, 0.0000E+00, -0.3410E+06
-0.3870 , -0.2157E+07, -0.2387 , 0.2103E+06
0.0000E+00, 0.0000E+00, 0.0000E+00, 0.0000E+00
0.0000E+00, 0.0000E+00, 0.0000E+00, 0.0000E+00
0.0000E+00
0.5881 , -0.5182E+06, 0.0000E+00, 0.2506E+07
2.845 , 0.1549E+08, 1.412 , -0.1244E+07
0.0000E+00, 0.7472E+07
0.6675E-06, -0.5881 , 0.0000E+00, 2.845
0.3229E-05, 17.59 , 0.1603E-05, -1.412
0.0000E+00, 8.481 , 0.9626E-05
-2.408 , 0.2121E+07, 0.0000E+00, -0.9867E+07
-11.20 , -0.6531E+08, -4.031 , 0.3552E+07
0.0000E+00, -0.2220E+08, -25.20 , 0.8553E+08
*UEL PROPERTY,ELSET=C 43
*USER ELEMENT,NODES=2,TYPE=U 44,LINEAR
1,2,3,4,5,6
*ELEMENT,TYPE=U 44,ELSET=C 44
120, 16, 14
*MATRIX,TYPE=STIFFNESS
0.5044E-06
0.2994 , 0.1777E+06
0.7005E-07, 0.4158E-01, 0.9729E-08
-0.7812 , -0.4636E+06, -0.1085 , 0.1403E+07
0.2770E-05, 1.644 , 0.3847E-06, -4.280
0.1540E-04
-6.211 , -0.3686E+07, -0.8627 , 0.8186E+07
-35.00 , 0.9062E+08
0.1906E-06, 0.1131 , 0.2648E-07, -0.2721
0.1317E-05, -3.669 , 0.5971E-06
0.1131 , 0.6715E+05, 0.1571E-01, -0.1615E+06
0.7817 , -0.2178E+07, 0.3544 , 0.2103E+06

```

```

0.2648E-07, 0.1571E-01, 0.3677E-08, -0.3779E-01
0.1829E-06, -0.5096 , 0.8292E-07, 0.4921E-01
0.1152E-07
-1.166 , -0.6917E+06, -0.1619 , 0.1579E+07
-7.585 , 0.2104E+08, -2.584 , -0.1534E+07
-0.3589 , 0.1166E+08
0.1147E-05, 0.6809 , 0.1593E-06, -1.650
0.7552E-05, -20.39 , 0.2998E-05, 1.780
0.4164E-06, -13.02 , 0.1523E-04
3.490 , 0.2071E+07, 0.4847 , -0.4318E+07
22.34 , -0.6439E+08, 5.791 , 0.3437E+07
0.8043 , -0.2833E+08, 28.70 , 0.8135E+08
*UEL PROPERTY,ELSET=C 44
*USER ELEMENT,NODES=2,TYPE=U 15,LINEAR
1,2,3,4,5,6
*ELEMENT,TYPE=U 15,ELSET=C 15
91, 1, 8
*MATRIX,TYPE=STIFFNESS
0.1332E+06
-0.7693E+05, 0.4442E+05
0.0000E+00, 0.0000E+00, 0.0000E+00
0.3320E+06, -0.1917E+06, 0.0000E+00, 0.8404E+06
0.5751E+06, -0.3320E+06, 0.0000E+00, 0.1456E+07
0.2521E+07
-0.3148E+07, 0.1818E+07, 0.0000E+00, -0.7712E+07
-0.1336E+08, 0.8865E+08
0.5036E+05, -0.2908E+05, 0.0000E+00, 0.1477E+06
0.2557E+06, -0.1868E+07, 0.1577E+06
-0.2908E+05, 0.1679E+05, 0.0000E+00, -0.8525E+05
-0.1477E+06, 0.1078E+07, -0.9107E+05, 0.5258E+05
0.0000E+00, 0.0000E+00, 0.0000E+00, 0.0000E+00
0.0000E+00, 0.0000E+00, 0.0000E+00, 0.0000E+00
0.0000E+00
0.2244E+06, -0.1295E+06, 0.0000E+00, 0.6266E+06
0.1085E+07, -0.7747E+07, 0.5387E+06, -0.3110E+06
0.0000E+00, 0.1868E+07
0.3886E+06, -0.2244E+06, 0.0000E+00, 0.1085E+07
0.1880E+07, -0.1342E+08, 0.9331E+06, -0.5387E+06
0.0000E+00, 0.3236E+07, 0.5604E+07
0.1837E+07, -0.1061E+07, 0.0000E+00, 0.4933E+07
0.8545E+07, -0.6531E+08, 0.3076E+07, -0.1776E+07
0.0000E+00, 0.1110E+08, 0.1923E+08, 0.8553E+08
*UEL PROPERTY,ELSET=C 15
**-----EDGE BEAMS
*BEAM SECTION,SECTION=RECT,MATERIAL=UWOOD,ELSET=E 5
12.25, 3.0
-0.0406, -0.0234, 0.9989
*TRANSVERSE SHEAR STIFFNESS
9972128.26, 9972128.26
*BEAM SECTION,SECTION=RECT,MATERIAL=UWOOD,ELSET=E 6
12.25, 3.0

```

0.0000, 0.0469, 0.9989
 *TRANSVERSE SHEAR STIFFNESS
 9972128.26, 9972128.26
 *BEAM SECTION,SECTION=RECT,MATERIAL=UWOOD,ELSET=E 48
 12.25, 3.0
 -0.0406, -0.0234, -0.9989
 *TRANSVERSE SHEAR STIFFNESS
 9972128.26, 9972128.26
 *BEAM SECTION,SECTION=RECT,MATERIAL=UWOOD,ELSET=E 60
 12.25, 3.0
 -0.0406, -0.0234, 0.9989
 *TRANSVERSE SHEAR STIFFNESS
 9972128.26, 9972128.26
 *BEAM SECTION,SECTION=RECT,MATERIAL=UWOOD,ELSET=E 19
 12.25, 3.0
 0.0406, -0.0234, -0.9989
 *TRANSVERSE SHEAR STIFFNESS
 9972128.26, 9972128.26
 *BEAM SECTION,SECTION=RECT,MATERIAL=UWOOD,ELSET=E 20
 12.25, 3.0
 0.0000, 0.0469, -0.9989
 *TRANSVERSE SHEAR STIFFNESS
 9972128.26, 9972128.26
 *BEAM SECTION,SECTION=RECT,MATERIAL=UWOOD,ELSET=E 34
 12.25, 3.0
 0.0406, -0.0234, -0.9989
 *TRANSVERSE SHEAR STIFFNESS
 9972128.26, 9972128.26
 *BEAM SECTION,SECTION=RECT,MATERIAL=UWOOD,ELSET=E 59
 12.25, 3.0
 0.0406, -0.0234, 0.9989
 *TRANSVERSE SHEAR STIFFNESS
 9972128.26, 9972128.26
 *BEAM SECTION,SECTION=RECT,MATERIAL=UWOOD,ELSET=E 47
 12.25, 3.0
 0.0000, 0.0469, -0.9989
 *TRANSVERSE SHEAR STIFFNESS
 9972128.26, 9972128.26
 *BEAM SECTION,SECTION=RECT,MATERIAL=UWOOD,ELSET=E 33
 12.25, 3.0
 -0.0406, -0.0234, -0.9989
 *TRANSVERSE SHEAR STIFFNESS
 9972128.26, 9972128.26
 *BEAM SECTION,SECTION=RECT,MATERIAL=UWOOD,ELSET=E 72
 12.25, 3.0
 0.0406, -0.0234, 0.9989
 *TRANSVERSE SHEAR STIFFNESS
 9972128.26, 9972128.26
 *BEAM SECTION,SECTION=RECT,MATERIAL=UWOOD,ELSET=E 71
 12.25, 3.0
 0.0000, 0.0469, 0.9989

```

*TRANSVERSE SHEAR STIFFNESS
 9972128.26, 9972128.26
**-----EDGE BEAMS/USER ELEMENTS
*USER ELEMENT,NODES=2,TYPE=U 5,LINEAR
1,2,3,4,5,6
*ELEMENT,TYPE=U 5,ELSET=C 5
 81, 3, 6
*MATRIX,TYPE=STIFFNESS
 0.1321E+06
-0.7749E+05, 0.4545E+05
 3553. , -2084. , 95.53
 0.5699E+06, -0.3343E+06, 0.1532E+05, 0.2514E+07
 0.8316E+06, -0.4878E+06, 0.2236E+05, 0.3647E+07
 0.5307E+07
-0.3055E+07, 0.1792E+07, -0.8215E+05, -0.1393E+08
-0.1987E+08, 0.8475E+08
 0.4993E+05, -0.2929E+05, 1343. , 0.2831E+06
 0.3992E+06, -0.1821E+07, 0.1564E+06
-0.2929E+05, 0.1718E+05, -787.6 , -0.1661E+06
-0.2341E+06, 0.1068E+07, -0.9173E+05, 0.5380E+05
 1343. , -787.6 , 36.11 , 7613.
 0.1073E+05, -0.4897E+05, 4205. , -2467.
 113.1
 0.1337E+06, -0.7840E+05, 3594. , 0.7214E+06
 0.1027E+07, -0.4415E+07, 0.4056E+06, -0.2379E+06
 0.1091E+05, 0.1106E+07
 0.3129E+06, -0.1835E+06, 8414. , 0.1680E+07
 0.2383E+07, -0.1050E+08, 0.8351E+06, -0.4898E+06
 0.2246E+05, 0.2214E+07, 0.4521E+07
 0.1855E+07, -0.1088E+07, 0.4987E+05, 0.9821E+07
 0.1377E+08, -0.6483E+08, 0.3134E+07, -0.1838E+07
 0.8426E+05, 0.7171E+07, 0.1627E+08, 0.8817E+08
*UEL PROPERTY,ELSET=C 5
*USER ELEMENT,NODES=2,TYPE=U 6,LINEAR
1,2,3,4,5,6
*ELEMENT,TYPE=U 6,ELSET=C 6
 82, 6, 2
*MATRIX,TYPE=STIFFNESS
 0.1342E+06
-0.7627E+05, 0.4334E+05
 3581. , -2035. , 95.54
 0.4387E+06, -0.2493E+06, 0.1170E+05, 0.1450E+07
 0.6240E+06, -0.3546E+06, 0.1665E+05, 0.2060E+07
 0.2954E+07
-0.3152E+07, 0.1791E+07, -0.8408E+05, -0.1048E+08
-0.1430E+08, 0.8816E+08
 0.5073E+05, -0.2883E+05, 1353. , 0.2058E+06
 0.2744E+06, -0.1869E+07, 0.1589E+06
-0.2883E+05, 0.1638E+05, -769.1 , -0.1169E+06
-0.1559E+06, 0.1062E+07, -0.9029E+05, 0.5131E+05
 1353. , -769.1 , 36.11 , 5490.

```

```

7320. , -0.4988E+05, 4239. , -2409.
113.1
0.2058E+06, -0.1169E+06, 5490. , 0.7953E+06
0.1070E+07, -0.7017E+07, 0.5246E+06, -0.2981E+06
0.1400E+05, 0.1750E+07
0.4483E+06, -0.2548E+06, 0.1196E+05, 0.1723E+07
0.2309E+07, -0.1539E+08, 0.1067E+07, -0.6066E+06
0.2848E+05, 0.3559E+07, 0.7293E+07
0.1835E+07, -0.1043E+07, 0.4897E+05, 0.6885E+07
0.9073E+07, -0.6484E+08, 0.3072E+07, -0.1746E+07
0.8196E+05, 0.1021E+08, 0.2195E+08, 0.8475E+08
*UEL PROPERTY,ELSET=C 6
*USER ELEMENT,NODES=2,TYPE=U 48,LINEAR
1,2,3,4,5,6
*ELEMENT,TYPE=U 48,ELSET=C 48
124, 17, 13
*MATRIX,TYPE=STIFFNESS
0.1321E+06
-0.7749E+05, 0.4545E+05
-3553. , 2084. , 95.53
-0.5699E+06, 0.3343E+06, 0.1532E+05, 0.2514E+07
-0.8316E+06, 0.4878E+06, 0.2236E+05, 0.3647E+07
0.5307E+07
-0.3055E+07, 0.1792E+07, 0.8215E+05, 0.1393E+08
0.1987E+08, 0.8475E+08
0.4993E+05, -0.2929E+05, -1343. , -0.2831E+06
-0.3992E+06, -0.1821E+07, 0.1564E+06
-0.2929E+05, 0.1718E+05, 787.6 , 0.1661E+06
0.2341E+06, 0.1068E+07, -0.9173E+05, 0.5380E+05
-1343. , 787.6 , 36.11 , 7613.
0.1073E+05, 0.4897E+05, -4205. , 2467.
113.1
-0.1337E+06, 0.7840E+05, 3594. , 0.7214E+06
0.1027E+07, 0.4415E+07, -0.4056E+06, 0.2379E+06
0.1091E+05, 0.1106E+07
-0.3129E+06, 0.1835E+06, 8414. , 0.1680E+07
0.2383E+07, 0.1050E+08, -0.8351E+06, 0.4898E+06
0.2246E+05, 0.2214E+07, 0.4521E+07
0.1855E+07, -0.1088E+07, -0.4987E+05, -0.9821E+07
-0.1377E+08, -0.6483E+08, 0.3134E+07, -0.1838E+07
-0.8426E+05, -0.7171E+07, -0.1627E+08, 0.8817E+08
*UEL PROPERTY,ELSET=C 48
*USER ELEMENT,NODES=2,TYPE=U 60,LINEAR
1,2,3,4,5,6
*ELEMENT,TYPE=U 60,ELSET=C 60
136, 18, 13
*MATRIX,TYPE=STIFFNESS
8.359
-1218. , 0.1776E+06
-28.26 , 4119. , 95.54
5996. , -0.8738E+06, -0.2027E+05, 0.4362E+07

```

```

-535.8 , 0.7809E+05, 1811. , -0.3789E+06
0.4203E+05
0.2487E+05, -0.3625E+07, -0.8408E+05, 0.1762E+08
-0.1924E+07, 0.8817E+08
3.159 , -460.5 , -10.68 , 2687.
-323.8 , 0.1475E+05, 9.895
-460.5 , 0.6711E+05, 1557. , -0.3916E+06
0.4719E+05, -0.2150E+07, -1442. , 0.2102E+06
-10.68 , 1557. , 36.11 , -9084.
1095. , -0.4987E+05, -33.45 , 4875.
113.1
3876. , -0.5649E+06, -0.1310E+05, 0.3140E+07
-0.3690E+06, 0.1684E+08, 9365. , -0.1365E+07
-0.3166E+05, 0.8989E+07
362.6 , -0.5285E+05, -1226. , 0.2837E+06
-0.3562E+05, 0.1620E+07, 626.6 , -0.9133E+05
-2118. , 0.6212E+06, 0.5370E+05
-0.1448E+05, 0.2111E+07, 0.4897E+05, -0.1130E+08
0.1426E+07, -0.6484E+08, -0.2424E+05, 0.3534E+07
0.8196E+05, -0.2412E+08, -0.2131E+07, 0.8476E+08
*UEL PROPERTY,ELSET=C 60
*USER ELEMENT,NODES=2,TYPE=U 19,LINEAR
1,2,3,4,5,6
*ELEMENT,TYPE=U 19,ELSET=C 19
95, 7, 9
*MATRIX,TYPE=STIFFNESS
0.1321E+06
0.7749E+05, 0.4545E+05
3553. , 2084. , 95.53
0.3186E+06, 0.1869E+06, 8566. , 0.7940E+06
-0.6865E+06, -0.4026E+06, -0.1846E+05, -0.1681E+07
0.3610E+07
0.3127E+07, 0.1834E+07, 0.8408E+05, 0.7146E+07
-0.1622E+08, 0.8816E+08
0.4993E+05, 0.2929E+05, 1343. , 0.1337E+06
-0.3129E+06, 0.1855E+07, 0.1564E+06
0.2929E+05, 0.1718E+05, 787.6 , 0.7840E+05
-0.1835E+06, 0.1088E+07, 0.9173E+05, 0.5380E+05
1343. , 787.6 , 36.11 , 3594.
-8414. , 0.4987E+05, 4205. , 2467.
113.1
0.2831E+06, 0.1661E+06, 7613. , 0.7214E+06
-0.1680E+07, 0.9821E+07, 0.6569E+06, 0.3853E+06
0.1766E+05, 0.2826E+07
-0.3992E+06, -0.2341E+06, -0.1073E+05, -0.1027E+07
0.2383E+07, -0.1377E+08, -0.9802E+06, -0.5750E+06
-0.2636E+05, -0.4180E+07, 0.6217E+07
-0.1821E+07, -0.1068E+07, -0.4897E+05, -0.4415E+07
0.1050E+08, -0.6483E+08, -0.3048E+07, -0.1788E+07
-0.8196E+05, -0.1391E+08, 0.1982E+08, 0.8475E+08
*UEL PROPERTY,ELSET=C 19

```

```

*USER ELEMENT,NODES=2,TYPE=U 20,LINEAR
1,2,3,4,5,6
*ELEMENT,TYPE=U 20,ELSET=C 20
96, 9, 2
*MATRIX,TYPE=STIFFNESS
0.1342E+06
0.7627E+05, 0.4334E+05
3581. , 2035. , 95.54
0.4387E+06, 0.2493E+06, 0.1170E+05, 0.1450E+07
-0.9166E+06, -0.5208E+06, -0.2445E+05, -0.3033E+07
0.6370E+07
0.3079E+07, 0.1750E+07, 0.8215E+05, 0.1024E+08
-0.2200E+08, 0.8475E+08
0.5073E+05, 0.2883E+05, 1353. , 0.2058E+06
-0.4483E+06, 0.1835E+07, 0.1589E+06
0.2883E+05, 0.1638E+05, 769.1 , 0.1169E+06
-0.2548E+06, 0.1043E+07, 0.9029E+05, 0.5131E+05
1353. , 769.1 , 36.11 , 5490.
-0.1196E+05, 0.4897E+05, 4239. , 2409.
113.1
0.2058E+06, 0.1169E+06, 5490. , 0.7953E+06
-0.1723E+07, 0.6885E+07, 0.5246E+06, 0.2981E+06
0.1400E+05, 0.1750E+07
-0.2744E+06, -0.1559E+06, -7320. , -0.1070E+07
0.2309E+07, -0.9073E+07, -0.7749E+06, -0.4403E+06
-0.2067E+05, -0.2586E+07, 0.3877E+07
-0.1869E+07, -0.1062E+07, -0.4987E+05, -0.7017E+07
0.1539E+08, -0.6484E+08, -0.3159E+07, -0.1795E+07
-0.8427E+05, -0.1050E+08, 0.1434E+08, 0.8817E+08
*UEL PROPERTY,ELSET=C 20
*USER ELEMENT,NODES=2,TYPE=U 34,LINEAR
1,2,3,4,5,6
*ELEMENT,TYPE=U 34,ELSET=C 34
110, 12, 10
*MATRIX,TYPE=STIFFNESS
8.359
1218. , 0.1776E+06
-28.26 , -4119. , 95.54
7995. , 0.1165E+07, -0.2703E+05, 0.7767E+07
-618.5 , -0.9015E+05, 2091. , -0.6140E+06
0.5366E+05
-0.2430E+05, -0.3542E+07, 0.8215E+05, -0.2417E+08
0.2132E+07, 0.8475E+08
3.159 , 460.5 , -10.68 , 3876.
-362.6 , -0.1449E+05, 9.895
460.5 , 0.6711E+05, -1557. , 0.5649E+06
-0.5285E+05, -0.2111E+07, 1442. , 0.2102E+06
-10.68 , -1557. , 36.11 , -0.1310E+05
1226. , 0.4897E+05, -33.45 , -4875.
113.1
2687. , 0.3916E+06, -9084. , 0.3140E+07

```

```

-0.2837E+06, -0.1130E+08, 7366. , 0.1074E+07
-0.2490E+05, 0.5585E+07
 323.8 , 0.4719E+05, -1095. , 0.3690E+06
-0.3562E+05, -0.1426E+07, 527.7 , 0.7690E+05
-1784. , 0.3716E+06, 0.4208E+05
 0.1475E+05, 0.2150E+07, -0.4987E+05, 0.1684E+08
-0.1620E+07, -0.6484E+08, 0.2493E+05, 0.3633E+07
-0.8427E+05, 0.1767E+08, 0.1924E+07, 0.8817E+08
*UEL PROPERTY,ELSET=C 34
*USER ELEMENT,NODES=2,TYPE=U 59,LINEAR
1,2,3,4,5,6
*ELEMENT,TYPE=U 59,ELSET=C 59
135, 7, 18
*MATRIX,TYPE=STIFFNESS
 8.359
 1218. , 0.1776E+06
 28.26 , 4119. , 95.54
-7995. , -0.1165E+07, -0.2703E+05, 0.7767E+07
 618.5 , 0.9015E+05, 2091. , -0.6139E+06
 0.5366E+05
-0.2430E+05, -0.3542E+07, -0.8215E+05, 0.2417E+08
-0.2132E+07, 0.8475E+08
 3.159 , 460.5 , 10.68 , -3876.
 362.6 , -0.1448E+05, 9.895
 460.5 , 0.6711E+05, 1557. , -0.5649E+06
 0.5284E+05, -0.2111E+07, 1442. , 0.2102E+06
 10.68 , 1557. , 36.11 , -0.1310E+05
 1226. , -0.4897E+05, 33.45 , 4875.
 113.1
-2687. , -0.3916E+06, -9084. , 0.3140E+07
-0.2837E+06, 0.1130E+08, -7366. , -0.1074E+07
-0.2490E+05, 0.5585E+07
-323.8 , -0.4719E+05, -1095. , 0.3690E+06
-0.3562E+05, 0.1426E+07, -527.7 , -0.7690E+05
-1784. , 0.3716E+06, 0.4208E+05
 0.1475E+05, 0.2150E+07, 0.4987E+05, -0.1684E+08
 0.1619E+07, -0.6484E+08, 0.2493E+05, 0.3633E+07
 0.8427E+05, -0.1767E+08, -0.1924E+07, 0.8817E+08
*UEL PROPERTY,ELSET=C 59
*USER ELEMENT,NODES=2,TYPE=U 47,LINEAR
1,2,3,4,5,6
*ELEMENT,TYPE=U 47,ELSET=C 47
123, 14, 17
*MATRIX,TYPE=STIFFNESS
 0.1342E+06
-0.7627E+05, 0.4334E+05
-3581. , 2035. , 95.54
-0.4387E+06, 0.2493E+06, 0.1170E+05, 0.1450E+07
-0.6240E+06, 0.3546E+06, 0.1665E+05, 0.2060E+07
 0.2954E+07
-0.3152E+07, 0.1791E+07, 0.8408E+05, 0.1048E+08

```

```

0.1430E+08, 0.8816E+08
0.5073E+05, -0.2883E+05, -1353. , -0.2058E+06
-0.2744E+06, -0.1869E+07, 0.1589E+06
-0.2883E+05, 0.1638E+05, 769.1 , 0.1169E+06
0.1559E+06, 0.1062E+07, -0.9029E+05, 0.5131E+05
-1353. , 769.1 , 36.11 , 5490.
7320. , 0.4987E+05, -4239. , 2409.
113.1
-0.2058E+06, 0.1169E+06, 5490. , 0.7953E+06
0.1070E+07, 0.7017E+07, -0.5246E+06, 0.2981E+06
0.1400E+05, 0.1750E+07
-0.4483E+06, 0.2547E+06, 0.1196E+05, 0.1723E+07
0.2309E+07, 0.1539E+08, -0.1067E+07, 0.6066E+06
0.2848E+05, 0.3559E+07, 0.7293E+07
0.1835E+07, -0.1043E+07, -0.4897E+05, -0.6885E+07
-0.9073E+07, -0.6484E+08, 0.3072E+07, -0.1746E+07
-0.8196E+05, -0.1021E+08, -0.2195E+08, 0.8475E+08
*UEL PROPERTY,ELSET=C 47
*USER ELEMENT,NODES=2,TYPE=U 33,LINEAR
1,2,3,4,5,6
*ELEMENT,TYPE=U 33,ELSET=C 33
109, 3, 12
*MATRIX,TYPE=STIFFNESS
8.359
-1218. , 0.1776E+06
28.26 , -4119. , 95.54
-5996. , 0.8738E+06, -0.2027E+05, 0.4362E+07
535.8 , -0.7808E+05, 1811. , -0.3789E+06
0.4203E+05
0.2487E+05, -0.3625E+07, 0.8408E+05, -0.1762E+08
0.1924E+07, 0.8817E+08
3.159 , -460.5 , 10.68 , -2687.
323.8 , 0.1475E+05, 9.895
-460.5 , 0.6711E+05, -1557. , 0.3916E+06
-0.4719E+05, -0.2150E+07, -1442. , 0.2102E+06
10.68 , -1557. , 36.11 , -9084.
1095. , 0.4987E+05, 33.45 , -4875.
113.1
-3876. , 0.5649E+06, -0.1310E+05, 0.3140E+07
-0.3690E+06, -0.1684E+08, -9365. , 0.1365E+07
-0.3166E+05, 0.8989E+07
-362.6 , 0.5284E+05, -1226. , 0.2837E+06
-0.3562E+05, -0.1619E+07, -626.6 , 0.9133E+05
-2118. , 0.6212E+06, 0.5370E+05
-0.1448E+05, 0.2111E+07, -0.4897E+05, 0.1130E+08
-0.1426E+07, -0.6484E+08, -0.2424E+05, 0.3533E+07
-0.8196E+05, 0.2412E+08, 0.2131E+07, 0.8475E+08
*UEL PROPERTY,ELSET=C 33
*USER ELEMENT,NODES=2,TYPE=U 72,LINEAR
1,2,3,4,5,6
*ELEMENT,TYPE=U 72,ELSET=C 72

```

```

148, 19, 10
*MATRIX,TYPE=STIFFNESS
0.1321E+06
0.7749E+05, 0.4545E+05
-3553. , -2084. , 95.53
-0.3186E+06, -0.1869E+06, 8566. , 0.7940E+06
0.6865E+06, 0.4026E+06, -0.1846E+05, -0.1681E+07
0.3610E+07
0.3127E+07, 0.1834E+07, -0.8408E+05, -0.7146E+07
0.1622E+08, 0.8816E+08
0.4993E+05, 0.2929E+05, -1343. , -0.1337E+06
0.3129E+06, 0.1855E+07, 0.1564E+06
0.2929E+05, 0.1718E+05, -787.6 , -0.7840E+05
0.1835E+06, 0.1088E+07, 0.9173E+05, 0.5380E+05
-1343. , -787.6 , 36.11 , 3594.
-8414. , -0.4987E+05, -4205. , -2467.
113.1
-0.2831E+06, -0.1661E+06, 7613. , 0.7214E+06
-0.1680E+07, -0.9821E+07, -0.6569E+06, -0.3853E+06
0.1766E+05, 0.2826E+07
0.3992E+06, 0.2341E+06, -0.1073E+05, -0.1027E+07
0.2383E+07, 0.1377E+08, 0.9802E+06, 0.5750E+06
-0.2636E+05, -0.4180E+07, 0.6217E+07
-0.1821E+07, -0.1068E+07, 0.4897E+05, 0.4415E+07
-0.1050E+08, -0.6483E+08, -0.3048E+07, -0.1788E+07
0.8196E+05, 0.1391E+08, -0.1982E+08, 0.8475E+08
*UEL PROPERTY,ELSET=C 72
*USER ELEMENT,NODES=2,TYPE=U 71,LINEAR
1,2,3,4,5,6
*ELEMENT,TYPE=U 71,ELSET=C 71
147, 14, 19
*MATRIX,TYPE=STIFFNESS
0.1342E+06
0.7627E+05, 0.4334E+05
-3581. , -2035. , 95.54
-0.4387E+06, -0.2493E+06, 0.1170E+05, 0.1450E+07
0.9166E+06, 0.5208E+06, -0.2445E+05, -0.3033E+07
0.6370E+07
0.3079E+07, 0.1750E+07, -0.8215E+05, -0.1024E+08
0.2200E+08, 0.8475E+08
0.5073E+05, 0.2883E+05, -1353. , -0.2058E+06
0.4483E+06, 0.1835E+07, 0.1589E+06
0.2883E+05, 0.1638E+05, -769.1 , -0.1169E+06
0.2548E+06, 0.1043E+07, 0.9029E+05, 0.5131E+05
-1353. , -769.1 , 36.11 , 5490.
-0.1196E+05, -0.4897E+05, -4239. , -2409.
113.1
-0.2058E+06, -0.1169E+06, 5490. , 0.7953E+06
-0.1723E+07, -0.6885E+07, -0.5246E+06, -0.2981E+06
0.1400E+05, 0.1750E+07
0.2744E+06, 0.1559E+06, -7320. , -0.1070E+07

```

```

0.2309E+07, 0.9073E+07, 0.7749E+06, 0.4403E+06
-0.2067E+05, -0.2586E+07, 0.3877E+07
-0.1869E+07, -0.1062E+07, 0.4987E+05, 0.7017E+07
-0.1539E+08, -0.6484E+08, -0.3159E+07, -0.1795E+07
0.8427E+05, 0.1050E+08, -0.1434E+08, 0.8817E+08
*UEL PROPERTY,ELSET=C 71
**-----MATERIAL PROPERTIES
*MATERIAL,NAME=WOOD
*ELASTIC
1.8E+06,4.625
*MATERIAL,NAME=UWOOD
*USER MATERIAL, CONSTANT=3
12.00,0.52,4.625
*MATERIAL,NAME=STEEL
*ELASTIC
2.9E+07,0.3
**-----BOUNDARY CONDITION
*BOUNDARY
SUPPORT,3
14,2
2,2
12,1
18,1
**-----APPLICATION OF DEAD LOAD
**-----NEWTON-RAPHSON STEP
*STEP,NLGEOM,INC=100,CYCLE=12
*STATIC,PTOL=20.,MTOL=2000.
0.1,1.,0.0, ,
**-----DEAD LOAD
*CLOAD
1, 3, -0.1687E+04
2, 3, -0.5581E+03
3, 3, -0.5581E+03
4, 3, -0.1682E+04
5, 3, -0.1682E+04
6, 3, -0.8391E+03
7, 3, -0.5581E+03
8, 3, -0.1682E+04
9, 3, -0.8391E+03
10, 3, -0.5581E+03
11, 3, -0.1682E+04
12, 3, -0.8391E+03
13, 3, -0.5581E+03
14, 3, -0.5581E+03
15, 3, -0.1682E+04
16, 3, -0.1682E+04
17, 3, -0.8391E+03
18, 3, -0.8391E+03
19, 3, -0.8391E+03
**-----NODE,ELEMENT SETS AND OUTPUTS
*NSET,NSET=APEX1

```

```

1
*ELSET,ELSET=ELE1
4
**-----OUTPUT REQUEST
*PRINT,RESIDUAL=NO
*NODE PRINT,NSET=APEX1,SUMMARY=NO,FREQUENCY=5
U
*NODE PRINT,NSET=APEX1,SUMMARY=NO,FREQUENCY=5
CF
*EL PRINT,ELSET=ELE1,SUMMARY=NO,FREQUENCY=20
3,23
S
*END STEP
**-----APPLICATION OF LIVE LOAD
**-----RIKS STEP
*STEP,NLGEOM,INC=25,CYCLE=12
*STATIC,PTOL=20.,MTOL=2000.,RIKS
0.1,1.,0.0, ,
**-----DEAD LOAD + SNOW LOAD
*CLOAD
  1, 3, -0.1687E+04
  2, 3, -0.5581E+03
  3, 3, -0.5581E+03
  4, 3, -0.1682E+04
  5, 3, -0.1682E+04
  6, 3, -0.8391E+03
  7, 3, -0.5581E+03
  8, 3, -0.1682E+04
  9, 3, -0.8391E+03
 10, 3, -0.5581E+03
 11, 3, -0.1682E+04
 12, 3, -0.8391E+03
 13, 3, -0.5581E+03
 14, 3, -0.5581E+03
 15, 3, -0.1682E+04
 16, 3, -0.1682E+04
 17, 3, -0.8391E+03
 18, 3, -0.8391E+03
 19, 3, -0.8391E+03
  1, 3, -0.2106E+04
  2, 3, -0.6972E+03
  3, 3, -0.6972E+03
  4, 3, -0.2101E+04
  5, 3, -0.2101E+04
  6, 3, -0.1048E+04
  7, 3, -0.6972E+03
  8, 3, -0.2101E+04
  9, 3, -0.1048E+04
 10, 3, -0.6971E+03
 11, 3, -0.2101E+04
 12, 3, -0.1048E+04

```

```

13, 3, -0.6971E+03
14, 3, -0.6972E+03
15, 3, -0.2101E+04
16, 3, -0.2101E+04
17, 3, -0.1048E+04
18, 3, -0.1048E+04
19, 3, -0.1048E+04
**-----NODE,ELEMENT SETS AND OUTPUTS
*NSET,NSET=APEX
1
*NSET,NSET=NWATCH
1,2,3,4,5,6
*ELSET,ELSET=EWATCH
5,6
**5,6,19,20,33,34,47,48,59,60,71,72
**-----OUTPUT REQUEST
*PRINT,RESIDUAL=NO
*EL PRINT,ELSET=EWATCH,POSITION=NODES
S
*NODE PRINT,NSET=NWATCH
U
*NODE PRINT,NSET=APEX,SUMMARY=NO
U
*NODE PRINT,NSET=APEX,SUMMARY=NO
CF
*NODE FILE,NSET=NALL
U
*END STEP
*USER SUBROUTINE
*****
*****      SUBROUTINE TO TEST USER SUBROUTINE UMAT      *****
*****
*****      NIKET M. TELANG .....10 APRIL'91      *****
*****
C
  SUBROUTINE UMAT(STRESS,STATEV,DDSDDE,SSE,SPD,SCD,
  1 RPL,DDSDDT,DRPLDE,DRPLDT,
  2 STRAN,DSTRAN,TIME,DTIME,TEMP,DTEMP,PREDEF,DPRED,CMNAME,
  3 NDI,NSHR,NTENS,NSTATV,PROPS,NPROPS,COORDS,DROT)
C
  IMPLICIT REAL*8(A-H,O-Z)
C
  CHARACTER*8 CMNAME
C
C
  DIMENSION STRESS(NTENS),STATEV(NSTATV),
  1 DDSDDE(NTENS,NTENS),
  2 DDSDDT(NTENS),DRPLDE(NTENS),
  3 STRAN(NTENS),DSTRAN(NTENS),PREDEF(1),DPRED(1),
  4 PROPS(NPROPS),COORDS(3),DROT(3,3)
C  DIMENSION DSTRES(2)

```

```

C
C
      DO 20 I=1,NTENS
        DO 10 J=1,NTENS
          DDSDDE(I,J)=0.0
10      CONTINUE
20      CONTINUE
C
C      SG=0.5200
C      WMC=12.0000
C
C      *LONGITUDINAL STRESS*
C
C      TS=0.0
C      TS=STRAN(1) + DSTRAN(1)
C
C      *TENSION ZONE*
C
C      IF(TS .GT. 0.0)THEN
C
C          BETA1=1805365.6
C          BETA2=1934700.0
C          BETA3=-45146768.0
C          AK1=1.43237E-03
C          AK2=0.02143
C          ALFA1=-92.62689
C          ALFA2=10496.5409
C
C          IF(TS .LT. AK1)THEN
C              DDSDDE(1,1)=BETA1
C              STRESS(1)=BETA1*TS
C          ELSEIF(TS .GE. AK1)THEN
C              DDSDDE(1,1)= BETA2 + (2.*BETA3*TS)
C              STRESS(1)=ALFA1 + BETA2*TS + BETA3*(TS**2)
C          ENDIF
C
C      *COMPRESSION ZONE*
C
C      ELSEIF(TS .LE. 0.0)THEN
CC
C          BETA1=2195036.0
C          BETA2=3229460.0
C          BETA3=-222916014.1
C          AK1=2.3202E-03
C          AK2=7.24367E-03
C          ALFA2=10496.5409
C          ALFA1=-1200.03
CC
C          AK1C=-AK1
C          AK2C=-AK2

```

```

CC      AK2C=-6.441551051E-03
      IF(TS .GE. AK1C)THEN
          DDSDDE(1,1)=BETA1
          STRESS(1)=-BETA1*ABS(TS)
      ELSEIF(TS .LT. AK1C .AND. TS .GE. AK2C)THEN
          DDSDDE(1,1)=BETA2 + 2.*BETA3*ABS(TS)
          STRESS(1)=- (ALFA1 + BETA2*ABS(TS) +
1          BETA3*((ABS(TS))**2))
      ELSEIF(TS .LT. AK2C)THEN
          DDSDDE(1,1)=0.0
          STRESS(1)=-ALFA2
      ENDIF
      ENDIF
C
C      *TORSIONAL SHEAR STRESS*
C
      TT=0.0
      TT=STRAN(2) + DSTRAN(2)
C
      DDSDDE(2,2)=(1.6000E+05)
      STRESS(2)=DDSDDE(2,2)*TT
C
      RETURN
      END

```

APPENDIX F

```

C*****
C PROGRAM TO COMPUTE THE DISPLACEMENT OF EACH NAILED JOINT
C ON MAIN BEAMS.
C
C BY MOSES TSANG ..... (703) 552-2801
C SANDEEP KAVI ..... (703) 953-0409
C
C THE PROGRAM REQUIRES SBEM1 DAT, SKS1 DAT, SDISP DAT,
C SNODE DAT AND MDISP1 EXEC FILES
C THE OUTPUT IS WRITTEN TO MDISP1 OUT FILE
C
C NOV. 30 ,1992
C*****
REAL S11,S21,S12,S22,S32,S42
REAL XCOS(1700),YCOS(1700),ZCOS(1700),XC(2700),YC(2700),ZC(2700),
1 XCC(2700),YCC(2700),ZCC(2700),ZCOS1(1700),
2 GDM1(6),GDM2(6),LDM1(6),LDM2(6),R(6,6),LDM(6),N(6),
3 T1(1700),T2(1700),T3(1700),N11(1700),N12(1700),N13(1700),
4 N21(1700),N22(1700),N23(1700),U1(1700),U2(1700),U3(1700),
5 RM1(1700),RM2(1700),RM3(1700)
OPEN(UNIT=10,STATUS='OLD')
OPEN(UNIT=15,STATUS='OLD')
OPEN(UNIT=20,STATUS='OLD')
OPEN(UNIT=25,STATUS='OLD')
OPEN(UNIT=30,STATUS='UNKNOWN')
C
C **THE BEAM TYPE.
WRITE(30,105)
C
CC ##### READ FROM SKS1 DAT
READ (25,*) S,H,NS,NMAX,NNODE,NELEM,NDISP
C
C***** READ FROM SKS1 DAT *****
C S=SPRING STIFFNESS, H=RIGID BEAM LENGTH,
C NS=NUMBER OF SPRINGS.
C NMAX=MAX. NUMBER OF ELEMENTS IN THE STRUCTURE
C NNODE=TOTAL NO. OF NODES.
C NELEM=NO. OF MAIN BEAM ELEMENTS.
C NDISP=NO. OF NODES OF DISPLACEMENTS
C*****
CC ##### READ NODES FROM, SNODE DAT A
DO 10 I=1,NNODE
READ (10,*) K, X, Y, Z
XCOS(K) = X

```

```

        YCOS(K) = Y
        ZCOS(K) = Z+1387.66
CC      ZCOS(K) = Z
CC
10  CONTINUE
CC#####READ GLOBAL NODE DISPLACEMENT FROM SDISP DAT A
    DO 11 I=1,NDISP
        READ (15,*) K,R1,R2,R3,R4,R5,R6
        U1(K)=R1
        U2(K)=R2
        U3(K)=R3
        RM1(K)=R4
        RM2(K)=R5
        RM3(K)=R6
11  CONTINUE
CC##### READ MAIN BEAMS 6.75X11.0, SBEM1 DAT A
C
    DO 100 K=1,NELEM
        READ (20,*) NE, N1, N2
C
C** ELEMENT NO.
        WRITE(30,175) NE
C
C***** READ FROM SBEM1 DAT *****
C        NE = THE ELEMENT NUMBER.
C        N1,N2=TO WHICH NODES THE BEAM ATTACHED.
C
C    IN ORDER TO OBTAIN THE NAIL DISPLACEMENT, WE NEED TO TRANSFORM
C    THE GLOBAL NODE DISPLACEMENTS INTO LOCAL DISPLACEMENTS, AND USE
C    BEAM INTERPOLATION FUNCTIONS AND BEAM END DISPLACEMENTS (FROM
C    NODE DISP.)
C    TO OBTAIN THE NAIL DISPLACEMENT. FIRST WE NEED THE ROTATION C
C    MATRIX FOR TRANSFORMATION
C
C    INITIALIZE THE ROTATION & TRANSPOSE ROTATION MATRICES.
C
    DO 40 I=1,6
        DO 45 J=1,6
            R(I,J) = 0.0
            GDM1(I)=0.0
            GDM2(I)=0.0
            LDM1(I)=0.0
            LDM2(I)=0.0
            LDM(I)=0.0
45  CONTINUE
40  CONTINUE
C
        T1(NE) = XCOS(N2) - XCOS(N1)
        T2(NE) = YCOS(N2) - YCOS(N1)
        T3(NE) = ZCOS(N2) - ZCOS(N1)
        TNORM = (T1(NE)**2+T2(NE)**2+T3(NE)**2)**0.5

```

```

C
N11(NE) = YCOS(N1) * ZCOS(N2) - ZCOS(N1) * YCOS(N2)
N12(NE) = -(XCOS(N1) * ZCOS(N2) - ZCOS(N1) * XCOS(N2))
N13(NE) = XCOS(N1) * YCOS(N2) - YCOS(N1) * XCOS(N2)
N1NORM = (N11(NE)**2+N12(NE)**2+N13(NE)**2) ** 0.5
C
N21(NE) = T2(NE)*N13(NE)-T3(NE)*N12(NE)
N22(NE) = T3(NE)*N11(NE)-T1(NE)*N13(NE)
N23(NE) = T1(NE)*N12(NE)-T2(NE)*N11(NE)
N2NORM = (N21(NE)**2+N22(NE)**2+N23(NE)**2) ** 0.5
CC
DO 50 I=1,4,3
R(I,I) = T1(NE)/TNORM
R(I,I+1)=T2(NE)/TNORM
R(I,I+2)=T3(NE)/TNORM
R(I+1,I)=N11(NE)/N1NORM
R(I+1,I+1)=N12(NE)/N1NORM
R(I+1,I+2)=N13(NE)/N1NORM
R(I+2,I)=N21(NE)/N2NORM
R(I+2,I+1)=N22(NE)/N2NORM
R(I+2,I+2)=N23(NE)/N2NORM
C ALTERNATIVELY >>
C R(I+2,I)=R(1,2)*R(2,3)-R(2,2)*R(1,3)
C R(I+2,I+1)=R(2,1)*R(1,3)-R(1,1)*R(2,3)
C R(I+2,I+2)=R(1,1)*R(2,2)-R(1,2)*R(2,1)
50 CONTINUE
C
CC##### PUT GLOBAL NODE DISPLACEMENT OF NODE N1 INTO GDM1(6)
C
GDM1(1)=U1(N1)
GDM1(2)=U2(N1)
GDM1(3)=U3(N1)
GDM1(4)=RM1(N1)
GDM1(5)=RM2(N1)
GDM1(6)=RM3(N1)
C
CC##### PUT GLOBAL NODE DISPLACEMENT OF NODE N2 INTO GDM2(6)
C
GDM2(1)=U1(N2)
GDM2(2)=U2(N2)
GDM2(3)=U3(N2)
GDM2(4)=RM1(N2)
GDM2(5)=RM2(N2)
GDM2(6)=RM3(N2)
C
CC##### TRANSFORM GLOBAL TO LOCAL NODE DISPLACEMENTS OF
CC NODE N1 AND N2, AND PUT THE LOCAL DISPLACEMENT INTO
CC LDM1(6) AND LDM2(6)
C
DO 60 I=1,6
DO 55 J=1,6

```

```

        LDM1(I)=LDM1(I)+R(I,J)*GDM1(J)
        LDM2(I)=LDM2(I)+R(I,J)*GDM2(J)
55    CONTINUE
60    CONTINUE
C
CC#### PUT THE NODE DISPLACEMENTS OF THE BEAM THAT ACTIVATE THE
CC    NAIL DISPLACEMENT INTO LDM(6), BE CAREFUL ABOUT THE LOCAL
C    AXIS OF THE MAIN BEAMS
C
        LDM(1)=LDM1(2)
        LDM(2)=LDM1(4)
        LDM(3)=LDM1(6)
        LDM(4)=LDM2(2)
        LDM(5)=LDM2(4)
        LDM(6)=LDM2(6)
C
C***** READ THE LOCATION OF SPRING AND DEFINE *****
C    INTERPOLATION FUNCTIONS
C *LOCAL AXIS OF EDGE BEAMS IS DIFFERENT FROM THAT OF THE EDGE BEAMS
C
        SPACE=TNORM/NS
C ##### SPACE=SPACING BETWEEN EACH SPRING
        DO 30 L=1,NS
            XI=SPACE*L/TNORM
            S11=1.-XI
            S21=XI
            S12=1.-3.*XI**2.+2.*XI**3.
            S22=-(XI-2.*XI**2.+XI**3.)*TNORM
            S32=3.*XI**2.-2.*XI**3.
            S42=(XI**2.-XI**3.)*TNORM
C
CC##### PUT THE INTERPOLATION FUNCTIONS INTO N(1,6)
CC    SEE THE HANDOUTS GIVEN BY DR.HOLZER ABOUT THE FORMULATION
CC    OF THE 3-D BEAM/CONNECTOR ELEMENTS. MAIN BEAM HAS A LITTLE
CC    DIFFERENT INTERPOLATION FUNCTIONS (JUST TWO OF THEM HAS
CC    SIGN CHANGE.)
C
        N(1)=-S12
        N(2)=H*S11
        N(3)=S22
        N(4)=-S32
        N(5)=H*S21
        N(6)=S42
C
CC##### COMPUTE THE NAIL DISPLACEMENT BY INTERPOLATION FUNCTIONS
CC    MULTIPLY N(1,6) WITH LDM(6)
C
CC##### SET NAIL DISPLACEMENT DISP TO ZERO
C
CC    WRITE(30,120) LDM(1),LDM(2),LDM(3),LDM(4),LDM(5),LDM(6)
CC120  FORMAT(6(F8.2))

```

```

DISP=0.0
DO 70 I=1,6
    DISP=DISP+N(I)*LDM(I)
70 CONTINUE
C
CC##### WRITE EACH NAIL DISPLACEMENT ACCORDING TO ITS LOCATION
CC      ON CERTAIN MAIN BEAM TO MDISP1 OUT
C
    WRITE(30,180) L,(XI*TNORM),N1
    WRITE(30,185) DISP
CC
175  FORMAT('**',35('-'),'ELEMENT',I4)
180  FORMAT('***',I4,' TH NAILED JOINT LOCATED',F8.2,' IN. FROM NODE',
1     I4)
185  FORMAT('NAIL DISPLACEMENT = ',G12.4,/)
30   CONTINUE
100  CONTINUE
105  FORMAT ('**',35('-'),'MAIN BEAMS/NAIL DISPLACEMENTS')
END

```

APPENDIX G

```

C*****
C PROGRAM TO COMPUTE THE DISPLACEMENT OF EACH NAILED JOINT
C ON EDGE BEAMS.
C
C BY MOSES TSANG ..... (703) 552-2801
C SANDEEP KAVI ..... (703) 953-0409
C
C THE PROGRAM REQUIRES SEBEM DAT, SKS3 DAT, SDISP DAT(GLOBAL DISP.)
C SNODE DAT AND MDISP3 EXEC FILES
C THE OUTPUT IS WRITTEN TO MDISP3 OUT FILE
C
C NOV. 30 ,1992
C*****
REAL S11,S21,S12,S22,S32,S42
REAL XCOS(1700),YCOS(1700),ZCOS(1700),XC(2700),YC(2700),ZC(2700),
1 XCC(2700),YCC(2700),ZCC(2700),ZCOS1(1700),
2 GDM1(6),GDM2(6),LDM1(6),LDM2(6),R(6,6),LDM(6),N(6),
3 T1(1700),T2(1700),T3(1700),N11(1700),N12(1700),N13(1700),
4 N21(1700),N22(1700),N23(1700),U1(1700),U2(1700),U3(1700),
5 RM1(1700),RM2(1700),RM3(1700)
OPEN(UNIT=10,STATUS='OLD')
OPEN(UNIT=15,STATUS='OLD')
OPEN(UNIT=20,STATUS='OLD')
OPEN(UNIT=25,STATUS='OLD')
OPEN(UNIT=30,STATUS='UNKNOWN')
C
C **THE BEAM TYPE.
WRITE(30,105)
C
CC ##### READ FROM SKS3 DAT
READ (25,*) S,H,NS,NMAX,NNODE,NELEM,NDISP
C
C***** READ FROM SKS3 DAT *****
C S=SPRING STIFFNESS, H=RIGID BEAM LENGTH,
C NS=NUMBER OF SPRINGS.
C NMAX=MAX. NUMBER OF ELEMENTS IN THE STRUCTURE
C NNODE=TOTAL NO. OF NODES.
C NELEM=NO. OF MAIN BEAM ELEMENTS.
C SDISP=NO. OF NODES OF DISPLACEMENTS
C*****
CC ##### READ NODES FROM, SNODE DAT A
DO 10 I=1,NNODE
READ (10,*) K, X, Y, Z
XCOS(K) = X

```

```

        YCOS(K) = Y
CC ###ZCOS1 = Z-190.46 FOR EDGE BEAMS NOT ON THE GREAT CIRCLE.
CC ###ZCOS1 = Z+1387.66 FOR EDGE BEAMS ON THE GREAT CIRCLE.
        ZCOS1(K) = Z-190.46
CC     ZCOS1(K) = Z+1387.66
CC
10  CONTINUE
CC#####READ GLOBAL NODE DISPLACEMENT FROM SDISP DAT A
    DO 11 I=1,NDISP
        READ (15,*) K,R1,R2,R3,R4,R5,R6
        U1(K)=R1
        U2(K)=R2
        U3(K)=R3
        RM1(K)=R4
        RM2(K)=R5
        RM3(K)=R6
11  CONTINUE
CC##### READ EDGE BEAMS 3.0 X 12.25 SEBEM DAT A
C
    DO 100 K=1,NELEM
        READ (20,*) NE, N1, N2
C
C** ELEMENT NO.
        WRITE(30,175) NE
C
C***** READ FROM SEBEM DAT *****
C     NE = THE ELEMENT NUMBER.
C     N1,N2=TO WHICH NODES THE BEAM ATTACHED.
C
C     IN ORDER TO OBTAIN THE NAIL DISPLACEMENT, WE NEED TO TRANSFORM
C     THE GLOBAL NODE DISPLACEMENTS INTO LOCAL DISPLACEMENTS, AND USE
C     BEAM INTERPOLATION FUNCTIONS AND BEAM END DISPLACEMENTS (FROM
C     NODE DISP.)
C     TO OBTAIN THE NAIL DISPLACEMENT. FIRST WE NEED THE ROTATION
C     MATRIX FOR TRANSFORMATION
C
C     INITIALIZE THE ROTATION & TRANSPOSE ROTATION MATRICES.
C
    DO 40 I=1,6
        DO 45 J=1,6
            R(I,J) = 0.0
            GDM1(I)=0.0
            GDM2(I)=0.0
            LDM1(I)=0.0
            LDM2(I)=0.0
            LDM(I)=0.0
45  CONTINUE
40  CONTINUE
C
        T1(NE) = XCOS(N2) - XCOS(N1)
        T2(NE) = YCOS(N2) - YCOS(N1)

```

```

T3(NE) = ZCOS1(N2) - ZCOS1(N1)
TNORM = (T1(NE)**2+T2(NE)**2+T3(NE)**2)**0.5
C
N11(NE) = YCOS(N1) * ZCOS1(N2) - ZCOS1(N1) * YCOS(N2)
N12(NE) = -(XCOS(N1) * ZCOS1(N2) - ZCOS1(N1) * XCOS(N2))
N13(NE) = XCOS(N1) * YCOS(N2) - YCOS(N1) * XCOS(N2)
N1NORM = (N11(NE)**2+N12(NE)**2+N13(NE)**2) ** 0.5
C
N21(NE) = T2(NE)*N13(NE)-T3(NE)*N12(NE)
N22(NE) = T3(NE)*N11(NE)-T1(NE)*N13(NE)
N23(NE) = T1(NE)*N12(NE)-T2(NE)*N11(NE)
N2NORM = (N21(NE)**2+N22(NE)**2+N23(NE)**2) ** 0.5
CC
DO 50 I=1,4,3
R(I,I) = T1(NE)/TNORM
R(I,I+1)=T2(NE)/TNORM
R(I,I+2)=T3(NE)/TNORM
R(I+1,I)=N11(NE)/N1NORM
R(I+1,I+1)=N12(NE)/N1NORM
R(I+1,I+2)=N13(NE)/N1NORM
R(I+2,I)=N21(NE)/N2NORM
R(I+2,I+1)=N22(NE)/N2NORM
R(I+2,I+2)=N23(NE)/N2NORM
C ALTERNATIVELY >>
C R(I+2,I)=R(1,2)*R(2,3)-R(2,2)*R(1,3)
C R(I+2,I+1)=R(2,1)*R(1,3)-R(1,1)*R(2,3)
C R(I+2,I+2)=R(1,1)*R(2,2)-R(1,2)*R(2,1)
50 CONTINUE
C
CC##### PUT GLOBAL NODE DISPLACEMENT OF NODE N1 INTO GDM1(6)
C
GDM1(1)=U1(N1)
GDM1(2)=U2(N1)
GDM1(3)=U3(N1)
GDM1(4)=RM1(N1)
GDM1(5)=RM2(N1)
GDM1(6)=RM3(N1)
C
CC##### PUT GLOBAL NODE DISPLACEMENT OF NODE N2 INTO GDM2(6)
C
GDM2(1)=U1(N2)
GDM2(2)=U2(N2)
GDM2(3)=U3(N2)
GDM2(4)=RM1(N2)
GDM2(5)=RM2(N2)
GDM2(6)=RM3(N2)
C
CC##### TRANSFORM GLOBAL TO LOCAL NODE DISPLACEMENTS OF
CC NODE N1 AND N2, AND PUT THE LOCAL DISPLACEMENT INTO
CC LDM1(6) AND LDM2(6), RESPECTIVELY
C

```

```

DO 60 I=1,6
  DO 55 J=1,6
    LDM1(I)=LDM1(I)+R(I,J)*GDM1(J)
    LDM2(I)=LDM2(I)+R(I,J)*GDM2(J)
55  CONTINUE
60  CONTINUE
C
CC##### PUT THE NODE DISPLACEMENTS OF THE BEAM THAT ACTIVATE THE
CC  NAIL DISPLACEMENT INTO LDM(6) ACCORDING TO THE LOCAL AXIS
CC  OF THE BEAM ## BE CAREFUL!
C
  LDM(1)=LDM1(3)
  LDM(2)=LDM1(4)
  LDM(3)=LDM1(5)
  LDM(4)=LDM2(3)
  LDM(5)=LDM2(4)
  LDM(6)=LDM2(5)
C
C***** READ THE LOCATION OF SPRING AND DEFINE *****
C  INTERPOLATION FUNCTIONS
C ***** ORIGINAL MATRIX WITH LOCAL AXIS FROM HOLZER'S BOOK *****
C ***** COMPATIBLE WITH LOCAL AXIS DIRECTION OF EDGE BEAMS *****
C
  SPACE=TNORM/NS
C ##### SPACE=SPACING BETWEEN EACH SPRING
  DO 30 L=1,NS
    XI=SPACE*L/TNORM
    S11=1.-XI
    S21=XI
    S12=1.-3.*XI**2.+2.*XI**3.
    S22=-(XI-2.*XI**2.+XI**3.)*TNORM
    S32=3.*XI**2.-2.*XI**3.
    S42=(XI**2.-XI**3.)*TNORM
C
CC##### PUT THE INTERPOLATION FUNCTIONS INTO N(1,6)
CC  SEE THE HANDOUTS GIVEN BY DR.HOLZER ABOUT THE FORMULATION
CC  OF THE 3-D BEAM/CONNECTOR ELEMENTS. EDGE BEAM HAS THE SAME
CC  INTERPOLATION FUNCTIONS
C
  N(1)=S12
  N(2)=H*S11
  N(3)=S22
  N(4)=S32
  N(5)=H*S21
  N(6)=S42
CC  WRITE(30,119) N(1),N(2),N(3),N(4),N(5),N(6)
CC119  FORMAT(6(F8.2))
C
CC##### COMPUTE THE NAIL DISPLACEMENT BY INTERPOLATION FUNCTIONS
CC  MULTIPLY N(1,6) WITH LDM(6)
C

```

```

CC##### SET NAIL DISPLACEMENT DISP TO ZERO
C
CC      WRITE(30,120) LDM(1),LDM(2),LDM(3),LDM(4),LDM(5),LDM(6)
CC120  FORMAT(6(F8.2))
      DISP=0.0
      DO 70 I=1,6
          DISP=DISP+N(I)*LDM(I)
70  CONTINUE
C
CC##### WRITE EACH NAIL DISPLACEMENT ACCORDING TO ITS LOCATION
CC      ON CERTAIN EDGE BEAM TO MDISP3 OUT
C
      WRITE(30,180) L,(XI*TNORM),N1
      WRITE(30,185) DISP
CC
175  FORMAT('**',35('-'),'ELEMENT',I4)
180  FORMAT('***',I4,' TH NAILED JOINT LOCATED',F8.2,' IN. FROM NODE',
1      I4)
185  FORMAT('NAIL DISPLACEMENT = ',G12.4,/)
30  CONTINUE
100 CONTINUE
105  FORMAT ('**',35('-'),'EDGE BEAMS/NAIL DISPLACEMENTS')
      END

```

VITA

Moses T. Tsang was born in Hong Kong in November, 1966. He graduated with the Bachelor of Science degree from National Cheng Kung University in Taiwan. He started his studies towards the Master of Science degree in Civil Engineering in August, 1990 at Virginia Polytechnic Institute and State University. He is a member of Chi Epsilon, which is a National Honor Society of Civil Engineering. He is planning to work as a Civil Engineer in the U.S.A. after he graduates.

A handwritten signature in cursive script that reads "Moses Tsang". The signature is written in black ink and is positioned on the right side of the page, below the main text block.